

# PONTE SULLO STRETTO DI MESSINA



## PROGETTO DEFINITIVO

### EUROLINK S.C.p.A.

IMPREGILO S.p.A. (MANDATARIA)  
 SOCIETÀ ITALIANA PER CONDOTTE D'ACQUA S.p.A. (MANDANTE)  
 COOPERATIVA MURATORI E CEMENTISTI - C.M.C. DI RAVENNA SOC. COOP. A.R.L. (MANDANTE)  
 SACYR S.A.U. (MANDANTE)  
 ISHIKAWAJIMA - HARIMA HEAVY INDUSTRIES CO. LTD (MANDANTE)  
 A.C.I. S.C.P.A. - CONSORZIO STABILE (MANDANTE)

<p>IL PROGETTISTA</p>  <p>Ing. E.M. Veje          Dott. Ing. E. Pagani          Ordine Ingegneri Milano          n° 15408</p> 	<p>IL CONTRAENTE GENERALE</p> <p>Project Manager          (Ing. P.P. Marcheselli)</p>	<p>STRETTO DI MESSINA</p> <p>Direttore Generale e          RUP Validazione          (Ing. G. Fiammenghi)</p>	<p>STRETTO DI MESSINA</p> <p>Amministratore Delegato          (Dott. P. Ciucci)</p>
--	---	--	---

<p><i>Unità Funzionale</i></p> <p><i>Tipo di sistema</i></p> <p><i>Raggruppamento di opere/attività</i></p> <p><i>Opera - tratto d'opera - parte d'opera</i></p> <p><i>Titolo del documento</i></p>	<p>OPERA DI ATTRAVERSAMENTO</p> <p>SOTTOSTRUTTURE</p> <p>BLOCCHI DI ANCORAGGIO</p> <p>Geotechnical Design Reports</p> <p>Sicily Anchor Block – earthquake induced displacements and safety against ultimate limit states, Annex</p>	<p><b>PF0064_F0</b></p>
---	---	-------------------------

CODICE	G C 1 0 0 0	P	C L	D	P	S T	B 4	B S	0 0	0 0	0 0	0 2	F0
--------	-------------	---	-----	---	---	-----	-----	-----	-----	-----	-----	-----	----

REV	DATA	DESCRIZIONE	REDATTO	VERIFICATO	APPROVATO
F0	20/06/2011	EMISSIONE FINALE	LM	GV	SR



		<b>Ponte sullo Stretto di Messina</b> <b>PROGETTO DEFINITIVO</b>		
Sicily Anchor Block – earthquake induced displacements and safety against ultimate limit states, Annex	<i>Codice documento</i> PF0064_F0_ANX	<i>Rev</i> F0	<i>Data</i> 20/06/2011	

## INDEX

1	Executive summary.....	5
2	Soil profile and geotechnical characterisation .....	13
3	Constitutive soil model and soil parameters .....	16
4	Anchor Blocks – Safety against sliding.....	19
4.1	Static conditions – governing equations.....	19
4.1.1	Global safety factor.....	19
4.1.2	Partial safety factors .....	19
4.2	Seismic conditions – governing equations .....	20
4.2.1	Pseudo-static approach.....	20
4.2.1.1	Global safety factor .....	21
4.2.1.2	Partial safety factors.....	21
4.2.2	Displacement-based approach .....	22
4.2.2.1	Critical seismic coefficient .....	23
4.2.2.2	Equation of relative motion under seismic conditions .....	23
5	Sicily Anchor Block – safety against sliding.....	25
5.1	Self weight of the anchor block.....	25
5.2	Sliding mechanisms.....	25
5.3	Evaluation of the sliding surface .....	26
5.4	Sliding resistance on the sides of the anchor block .....	29
5.5	Passive resistance in front of the block.....	30
5.5.1	Pseudo static approach .....	30
5.5.2	Displacement based approach .....	31
5.6	Evaluation of safety against sliding – pseudostatic approach .....	33
5.7	Evaluation of sliding performance – displacement based approach.....	35
5.7.1	Seismic action .....	35
5.7.2	Critical seismic coefficient.....	41
5.7.3	Earthquake-induced displacements.....	41
6	Sicily Anchor Block – Safety against rotation .....	45
7	Sicily Anchor Block – Bearing capacity .....	47
8	Conclusions .....	51

		<b>Ponte sullo Stretto di Messina</b> <b>PROGETTO DEFINITIVO</b>		
Sicily Anchor Block – earthquake induced displacements and safety against ultimate limit states, Annex	<i>Codice documento</i> PF0064_F0_ANX	<i>Rev</i> F0	<i>Data</i> 20/06/2011	

9	Figures.....	53
	Appendices .....	87
	Appendix A – Sliding resistance along the block sides .....	88
	Appendix B – Passive earth resistance in front of the anchor block .....	97
	Appendix C – Safety against sliding, pseudo-static approach.....	100
	Appendix D – Time histories.....	104
	Appendix E – Updated cable forces obtained from global IBDAS model version 3.3b .....	135
	Appendix F – Updated cable forces obtained from global IBDAS model version 3.3f .....	138
	References .....	141

		<b>Ponte sullo Stretto di Messina</b> <b>PROGETTO DEFINITIVO</b>		
Sicily Anchor Block – earthquake induced displacements and safety against ultimate limit states, Annex	<i>Codice documento</i> PF0064_F0_ANX	<i>Rev</i> F0	<i>Data</i> 20/06/2011	

## 1 Executive summary

In this report the geotechnical safety of Sicily anchor block is evaluated against ultimate limit state using the pseudo-static approach, including safety against sliding and rotation and bearing capacity failure, while earthquake-induced block displacements are evaluated using the displacement-based approach. The most likely sliding mechanisms to be used for computing the earthquake-induced displacements was estimated through plane strain FE analyses. Computations were carried out using the cable forces provided by the tender design that, for the ULS load combination, result slightly higher than the values obtained from the global IBDAS model (5.8% for the version 3.3b, 8% for the version 3.3f) this resulting in a conservative estimate of the behaviour of the Sicilia Anchor Block.

The companion report “Sicily Anchor Block – evaluation of block behaviour via 3D FE analyses and of bearing capacity” describes results from static 3D FE analyses of Sicily Anchor Block.

**Chapter 2** describes the soil profile on the Sicily shore (Figure 2.1).

Starting from ground level and moving downwards the following units are encountered: *Depositi Costieri* (Coastal Deposits); *Ghiaie di Messina* (Messina Gravel)/*Sedimenti dei terrazzi* (Terrace Deposits); *Depositi Continentali* (Continental Deposits)/*Calcarenite di Vinco* (Vinco Calcarenite); *Conglomerato di Pezzo* (Pezzo Conglomerate); *Cristallino* (Crystalline bedrock). A plan view at the site of the Sicily Anchor Block is shown in Figure 2.2. The two longitudinal sections and the cross section indicated in Figure 2.2 are shown in Figure 2.3 – 2.5. The sections in the figures show that the Messina Gravel/Terrace Deposits unit extends from the ground level over a thickness of about 200m. Hence it is the only geological units of relevance. Table 2.1 summarises the main mechanical parameters obtained from the geotechnical characterisation.

**Chapter 3** details the constitutive model adopted in the FE analyses discussed in the report.

This is an elastic-plastic rate independent model with isotropic hardening (Hardening Soil) available in the library of the code *Plaxis*. In the model, the elastic behaviour is defined by isotropic elasticity through a stress-dependent Young’s modulus,  $E'$ . For plastic loading from isotropic stress states, the model predicts a non linear stress-strain relationship with tangent initial modulus equal to  $E'$ . Values of  $E'$  were related to the shear modulus at small-strain  $G_0$  obtained from the cross-hole test carried out in the site. In particular, values of the parameters reported in Table 3.1

		<b>Ponte sullo Stretto di Messina</b> <b>PROGETTO DEFINITIVO</b>		
Sicily Anchor Block – earthquake induced displacements and safety against ultimate limit states, Annex	<i>Codice documento</i> PF0064_F0_ANX	<i>Rev</i> F0	<i>Data</i> 20/06/2011	

were obtained by best fitting the cross-hole test results in Figure 3.2. The values of the Hradening soil parameters adopted in the FE analyses discussed in the report are given in Table 3.2.

**Chapter 4** examines the governing equations for the safety of anchor blocks against sliding.

In static conditions (section 4.1) and following the global safety factor approach (section 4.1.1), safety against sliding can be expressed through the global safety factor given in eq.(1). For the meaning of the symbols in eq.(1) refer to Figure 4.1 of the report. Following the partial safety factors approach (section 4.1.2), the design values of the actions  $E_d$  and the resistance  $R_d$  are computed from the corresponding characteristic values applying partial safety factors to actions, resistances and strength parameters. Condition  $R_d \geq E_d$  must then be satisfied (D.M. 14.01.2008). The characteristic actions and the characteristic resistance are defined in eq. (2). Following Approach 1, Combination 2 to study geotechnical (GEO) limit states (section 2.6.1 - D.M. 14.01.2008), the design actions and resistances can be computed from eq.(3) in which:  $\gamma_\phi = 1.25$  and  $\gamma_p = 1.1$ , the cable forces,  $T$ , are inclusive of partial load factors as provided by structural analyses of the tender design for each limit state and therefore are not factored, the weight of the anchor block (permanent load) is multiplied by the same load factor,  $\gamma_{G1} = 1$ , irrespective of its effect (D.M. 14.01.2008), and the components of  $S_a$  and  $R_p$  normal to the sliding surface are neglected. Safety against sliding under static loading conditions is not evaluated in the report since the pseudo-static loading conditions are the most critical.

Analysis of the anchor blocks under seismic conditions (section 4.2) is carried out using the pseudo-static approach and the displacement-based sliding block approach. In the pseudo-static approach (section 4.2.1), the stability of the block is measured either by a global factor of safety  $F$ , that is the ratio of the total resisting force to the total driving force (section 4.2.1.1) or using partial safety factors (section 4.2.1.2). The global factor of safety against sliding is given in eq.(4). For the meaning of the symbols in eq.(4) refer to Figure 4.2 of the report. In the partial safety factors approach (section 4.2.1.2) the stability of the block is measured by a comparison of the design action with the design resistance. The design values of the actions  $E_d$  and the resistance  $R_d$  are computed from the corresponding characteristic values applying partial safety factors to actions, resistances and strength parameters. Condition  $R_d \geq E_d$  must then be satisfied. Under seismic condition the load factors of the design actions are set equal to unity:  $\gamma_G = \gamma_Q = 1$  (§ 7.11.1 - D.M. 14.01.2008) and are therefore omitted in the relevant equations. The characteristic actions and the characteristic resistance are defined in eq. (5). Following Approach 1, Combination 2, to study geotechnical (GEO) limit states, the design actions and resistances can be computed from eq.(6)

		<b>Ponte sullo Stretto di Messina</b> <b>PROGETTO DEFINITIVO</b>		
Sicily Anchor Block – earthquake induced displacements and safety against ultimate limit states, Annex	<i>Codice documento</i> PF0064_F0_ANX	<i>Rev</i> F0	<i>Data</i> 20/06/2011	


in which:  $\gamma_\phi = 1.25$  and  $\gamma_p = 1.1$ , the cable forces,  $T$ , are inclusive of partial load factors, as provided by structural analyses of the tender design for each limit state, and the components of  $S_a$  and  $R_p$  normal to the sliding surface are neglected. In the displacement-based approach (section 4.2.2), the safety of the anchor block is evaluated comparing the permanent displacement developed during the earthquake with a threshold value. The critical acceleration is first determined using the pseudo-static approach and then the cumulative displacement of the potentially sliding mass is evaluated using the sliding block analysis. The sliding mass is treated as a rigid body with permanent displacements taking place whenever the ground acceleration exceeds the critical acceleration. The permanent displacement is calculated by integrating twice the relative acceleration time history over the time intervals in which the velocity of the sliding mass relative to the ground is positive. The critical acceleration is evaluated using the characteristic values of the strength parameters  $c'_k$  and  $\phi'_k$ ; under seismic conditions load factors are equal to one. The pseudo-static seismic action acts with an angle  $(\alpha-\theta)$  with respect to the sliding surface (Figure 4.3). Assuming conditions of limit equilibrium ( $F = 1$ ) and neglecting the contributions of passive and active earth thrusts, the expression of  $K$  given in eq.(8) is obtained. The minimum value of  $K$ , that is the critical seismic coefficient  $K_c$ , is obtained for  $\theta = \alpha + \phi'_s \Rightarrow \alpha - \theta = -\phi'_s$  (Figure 4.3) and has the expression given in eq.(9). During sliding ( $K > K_c$ ), it can be assumed that the net earth thrust  $\Delta R$  increases with increasing block displacements  $u$  as per eq.(10), in which  $k_d$  is a non linear spring stiffness, depending on relative displacement (Figure 4.4). The effect of  $\Delta R$  is explicitly included in the equation of relative motion used for computing the earthquake-induced displacement of the anchor block. Separating the horizontal and vertical components of the acceleration time histories, and for  $\theta = \alpha + \phi'_s \Rightarrow \alpha - \theta = -\phi'_s$ , the equation of relative motion can be written as in eq. (21).

**Chapter 5** examines safety against sliding for the Sicily Anchor Block.

The self-weight of the anchor block (section 5.1) was calculated on the basis of the drawings the tender design (Figure 5.2). Relevant data are listed in Table 5.1.

Three possible sliding mechanisms (section 5.2) were considered in the analyses (Figure 5.3), characterised by angles  $\alpha = 38^\circ$ ,  $26^\circ$  and  $8^\circ$  on the horizontal; in each mechanism, the contribution of soil between the sliding surface and the anchor is considered as an added weight, as reported in Table 5.2.

In order to estimate the most likely sliding mechanism (section 5.3), plane strain FE analyses were carried out using *Plaxis 8* (Figure 5.4). Soil-anchor block contact was modelled through interface

		<b>Ponte sullo Stretto di Messina</b> <b>PROGETTO DEFINITIVO</b>		
Sicily Anchor Block – earthquake induced displacements and safety against ultimate limit states, Annex	<i>Codice documento</i> PF0064_F0_ANX	<i>Rev</i> F0	<i>Data</i> 20/06/2011	

elements with reduced shear strength and stiffness. The anchor block was assumed to behave as an elastic non-porous material. The analyses were carried out in terms of effective stresses, assuming drained conditions. The presence of diaphragm walls in front and behind the anchor block were not accounted for in the analyses. Table 5.3 summarises the equivalent unit weight,  $\gamma_{eq}$ , of both the cable chambers and the filled chambers that were used in the plane strain FE analyses. ULS loading conditions were considered in the analyses, spreading the cable load  $T$  over the width  $B = 100$  m of the anchor block, to account for plane strain conditions. Table 5.4 details the sequence of computation steps. To estimate the most likely sliding surface, the block displacement and its direction were evaluated as the average between the displacements of the centre of gravity and of four nodes of the block at the contact with the soil (Figures 5.8 -5.9). Table 5.5 shows the results obtained. Under ULS loading condition, the average direction is  $14.2^\circ$  on the horizontal. The most likely sliding mechanism is therefore between the second and the third mechanism.

The sliding resistance  $T_L$  developed on the sides of the anchor block (section 5.4) was computed under the conservative hypothesis that active limit equilibrium is achieved behind the diaphragm walls during the excavation stages, reducing  $\tan\phi'$  and  $\tan\phi'_s$  by factor  $\gamma_\phi = 1.25$  as prescribed by D.M. 14.01.2008. Table 5.7 lists the characteristics and design values of lateral resistance  $T_L$ . The former are used to evaluate the critical seismic coefficient  $K_{c(red)}$  given by eq.(9), while the latter is used in the pseudostatic approach. Appendix A gives computation details.

The passive resistance  $R_p$  developed in front of the block on sliding is dealt with section 5.5. In the pseudostatic approach (section 5.5.1)  $R_p$  was computed using the solution obtained by Chen and Liu (1990) reducing  $\tan\phi'$  by factor  $\gamma_\phi = 1.25$  (D.M. 14.01.2008). Table 5.9 reports the values of characteristic and design passive earth pressure coefficients,  $K_{PK}$  and  $K_{Pd}$ , respectively. Values of  $K_h$  and  $K_v$  used in computation are also listed in Table 5.9. These were obtained assuming the values of  $a_g$  specified in document GCG.F.04.01. Site effects were accounted for assuming a topographic amplification factor  $S_T = 1.2$  and a subsoil amplification factor  $S_S = 1.0$ ; a coefficient  $\beta_m = 0.31$  was used for computing  $K_h$  (D.M. 14.01.2008). Table 5.10 summarises the computed design values of passive resistance  $R_{Pd}$  developed in front of the block; for comparison the characteristic values of  $R_p$  are also given in the Table. Appendix B gives computation details. In the displacement based approach (section 5.1.2),  $R_p$  is assumed to increase progressively with the relative displacement  $u$  induced by the earthquake loading. To obtain the analytical relationship between  $R_p$  and  $u$ , plane strain FE analyses were carried out with reference to mechanisms 2 ( $\alpha = 26^\circ$ ) and 3 ( $\alpha = 8^\circ$ ) in which an ideal perfectly smooth wall, located in the position



		<b>Ponte sullo Stretto di Messina</b> <b>PROGETTO DEFINITIVO</b>		
Sicily Anchor Block – earthquake induced displacements and safety against ultimate limit states, Annex	<i>Codice documento</i> PF0064_F0_ANX	<i>Rev</i> F0	<i>Data</i> 20/06/2011	

corresponding to the front of the anchor block and extending to the depth of the sliding mechanism modelled in the analysis, was progressively displaced towards the soil. The assumption of smooth soil-wall interface and plane strain conditions are both conservative. For each value of the applied displacement,  $u$  ( $= 1 \text{ mm to } 1 \text{ m}$ ), the earth resistance  $\Delta R$  was calculated as the integral of the difference of the horizontal stresses acting on the wall for the given displacement and under geostatic conditions over the length of the wall. The relationship between  $\Delta R$  and  $u$  and the ultimate value of  $\Delta R$  were obtained by hyperbolic interpolation of the resulting data. The results obtained are summarised in Table 5.12 and Figure 5.11.

In the pseudo-static approach (section 5.6), safety against sliding was evaluated using eq.(6) with the prescriptions of D.M. 14.01.2008. The design resistances were computed considering the contributions of sliding resistance at the base and at the block sides and the passive resistance in front of the block; the active earth thrust behind the block was accounted for only along the vertical portion of the back wall. Design actions and resistances were computed using the pseudo-static seismic coefficients reported in Table 5.9. Table 5.13 gives the values of  $T$  provided by structural analyses of the tender design for each limit state. The characteristic value of  $\phi'_s$  mobilised on the sliding surface was assumed to be the angle of shearing resistance at constant volume; its value was estimated using the relationship proposed by Bolton (1986):  $\phi'_{sk} = \phi'_{cv} = \phi'_p - 3 D_R(10 - \ln p') + 3^\circ$ , that for  $\phi'_p = 40^\circ$ ,  $D_R = 50\%$  and  $p' = 200 \text{ kPa}$  provides  $\phi'_{sk} = \phi'_{cv} = 36^\circ$ . Table 5.15 reports the pseudostatic seismic coefficients, the active earth pressure coefficients and the active earth thrust used for computations. Table 5.16 a-b report the comparison between design resistances and design actions for the three sliding mechanisms assumed in the analyses: in all cases  $\Sigma R_d / \Sigma E_d > 1$  and safety against sliding is satisfied. Appendix C gives computation details.

The first step of the displacement based approach (section 5.7), is the selection of acceleration time histories (section 5.7.1). These were 22 real accelerograms from the PEER strong-motion database with magnitudes between 6.5 and 7.28, hypocentral distances between 12 and 82 km, and peak acceleration between 0.29 and 1.16 g, and 8 artificial strong motion accelerograms, fully compatible with the response spectrum of the preliminary design. Table 5.17 and 5.18 report the main parameters of their horizontal and vertical components, respectively. Each horizontal component was scaled to the design peak acceleration  $a_{max} = 0.58g$  and the corresponding vertical component was scaled by the same factor (Tables 5.19 and 5.20). The horizontal components of each event were independently considered and combined with the vertical component. The analyses were also repeated using the scaled horizontal component combined with the vertical

		<b>Ponte sullo Stretto di Messina</b> <b>PROGETTO DEFINITIVO</b>		
Sicily Anchor Block – earthquake induced displacements and safety against ultimate limit states, Annex	<i>Codice documento</i> PF0064_F0_ANX	<i>Rev</i> F0	<i>Data</i> 20/06/2011	

component scaled to 0.58g (Table 5.21). Figures 5.18–5.22 show the elastic response spectra of the selected accelerograms, compared to the design response spectrum.

The values of critical seismic coefficients (section 5.7.2) were evaluated for each limit state, considering the contribution of the base and the lateral sides of the block and a passive earth resistance in front of the block gradually increasing with block displacement. The values of  $K_c$ , computed using eq.(9) are listed in Table 5.22. The lowest values of  $K_c$  were obtained for the ULS condition and therefore the displacements were computed only for this condition.

The earthquake-induced displacements (section 5.7.3) were computed by numerical integration of equation (21) for mechanisms 2 and 3 only, as the pseudo-static analyses showed that mechanism 1 is the less critical and the FE analyses showed that the most likely sliding surface is between mechanisms 2 and 3. Each scaled horizontal component was combined with the corresponding vertical component, first scaled by the same factor and then scaled to 0.58g and the analyses repeated considering both directions of applications of the horizontal components. The maximum computed displacements are summarised in Table 5.23. The highest displacements were obtained for mechanism 3 ( $\alpha = 8^\circ$ ), when the vertical components are scaled to 0.58g. The results obtained for each accelerogram are summarised in Table 5.24 – 5.25. Appendix D reports time histories of acceleration, velocity and displacement obtained for each seismic input for sliding mechanism 3.

**Chapter 6** examines safety against sliding for the Sicily Anchor Block.

Safety against rotation was evaluated by imposing momentum equilibrium around point O belonging to the plane of motion (Figure 6.1). The load factors of the design actions are set equal to unity (seismic conditions § 7.11.1 - D.M. 14.01.2008). Safety against rotation is treated as an equilibrium limit state of rigid body (EQU) using the partial safety factor of group M2 and is ensured when the resistant moments are equal or larger than driving moments, as per eq.(28), in which:  $e_i$  is the distance of the line of action of each force from point O, factored values of the cable force T are introduced as provided by structural analyses of the tender design; the passive earth resistance  $R_{Pd}$  refers to mechanism 3, and the contribution of slide resistance  $T_{Ld}$  developed along the sides of the anchor block is neglected. Table 6.2 and 6.3 report the resistant and the driving actions. The ratio of the resisting actions and the driving actions is equal to 2.42. Hence the requirements of D.M. 14.01.2008 are fulfilled.

**Chapter 7** examines safety against bearing capacity failure for the Sicily Anchor Block.

		<b>Ponte sullo Stretto di Messina</b> <b>PROGETTO DEFINITIVO</b>		
Sicily Anchor Block – earthquake induced displacements and safety against ultimate limit states, Annex	<i>Codice documento</i> PF0064_F0_ANX	<i>Rev</i> F0	<i>Data</i> 20/06/2011	

Safety against bearing capacity failure was evaluated using Approach 1, Combination 2 (D.M. 14.01.2008). The loads considered for the evaluation of bearing capacity are the cable force  $T$ , the weight of the anchor block  $W$  and the horizontal and vertical components of the pseudostatic inertial force,  $K_h W$  and  $K_v W$ . The sliding resistance developed on the side walls of the anchor block the passive earth resistance were neglected. Both assumptions are conservative.

The bearing capacity was evaluated in terms of effective stress using appropriate correction factors to take into account the inclination of the applied load, the shape of the foundation, and the inclination of the foundation base, using Terzaghi's theory as from eq.(30). To account for the eccentricity of the load, the bearing capacity was computed for an equivalent rectangular foundation with reduced width  $B'$  and length  $L'$ . Design values of resistances and forces were obtained from the corresponding characteristic values and are those acting normally to the foundation plane. Safety against bearing capacity failure is ensured if  $R_d \geq E_d$ . The partial safety factors of the design actions are set equal to one:  $\gamma_G = \gamma_Q = 1$  (seismic conditions: § 7.11.1 - D.M. 14.01.2008). However, the cable forces used to compute the design components of the loads acting normally and tangentially to the foundation plane in eqs. (31) and (32) are inclusive of partial load factors, as provided by structural analyses of the tender design. Calculations were carried out with reference to the ULS loading condition. Tables 7.2 and 7.3 give the values of the design loads acting normally and tangentially to the foundation plane. The ratio of the design bearing resistance and the normal design load is equal to 3.2. Hence the requirements of D.M. 14.01.2008 are fulfilled.

**Chapter 8** summarises the contents of the report.

The seismic performance of the Sicily anchor block was evaluated using the pseudo-static approach, in which the anchor block is assumed to be in a state of limit equilibrium under the action of inertial and static forces, and the displacement-based approach, in which the earthquake-induced displacements of the anchor block are evaluated for a number of input seismic motions. Three possible sliding mechanisms were examined, characterised by angles of inclination  $\alpha = 38^\circ$ ,  $26^\circ$  and  $8^\circ$ . Companion plane strain FE analyses of the anchor block permitted to evaluate that the prevailing inclination of the displacement vectors is in the range  $8^\circ$ - $26^\circ$  so that the second and the third mechanisms were recognised to be the most likely to occur. As far as the pseudo-static conditions are concerned, both design actions and design resistances were computed using the pseudo-static seismic coefficients given by the Italian building code (D.M. 14.01.2008). The obtained results showed that safety against sliding is adequately satisfied for each of the loading

		<b>Ponte sullo Stretto di Messina</b> <b>PROGETTO DEFINITIVO</b>		
Sicily Anchor Block – earthquake induced displacements and safety against ultimate limit states, Annex	<i>Codice documento</i> PF0064_F0_ANX	<i>Rev</i> F0	<i>Data</i> 20/06/2011	

condition provided by structural analyses of the tender design. Earthquake-induced displacements were computed using 30 input accelerograms. The horizontal component of the selected acceleration time histories was scaled to 0.58 g, while the vertical component was scaled either by the same factor used for the corresponding horizontal component, or to 0.58 g as well. The earthquake-induced displacements decrease with increasing inclination of the sliding mechanism. The maximum displacement is equal to 1 mm for mechanism 2 ( $\alpha = 26^\circ$ ) and equal to 33 mm for mechanism 3 ( $\alpha = 8$ ). Finally, bearing capacity and safety against rotation were estimated following the prescriptions of D.M. 14.01.2008, the results showing that both the requirements are satisfied for the considered loading conditions.

#### **Appendix E and appendix F. Updated cable forces obtained from global IBDAS model version 3.3b and version 3.3f**

The forces transmitted by the main cables to the Sicilia Anchor Block have been re-evaluated using the global IBDAS model version 3.3b and version 3.3f. The worst load combinations were selected for each limit state (SILS, SLS2 and ULS) for both static and seismic conditions, using 6 different criteria (Table E.1 – Table E.2 for version 3.3b and Table F.1 – Table F.2 for version 3.3f). For both IBDAS model versions a low difference is observed between the tender design and the updated (IBDAS) cable forces, the ratio being in the range of 1.06 to 0.90 for version 3.3b (Table E.3) and in the range of 1.08 to 0.93 for version 3.3f (Table F.3); the higher value refers to the ULS load combination, while the lower is obtained for the SILS load combination. For the Ultimate Limit State (ULS) cable forces provided by the tender design are 5.8% higher than the corresponding IBDAS 3.3b values and are 8% higher than the corresponding IBDAS 3.3f values, this resulting in a conservative estimate of the behaviour of the Sicilia Anchor Block.

		<b>Ponte sullo Stretto di Messina</b> <b>PROGETTO DEFINITIVO</b>		
Sicily Anchor Block – earthquake induced displacements and safety against ultimate limit states, Annex	<i>Codice documento</i> PF0064_F0_ANX	<i>Rev</i> F0	<i>Data</i> 20/06/2011	

## 2 Soil profile and geotechnical characterisation

Figure 2.1 shows the soil profile on the Sicilian shore of the strait. Starting from ground level and moving downwards the following units are encountered:

- *Depositi Costieri* (Coastal Deposits). Sand and gravel with very little or no fine content; occasionally, silty peaty layers appear in the lower part of the formation. The thickness of this formation is difficult to evaluate as it rests on the very similar formation of the *Ghiaie di Messina*.
- *Ghiaie di Messina* (Messina Gravel)/*Sedimenti dei terrazzi* (Terrace Deposits). Gravel and sand, with very occasional silty layers. The thickness of this formation can reach more than 170 m.
- *Depositi Continentali* (Continental Deposits)/*Calcarenite di Vinco* (Vinco Calcarenite). Clayey-sandy deposit, consisting of layers of silt or silt and sand, with significant gravel content/Bio-calcarenite and fossiliferous calcarenite, with thin silty layers.
- *Conglomerato di Pezzo* (Pezzo Conglomerate). Soft rock, consisting of clasts of different dimensions in a silty-sandy matrix and sandstone. The thickness of this formation is larger than 200 m.
- *Cristallino* (Crystalline bedrock). Tectonised granite.



A plan view at the site of the Sicily Anchor Block is shown in Figure 2.2 together with the location of the available site investigations. The actual level of the ground is in between 22 m a.s.l. and 59 a.s.l. and the groundwater level coincides with the sea level, at 0 m a.s.l.

The three longitudinal sections and the cross section indicated in Figure 2.2 are shown in Figure 2.3 – 2.6. The sections in the figures show that the Messina Gravel/Terrace Deposits unit extends from the ground level over a thickness of about 200m. Hence it is the only geological units of relevance.

The permeability of the deposits was evaluated by pumping tests carried out from a well located in the area of the Sicilian Tower, extending 40 m b.g.l., and by Lefranc permeability tests carried out in a borehole at depths between 10 m b.g.l. and 38 m b.g.l..

The results of pumping tests show a value of the horizontal permeability  $k_h$  of  $5 \times 10^{-3}$  m/s.

Lefranc permeability tests have a more local character than well pumping tests and are affected by the disturbance created by borehole formation; moreover their interpretation depends on the assumed ratio  $k_h/k_v$ . Their results must therefore be considered reliable within one order of

		<b>Ponte sullo Stretto di Messina</b> <b>PROGETTO DEFINITIVO</b>		
Sicily Anchor Block – earthquake induced displacements and safety against ultimate limit states, Annex	<i>Codice documento</i> PF0064_F0_ANX	<i>Rev</i> F0	<i>Data</i> 20/06/2011	

magnitude. The values of  $k_v$  obtained for  $k_h/k_v = 10$  range from  $2 \times 10^{-3}$  to  $5 \times 10^{-2}$  (m/s); for  $k_v/k_h = 1$ ,  $k_v$  ranges from  $2.6 \times 10^{-4}$  to  $5.8 \times 10^{-3}$  (m/s) being in a fair agreement with the values obtained by the well pumping test.

In the area of the Sicily Anchor Block erosion phenomena for the Messina Gravel are less important than in the site of Sicily Tower, so that deviation of  $K_0$  from its normally consolidated value is mainly due to ageing effects:

$$\frac{K_0}{K_0(\text{NC})} = \left( \frac{t}{t_p} \right)^{C_{\alpha e}/C_c}$$

in which  $t$  is the time elapsed from the deposition of the Messina Gravel, between  $4 \times 10^5$  and  $6 \times 10^5$  years,  $t_p$  is the end of primary consolidation time, about  $10^{-2}$  year,  $C_{\alpha e}$  is the secondary compression coefficient, and  $C_c$  is the compression index. For granular soils typical values of the ratio  $C_{\alpha e}/C_c$  are about 0.02 (Mesri, 1989) and therefore the maximum estimated increase of  $K_0$  due to ageing effects is of the order of 42%.

It follows:

$$K_0 = 1.42 \times K_0(\text{NC}) = 1.42 \times (1 - \sin \varphi'_p) = 0.47$$

in which  $\varphi'_p = 42^\circ$  as described ahead.

The relative density of the Messina Gravel was estimated from the SPT and LPT results using the procedure proposed by Cubrinovski and Ishihara (1999): values of  $D_R = 40\%$  to  $60\%$  were obtained as shown in Figure 2.7. The angle of shearing resistance at peak  $\varphi'_p = 41^\circ - 44^\circ$  was then evaluated through the relationship proposed by Schmertmann (1975) (Figure 2.7).

The constant-volume friction angle was evaluated following Bolton (1986):

$$\varphi'_{cv} = \varphi'_p - 3 D_R (10 - \ln p') + 3^\circ$$

That, for  $\varphi'_p = 40^\circ$ ,  $D_R = 50\%$  and  $p' = 200$  kPa, provides  $\varphi'_{cv} = 36^\circ$ .

The stiffness profile of Messina gravel was obtained from two cross-hole tests carried out in the vicinity of the Sicily Anchor Block, down to a depth of 100 m b.g.l. The results of the cross-hole tests in terms of shear wave velocity,  $V_s$ , versus depth are given in Figure 2.8. The same results are shown in the figure as profiles of small strain shear modulus,  $G_0$ :

$$G_0 = \rho V_s^2$$



		<b>Ponte sullo Stretto di Messina</b> <b>PROGETTO DEFINITIVO</b>		
Sicily Anchor Block – earthquake induced displacements and safety against ultimate limit states, Annex	<i>Codice documento</i> PF0064_F0_ANX	<i>Rev</i> F0	<i>Data</i> 20/06/2011	

$G_0$  increases from about 50-100 MPa at the ground level to about 400 MPa at a depth of 80 m b.g.l.; below this depth the data are more dispersed with an average higher value of 450 MPa.

Table 2.1 summarises the main mechanical parameters obtained from the geotechnical characterization above.

Table 2.1. Summary of main mechanical parameters from geotechnical characterization

	depth (m bgl)	$K_0$	$\varphi'_p$ (°)	$\varphi'_{cv}$ (°)	$K_h$ (m/s)	$G_0$ (MPa)
Messina Gravel	0-20	0.43	44	35	$5 \times 10^{-3}$	50-150
Messina Gravel	20-80	0.47	42	37	$5 \times 10^{-3}$	150-400
Messina Gravel	>80	0.47	42	37	$5 \times 10^{-3}$	450

		<b>Ponte sullo Stretto di Messina</b> <b>PROGETTO DEFINITIVO</b>		
Sicily Anchor Block – earthquake induced displacements and safety against ultimate limit states, Annex	<i>Codice documento</i> PF0064_F0_ANX	<i>Rev</i> F0	<i>Data</i> 20/06/2011	

### 3 Constitutive soil model and soil parameters

In the FE analyses discussed in the following sections, the mechanical behaviour of the soil was described using the constitutive model Hardening Soil available in the model library of the code Plaxis. The model is capable of reproducing soil non-linearity due to the occurrence of plastic strains from the early beginning of a loading process. The computed non linear stress-strain relationship has tangent initial modulus equal to  $E'_0$ ; upon unloading, the model assumes elastic behaviour with Young's modulus  $E'_0$ , thus reproducing a significant change in stiffness. In the model, soil stiffness depends on the effective stress state.

Hardening soil model is an elastic-plastic rate independent model with isotropic hardening. The elastic behaviour is defined by isotropic elasticity through a stress-dependent Young's modulus:

$$E' = E^{\text{ref}} \left( \frac{c' \cdot \cot \varphi' + \sigma_3'}{c' \cdot \cot \varphi' + p^{\text{ref}}} \right)^m$$

where  $\sigma_3'$  is the minimum principal effective stress,  $c'$  is the cohesion,  $\varphi'$  is the angle of shearing resistance,  $p^{\text{ref}} = 100$  kPa is a reference pressure;  $E^{\text{ref}}$  and  $m$  are model parameters.

The model has two yield surfaces  $f_s$  and  $f_v$  with independent isotropic hardening depending on distortional plastic strain  $\gamma^p = (2 \cdot \varepsilon_1^p - \varepsilon_v^p)$  and on volumetric plastic strains  $\varepsilon_v^p$ , respectively; the two surfaces have the following equations:



$$f_s = \frac{1}{E'_{50}} \frac{q}{(1 - 0.9 \cdot q/q_f)} - \frac{2q}{E'} - \gamma^p = 0$$

$$f_v = \frac{\tilde{q}^2}{\alpha^2} + p'^2 - p_c'^2 = 0$$

Parameter  $E'_{50}$  is given by an expression similar to  $E'$ , but, in contrast to it, it is not used within a concept of elasticity. Hardening of the  $f_s$  surface is isotropic and depends on the plastic distortional strain  $\gamma^p = (2 \cdot \varepsilon_1^p - \varepsilon_v^p)$ .

In the equations above,  $p'$  is the mean effective stress;  $\tilde{q}$  is a generalised deviator stress, that accounts for the dependence of strength on the intermediate principal effective stress  $\sigma_2'$ ;  $\alpha$  controls the shape of the  $f_v$  surface in the  $\tilde{q} - p'$  plane and can be related to the coefficient of earth pressure at rest  $K_0$  for normally consolidated states. The hardening parameter  $p'_c$  is the size of the current  $f_v$  surface and is related to the plastic volumetric strains  $\varepsilon_v^p$  through the hardening law, written in the incremental form as:



		<b>Ponte sullo Stretto di Messina</b> <b>PROGETTO DEFINITIVO</b>		
Sicily Anchor Block – earthquake induced displacements and safety against ultimate limit states, Annex	<i>Codice documento</i> PF0064_F0_ANX	<i>Rev</i> F0	<i>Data</i> 20/06/2011	

$$d\varepsilon_V^p = \frac{\beta}{p_{ref}} \left( \frac{p'_c}{p_{ref}} \right)^m \cdot dp'_c$$

where  $\beta$  is a parameter that controls the variation of  $p'_c$  with the plastic volumetric strains. In the model formulation implemented in Plaxis, the parameter  $E'_{oed}$ , which is related to  $\beta$ , has to be specified. This is the constrained modulus for one-dimensional plastic loading, and depends on the maximum principal effective stress  $\sigma'_1$  through the relationship:

$$E'_{oed} = E'_{oed,ref} \cdot \left( \frac{c' \cdot \cot \varphi' + \sigma'_1}{c' \cdot \cot \varphi' + p_{ref}} \right)^m$$

where  $\sigma'_1$  is the maximum principal effective stress.

The initial value of the hardening parameter  $p'_c$  is related to the one-dimensional vertical yield stress, and can therefore be specified by assigning a value for the overconsolidation ratio OCR. It is worth mentioning that OCR has to be regarded as a yield stress ratio (YSR) defined in the framework of strain hardening plasticity, so that values of  $OCR > 1$  can be specified also for geologically normally consolidated soil deposits exhibiting a yield stress larger than the in situ stress.

The flow rule is associated for states lying on the surface  $f_v$ , while a non associated flow rule is used for states on the surface  $f_s$ . The latter is derived from the theory of stress dilatancy by Rowe (1962): the mobilised dilatancy angle  $\psi_m$  depends on the current stress state through the angle of mobilised friction  $\varphi'_m$  and the angle of friction at constant volume  $\varphi'_{cv}$ :



$$\sin \psi_m = \frac{\sin \varphi'_m - \sin \varphi'_{cv}}{1 - \sin \varphi'_m \sin \varphi'_{cv}}$$

In turn,  $\varphi'_{cv}$  can be obtained from the angle of shearing resistance  $\varphi'$  and the angle of dilatancy  $\psi$  at failure:

$$\sin \varphi'_{cv} = \frac{\sin \varphi' - \sin \psi}{1 - \sin \varphi' \sin \psi}$$

Figure 3.1 shows the shape of the yield surfaces  $f_v$  and  $f_s$  and schematically indicates their evolution.

For plastic loading from isotropic stress states, the model predicts a non linear stress-strain relationship with tangent initial modulus equal to  $E'$ . Therefore, values of  $E'$  were related to the shear modulus at small-strain  $G_0$  obtained from the cross-hole tests carried out at the site. In

		<b>Ponte sullo Stretto di Messina</b> <b>PROGETTO DEFINITIVO</b>		
Sicily Anchor Block – earthquake induced displacements and safety against ultimate limit states, Annex	<i>Codice documento</i> PF0064_F0_ANX	<i>Rev</i> F0	<i>Data</i> 20/06/2011	

particular, values of  $E'^{ref}$  and  $m$  were obtained by best fitting the cross-hole test results using the equation given above for  $E'$  and assuming  $\nu' = 0.2$ .

Figure 3.2 shows the profile of  $G_0$  against depth b.g.l.. The continuous line in the figure represents the prediction of  $G_0$  obtained with the values of  $c'$ ,  $\phi'$ ,  $E'^{ref}$  and  $m$  reported in Table 3.1. Specifically, the values of  $\sigma'_3$  were obtained using the values of  $K_0$  given in Table 3.1. For the Messina Gravel, a non zero value of cohesion was introduced in the FE analyses to simulate non zero values of stiffness at shallow depths; this low value of cohesion does not significantly affect the behaviour of the layer in terms of strength.



Table 3.1. Best fitting of cross hole test results

Soil	$\gamma$ (kN/m <sup>3</sup> )	$c'$ (kPa)	$\phi'$ (°)	$K_0$	$E'^{ref}$ (kPa)	$m$
Messina gravel (z<80 m)	20	20	42	0.47	$4.08 \cdot 10^5$	0.6
Messina gravel (z>80 m)	20	20	42	0.47	$1.08 \cdot 10^6$	0.1

The soil parameters assumed in the FE analyses discussed in the following are reported in Table 3.2. Stiffness decay with shear strain was described using ratios of  $E'^{ref} / E'_{50}^{ref} = 20$  and of  $E'_{50}^{ref} / E'_{oed}^{ref} = 1.0$  and a value for the angle of dilatancy at failure  $\psi = 0$ .

Table 3.2. Hardening soil parameters for FE analyses of the anchor block

Soil	$\gamma$ (kN/m <sup>3</sup> )	$c'$ (kPa)	$\phi'$ (°)	$K_0$	YSR	$E'^{ref}$ (kPa)	$m$	$E'_{50}^{ref}$ (kPa)	$E'_{oed}^{ref}$ (kPa)
Messina gravel (z<80 m)	20.0	20.0	42	0.47	2.0	$4.08 \cdot 10^5$	0.6	$2.04 \cdot 10^4$	$2.04 \cdot 10^4$
Messina gravel (z>80 m)	20.0	20.0	42	0.47	2.0	$1.08 \cdot 10^6$	0.1	$5.40 \cdot 10^4$	$5.40 \cdot 10^4$

		<b>Ponte sullo Stretto di Messina</b> <b>PROGETTO DEFINITIVO</b>		
Sicily Anchor Block – earthquake induced displacements and safety against ultimate limit states, Annex	<i>Codice documento</i> PF0064_F0_ANX	<i>Rev</i> F0	<i>Data</i> 20/06/2011	

## 4 Anchor Blocks – Safety against sliding

### 4.1 Static conditions – governing equations

#### 4.1.1 Global safety factor

The global factor of safety against sliding can be written as:

$$F = \frac{[W' \cos \alpha + T \sin(\alpha - i)] \tan \varphi'_s + T_L + R_p \cos(\alpha - \delta)}{T \cos(\alpha - i) - W' \sin \alpha + S_a \cos \alpha} \quad (1)$$

where (Figure 4.1):

- $W'$  = submerged weight of the anchor block
- $T$  = force transmitted by the cables
- $\alpha$  = inclination of the sliding surface
- $i$  = inclination of the forces transmitted by the cables
- $\varphi'_s$  = angle of shearing resistance on the sliding surface
- $T_L$  = sliding resistance developed on the lateral sides of the block
- $R_p$  = passive earth resistance developed in the front of the block
- $S_a$  = active earth thrust developed behind the block (computed assuming  $\delta = 0$ )
- $\delta$  = friction angle at the soil-concrete interface

The safety factor against sliding becomes  $F = \infty$  if  $T \cos(\alpha - i) = W' \sin \alpha - S_a \cos \alpha$ . Values of  $F < 0$  are meaningless; in these cases only part of the block weight acts on the sliding surfaces and  $F = \infty$  can be assumed.

#### 4.1.2 Partial safety factors



In D.M. 14.01.2008 – “Nuove norme tecniche per le costruzioni”, partial safety factors are applied to actions, resistances and strength parameters. Once the design values of the actions  $E_d$  and the resistance  $R_d$  are computed, condition  $R_d \geq E_d$  must be satisfied.

For the case at hand the characteristic actions and the characteristic resistance are defined as:

$$E_k = T_k \cos(\alpha - i) - W'_k \sin \alpha + S_{ak} \cos \alpha$$

$$R_k = [W'_k \cos \alpha + T_k \sin(\alpha - i)] \tan \varphi'_s + T_{Lk} + R_{Pk} \cos(\alpha - \delta) \quad (2)$$

In section 2.6.1 of D.M. 14.01.2008 two alternative approaches are defined: the Approach 1 and the Approach 2. In Approach 1, two combinations of partial safety factors are used, in which the design actions are multiplied by factors of group A, the strength parameters are divided by factors of group M and the global resistance of the system is divided by factors of group R. Combination 1

		<b>Ponte sullo Stretto di Messina</b> <b>PROGETTO DEFINITIVO</b>		
Sicily Anchor Block – earthquake induced displacements and safety against ultimate limit states, Annex	<i>Codice documento</i> PF0064_F0_ANX	<i>Rev</i> F0	<i>Data</i> 20/06/2011	

(C1), named STR, is used for limit state verifications of structural components, while Combination 2 (C2), named GEO, is used to study limit states that involve collapse mechanisms of the soil interacting with the structure. Specifically, the actions are mainly amplified in combination 1, while the soil resistances are mainly reduced in combination 2.

In Approach 2, a single combination of partial safety factors is defined.

Following Approach 1, Combination 2 to study geotechnical (GEO) limit states, it is:

$$\begin{aligned}
 E_d &= T_d \cos(\alpha - i) - \gamma_{G1} \cdot W'_k \sin \alpha + \gamma_{G1} \cdot S_{ad} \cos \alpha \\
 R_d &= \frac{1}{\gamma_R} \left\{ \left[ \gamma_{G1} \cdot W'_k \cos \alpha + T_d \sin(\alpha - i) \right] \frac{\tan \varphi'_{sk}}{\gamma_\varphi} + \gamma_{G1} \cdot T_{Ld} + \gamma_{G1} \cdot R_{Pd} \cos(\alpha - \delta) \right\} \quad (3)
 \end{aligned}$$

where  $\gamma_\varphi = 1.25$  and  $\gamma_R = 1.1$

In equation (3):

- the shear resistance on the lateral sides of the block, the passive earth resistance in front of the block and the active earth thrust are computed using reduced values of the angle of shearing resistance acting on the sliding surface  $\varphi'_{sd} = \arctan [(\tan \varphi'_{sk})/\gamma_\varphi]$ ;
- the cable forces are inclusive of partial load factors, as provided by structural analyses of the tender design for each limit state and therefore are not factored;
- according to D.M. 14.01.2010, the weight of the anchor block (permanent load), present in both the action  $E_d$  and the resistance  $R_d$ , is multiplied by the same load factor  $\gamma_{G1} = 1$ , irrespective of its effect;
- components of  $S_a$  and  $R_p$  normal to the sliding surface are neglected.



Safety against sliding under static loading conditions will not be evaluated in the following since the pseudo-static loading conditions are the most critical.

## 4.2 Seismic conditions – governing equations

Analysis of the anchor blocks under seismic conditions is carried out using the force-based pseudo-static approach and the displacement-based sliding block approach.

### 4.2.1 Pseudo-static approach

In the pseudo-static approach, the anchor block is assumed to behave as a rigid block and to be in a state of equilibrium under the action of inertial and static forces. The stability of the block is measured either by a global factor of safety  $F$  that is the ratio of the total resisting force to the total driving force, or by a comparison of the design action with the design resistance, both including the effect of partial safety factors.

		<b>Ponte sullo Stretto di Messina</b> <b>PROGETTO DEFINITIVO</b>		
Sicily Anchor Block – earthquake induced displacements and safety against ultimate limit states, Annex		<i>Codice documento</i> PF0064_F0_ANX	<i>Rev</i> F0	<i>Data</i> 20/06/2011

#### 4.2.1.1 Global safety factor

The global factor of safety against sliding can be written as:

$$F = \frac{[W' \cos \alpha + T \sin(\alpha - i) + W(K_h \sin \alpha \pm K_v \cos \alpha)] \tan \varphi'_s + T_L + R_{pE} \cos(\alpha - \delta)}{T \cos(\alpha - i) - W' \sin \alpha + S_{aE} \cos \alpha + W(K_h \cos \alpha \pm K_v \sin \alpha)} \quad (4)$$

where (Figure 4.2):

- $W'$  = submerged weight of the anchor block
- $W$  = weight of the anchor block
- $T$  = force transmitted by the cables
- $\alpha$  = inclination of the sliding surface
- $i$  = inclination of the forces transmitted by the cables
- $\varphi'_s$  = angle of shearing resistance on the sliding surface
- $T_L$  = sliding resistance developed on the lateral sides of the block
- $R_{pE}$  = pseudostatic passive earth resistance developed on the front of the block
- $S_{aE}$  = pseudostatic active earth thrust developed behind the block
- $\delta$  = friction angle at the soil-concrete interface
- $K_h$  = horizontal seismic coefficient
- $K_v$  = vertical seismic coefficient

#### 4.2.1.2 Partial safety factors



In D.M. 14.01.2008 – “Nuove Norme Tecniche per le Costruzioni”, partial safety factors are applied to actions, resistances and strength parameters. However, under seismic condition the load factors of the design actions are set equal to unity:  $\gamma_G = \gamma_Q = 1$  (§ 7.11.1 - D.M. 14.01.2008); accordingly these factors are omitted in the following.

Once the design values of the actions  $E_d$  and the resistance  $R_d$  are computed, condition  $R_d \geq E_d$  must be satisfied.

For the case at hand the characteristic actions and the characteristic resistance are defined as:

$$\begin{aligned} E_k &= T_k \cos(\alpha - i) - W'_k \sin \alpha + S_{aE(k)} \cos \alpha + W_k (K_h \cos \alpha \pm K_v \sin \alpha) \\ R_k &= [W'_k \cos \alpha + T_k \sin(\alpha - i) + W_k (K_h \sin \alpha \pm K_v \cos \alpha)] \tan \varphi'_s + T_{Lk} + R_{pE(k)} \cos(\alpha - \delta) \end{aligned} \quad (5)$$

Following, as above, the Approach 1, Combination 2, it can be written:

		<b>Ponte sullo Stretto di Messina</b> <b>PROGETTO DEFINITIVO</b>		
Sicily Anchor Block – earthquake induced displacements and safety against ultimate limit states, Annex		<i>Codice documento</i> PF0064_F0_ANX	<i>Rev</i> F0	<i>Data</i> 20/06/2011

$$E_d = T_d \cos(\alpha - i) - W'_k \sin \alpha + S_{aE(d)} \cos \alpha + W_k (K_h \cos \alpha \pm K_v \sin \alpha)$$

$$R_d = \frac{1}{\gamma_R} \left\{ [W'_k \cos \alpha + T_d \sin(\alpha - i) + W_k (K_h \sin \alpha \pm K_v \cos \alpha)] \frac{\tan \phi'_s}{\gamma_\phi} + T_{Ld} + R_{pE(d)} \cos(\alpha - \delta) \right\} \quad (6)$$

with  $\gamma_\phi = 1.25$  and  $\gamma_R = 1.1$



In equation (6):

- the shear resistance on the lateral sides of the block, the passive earth resistance in front of the block and the active earth thrust behind the block are computed using reduced values of the angle of shearing resistance acting on the sliding surface  $\phi'_{sd} = \text{atan} [(\tan \phi'_{sk})/\gamma_\phi]$ ;
- the cable forces are inclusive of partial load factors, as provided by the structural analyses of the tender design for each limit state;
- components of  $S_{aE}$  and  $R_{pE}$  normal to the sliding surface are neglected.

#### 4.2.2 Displacement-based approach

In the displacement-based approach, the safety of the anchor block is evaluated by comparing the permanent displacement developed during the earthquake with a threshold value. The earthquake-induced displacement of the potential sliding mass is determined following a two step procedure: first, the critical acceleration is determined by the pseudo-static approach; then, the cumulative displacement of the potential sliding mass is evaluated using the sliding block analysis. In the analysis, the potential sliding mass is treated as a rigid body and permanent displacements take place whenever the ground acceleration exceeds the critical acceleration. For a given earthquake, the permanent displacement is calculated by integrating twice the acceleration time history with the critical acceleration used as the reference datum; more specifically, numerical integration is extended to the time intervals in which the velocity of the sliding mass relative to the ground is positive.

According to section C.7.11 of Circolare No.617 dated 02.02.09 (Istruzioni per l'applicazione delle "Nuove norme tecniche per le costruzioni" di cui al D.M. 14.01.08), the critical acceleration must be evaluated using the characteristic values of the strength parameters  $c'_k$  and  $\phi'_k$ . Recalling that under seismic conditions the load factor are equal to unity, in the following suffix k and coefficients  $\gamma_G$  and  $\gamma_Q$  are omitted for simplicity.

		<b>Ponte sullo Stretto di Messina</b> <b>PROGETTO DEFINITIVO</b>		
Sicily Anchor Block – earthquake induced displacements and safety against ultimate limit states, Annex		<i>Codice documento</i> PF0064_F0_ANX	<i>Rev</i> F0	<i>Data</i> 20/06/2011

#### 4.2.2.1 Critical seismic coefficient

The pseudo-static seismic action is assumed to act with an angle  $(\alpha-\theta)$  with respect to the sliding surface (Figure 4.3). Assuming conditions of limit equilibrium ( $F = 1$ ) and neglecting at this stage the contributions of passive and active earth thrusts, the following expression for  $K$  is obtained:

$$F = \frac{[W' \cos \alpha + T \sin(\alpha - i) + KW \sin(\alpha - \theta)] \tan \varphi'_s + T_L}{T \cos(\alpha - i) - W' \sin \alpha + KW \cos(\alpha - \theta)} = 1 \quad (7)$$

$$K = \frac{[W' \cos \alpha + T \sin(\alpha - i)] \tan \varphi'_s - T \cos(\alpha - i) + W' \sin \alpha + T_L}{W [\cos(\alpha - \theta) - \sin(\alpha - \theta) \tan \varphi'_s]} \quad (8)$$

The minimum value of  $K$ , that is the critical seismic coefficient  $K_c$ , is obtained for  $\theta = \alpha + \varphi'_s \Rightarrow \alpha - \theta = -\varphi'_s$  (Figure 4.3):

$$K_{c(\text{red})} = \frac{[W' \cos \alpha + T \sin(\alpha - i)] \tan \varphi'_s - T \cos(\alpha - i) + W' \sin \alpha + T_L}{W [\cos(-\varphi'_s) - \sin(-\varphi'_s) \tan \varphi'_s]} \quad (9)$$

During sliding ( $K > K_c$ ), it can be assumed that a net earth thrust  $\Delta R$ , obtained as the difference between the normal stresses acting in front and behind the anchor block increases gradually with increasing block displacements. Therefore, the effect of  $\Delta R$  is explicitly included in the equation of relative motion used for computing the earthquake-induced displacement of the anchor block.

$\Delta R$  is a function of the relative displacement cumulated during the earthquake loading:

$$\Delta R(u) = k_d(u) \cdot u(t) \quad (10)$$

where  $k_d$  is a non linear spring stiffness, depending on relative displacement  $u$  (Figure 4.4).

#### 4.2.2.2 Equation of relative motion under seismic conditions

The equation of relative motion of the anchor block can be written in its simplest form as:

$$m\ddot{u}(t) = [E_d(K) - E_d(K_{c(\text{red})})] - [R_d(K) - R_d(K_{c(\text{red})})] \quad (11)$$



where

$$[E_d(K) - E_d(K_{c(\text{red})})] = \text{net driving action relative to limit equilibrium conditions}$$

$$[R_d(K) - R_d(K_{c(\text{red})})] = \text{net resisting force relative to limit equilibrium conditions}$$

Since it is:

$$\begin{aligned} E_d(K) &= [T \cos(\alpha - i) - W' \sin \alpha + K(t)W \cos(\alpha - \theta)] \\ E_d(K_{c(\text{red})}) &= [T \cos(\alpha - i) - W' \sin \alpha + K_{c(\text{red})}W \cos(\alpha - \theta)] \end{aligned} \quad (12)$$

		<b>Ponte sullo Stretto di Messina</b> <b>PROGETTO DEFINITIVO</b>		
Sicily Anchor Block – earthquake induced displacements and safety against ultimate limit states, Annex		<i>Codice documento</i> PF0064_F0_ANX	<i>Rev</i> F0	<i>Data</i> 20/06/2011

and

$$\begin{aligned}
 [R_d(K)] &= [W' \cos \alpha + T \sin(\alpha - i) + K(t) W \sin(\alpha - \theta)] \tan \varphi'_s + T_L \\
 [R_d(K_{c(\text{red})})] &= [W' \cos \alpha + T \sin(\alpha - i) + K_{c(\text{red})} W \sin(\alpha - \theta)] \tan \varphi'_s + T_L + \Delta R(u)
 \end{aligned} \quad (13)$$

it can be obtained:

$$\begin{aligned}
 [E_d(K) - E_d(K_{c(\text{red})})] &= [K(t) - K_{c(\text{red})}] \cdot W \cos(\alpha - \theta) \\
 [R_d(K) - R_d(K_{c(\text{red})})] &= [K(t) - K_{c(\text{red})}] \cdot W \sin(\alpha - \theta) \tan \varphi'_s + \Delta R(u)
 \end{aligned} \quad (14)$$

and

$$\frac{W}{g} \ddot{u}(t) = [K(t) - K_{c(\text{red})}] \cdot W \frac{\cos(\alpha - \theta + \varphi'_s)}{\cos \varphi'_s} - k_d(u) \cdot u(t) \quad (15)$$

that, for  $\theta = \alpha + \varphi'_s \Rightarrow \alpha - \theta = -\varphi'_s$ , provides:

$$\ddot{u}(t) + g \frac{k_d(u)}{W} \cdot u(t) = g [K(t) - K_{c(\text{red})}] \frac{1}{\cos \varphi'_s} \quad (16)$$

Finally, separating the horizontal and vertical components of the acceleration time histories, it can be written:

$$\begin{aligned}
 E_d(K) &= [T \cos(\alpha - i) - W' \sin \alpha + W(K_h \cos \alpha + K_v \sin \alpha)] \\
 E_d(K_{c(\text{red})}) &= [T \cos(\alpha - i) - W' \sin \alpha + K_{c(\text{red})} W \cos(\alpha - \theta)]
 \end{aligned} \quad (17)$$

$$\begin{aligned}
 [R_d(K)] &= [W' \cos \alpha + T \sin(\alpha - i) + W(K_h \sin \alpha - K_v \cos \alpha)] \tan \varphi'_s + T_L \\
 [R_d(K_{c(\text{red})})] &= [W' \cos \alpha + T \sin(\alpha - i) + K_{c(\text{red})} W \sin(\alpha - \theta)] \tan \varphi'_s + T_L + \Delta R(u)
 \end{aligned} \quad (18)$$

the net driving action and resisting force being:

$$\begin{aligned}
 [E_d(K) - E_d(K_{c(\text{red})})] &= W [K_h \cos \alpha + K_v \sin \alpha - K_{c(\text{red})} \cos(\alpha - \theta)] \\
 [R_d(K) - R_d(K_{c(\text{red})})] &= W [K_h \sin \alpha - K_v \cos \alpha - K_{c(\text{red})} \sin(\alpha - \theta)] \tan \varphi'_s + \Delta R(u)
 \end{aligned} \quad (19)$$

so that the equation of relative motion is:

$$\frac{W}{g} \ddot{u}(t) = W \{ K_h (\cos \alpha - \sin \alpha \tan \varphi'_s) + K_v (\sin \alpha + \cos \alpha \tan \varphi'_s) - K_{c(\text{red})} [\cos(\alpha - \theta) - \sin(\alpha - \theta) \tan \varphi'_s] \} + k_d \cdot u(t) \quad (20)$$

that, for  $\theta = \alpha + \varphi'_s \Rightarrow \alpha - \theta = -\varphi'_s$ , provides:

$$\ddot{u}(t) + g \frac{k_d(u)}{W} u(t) = g \left\{ [K_h(t) + K_v(t) \tan(\alpha + \varphi'_s)] \cos(\alpha + \varphi'_s) - K_{c(\text{red})} \right\} \frac{1}{\cos \varphi'_s} \quad (21)$$



		<b>Ponte sullo Stretto di Messina</b> <b>PROGETTO DEFINITIVO</b>		
Sicily Anchor Block – earthquake induced displacements and safety against ultimate limit states, Annex	<i>Codice documento</i> PF0064_F0_ANX	<i>Rev</i> F0	<i>Data</i> 20/06/2011	

## 5 Sicily Anchor Block – safety against sliding

### 5.1 Self weight of the anchor block

Figure 5.1 shows a plan view and a section of the Sicily anchor block. The weight of the anchor block was calculated using a Cad scheme based on drawings from the tender design (Figure 5.2). The original design includes the presence of two chambers filled with granular material. Since the ground water level is located slightly below the anchor block ( $H_w = 0$  m a.s.l.), the resulting pore water pressure force is equal to zero. Relevant data are listed in Tables 5.1.

Table 5.1. Weight of Sicily anchor block



	volume (m <sup>3</sup> )	$\gamma$ (kN/m <sup>3</sup> )	weight (MN)
concrete	282588	24	6782
fill chambers (x2)	36004	20	720
pore water pressure resulting force	0	10	0
<b>Total</b>			<b>7502</b>

### 5.2 Sliding mechanisms

Three possible sliding mechanisms have been considered in the analyses (Figure 5.3), characterised by angles of inclination  $\alpha = 38^\circ$ ,  $26^\circ$  and  $8^\circ$ , as reported in Table 5.2; all the mechanisms develop within the soil. In the first mechanism it is assumed that the diaphragm wall in front of the block collapses and the sliding surface trespass it; in the second one, the sliding plane is assumed to develop under the diaphragm tip; in the third mechanism, sliding is assumed to occur at the lowest inclination of the block base. The contribution of soil between the sliding surface and the anchor is considered as an added weight, as it is assumed to move together with the anchor block.

Table 5.2: sliding mechanisms of Sicily anchor block

	inclination (°)	anchor block weight (MN)	soil weight (MN)	total weight (MN)
mechanism 1	38	7502.0	346.8	7848.8
mechanism 2	26	7502.0	658.0	8160.0
mechanism 3	8	7502.0	1036.7	8538.7

		<b>Ponte sullo Stretto di Messina</b> <b>PROGETTO DEFINITIVO</b>		
Sicily Anchor Block – earthquake induced displacements and safety against ultimate limit states, Annex	<i>Codice documento</i> PF0064_F0_ANX	<i>Rev</i> F0	<i>Data</i> 20/06/2011	

It can be anticipated that companion FE analyses carried under plane strain conditions indicate that, under ULS loading conditions, the prevailing inclination of the displacement vectors is of 14°, in between 8° and 26° so that the second and the third mechanisms are the most likely to occur.

### 5.3 Evaluation of the sliding surface

In order to estimate the most likely sliding mechanism, plane strain FE analyses were carried out using the code Plaxis 8. Figure 5.4 show the adopted mesh, made of 1617 15-node triangular elements with fourth order interpolation for displacements and third order interpolation for pore water pressure. The mesh is 800 m wide, its height ranging from 167.1 m to 264.15 m. At the lower boundary displacements are restrained both in vertical and horizontal direction, while at the side boundaries only horizontal displacements are restrained.

The geometry of the anchor block is based on the drawings provided in the tender design.

Soil-anchor block contact is modelled through interface elements with reduced shear strength and stiffness.

As illustrated in section 2, soil behaviour was described using the constitutive model Hardening Soil available in the model library of the code Plaxis. It is an elastic-plastic rate independent model with isotropic hardening and Mohr-Coulomb failure criterion.

The cross-hole test carried out at the site was used to evaluate the shear modulus at small strains  $G_0$ . Stiffness decay with shear strain was described using ratios of  $E^{ref} / E'_{50}{}^{ref} = 20$  and of  $E'_{50}{}^{ref} / E'_{oed}{}^{ref} = 1.0$  and a value for the angle of dilatancy at failure  $\psi = 0$ . Soil parameters adopted in the analyses are those listed in Table 3.2 (see section 2).

An elastic-plastic model was used to describe the mechanical behaviour of interface elements. The strength and stiffness parameters were reduced by applying the following rules:



$$\begin{aligned}
 \tan \phi'_{int} &= R_{int} \tan \phi'_{soil} \\
 c'_{int} &= R_{int} c'_{soil} \\
 \psi'_{int} &= 0^\circ \\
 G_{int} &= R_{int}^2 G_{soil}
 \end{aligned}
 \tag{22}$$

where  $R_{int}$  is a reduction factor; in the analyses a value of  $R_{int} = 0.67$  was adopted.

The anchor block is assumed to behave as an elastic non-porous material with Poisson's ratio  $\nu = 0.15$  and Young's modulus  $E = 3 \cdot 10^7$  MPa

The analyses were carried out in terms of effective stresses, assuming drained conditions.

In order to carry out plane strain analyses, the equivalent unit weight of both the cable chambers and the filled chambers are to be estimated. This was obtained by making the self-weight of the

		<b>Ponte sullo Stretto di Messina</b> <b>PROGETTO DEFINITIVO</b>		
Sicily Anchor Block – earthquake induced displacements and safety against ultimate limit states, Annex	<i>Codice documento</i> PF0064_F0_ANX	<i>Rev</i> F0	<i>Data</i> 20/06/2011	

anchor block equal to that of the equivalent 2D scheme. For each item (cable chamber or filled chamber), the equivalent unit weight  $\gamma_{eq}$  is given by the equation

$$\gamma_{eq} V_{eq} = \gamma_{conc} (V_{eq} - V) + \gamma V \quad (23)$$

where

- $V_{eq}$  is the volume of either the cable chambers or the filled chambers in the equivalent 2D configuration (i.e. distributed along the whole width of the anchor block, equal to 100 m);
- $\gamma_{conc} = 25 \text{ kN/m}^3$  is the unit weight of the reinforced concrete;
- $\gamma$  is the unit weight of the material;
- $V$  is the real volume of either the cable chambers or the filled chambers.

From the previous equation it follows that

$$\gamma_{eq} = \gamma_{conc} + (\gamma - \gamma_{conc}) \frac{V}{V_{eq}} \quad (24)$$

Table 5.3 summarises the values of  $\gamma_{eq}$  used in the plane strain FE analyses.

Table 5.3. Equivalent unit weights assumed in the 2D F.E. analyses

	$V$ ( $\text{m}^3$ )	$V_{eq}$ ( $\text{m}^3$ )	$\gamma$ ( $\text{kN/m}^3$ )	$\gamma_{conc}$ ( $\text{kN/m}^3$ )	$\gamma_{eq}$ ( $\text{kN/m}^3$ )
Cable chambers (x2)	12225	31120	0	25	14.57
Filled chambers (x2)	35388	44401	20	25	20.81

The aim of the 2D FE analyses is to estimate the behaviour of the anchor block in a condition of ultimate limit state. To this purpose, ULS loading conditions were considered in the analyses, spreading the cable load  $T$  over an average width  $B = 100 \text{ m}$  of the anchor block, to account for plane strain conditions.

The following sequence of steps was applied in the analyses: computation of the initial stress state; activation of the anchor block; application of the cable load  $T$  (Table 5.4).

Table 5.4. Sequence of steps for calculations

step	description
0	initial stress state assuming $K_0$ stress conditions
1	application of gravity loading (to account for non horizontal ground surface)
2	displacement reset and activation of the anchor block
3	displacement reset and activation of cable load $T$

		<b>Ponte sullo Stretto di Messina</b> <b>PROGETTO DEFINITIVO</b>		
Sicily Anchor Block – earthquake induced displacements and safety against ultimate limit states, Annex	<i>Codice documento</i> PF0064_F0_ANX	<i>Rev</i> F0	<i>Data</i> 20/06/2011	

The cable load  $T$  is applied with an inclination  $i = 15^\circ$  to the horizontal; the value corresponding to limit state ULS,  $T = 3964$  MN, was provided by the structural analyses of the tender design. The presence of diaphragm walls in front and behind the anchor block were not accounted for in the analyses.

Figures 5.5 shows the contours of mobilized shear strength, expressed in terms of the ratio  $t/t_{max}$  where  $t = (\sigma_1' - \sigma_3')/2$  and  $\sigma_1'$  and  $\sigma_3'$  are the maximum and minimum principal effective stresses; as values of  $t/t_{max}$  approach unity, the full shear strength of the soil is attained. At step 3, when ULS conditions are applied, part of the shear strength is mobilized at both the base and in front of the anchor block, and a wedge of plastic soil can be recognised as the anchor block is pulled by the cable force. Figures 5.6 shows the deformed mesh obtained at this stage.

In order to estimate the most likely sliding surface, the block displacement and its direction was evaluated as the average between the displacements of the centre of gravity and of four nodes of the block at the contact with the soil (Figures 5.7). The results obtained are showed in Table 5.5 and Figure 5.8.

Table 5.5: displacements of the anchor block at the end of step 3

Points	X m	Y m	$u_x$ m	$u_y$ m	$u$ m	inclination °
A	-96.530	0.850	0.150	0.088	0.174	30.299
B	-36.180	10.000	0.158	0.036	0.162	12.979
C	-29.100	25.500	0.171	0.032	0.174	10.615
D	2.470	38.960	0.183	0.001	0.183	0.380
G (centre of gr.)	-53.596	29.533	0.175	0.053	0.182	16.772
average					0.175	14.209

Under ULS loading condition, the average displacement is of 175 mm and the average inclination is of  $14.2^\circ$  to the horizontal. Hence the most likely sliding mechanism is in between the second and the third mechanism.

The inclination of the displacement vector of the block computed in the 2D analyses ( $14.2^\circ$ ) is nearly coincident with that obtained in the three-dimensional analyses ( $14^\circ$ ), as shown in the companion report “*Sicily anchor block: evaluation of block behaviour via 3D FE analyses and of bearing capacity*”. Maximum block displacement computed in the 2D analyses ( $u = 17.5$  cm) is however greater than that computed in the 3D analyses ( $u = 3.5$  cm) due to the influence of different geometrical conditions.

		<b>Ponte sullo Stretto di Messina</b> <b>PROGETTO DEFINITIVO</b>		
Sicily Anchor Block – earthquake induced displacements and safety against ultimate limit states, Annex	<i>Codice documento</i> PF0064_F0_ANX	<i>Rev</i> F0	<i>Data</i> 20/06/2011	

#### 5.4 Sliding resistance on the sides of the anchor block

The sliding resistance  $T_L$  developed on the sides of the anchor block was computed under the conservative hypothesis that active limit equilibrium is achieved behind the diaphragm walls during the excavation stages. The shear stress at the contact of the side walls with the soil can be written as:

$$\tau_s = \sigma'_n \cdot \tan \varphi'_s = K_a \sigma'_v \cdot \tan \varphi'_s$$

where the active earth pressure coefficient  $K_a$  is conservatively calculated using the characteristic angle of the shearing resistance of the soil  $\varphi'_k = 40^\circ$ , while a friction angle  $\varphi'_s \approx \text{atan}[(2/3)\tan \varphi']$  is assumed at the block – soil interface; the corresponding characteristic values were  $\varphi'_k = 40^\circ$  and  $\varphi'_{sk} = 30^\circ$ .

The sliding resistance was computed reducing the  $\tan \varphi'_k$  and  $\tan \varphi'_{sk}$  by the factor  $\gamma_\varphi = 1.25$  prescribed by D.M. 14.01.2008 – “Nuove norme tecniche per le costruzioni” (Table 5.6).

Table 5.6. Sliding resistance on the sides of the anchor block  $T_L$

	$\varphi'_k$ (°)	$\varphi'_d$ (°)	$c'_k$ (kPa)	$c'_d$ (kPa)
active earth pressure coefficient $K_a$	40	-	-	-
friction angle at block sides $\varphi'_s \approx \text{atan}[(2/3)\tan \varphi']$	30	24.8	0	0

Table 5.7 lists the characteristics and design values of lateral resistance  $T_L$  assumed in computation to account for the contribution of the block sides to sliding resistance. The former are used to evaluate the critical seismic coefficient  $K_{c(\text{red})}$  given by eq. (9), while the latter is used in the pseudostatic approach. The depth of block sides accounted for in calculation of sliding resistance changes according to the sliding mechanism. The Tables in Appendix A give computation details.

Table 5.7. Sliding resistance on the block sides

mechanism	$\varphi'_{sk}$ (°)	$T_{Lk}$ (MN)	$\varphi'_{sd}$ (°)	$T_{Ld}$ (MN)
(1)	30	303.1	24.8	242.5
(2)	30	333.9	24.8	267.1
(3)	30	403.6	24.8	322.9

		<b>Ponte sullo Stretto di Messina</b> <b>PROGETTO DEFINITIVO</b>		
Sicily Anchor Block – earthquake induced displacements and safety against ultimate limit states, Annex	<i>Codice documento</i> PF0064_F0_ANX	<i>Rev</i> F0	<i>Data</i> 20/06/2011	

## 5.5 Passive resistance in front of the block

### 5.5.1 Pseudo static approach

The passive resistance developed in front of the block on sliding was computed using the solution obtained by Chen and Liu (1990) via the kinematic theorem of limit analysis. For a value of  $\varphi'_k=40^\circ$  it was assumed  $\delta_k = \varphi'_k/2 = 20^\circ$  and  $\delta_d = \varphi'_d/2 = 17^\circ$ . Again, according to D.M. 14.01.2008, passive resistance was calculated reducing the  $\tan\varphi'$  by the factor  $\gamma_\phi = 1.25$  (Table 5.8)

Table 5.8. Passive resistance in front of the block  $R_p$

	$\varphi'_k$ (°)	$\varphi'_d$ (°)	$c'_k$ (kPa)	$c'_d$ (kPa)
passive earth pressure coefficient $K_p$	40	33.9	-	-
friction angle at the soil block interfaces $\delta_k = \varphi'_k/2$	20	17	-	-

Table 5.9 reports the values of passive earth pressure coefficients,  $K_{Pk}$  and  $K_{Pd}$ , evaluated using the characteristic ( $\varphi'_k = 40^\circ$ ) and the design ( $\varphi'_d = 33.9^\circ$ ) values of the angle of shearing resistance, respectively.

Values of  $K_h$  and  $K_v$  used in computation are also listed in Table 5.9. These were obtained assuming the values of  $a_g$  specified in document GCG.F.04.01 “Fondamenti progettuali e prestazioni attese per l’Opera di attraversamento”. Site effects were accounted for by assuming a topographic amplification factor  $S_T = 1.2$  and a subsoil amplification factor  $S_S = 1.0$ . According to D.M. 14.01.2008, coefficient  $\beta_m = 0.31$  was used for computing  $K_h$ .

Table 5.9. Pseudo-static seismic coefficients and passive earth pressure coefficients

Limit state	$a_g$ (g)	$K_h$	$K_v$	$K_{Pk}$ ( $\varphi'_k = 40^\circ$ )	$K_{Pd}$ ( $\varphi'_d = 33.9^\circ$ )
SLS2	0.26	0.097	0.049	9.005	5.481
ULS	0.58	0.216	0.108	7.655	4.577
SILS	0.64	0.238	0.119	7.395	4.401

The passive resistance was computed from the head of diaphragm walls (49.5 m a.s.l.,  $z = 6.5$  m b.g.l.) down to different depths according to the sliding mechanism considered in the analyses; a length  $L = 80$  m was assumed in the calculation. Table 5.10 summarises the computed design values of passive resistance  $R_{Pd}$  developed in front of the block; for comparison the characteristic values of  $R_p$  are also given in the Tables. Appendix B, gives computation details.

		<b>Ponte sullo Stretto di Messina</b> <b>PROGETTO DEFINITIVO</b>		
Sicily Anchor Block – earthquake induced displacements and safety against ultimate limit states, Annex		<i>Codice documento</i> PF0064_F0_ANX	<i>Rev</i> F0	<i>Data</i> 20/06/2011

Table 5.10. Passive earth resistance in front of the block

sliding mechanism	SLS2		ULS		SILS	
	R <sub>Pk</sub> (MN)	R <sub>Pd</sub> (MN)	R <sub>Pk</sub> (MN)	R <sub>Pd</sub> (MN)	R <sub>Pk</sub> (MN)	R <sub>Pd</sub> (MN)
(1) z = 18.8 m	2241.8	1364.5	1905.7	1139.5	1841.0	1095.6
(2) z = 29.2 m	5838.0	3553.4	4962.8	2967.3	4794.3	2853.2
(3) z = 47.6 m	16018.2	9749.6	13616.8	8141.6	13154.3	7828.5

### 5.5.2 Displacement based approach

In the displacement based approach, the passive earth resistance  $R_p$  in front of the block is assumed to progressively increase with the relative displacement  $u$  induced by the earthquake loading. For computations, an analytical relationship between  $R_p$  and  $u$  is needed. To this aim, plane strain FE analyses were carried out with reference to mechanism 2 ( $\alpha = 26^\circ$ ) and mechanism 3 ( $\alpha = 8^\circ$ ) that were seen to be an upper and a lower bound for the inclination of the sliding surface. Figures 5.9 and 5.10 show the FE meshes used for calculations. The same soil profile was assumed in the analyses as discussed in § 2 and 3. In the analyses, an ideal wall characterised by perfectly smooth contact with the soil is located in the position corresponding to the front of the anchor block; the wall length extends to the depth of the sliding mechanism modelled in the analysis ( $z = 29.2$  m and  $z = 47.6$  m).

An uniform displacement is applied to the wall that progressively increases from 1 mm to about 1 m. For each value of the applied displacement, the earth resistance  $\Delta R$  for unit length is given by:

$$\Delta R = \int_L (\sigma_h - \sigma_{h0}) dl \quad (25)$$


where  $\sigma_h$  and  $\sigma_{h0}$  are the horizontal stresses acting on the wall for a given displacement  $u$  and under geostatic conditions, respectively, and  $L$  is the height of the ideal wall. The relationship between earth resistance in front of the wall  $\Delta R$  and wall displacement  $u$  was obtained by best-fitting the  $u - \Delta R$  data through the equation

$$\Delta R(u) = \frac{u}{b + m \cdot u} \quad (26)$$

where  $b$  and  $m$  are constants. In such condition, the ultimate value of  $\Delta R$  is given by

$$\Delta R_{\max} = \lim_{u \rightarrow \infty} \frac{u}{b + m \cdot u} = \frac{1}{m} \quad (27)$$

It is worth noting that the assumptions of smooth soil-wall interface yield to a conservative estimate of passive resistance. Also, the hypothesis of plane strain conditions is conservative as well in that

		<b>Ponte sullo Stretto di Messina</b> <b>PROGETTO DEFINITIVO</b>		
Sicily Anchor Block – earthquake induced displacements and safety against ultimate limit states, Annex	<i>Codice documento</i> PF0064_F0_ANX	<i>Rev</i> F0	<i>Data</i> 20/06/2011	

greater displacements are induced by a given pressure under 2D conditions; as a consequence a more deformable non linear spring is obtained.

In the analyses, the mechanical soil behaviour was described using the constitutive model Hardening Soil, that is capable of describing the non linear soil behaviour from the early beginning of the loading process; the same parameters listed in Table 3.2 were used to this purpose.

The sequence of steps adopted in the analyses is summarised in Table 5.11.

Table 5.11. Sequence of steps for calculations

step	description
0	initial stress state assuming $K_0$ stress conditions
1	application of gravity loading
2	displacement reset and application of constant displacement along the wall
3	application of the first displacement increment
⋮	⋮
$n$	application of the last displacement increment

The results obtained are reported in Table 5.12 and are showed in Figure 5.11 in terms of  $u - \Delta R$  relationships. The value of earth resistance for unit length has been multiplied for the anchor block width (equal to 80 m) to obtain a  $\Delta R$  value expressed in term of force (MN). Figure 5.12, Figure 5.13 and Figure 5.14 show the plastic points, the contours of horizontal displacement and the contours of mobilised shear strength ( $t/t_{lim}$ ) obtained for mechanism 2. Figure 5.15, Figure 5.16 and Figure 5.17 show the plastic points, the contours of horizontal displacement and the contours of mobilised shear strength ( $t/t_{lim}$ ) obtained for mechanism 3.

Table 5.12. F.E. analysis of passive earth resistance

	<i>Mechanism 2</i>	<i>Mechanism 3</i>
$m$ (1/MN)	$3.149 \times 10^{-4}$	$1.582 \times 10^{-4}$
$b$ (m/MN)	$4.145 \times 10^{-5}$	$3.039 \times 10^{-5}$
$\Delta R_{max}$ (MN)	3176	6321



		<b>Ponte sullo Stretto di Messina</b> <b>PROGETTO DEFINITIVO</b>		
Sicily Anchor Block – earthquake induced displacements and safety against ultimate limit states, Annex	<i>Codice documento</i> PF0064_F0_ANX	<i>Rev</i> F0	<i>Data</i> 20/06/2011	

## 5.6 Evaluation of safety against sliding – pseudostatic approach

In evaluating the safety against sliding through the pseudo-static approach, equation 6 was used and the prescriptions of D.M. 14.01.2008 were followed.

The design resistances are computed considering the contributions of sliding resistance at the base and at the block sides and the passive resistance in front of the block. The active earth thrust behind the block was accounted for down to a depth of 20 m (the vertical portion of the back wall) and along a width of 120 m (the width of the rear side). Both design actions and design resistances were computed using the pseudo-static seismic coefficients reported in Table 5.9.

The cable force  $T$  is inclined to the horizontal of an angle  $i = 15^\circ$ . Table 5.13 reports the values of  $T$  provided by structural analyses of the tender design for each limit state. In the following, computations are carried out for each limit state although safety against sliding should be verified for ULS loading condition only. For this condition, cable forces provided by the tender design are higher than the corresponding values provided by the global IBDAS model (5.8% for the version 3.3b and 8% for the version 3.3f), this resulting in a conservative estimate of safety against sliding of Sicilia Anchor Block.

Table 5.13. Cable force T

Limit state	SLS	ULS	SLIS
T (MN)	3250	3964	3146

The characteristic value of  $\phi'_s$  mobilised on the sliding surface was assumed to be the angle of shearing resistance at constant volume; its value was estimated using the relationship proposed by Bolton (1986):

$$\phi'_{sk} = \phi'_{cv} = \phi'_p - 3 D_R(10 - \ln p') + 3^\circ$$

that for  $\phi'_p = 40^\circ$ ,  $D_R = 50\%$  and  $p' = 200$  kPa provides  $\phi'_{sk} = \phi'_{cv} = 36^\circ$  (Table 5.14).

Table 5.14. Sliding surface

	$\phi'_k$ (°)	$\phi'_d$ (°)	$c'_k$ (kPa)	$c'_d$ (kPa)
<sup>(1)</sup> mobilized shear resistance $\phi'_{sk} = \phi'_{cv}$	36	30.2	0	0

<sup>(1)</sup>  $\phi'_{sk} = \phi'_{cv}$ , for  $\phi'_p = 40^\circ$ ,  $D_R = 50\%$  and  $p' = 200$  kPa

		<b>Ponte sullo Stretto di Messina</b> PROGETTO DEFINITIVO		
Sicily Anchor Block – earthquake induced displacements and safety against ultimate limit states, Annex		Codice documento PF0064_F0_ANX	Rev F0	Data 20/06/2011

Table 5.15 reports the pseudostatic seismic coefficients, the active earth pressure coefficients and the active earth thrust used for computations.

Table 5.15. Pseudo-static seismic coefficients, active earth pressure coefficients and active earth thrust

Limit state	$a_g$ (g)	$K_h$	$K_v$	$K_{ak}$ ( $\varphi'_k=40^\circ$ )	$K_{ad}$ ( $\varphi'_k=33.9^\circ$ )	$S_{aE(k)}$ (MN, $\varphi'_k=40^\circ$ )	$S_{aE(d)}$ (MN, $\varphi'_k=33.9^\circ$ )
SLS2	0.26	0.097	0.048	0.269	0.343	129.2	164.7
ULS	0.58	0.216	0.108	0.357	0.445	171.4	213.7
SLIS	0.64	0.238	0.119	0.378	0.470	181.3	225.4

Table 5.16 a-b report the comparison between design resistances and design actions for the three sliding mechanisms assumed in the analyses. The Tables in Appendix C give computation details.

Table 5.16 a. Safety against sliding, active earth pressure neglected

	SLS2			ULS			SILS		
	$\Sigma R_d$	$\Sigma E_d$	$\Sigma R_d / \Sigma E_d$	$\Sigma R_d$	$\Sigma E_d$	$\Sigma R_d / \Sigma E_d$	$\Sigma R_d$	$\Sigma E_d$	$\Sigma R_d / \Sigma E_d$
Mechanism 1	5406.0	-1008.7	(-)	5471.9	672.4	8.1	5286.4	111.4	47.4
Mechanism 2	7631.3	495.5	15.4	7171.4	4	3.1	6985.5	1683.0	4.2
Mechanism 3	13152.5	2912.7	4.5	11471.3	4698.7	2.4	11206.9	4088.8	2.7

(-) The component of the submerged weight of the anchor block parallel to the sliding surface  $W' \sin \alpha$  is larger than the sum of the other driving forces.

Table 5.16 b. Safety against sliding, active earth pressure included

	SLS2			ULS			SILS		
	$\Sigma R_d$	$\Sigma E_d$	$\Sigma R_d / \Sigma E_d$	$\Sigma R_d$	$\Sigma E_d$	$\Sigma R_d / \Sigma E_d$	$\Sigma R_d$	$\Sigma E_d$	$\Sigma R_d / \Sigma E_d$
Mechanism 1	5406.0	-878.9	(-)	5471.9	840.8	6.5	5286.4	289.0	18.3
Mechanism 2	7631.3	643.5	11.9	7171.4	2474.4	2.9	6985.5	1885.6	3.7
Mechanism 3	13152.5	3075.8	4.3	11471.3	4910.3	2.3	11206.9	4312.0	2.6

(-) The component of the submerged weight of the anchor block parallel to the sliding surface  $W' \sin \alpha$  is larger than the sum of the other driving forces.

Comparison of Tables 5.16 a-b shows that the active earth thrust reduces the ratio  $\Sigma R_d / \Sigma E_d$ . However the reduction is negligible in the ULS loading condition for mechanism 2 and mechanism 3, which are characterized by the lowest values of the ratio  $\Sigma R_d / \Sigma E_d$  and have been showed to be the upper and the lower boundary for the most likely sliding surface.

		<b>Ponte sullo Stretto di Messina</b> <b>PROGETTO DEFINITIVO</b>		
Sicily Anchor Block – earthquake induced displacements and safety against ultimate limit states, Annex	<i>Codice documento</i> PF0064_F0_ANX	<i>Rev</i> F0	<i>Data</i> 20/06/2011	

In all the cases examined the ratio  $\Sigma R_d / \Sigma E_d$  is greater than 1 and safety against sliding is satisfied.

## 5.7 Evaluation of sliding performance – displacement based approach

### 5.7.1 Seismic action

In the displacement based approach, a number of input accelerograms are to be selected. To this purpose, 22 acceleration time histories were selected from the PEER strong-motion database specifying a range of magnitude  $M = 6.5\text{--}7.28$ , and hypocentral distances in the range of 12 to 82 km. The peak acceleration of the input accelerograms ranges from 0.29 g, that is half of the design peak acceleration (0.58 g), to 1.16 g, that is twice the design peak acceleration. In addition to the real acceleration time histories, 8 artificial strong motion accelerograms, fully compatible with the response spectrum of the preliminary design, were also used as input motion to the sliding block analyses.

Table 5.17 reports the main parameters of the horizontal components of the selected accelerograms: the peak acceleration  $a_{\max}$ , the peak velocity  $v_{\max}$ , the Arias intensity  $I_a$ , the predominant period of Fourier spectrum  $T_P$ , and the duration between the first and the last exceedance of 0.05g ( $D_{0.05g}$ ). In Table 5.18, the same parameters are listed for the vertical component of the accelerograms .

Each horizontal component was scaled to the design peak acceleration  $a_{\max} = 0.58g$  and the corresponding vertical component was scaled by the same factor. Table 5.19 and Table 5.20 show the parameters of the scaled accelerograms.

The horizontal components of each seismic event was independently considered and combined with the vertical component. The analyses were also repeated using the scaled horizontal component combined with the vertical component scaled to 0.58g as well (Table 5.21).

Figures 5.18–5.22 show the elastic response spectra of the selected accelerograms, compared to the design response spectrum.

		<b>Ponte sullo Stretto di Messina</b> <b>PROGETTO DEFINITIVO</b>		
Sicily Anchor Block – earthquake induced displacements and safety against ultimate limit states, Annex	<i>Codice documento</i> PF0064_F0_ANX	<i>Rev</i> F0	<i>Data</i> 20/06/2011	

Table 5.17. Parameters of the selected accelerograms, horizontal components

Time history	$a_{MAX}$ (g)	$v_{MAX}$ (m/s)	$I_a$ (m/s)	$T_P$ (s)	$D_{0.05g}$ (s)
Friuli 76 TOLXC	0.357	0.210	0.799	0.494	7.48
Friuli 76 TOLYC	0.316	0.326	1.169	0.661	6.09
Imperial Valley 1979 DLT352	0.351	0.330	3.289	1.672	70.53
Kobe 1995 TAZ000	0.693	0.683	3.070	1.638	14.92
Kobe 1995 TAZ090	0.694	0.853	3.935	0.488	12.15
Landers 1992 CLWTR	0.417	0.423	2.172	0.706	18.50
Landers 1992 LCN260	0.727	1.465	6.977	0.106	33.26
Landers 1992 LCN345	0.789	0.324	6.585	0.088	33.33
Loma Prieta 1989 CYC285	0.484	0.397	1.503	0.650	16.92
Loma Prieta 1989 G03000	0.555	0.357	2.087	0.569	9.99
Loma Prieta 1989 G03090	0.367	0.447	1.348	1.862	16.59
Loma Prieta 1989 G04000	0.417	0.388	1.241	0.394	14.73
Manjil 90 ABBL	0.515	0.425	4.656	0.340	49.16
Manjil 90 ABBT	0.496	0.521	7.589	0.218	45.24
Northridge 94 CEN245	0.322	0.229	0.994	0.853	14.16
Northridge 94 LAC180	0.316	0.140	1.051	0.339	16.21
Umbria Marche 97 NCRXC	0.524	0.320	3.304	0.159	12.38
Umbria Marche 97 NCRYC	0.463	0.291	2.822	0.378	10.84
Imperial Valley 79 BC230	0.775	0.460	5.987	0.621	19.09
Irpinia 80 STUYC	0.323	0.546	1.506	2.341	43.48
Montenegro 79 ULCXC	0.294	0.386	1.851	1.092	30.90
Montenegro 79 PETXC	0.454	0.389	4.527	0.458	18.67
Art. 1 comp. 1	0.642	0.757	7.457	0.803	36.58
Art. 1 comp. 2	0.633	0.805	7.667	0.819	27.98
Art. 2 comp. 1	0.656	0.667	6.239	0.910	26.93
Art. 2 comp. 2	0.640	0.742	5.835	0.694	24.92
Art. 3 comp. 1	0.675	0.709	9.664	0.759	37.31
Art. 3 comp. 2	0.611	0.722	8.733	0.890	33.92
Art. 4 comp. 1	0.608	0.782	9.588	0.881	59.59
Art. 4 comp. 2	0.534	1.178	6.276	0.433	51.41

		<b>Ponte sullo Stretto di Messina</b> <b>PROGETTO DEFINITIVO</b>		
Sicily Anchor Block – earthquake induced displacements and safety against ultimate limit states, Annex	<i>Codice documento</i> PF0064_F0_ANX	<i>Rev</i> F0	<i>Data</i> 20/06/2011	

Table 5.18. Parameters of the selected accelerograms, vertical components

Time history	$a_{MAX}$ (g)	$v_{MAX}$ (m/s)	$I_a$ (m/s)	$T_P$ (s)	$D_{0.05g}$ (s)
Friuli 76 TOLZC	0.267	0.103	0.336	0.174	6.09
Imperial Valley 1979 DLTDW	0.145	0.148	0.538	4.312	20.45
Kobe 1995 TAZUP	0.433	0.348	1.051	0.466	4.12
Landers 1992 CLWUP	0.174	0.099	0.617	0.146	21.35
Landers 1992 LCNUP	0.818	0.460	8.226	0.075	33.54
Loma Prieta 1989 CYCUP	0.082	0.095	0.122	1.107	8.92
Loma Prieta 1989 G03UP	0.338	0.155	0.807	1.280	12.93
Loma Prieta 1989 G04UP	0.159	0.146	0.315	1.781	12.97
Manjil 90 ABBV	0.538	0.440	4.676	0.134	47.58
Northridge 94 CENUP	0.109	0.106	0.254	1.517	12.66
Northridge 94 LACUP	0.135	0.076	0.215	0.410	11.67
Umbria Marche 97 NCRZC	0.419	0.284	0.711	0.158	5.27
Imperial Valley 79 BCUP	0.425	0.122	1.123	0.146	17.91
Irpinia 80 STUZC	0.235	0.204	0.561	1.707	12.40
Montenegro 79 ULCZC	0.458	0.163	2.512	0.079	16.23
Montenegro 79 PETZC	0.213	0.132	0.577	0.410	15.79
Art. 1 comp. V	0.515	0.463	6.922	0.494	33.86
Art. 2 comp. V	0.656	0.566	4.249	0.706	22.46
Art. 3 comp. V	0.630	0.656	6.408	0.445	27.06
Art. 4 comp. V	0.699	0.576	7.344	0.394	56.42

		<b>Ponte sullo Stretto di Messina</b> <b>PROGETTO DEFINITIVO</b>		
Sicily Anchor Block – earthquake induced displacements and safety against ultimate limit states, Annex	<i>Codice documento</i> PF0064_F0_ANX	<i>Rev</i> F0	<i>Data</i> 20/06/2011	

Table 5.19. Parameters of the selected accelerograms scaled to 0.58g. Horizontal components

Time history	$a_{MAX}$ (g)	$v_{MAX}$ (m/s)	$I_a$ (m/s)	$T_P$ (s)	$D_{0.05g}$ (s)
Friuli 76 TOLXC	0.580	0.341	2.112	0.494	8.88
Friuli 76 TOLYC	0.580	0.599	3.948	0.661	12.66
Imperial Valley 1979 DLT352	0.580	0.545	8.974	1.672	77.41
Kobe 1995 TAZ000	0.580	0.571	2.148	1.638	9.53
Kobe 1995 TAZ090	0.580	0.713	2.752	0.488	12.01
Landers 1992 CLWTR	0.580	0.589	4.204	0.706	20.40
Landers 1992 LCN260	0.580	1.169	4.442	0.106	33.26
Landers 1992 LCN345	0.580	0.238	3.557	0.088	33.30
Loma Prieta 1989 CYC285	0.580	0.476	2.159	0.650	17.44
Loma Prieta 1989 G03000	0.580	0.373	2.279	0.569	11.80
Loma Prieta 1989 G03090	0.580	0.705	3.360	1.862	22.84
Loma Prieta 1989 G04000	0.580	0.540	2.408	0.394	21.55
Manjil 90 ABBL	0.580	0.479	5.916	0.340	49.30
Manjil 90 ABBT	0.580	0.609	10.363	0.218	45.24
Northridge 94 CEN245	0.580	0.412	3.232	0.853	21.26
Northridge 94 LAC180	0.580	0.257	3.535	0.339	24.64
Umbria Marche 97 NCRXC	0.580	0.354	4.052	0.159	12.38
Umbria Marche 97 NCRYC	0.580	0.365	4.435	0.378	11.95
Imperial Valley 79 BC230	0.580	0.344	3.355	0.621	16.11
Irpinia 80 STUYC	0.580	0.982	4.797	2.341	46.29
Montenegro 79 ULCXC	0.580	0.761	7.225	1.092	35.88
Montenegro 79 PETXC	0.580	0.497	7.392	0.458	31.58
Art. 1 comp. 1	0.580	0.683	6.080	0.803	36.56
Art. 1 comp. 2	0.580	0.738	6.444	0.819	27.96
Art. 2 comp. 1	0.580	0.590	4.879	0.910	24.75
Art. 2 comp. 2	0.580	0.672	4.791	0.694	24.91
Art. 3 comp. 1	0.580	0.609	7.138	0.759	32.85
Art. 3 comp. 2	0.580	0.685	7.876	0.890	30.57
Art. 4 comp. 1	0.580	0.746	8.724	0.881	59.59
Art. 4 comp. 2	0.580	1.279	7.395	0.433	51.42

		<b>Ponte sullo Stretto di Messina</b> <b>PROGETTO DEFINITIVO</b>		
Sicily Anchor Block – earthquake induced displacements and safety against ultimate limit states, Annex	<i>Codice documento</i> PF0064_F0_ANX	<i>Rev</i> F0	<i>Data</i> 20/06/2011	

Table 5.20. Parameters of the vertical components scaled by the same factor of the corresponding horizontal components

Time history	scale factor	$a_{MAX}$ (g)	$v_{MAX}$ (m/s)	$I_a$ (m/s)	$T_P$ (s)	$D_{0.05g}$ (s)
Friuli 76 TOLZC	1.6246	0.434	0.167	0.886	0.174	7.05
Friuli 76 TOLZC	1.8354	0.490	0.188	1.130	0.174	8.62
Imperial Valley 1979 DLTDW	1.6524	0.240	0.244	1.469	4.120	57.14
Kobe 1995 TAZUP	0.8369	0.362	0.292	0.736	0.466	3.12
Kobe 1995 TAZUP	0.8357	0.362	0.291	0.734	0.466	3.12
Landers 1992 CLWUP	1.3909	0.242	0.138	1.193	0.146	23.19
Landers 1992 LCNUP	0.7978	0.653	0.367	5.236	0.075	33.52
Landers 1992 LCNUP	0.7351	0.601	0.338	4.445	0.075	25.08
Loma Prieta 1989 CYCUP	1.1983	0.098	0.114	0.175	1.107	8.99
Loma Prieta 1989 G03UP	1.0450	0.353	0.162	0.881	1.280	12.94
Loma Prieta 1989 G03UP	1.5804	0.534	0.244	2.016	1.280	20.44
Loma Prieta 1989 G04UP	1.3909	0.221	0.203	0.610	1.781	14.12
Manjil 90 ABBV	1.1262	0.606	0.495	5.931	0.134	47.60
Manjil 90 ABBV	1.1694	0.629	0.514	6.395	0.134	47.60
Northridge 94 CENUP	1.8012	0.196	0.191	0.824	1.517	21.90
Northridge 94 LACUP	1.8354	0.248	0.139	0.724	0.410	17.60
Umbria Marche 97 NCRZC	1.1069	0.464	0.314	0.871	0.158	6.18
Umbria Marche 97 NCRZC	1.2527	0.525	0.356	1.157	0.158	7.49
Imperial Valley 79 BCUP	0.7484	0.318	0.091	0.629	0.146	11.59
Irpinia 80 STUZZC	1.7957	0.422	0.367	1.809	1.707	44.99
Montenegro 79 ULCZC	1.9728	0.904	0.321	9.776	0.079	30.24
Montenegro 79 PETZC	1.2775	0.272	0.169	0.941	0.410	17.61
Art. 1 comp. V	0.9034	0.465	0.418	5.649	0.494	30.44
Art. 1 comp. V	0.9163	0.472	0.424	5.812	0.494	30.44
Art. 2 comp. V	0.8841	0.580	0.500	3.321	0.706	21.79
Art. 2 comp. V	0.9063	0.595	0.513	3.490	0.706	21.79
Art.3 comp. V	0.8593	0.541	0.564	4.732	0.445	27.03
Art. 3 comp. V	0.9493	0.598	0.623	5.775	0.445	27.05
Art. 4 comp. V	0.9539	0.667	0.549	6.682	0.394	56.40
Art. 4 comp. V	1.0861	0.759	0.625	8.663	0.394	56.42


		<b>Ponte sullo Stretto di Messina</b> <b>PROGETTO DEFINITIVO</b>		
Sicily Anchor Block – earthquake induced displacements and safety against ultimate limit states, Annex	<i>Codice documento</i> PF0064_F0_ANX	<i>Rev</i> F0	<i>Data</i> 20/06/2011	

Table 5.21. Parameters of the selected accelerograms scaled to 0.58g. Vertical components

Time history	$a_{MAX}$ (g)	$v_{MAX}$ (m/s)	$I_a$ (m/s)	$T_P$ (s)	$D_{0.05g}$ (s)
Friuli 76 TOLZC	0.580	0.223	1.579	0.174	4.12
Imperial Valley 1979 DLTDW	0.580	0.592	8.612	4.120	30.57
Kobe 1995 TAZUP	0.580	0.467	1.882	0.466	2.79
Landers 1992 CLWUP	0.580	0.332	6.885	0.146	16.52
Landers 1992 LCNUP	0.580	0.323	4.131	0.075	25.08
Loma Prieta 1989 CYCUP	0.580	0.678	6.160	1.107	31.40
Loma Prieta 1989 G03UP	0.580	0.265	2.373	1.280	20.44
Loma Prieta 1989 G04UP	0.580	0.534	4.211	1.781	23.16
Manjil 90 ABBV	0.580	0.474	5.438	0.134	47.60
Northridge 94 CENUP	0.580	0.566	7.216	1.517	27.44
Northridge 94 LACUP	0.580	0.326	3.992	0.410	30.29
Umbria Marche 97 NCRZC	0.580	0.393	1.362	0.158	7.49
Imperial Valley 79 BCUP	0.580	0.166	2.093	0.146	17.93
Irpinia 80 STUZZ	0.580	0.503	3.409	1.707	46.03
Montenegro 79 ULCZC	0.580	0.206	4.034	0.079	28.45
Montenegro 79 PETZC	0.580	0.361	4.292	0.410	32.63
Art. 1 comp. V	0.580	0.521	8.776	0.494	34.18
Art. 2 comp. V	0.580	0.500	3.320	0.706	21.79
Art. 3 comp. V	0.580	0.604	5.433	0.445	27.05
Art. 4 comp. V	0.580	0.478	5.062	0.394	52.24



		<b>Ponte sullo Stretto di Messina</b> <b>PROGETTO DEFINITIVO</b>		
Sicily Anchor Block – earthquake induced displacements and safety against ultimate limit states, Annex	<i>Codice documento</i> PF0064_F0_ANX	<i>Rev</i> F0	<i>Data</i> 20/06/2011	

### 5.7.2 Critical seismic coefficient

The values of critical seismic coefficients were evaluated for each limit state, considering the contribution of the base and the lateral sides of the block, while the passive earth resistance in front of the block is assumed to gradually increase as the block displacement relative to the ground develops.

The values of  $K_c$ , computed using equation (9), with  $\varphi'_{sk} = 36^\circ$ , are listed in Table 5.22.

Table 5.22. Critical seismic coefficients  $K_c$

	SLS2	ULS	SILS
Mechanism 1	0.78	0.73	0.79
Mechanism 2	0.64	0.58	0.65
Mechanism 3	0.40	0.33	0.41

The lowest values of  $K_c$  are obtained for the ULS condition. For this reason the earthquake-induced displacement computed for the Sicily anchor block are in the following referred to the ULS condition only.

### 5.7.3 Earthquake-induced displacements

The pseudo-static analyses show that mechanism 1 is the less critical among the three assumed mechanisms, in terms of both safety against sliding and critical seismic coefficient  $K_c$ . In addition, the FE analyses showed that the inclination of the most likely sliding surface is in between mechanisms 2 and 3. For these reasons the earthquake-induced displacements were evaluated for these mechanisms.

Calculations were carried out combining each scaled horizontal component with the corresponding vertical component first scaled by the same factor and then scaled to 0.58g as well. The analyses were also repeated considering the inverse accelerograms, i.e.  $a_{\text{inverse}}(t) = -a(t)$ .

Earthquake induced displacements were computed through numerical integration of equation (21), with  $\varphi'_{sk} = 36^\circ$ . Maximum computed displacement are summarised in Table 5.23.

For mechanism 2, the maximum computed displacement of the anchor block is  $u_{\max} = 1$  mm, whereas for mechanism 3 is  $u_{\max} = 33$  mm.

The highest displacements induced by the selected seismic events are obtained for mechanism 3, characterised by the lower inclination of the sliding plane ( $\alpha = 0$ ).

		<b>Ponte sullo Stretto di Messina</b> <b>PROGETTO DEFINITIVO</b>		
Sicily Anchor Block – earthquake induced displacements and safety against ultimate limit states, Annex	<i>Codice documento</i> PF0064_F0_ANX	<i>Rev</i> F0	<i>Data</i> 20/06/2011	

The results obtained for each accelerogram are summarised in Table 5.24, while Appendix D report time histories of acceleration, velocity and displacement obtained for each seismic input considering sliding mechanism 3, that was recognised to be the most critical.

Table 5.23. Earthquake-induced displacements (mm)

	$a_{v,max} \neq 0.58g$	$a_{v,max} = 0.58g$
Mechanism 2	1	1
Mechanism 3	24	33

Finally, two comparative analyses were carried out in which the inclination of the sliding surface is  $\alpha = 14^\circ$ , as obtained from the 2D and 3D FE analyses, and  $\alpha = 8^\circ$ . In these analyses, the following conservative assumptions were made: values of  $T_L$  corresponding to mechanism 1 were considered; the net earth thrust  $\Delta R$  was computed down to the depth of the diaphragm wall (mechanism 2); the weight of the anchor block only was considered in computations. The results reported in Table 5.25 show that, under these conservative hypotheses, the permanent displacement of the anchor block induced by earthquake loading is in the range 25 – 58 mm.

		<b>Ponte sullo Stretto di Messina</b> <b>PROGETTO DEFINITIVO</b>		
Sicily Anchor Block – earthquake induced displacements and safety against ultimate limit states, Annex	<i>Codice documento</i> PF0064_F0_ANX	<i>Rev</i> F0	<i>Data</i> 20/06/2011	

Table 5.24. Earthquake-induced displacements (mm)

Time history	Mechanism 2		Mechanism 3	
	$a_{v,max} \neq 0.58g$	$a_{v,max} = 0.58g$	$a_{v,max} \neq 0.58g$	$a_{v,max} = 0.58g$
Friuli 76 TOLXC	0	0	1	3
Friuli 76 TOLYC	0	0	12	13
Imperial Valley 1979 DLT352	0	0	2	5
Kobe 1995 TAZ000	0	0	1	5
Kobe 1995 TAZ090	0	1	20	33
Landers 1992 CLWTR	0	0	8	8
Landers 1992 LCN260	0	0	8	7
Landers 1992 LCN345	0	0	2	2
Loma Prieta 1989 CYC285	0	0	1	5
Loma Prieta 1989 G03000	0	0	1	1
Loma Prieta 1989 G03090	0	0	9	10
Loma Prieta 1989 G04000	0	0	8	10
Manjil 90 ABBL	0	0	6	5
Manjil 90 ABBT	0	0	14	12
Northridge 94 CEN245	0	0	6	8
Northridge 94 LAC180	0	0	4	11
Umbria Marche 97 NCRXC	0	0	7	9
Umbria Marche 97 NCRYC	0	0	5	6
Imperial Valley 79 BC230	0	0	3	3
Irpinia 80 STUYC	0	0	1	2
Montenegro 79 ULCXC	1	0	15	7
Montenegro 79 PETXC	0	0	10	29
Art. 1 comp. 1	0	0	6	12
Art. 1 comp. 2	0	0	14	21
Art. 2 comp. 1	0	0	13	13
Art. 2 comp. 2	0	0	24	23
Art. 3 comp. 1	0	0	13	16
Art. 3 comp. 2	0	0	11	10
Art. 4 comp. 1	0	0	18	16
Art. 4 comp. 2	0	0	13	9

		<b>Ponte sullo Stretto di Messina</b> <b>PROGETTO DEFINITIVO</b>		
Sicily Anchor Block – earthquake induced displacements and safety against ultimate limit states, Annex	<i>Codice documento</i> PF0064_F0_ANX	<i>Rev</i> F0	<i>Data</i> 20/06/2011	

Table 5.25. Comparative analysis: earthquake-induced displacements (mm); scaled horizontal component and corresponding vertical component scaled to 0.58g

Time history	$\alpha=14^\circ, K_c=0.366$		$\alpha=8^\circ, K_c=0.265$	
	$a_{vmax}<>0.58g$	$a_{vmax}=0.58g$	$a_{vmax}<>0.58g$	$a_{vmax}=0.58g$
Friuli 76 TOLXC	1	3	4	8
Friuli 76 TOLYC	4	7	21	24
Imperial Valley 1979 DLT352	0	3	3	12
Kobe 1995 TAZ000	0	5	3	22
Kobe 1995 TAZ090	9	25	35	57
Landers 1992 CLWTR	0	4	16	22
Landers 1992 LCN260	5	4	16	13
Landers 1992 LCN345	1	1	6	6
Loma Prieta 1989 CYC285	0	2	3	12
Loma Prieta 1989 G03000	0	0	2	4
Loma Prieta 1989 G03090	3	4	16	18
Loma Prieta 1989 G04000	0	2	15	20
Manjil 90 ABBL	4	3	16	15
Manjil 90 ABBT	8	5	32	29
Northridge 94 CEN245	0	3	11	17
Northridge 94 LAC180	0	6	7	27
Umbria Marche 97 NCRXC	2	5	15	21
Umbria Marche 97 NCRYC	2	3	12	13
Imperial Valley 79 BC230	0	1	7	7
Irpinia 80 STUYC	0	0	4	6
Montenegro 79 ULCXC	11	2	32	17
Montenegro 79 PETXC	1	18	26	58
Art. 1 comp. 1	3	11	19	32
Art. 1 comp. 2	8	15	31	42
Art. 2 comp. 1	12	12	23	23
Art. 2 comp. 2	21	20	39	38
Art. 3 comp. 1	6	8	35	39
Art. 3 comp. 2	3	2	32	30
Art. 4 comp. 1	9	5	37	31
Art. 4 comp. 2	12	3	34	22
max	21	25	39	58

		<b>Ponte sullo Stretto di Messina</b> <b>PROGETTO DEFINITIVO</b>		
Sicily Anchor Block – earthquake induced displacements and safety against ultimate limit states, Annex	<i>Codice documento</i> PF0064_F0_ANX	<i>Rev</i> F0	<i>Data</i> 20/06/2011	

## 6 Sicily Anchor Block – Safety against rotation

Safety against rotation ensures that the resultant force transmitted to the foundation acts within the foundation plane; it was evaluated by imposing momentum equilibrium around point O belonging to the plane of motion (Figure 6.1).

According to D.M. 14.01.2008, safety against rotation is treated as an equilibrium limit state of rigid body (EQU) using the partial safety factor of group M2 to evaluate the earth pressures. Moreover, under seismic conditions the load factors of the design actions are set equal to unity (§ 7.11.1 - D.M. 14.01.2008); accordingly these factors are omitted in the following

A conservative estimate of safety against rotation was obtained through the following assumptions:

- the passive earth resistance  $R_{Pd}$  accounted for in computations was referred to mechanism 3, corresponding to the lower resistant moment;
- the contribution of slide resistance  $T_{Ld}$  developed along the sides of the anchor block was neglected.

Safety against rotation is ensured when the resistant moments are equal or larger than driving moments:

$$\frac{\sum M_{Rd}}{\sum M_{Dd}} = \frac{W' \cdot e_W + R_{Pd} \cos \delta \cdot e_{RP}}{K_h W \cdot e_{K_h} + K_v W \cdot e_{K_v} + T \cos i \cdot e_{T_h} + T \sin i \cdot e_{T_v}} \geq 1 \quad (28)$$

where  $e_i$  is the distance of the line of action of each force from point O. Factored values of the cable force  $T$  were introduced in equation (28), as provided by structural analyses. of the tender design, for the ULS loading condition

Table 6.1 reports the shear strength parameters used in the computations.

Table 6.1. Safety against rotation

	$\varphi_k'$	$\varphi_d'$	$c_k'$	$c_d'$
	(°)	(°)	(kPa)	(kPa)
passive earth resistance $R_p$	40	33.9	0	0

		<b>Ponte sullo Stretto di Messina</b> <b>PROGETTO DEFINITIVO</b>		
Sicily Anchor Block – earthquake induced displacements and safety against ultimate limit states, Annex		<i>Codice documento</i> PF0064_F0_ANX	<i>Rev</i> F0	<i>Data</i> 20/06/2011

Table 6.2 and Table 6.3 report the resistant and the driving actions, respectively.

Table 6.2. Design resistance

	resistance (MN)	distance (m)	$M_{Rd}$ (MN·m)
$W'$	7502	57.6	432115
$R_{Pd} \cos \delta$	7788	13.7	206702
$\Sigma M_{Rd}$			538818



Table 6.3. Driving forces

	action (MN)	distance (m)	$M_{Dd}$ (MN·m)
$K_h W$	1619	12.9	20880
$K_v W$	809	57.6	46617
$T_h$	3829	38.1	145882
$T_v$	1026	9.0	9234
$\Sigma M_{Dd}$			222613

It follows that

$$\frac{\Sigma M_{Rd}}{\Sigma M_{Dd}} = 2.42$$

Hence the requirements of D.M. 14.01.2008 are fulfilled.

		<b>Ponte sullo Stretto di Messina</b> <b>PROGETTO DEFINITIVO</b>		
Sicily Anchor Block – earthquake induced displacements and safety against ultimate limit states, Annex	<i>Codice documento</i> PF0064_F0_ANX	<i>Rev</i> F0	<i>Data</i> 20/06/2011	

## 7 Sicily Anchor Block – Bearing capacity

Safety against bearing capacity failure was evaluated using Approach 1, Combination 2 of Italian Building Code (D.M. 14.01.2008, “Nuove norme tecniche per le costruzioni”).

The loads to be considered for evaluation of bearing capacity are the cable force  $T$ , the weight of the anchor block  $W$  and the horizontal and vertical components of the pseudostatic inertial force,  $K_h W$  and  $K_v W$ .

The conservative assumptions adopted in computation were as follows:

- the sliding resistance developed on the side walls of the anchor block were not taken into account;
- the passive earth resistance was neglected assuming that it was not fully mobilised when bearing capacity is attained.

The bearing capacity is evaluated in terms of effective stress using appropriate correction factors to take into account the inclination of the applied load, the shape of the foundation, and the inclination of the foundation base. To this aim, the geometry of the anchor block considered in the analysis is as shown in Figure 6.1. To account for the eccentricity of the load, the bearing capacity is computed for an equivalent rectangular foundation with reduced width  $B'$  and length  $L'$ .

Safety against bearing capacity failure is ensured if the design resistance  $R_d$  is equal or larger than design loads  $E_d$ :

$$\frac{R_d}{E_d} \geq 1$$


Design values of resistances and forces are obtained from the corresponding characteristic values and are those acting normally to the foundation plane.

The design resistance is:

$$R_{N_d} = \frac{1}{\gamma_R} R_{N_k} = \frac{1}{\gamma_R} (Q'_{ult_d} + U_{bd}) \quad (29)$$

with  $\gamma_R = 1.8$ . In equation (29):

- $Q'_{ult_d} = A \cdot q'_{ult_d}$  is the ultimate effective bearing capacity provided by Terzaghi equation;
- $A$  is the area of the foundation base of the anchor block;
- $q'_{ult_d}$  is the ultimate effective bearing pressure computed using the reduced values of the angle of shearing resistance acting on the failure surface  $\phi'_d = \arctan [(\tan \phi'_k) / \gamma_\phi]$ , with  $\gamma_\phi = 1.25$ ;
- $U_{bd} = U_{bk}$  is the resultant of the pore water pressure acting at the foundation level.

		<b>Ponte sullo Stretto di Messina</b> <b>PROGETTO DEFINITIVO</b>		
Sicily Anchor Block – earthquake induced displacements and safety against ultimate limit states, Annex		<i>Codice documento</i> PF0064_F0_ANX	<i>Rev</i> F0	<i>Data</i> 20/06/2011

According to Terzaghi's theory, the ultimate effective bearing pressure  $q'_{ult}$  is given by the equation

$$q'_{ult} = N_q \cdot q' \cdot \zeta_q \cdot \xi_q \cdot \alpha_q + N_c \cdot c'_d \cdot \zeta_c \cdot \xi_c \cdot \alpha_c + N_\gamma \cdot \gamma_{av} \cdot \frac{B'}{2} \cdot \zeta_\gamma \cdot \xi_\gamma \cdot \alpha_\gamma \quad (30)$$

where

- $q' = \gamma z_w + \gamma'(D - z_w)$  is the vertical effective stress acting at the foundation level;
- $z_w$  is the depths of the groundwater table;
- $D$  is the minimum depth of the foundation base below ground level;
- $\gamma_{av}$  is the average unit weight of the soil below the foundation level.

Soil parameters used in computations are those listed in Table 3.2.

When evaluating the effect of seismic actions, the Italian Building Code (§ 7.11.1 - D.M. 14.01.2008) specifies that the partial safety factors of the design actions are set equal to unity:  $\gamma_G = \gamma_Q = 1$ . Accordingly, load factors  $\gamma_F$  ( $\gamma_G$  and  $\gamma_Q$ ) are omitted in the following.

The design components of the loads acting normally to the foundation plane are:

$$E_{N_d} = \gamma_F E_{N_k} = W'_k \cos \varepsilon + T \sin(\varepsilon - i) + K_h W \sin \varepsilon \pm K_v W \cos \varepsilon \quad (31)$$

The design components of the loads acting tangentially to the foundation plane are:

$$E_{S_d} = \gamma_F E_{S_k} = W'_k \sin \varepsilon - T \cos(\varepsilon - i) - K_h W \cos \varepsilon \mp K_v W \sin \varepsilon \quad (32)$$

Note, however, that in equations 31 and 32 the cable forces are inclusive of partial load factors, as provided by structural analyses of the tender design.

Calculations were carried out with reference to the ULS loading condition.

Table 7.1 reports the shear strength parameters used in the computations.

Table 7.1. Strength parameters for bearing capacity

	$\varphi'_k$	$\varphi'_d$	$c'_k$	$c'_d$
	(°)	(°)	(kPa)	(kPa)
shearing resistance	40	33.9	0	0

Table 7.2 lists the values of the design loads acting normally to the foundation plane, while Table 7.3 summarises the those acting tangentially to the foundation plane:



		<b>Ponte sullo Stretto di Messina</b> <b>PROGETTO DEFINITIVO</b>		
Sicily Anchor Block – earthquake induced displacements and safety against ultimate limit states, Annex		<i>Codice documento</i> PF0064_F0_ANX	<i>Rev</i> F0	<i>Data</i> 20/06/2011

Table 7.2. normal design loads

	$E_{Nd}$ (MN)
$W'_k \cos \varepsilon$	7239.6
$T \sin(\varepsilon - i)$	13.8
$k_h W \sin \varepsilon$	424.4
$-K_v W \cos \varepsilon$	-781.0
$\Sigma E_{Nd}$	6896.8

Table 7.3. tangent design loads

	$E_{Sd}$ (MN)
$W'_k \sin \varepsilon$	1966.9
$-T \cos(\varepsilon - i)$	-3964.0
$-k_h W \cos \varepsilon$	-1562.0
$-K_v W \sin \varepsilon$	-212.2
$\Sigma E_{Sd}$	-3771.2

To evaluate the design resistance, the reduced width  $B'$  is first calculated through equation

$$B' = B - 2e$$

where  $B = 102.6$  m is the original width and  $e = 10.95$  m is the eccentricity of  $E_{Nd}$  from the centre of gravity of the foundation plane. The reduced width is then  $B' = 80.7$  m.

The average length of the foundation surface is  $L = 100$  m and no correction is needed as the loads are centred in the longitudinal direction.

According to Approach 1, Combination 2 of D.M. 14.01.2008, the design strength parameters adopted for evaluation of bearing capacity were  $\phi'_d = \tan^{-1}[(\tan \phi'_k)/1.25] = 33.9^\circ$  and  $c'_d = 0$  kPa.

For the hypotheses mentioned above, the following was obtained:

- bearing capacity coefficients:

$$N_{qd} = 28.99$$



$$N_{\gamma d} = 40.26$$

- correction factors for load inclination:

$$\zeta_q = (1 - E_{Sd}/E_{Nd})^m = 0.292 \quad m = (2 + B'/L)/(1 + B'/L) = 1.55$$

$$\zeta_\gamma = (1 - E_{Sd}/E_{Nd})^{m+1} = 0.133$$

- correction factors for foundation shape:

		<b>Ponte sullo Stretto di Messina</b> <b>PROGETTO DEFINITIVO</b>		
Sicily Anchor Block – earthquake induced displacements and safety against ultimate limit states, Annex	<i>Codice documento</i> PF0064_F0_ANX	<i>Rev</i> F0	<i>Data</i> 20/06/2011	

$$\xi_q = 1 + (B'/L) \cdot \tan \varphi'_d = 1.54$$

$$\xi_\gamma = 1 - 0.4 \times (B'/L) = 0.68$$

– correction factors for inclination of foundation plane ( $\varepsilon = 15.2^\circ$ ):

$$\alpha_q = \alpha_\gamma = (1 - \varepsilon \tan \varphi'_d)^2 = 0.676$$

At the site of Sicily anchor block the minimum thickness of soil adjacent to the anchor block is  $D = 20$  m and the water level is slightly below the deepest point of the foundation plane. For the calculations it was assumed  $z_w = 20$  m =  $D$ ; hence no water pressure is to be considered in calculating  $q'$ .

The unit weight of the soil below the foundation plane was conservatively assumed to be equal to the submerged unit weight  $\gamma' = \gamma - \gamma_w = 10$  kN/m<sup>3</sup>.

The computed ultimate effective bearing pressure is:

$$q'_{ultd} = 4517 \text{ kPa}$$

Since  $z_w = D$ , it follows that the pore water pressure resultant  $U$  at the foundation plane is equal to zero.

Then, the design bearing resistance is

$$R_{N_d} = \frac{1}{\gamma_R} (q'_{ultd} \cdot B'L + U_{bd}) = 20248 \text{ MN}$$

and the ratio  $\frac{R_{N_d}}{E_{N_d}} = \frac{22091}{6897} = 2.94 \geq 1$ , that satisfies requirements of D.M. 14.01.2008.

		<b>Ponte sullo Stretto di Messina</b> <b>PROGETTO DEFINITIVO</b>		
Sicily Anchor Block – earthquake induced displacements and safety against ultimate limit states, Annex	<i>Codice documento</i> PF0064_F0_ANX	<i>Rev</i> F0	<i>Data</i> 20/06/2011	

## 8 Conclusions

Seismic performance of Sicily anchor block was evaluated using two approaches: the pseudo-static approach, in which the anchor block is assumed to be in a state of limit equilibrium under the action of inertial and static forces, and the displacement-based approach, in which the earthquake-induced displacements of the anchor block are evaluated for a number of input seismic motions. Computations were carried out using the cable forces provided by the tender design that for the ULS load combination result slightly higher than the values obtained from the global IBDAS model (5.8% for the version 3.3b – Table E.3 – and 8% for the version 3.3f – Table F.3), this resulting in a conservative estimate of the behaviour of the Sicilia Anchor Block. In the pseudostatic approach, according to the Italian Building Code (D.M. 14.01.2008), safety of the block against eventual failure mechanisms is ensured comparing the design actions with the design resistances, the first increased and the second reduced by partial factors of safety. In the displacement-based approach, the critical acceleration is first determined through the pseudo-static approach and the cumulative displacement of the potential sliding mass is then evaluated using the sliding block analysis, in which the equation of the relative motion is integrated twice with the critical acceleration used as a reference datum.

For evaluation of safety against sliding, design resistances were computed considering the contributions of the sliding resistance at the base and at the block sides and that of the passive resistance in front of the block.

In the analyses three possible sliding mechanisms were assumed, characterised by angles of inclination  $\alpha = 38^\circ$ ,  $26^\circ$  and  $8^\circ$ . Companion plane strain FE analyses of the anchor block permitted to evaluate that under ULS loading conditions the prevailing inclination of the displacement vectors is in the range  $8^\circ$ - $26^\circ$  so that the second and the third mechanisms were recognised to be the most likely to occur.

As far as the pseudo-static conditions are concerned, both design actions and design resistances were computed using the pseudo-static seismic coefficients given by the Italian building code (D.M. 14.01.2008). The obtained results showed that safety against sliding is adequately satisfied for each of the loading condition provided by the structural analyses of the tender design.

In the displacement-based approach, the earth resistance  $\Delta R$  mobilised in front of the block was assumed to progressively increase with increasing relative displacement  $u$  induced by earthquake loading. In this conditions, its contribution was neglected in the expression of the critical seismic coefficient and was included in the equation of relative motion. The relationship between  $\Delta R$  and



		<b>Ponte sullo Stretto di Messina</b> <b>PROGETTO DEFINITIVO</b>		
Sicily Anchor Block – earthquake induced displacements and safety against ultimate limit states, Annex	<i>Codice documento</i> PF0064_F0_ANX	<i>Rev</i> F0	<i>Data</i> 20/06/2011	

relative displacement was evaluated by best fitting the  $u - \Delta R$  data as obtained from 2D FE analyses in which a uniform horizontal displacements are applied to an ideal smooth wall.

Earthquake-induced displacements were computed using 30 input accelerograms. The horizontal component of the selected acceleration time histories was scaled to 0.58 g, while the vertical component was scaled either by the same factor used for the corresponding horizontal component, or to 0.58 g as well. Computation were repeated assuming both directions of applications of the horizontal accelerograms.

The results show that the earthquake-induced displacements decrease with decreasing inclination of the sliding mechanism, the maximum displacement being equal to 1 mm for mechanism 2 ( $\alpha = 26^\circ$ ) and equal to 33 mm for mechanism 3 ( $\alpha = 8^\circ$ ). Two comparative analyses carried out under conservative hypotheses provided maximum values of the earthquake-induced displacements in the range 25 – 58 mm.

Finally, bearing capacity and safety against rotation were estimated following the prescriptions of D.M. 14.01.2008, the results showing that both the requirements are satisfied for the considered loading conditions.

		<b>Ponte sullo Stretto di Messina</b> <b>PROGETTO DEFINITIVO</b>		
Sicily Anchor Block – earthquake induced displacements and safety against ultimate limit states, Annex	<i>Codice documento</i> PF0064_F0_ ANX		<i>Rev</i> F0	<i>Data</i> 20/06/2011

## 9 Figures

		<b>Ponte sullo Stretto di Messina</b> <b>PROGETTO DEFINITIVO</b>		
Sicily Anchor Block – earthquake induced displacements and safety against ultimate limit states, Annex	<i>Codice documento</i> PF0064_F0_ANX		<i>Rev</i> F0	<i>Data</i> 20/06/2011

		<b>Ponte sullo Stretto di Messina</b> PROGETTO DEFINITIVO		
Sicily Anchor Block – earthquake induced displacements and safety against ultimate limit states, Annex	<i>Codice documento</i> PF0064_F0_ANX	<i>Rev</i> F0	<i>Data</i> 20/06/2011	

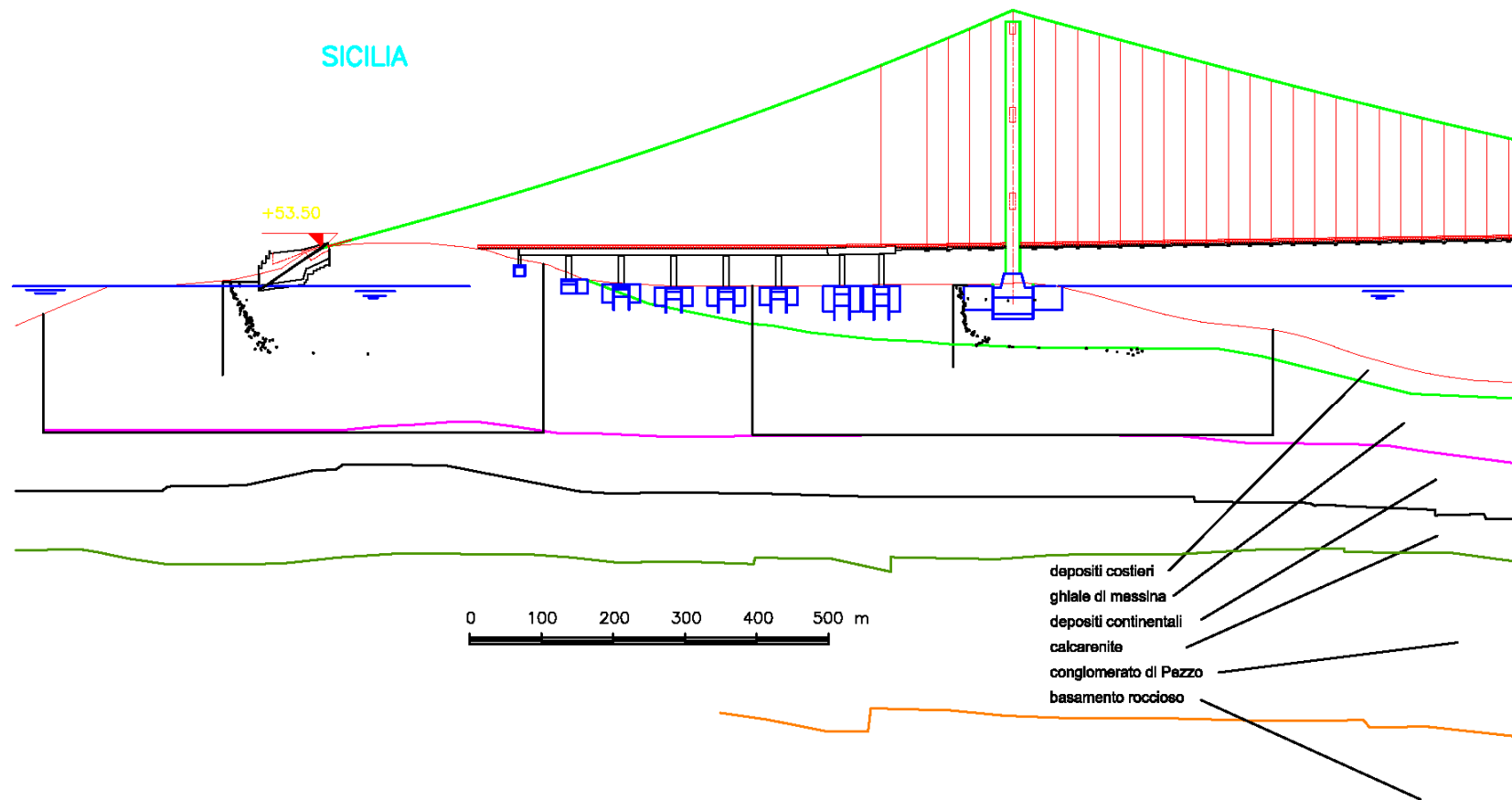




Figure 2.1. Soil profile on Sicilian shore of Messina Strait

		<b>Ponte sullo Stretto di Messina</b> <b>PROGETTO DEFINITIVO</b>		
Sicily Anchor Block – earthquake induced displacements and safety against ultimate limit states, Annex	Codice documento PF0064_F0_ANX	Rev F0	Data 20/06/2011	

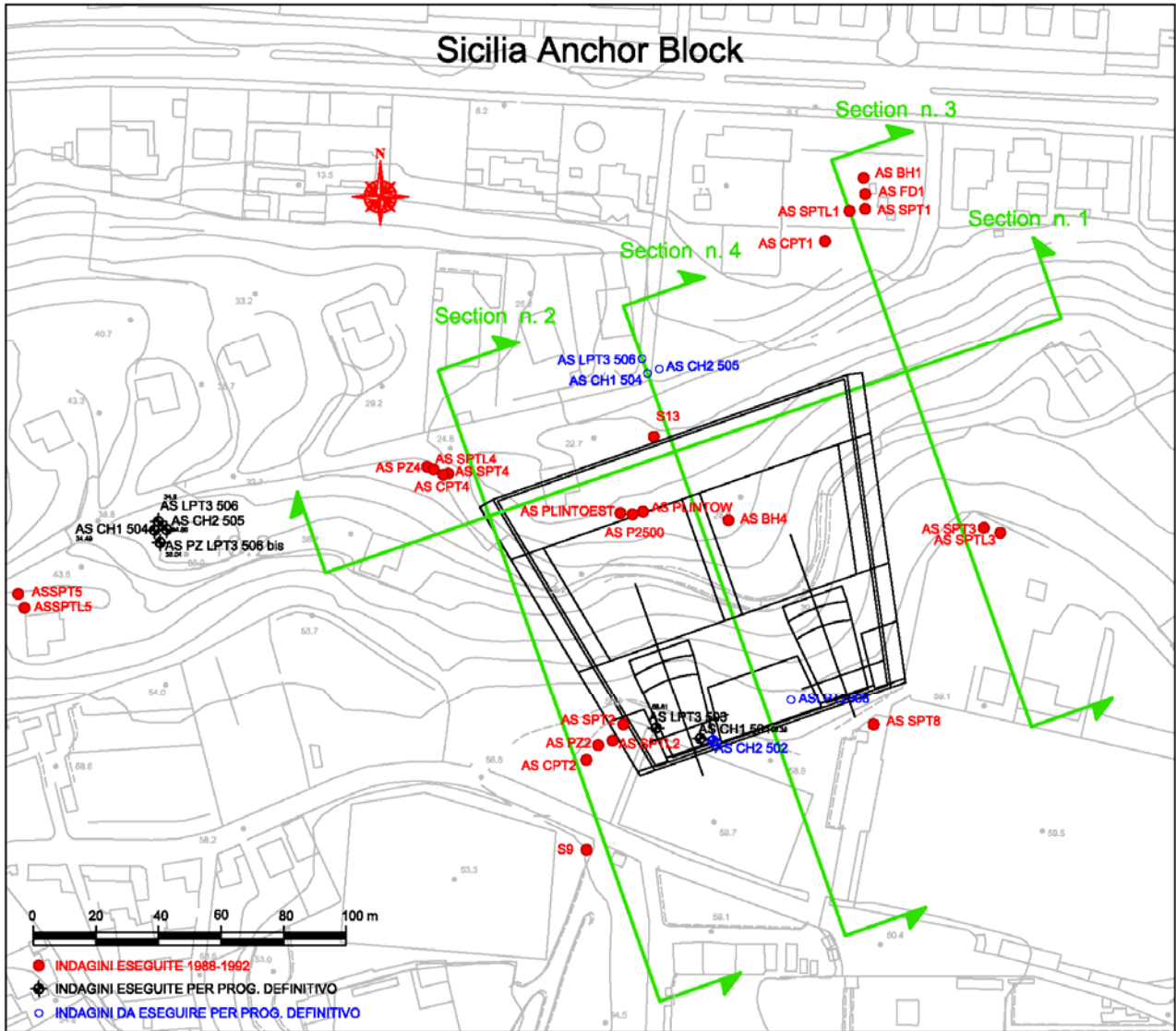


Figure 2.2. Plan view at the location of Sicily Anchor Block



SECTION N. 1

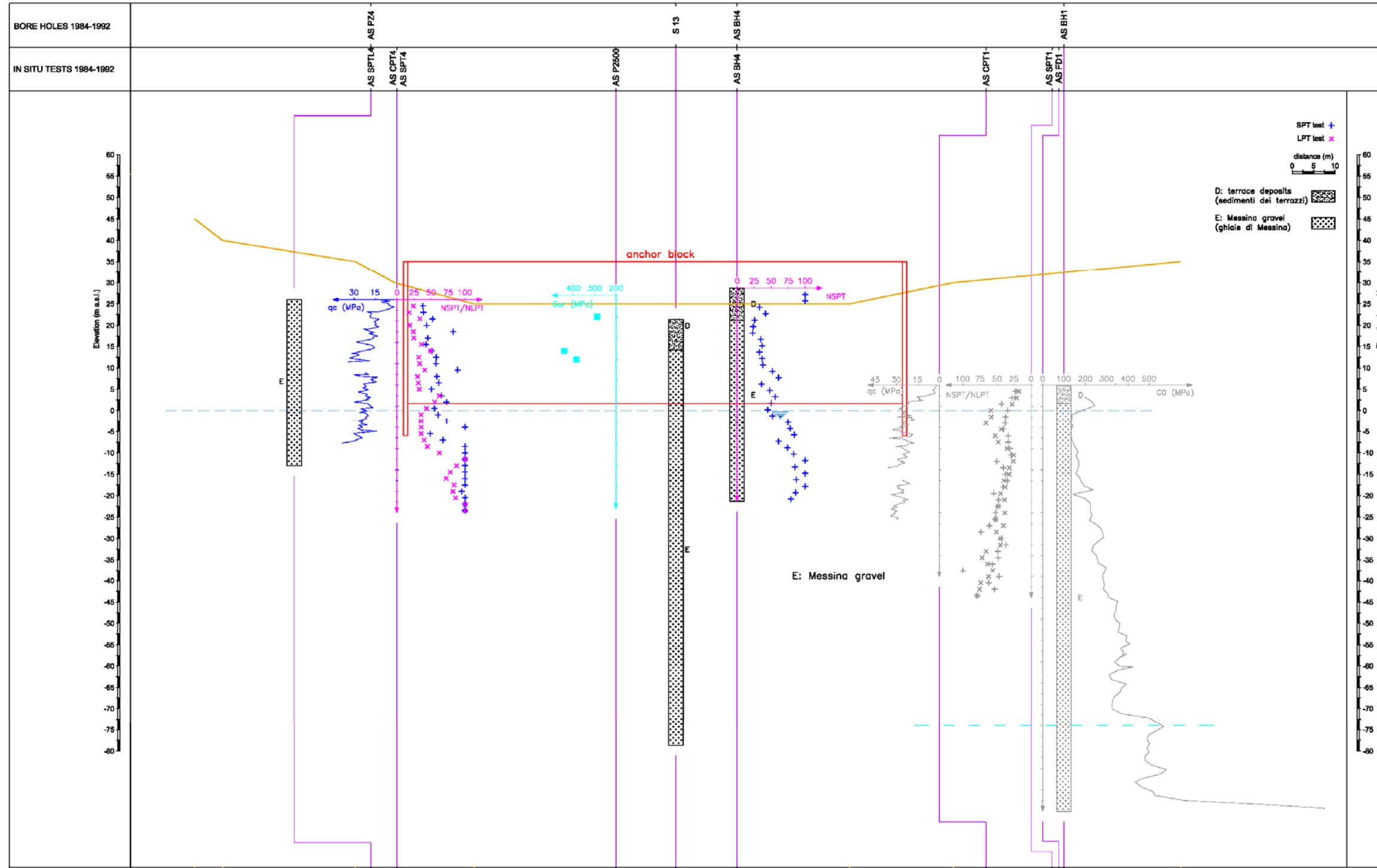


Figure 2.3. Sicily Anchor Block, cross section (section No. 1)

		<p align="center"><b>Ponte sullo Stretto di Messina</b> PROGETTO DEFINITIVO</p>		
<p>Sicily Anchor Block – earthquake induced displacements and safety against ultimate limit states, Annex</p>	<p><i>Codice documento</i> PF0064_F0_ANX</p>	<p><i>Rev</i> F0</p>	<p><i>Data</i> 20/06/2011</p>	

**SECTION N. 2**

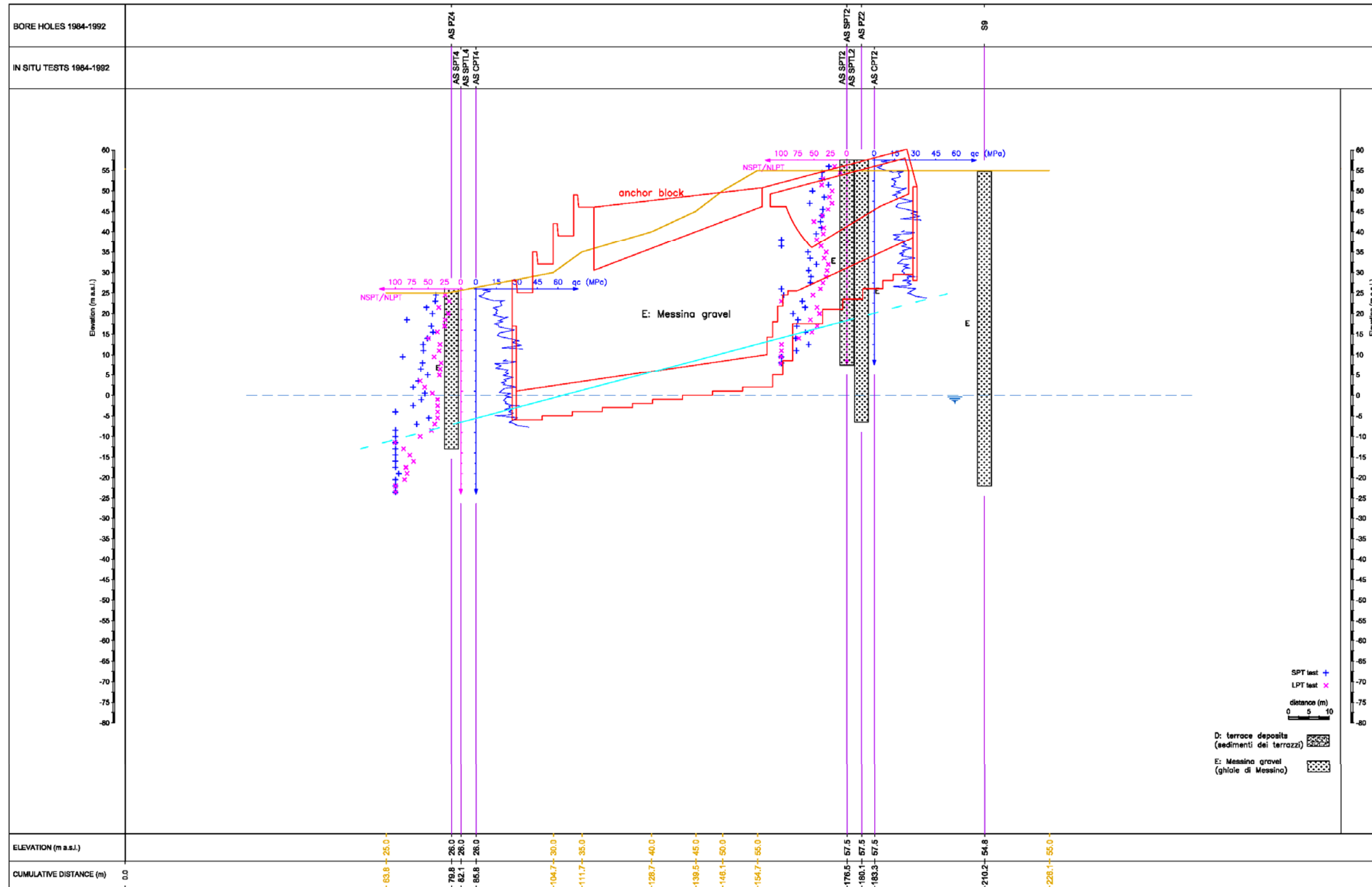




Figure 2.4. Sicily Anchor Block, longitudinal section (Section No. 2)

		<p align="center"><b>Ponte sullo Stretto di Messina</b> PROGETTO DEFINITIVO</p>		
<p>Sicily Anchor Block – earthquake induced displacements and safety against ultimate limit states, Annex</p>	<p><i>Codice documento</i> PF0064_F0_ANX</p>	<p><i>Rev</i> F0</p>	<p><i>Data</i> 20/06/2011</p>	

**SECTION N. 3**

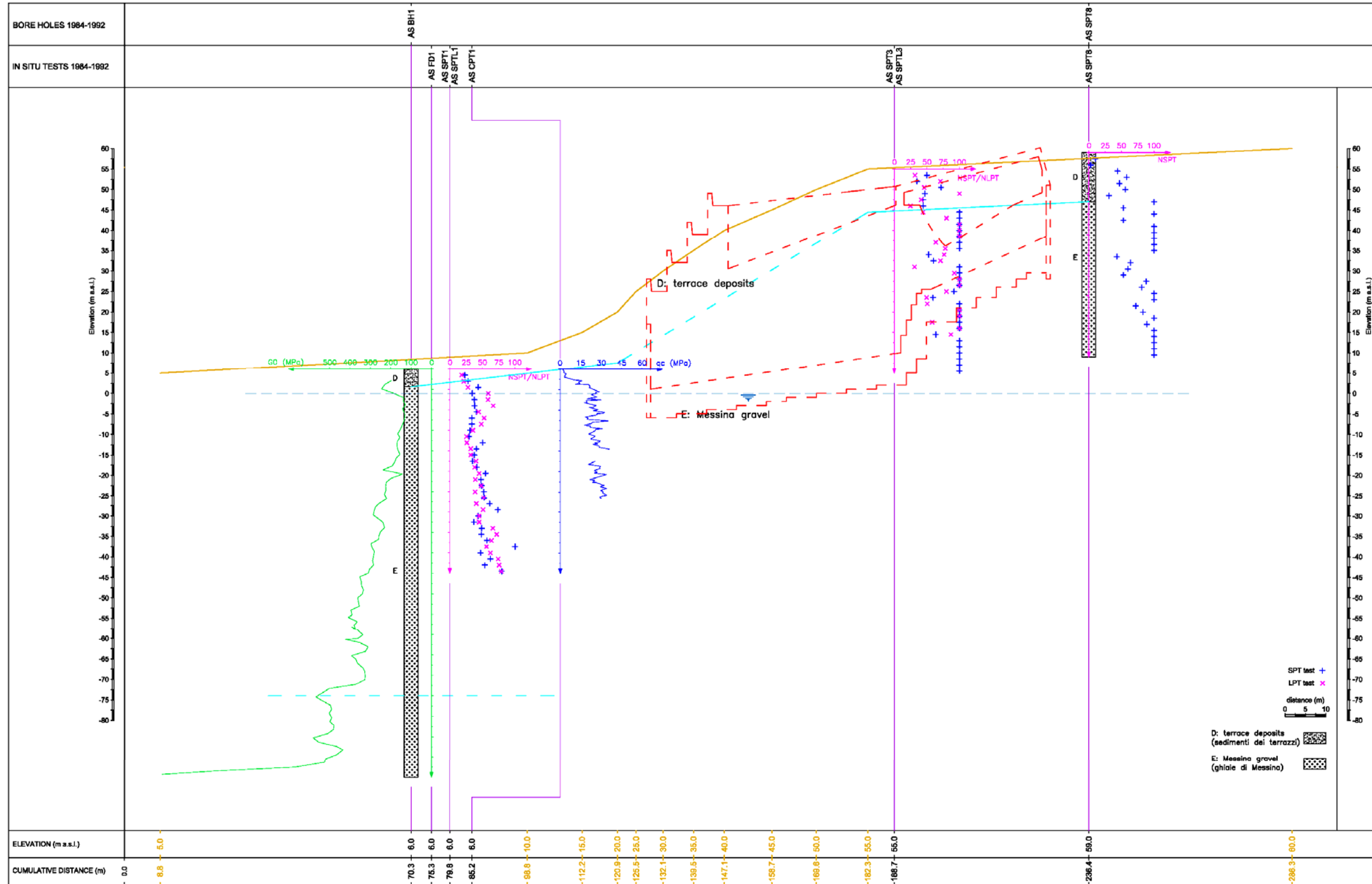


Figure 2.5. Sicily Anchor Block, longitudinal section (Section No. 3)

		<p align="center"><b>Ponte sullo Stretto di Messina</b> PROGETTO DEFINITIVO</p>		
<p>Sicily Anchor Block – earthquake induced displacements and safety against ultimate limit states, Annex</p>	<p><i>Codice documento</i> PF0064_F0_ANX</p>	<p><i>Rev</i> F0</p>	<p><i>Data</i> 20/06/2011</p>	

SECTION N. 4

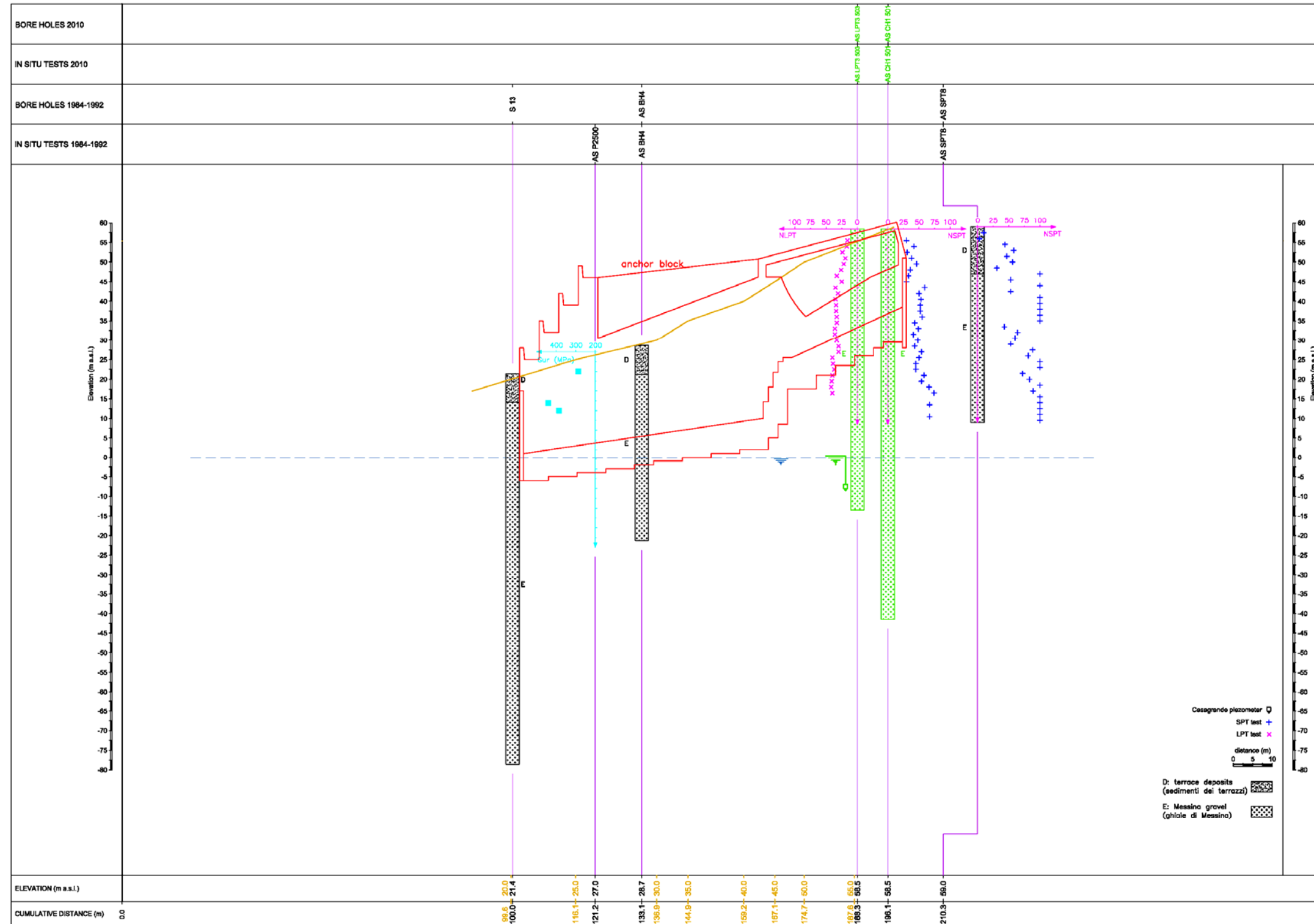




Figure 2.6. Sicily Anchor Block, longitudinal section (Section No. 4)

		<p align="center"><b>Ponte sullo Stretto di Messina</b> PROGETTO DEFINITIVO</p>		
<p>Sicily Anchor Block – earthquake induced displacements and safety against ultimate limit states, Annex</p>	<p><i>Codice documento</i> PF0064_F0_ANX</p>	<p><i>Rev</i> F0</p>	<p><i>Data</i> 20/06/2011</p>	



		<b>Ponte sullo Stretto di Messina</b> <b>PROGETTO DEFINITIVO</b>		
Sicily Anchor Block – earthquake induced displacements and safety against ultimate limit states, Annex		<i>Codice documento</i> PF0064_F0_ANX	<i>Rev</i> F0	<i>Data</i> 20/06/2011

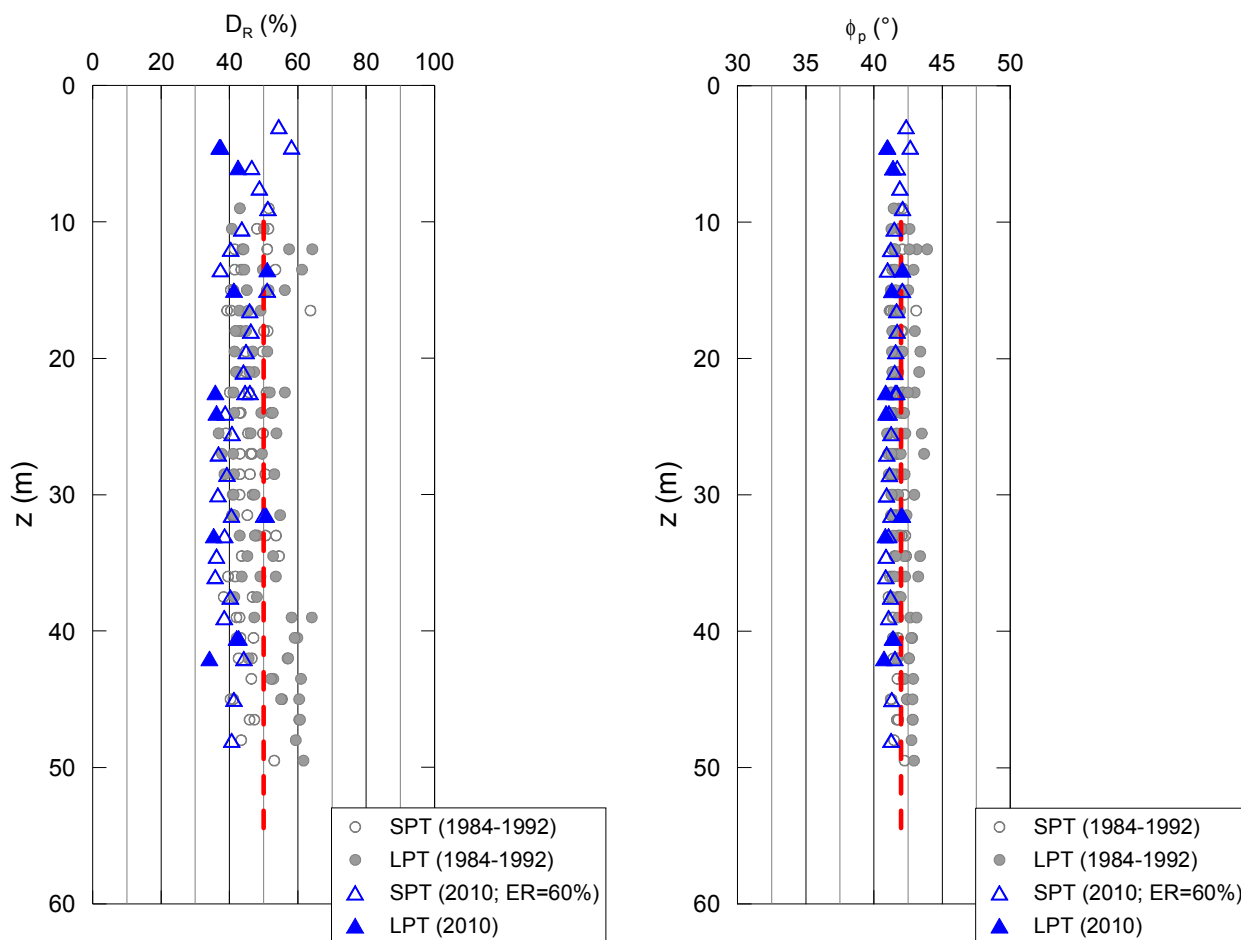




Figure 2.7. Sicily Anchor Block: relative density and angle of shearing resistance from SPT and LPT test results

		<b>Ponte sullo Stretto di Messina</b> <b>PROGETTO DEFINITIVO</b>	
Sicily Anchor Block – earthquake induced displacements and safety against ultimate limit states, Annex	<i>Codice documento</i> PF0064_F0_ANX	<i>Rev</i> F0	<i>Data</i> 20/06/2011

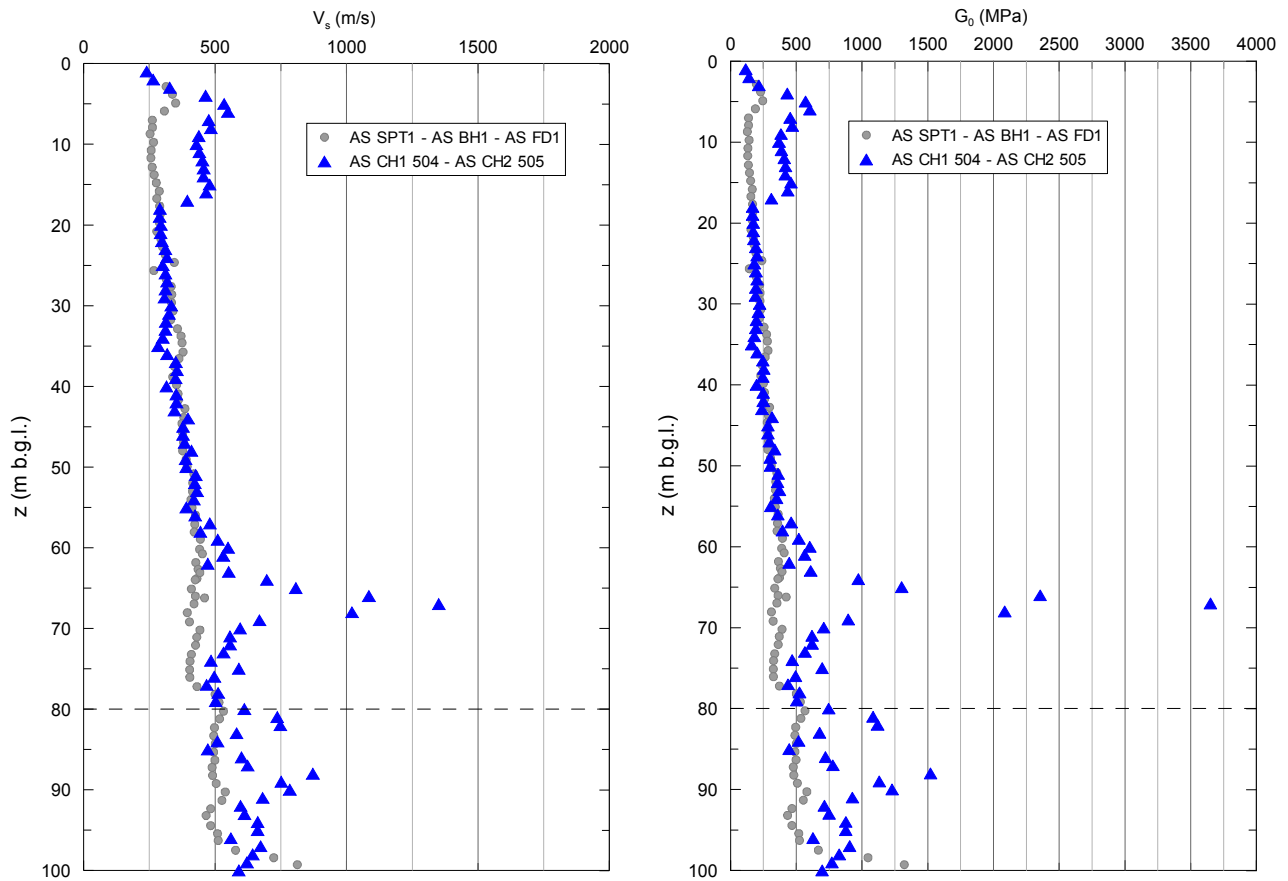


Figure 2.8. Sicily Anchor Block,  $V_s$  and  $G_0$  profiles from cross-hole tests

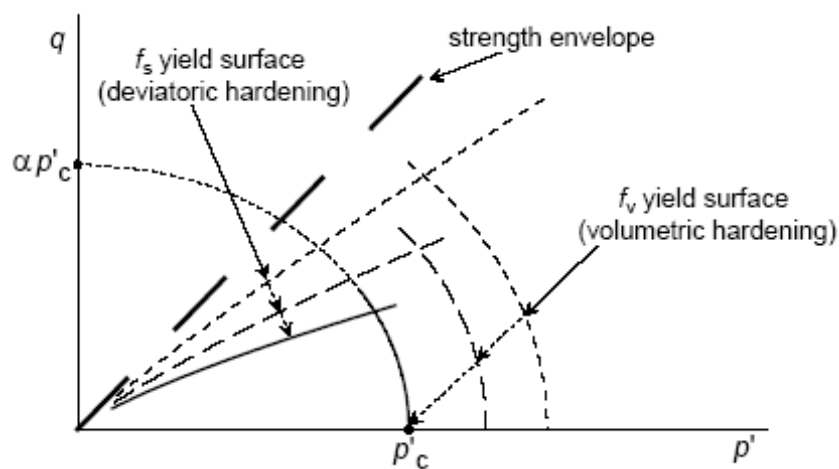




Figure 3.1. Yield surfaces of the Hardening Soil model and their evolution

		<b>Ponte sullo Stretto di Messina</b> <b>PROGETTO DEFINITIVO</b>		
Sicily Anchor Block – earthquake induced displacements and safety against ultimate limit states, Annex	<i>Codice documento</i> PF0064_F0_ANX	<i>Rev</i> F0	<i>Data</i> 20/06/2011	

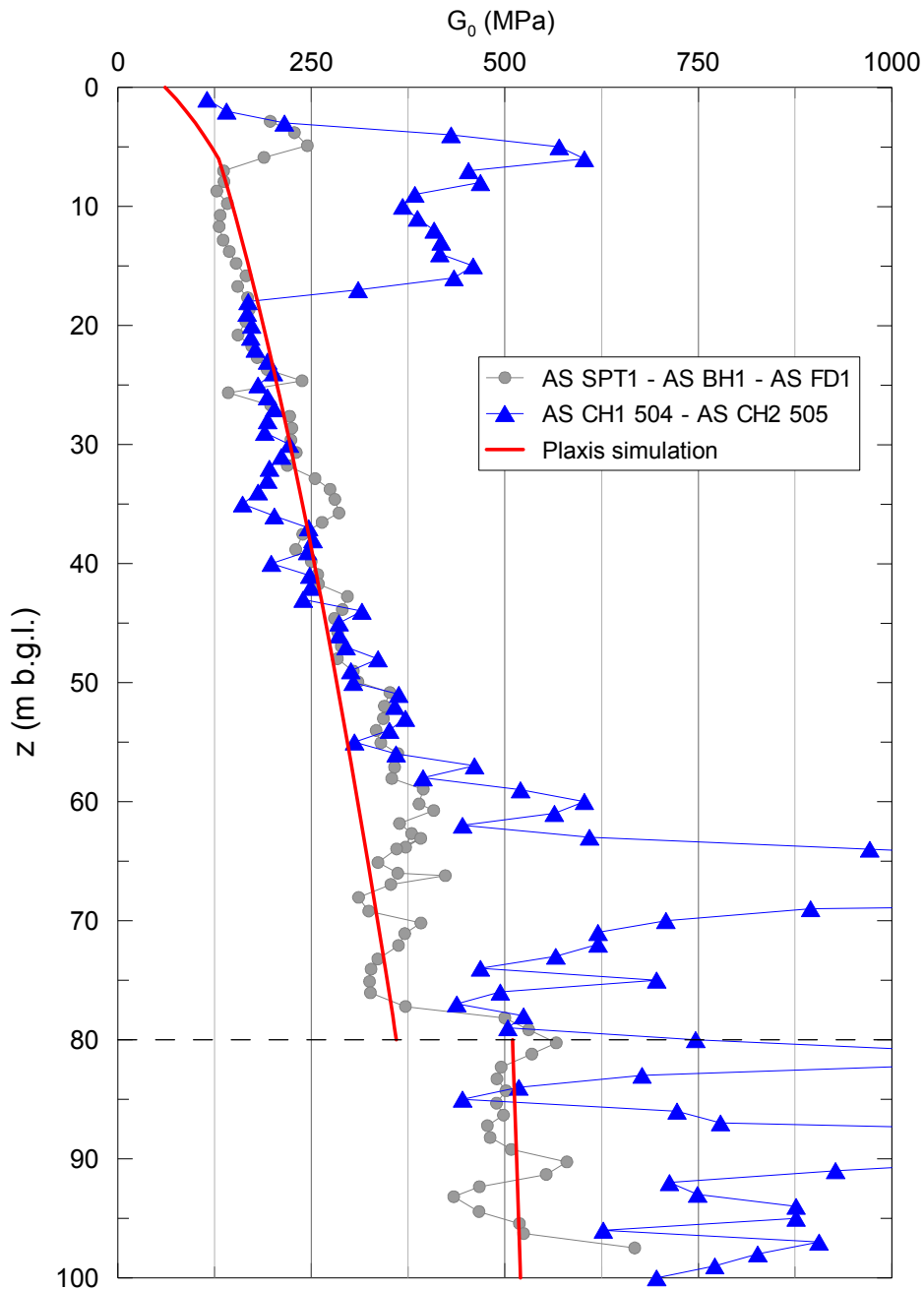




Figure 3.2. Sicily Anchor Block,  $G_0$  profiles from cross-hole tests and HS model prediction

		<b>Ponte sullo Stretto di Messina</b> <b>PROGETTO DEFINITIVO</b>		
Sicily Anchor Block – earthquake induced displacements and safety against ultimate limit states, Annex		<i>Codice documento</i> PF0064_F0_ANX	<i>Rev</i> F0	<i>Data</i> 20/06/2011

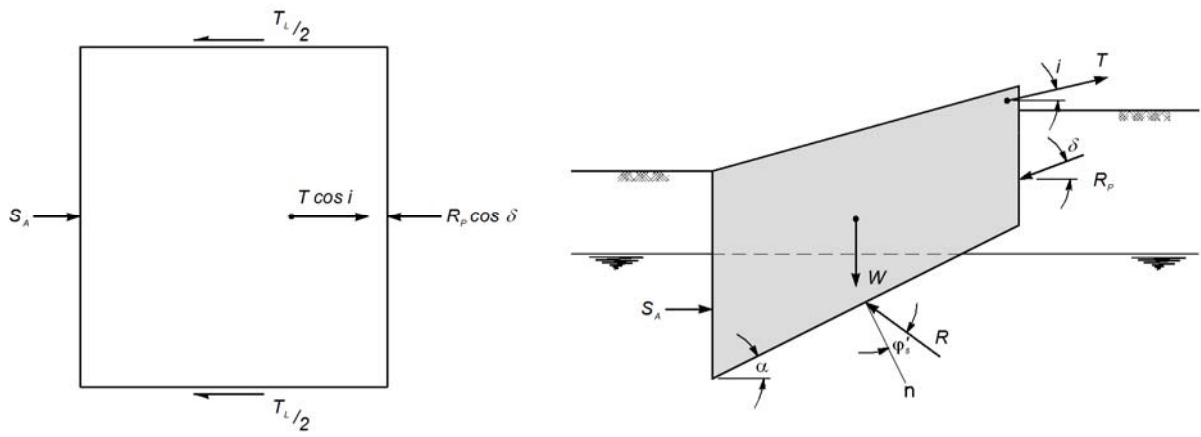


Figure 4.1. Rigid block, static conditions

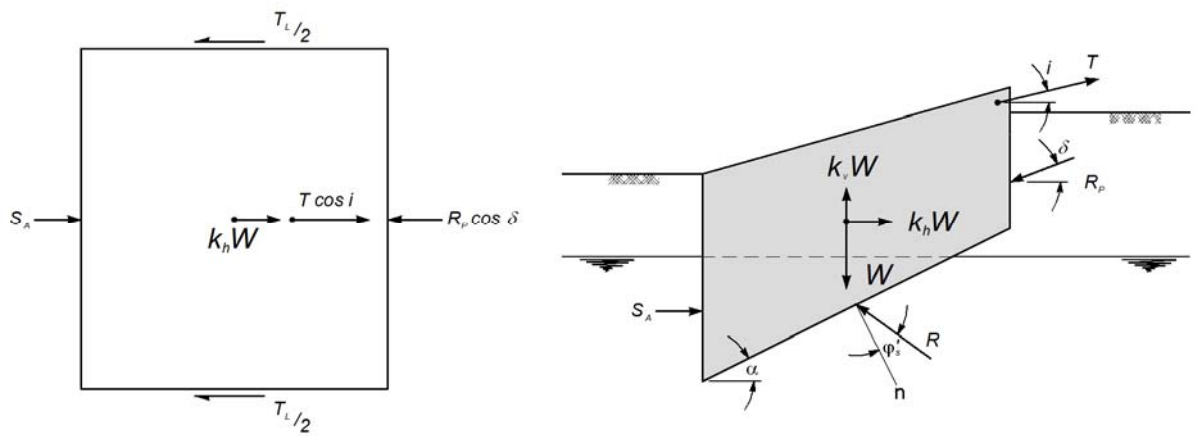




Figure 4.2. Rigid block, pseudo-static conditions

		<b>Ponte sullo Stretto di Messina</b> <b>PROGETTO DEFINITIVO</b>		
Sicily Anchor Block – earthquake induced displacements and safety against ultimate limit states, Annex		<i>Codice documento</i> PF0064_F0_ANX	<i>Rev</i> F0	<i>Data</i> 20/06/2011

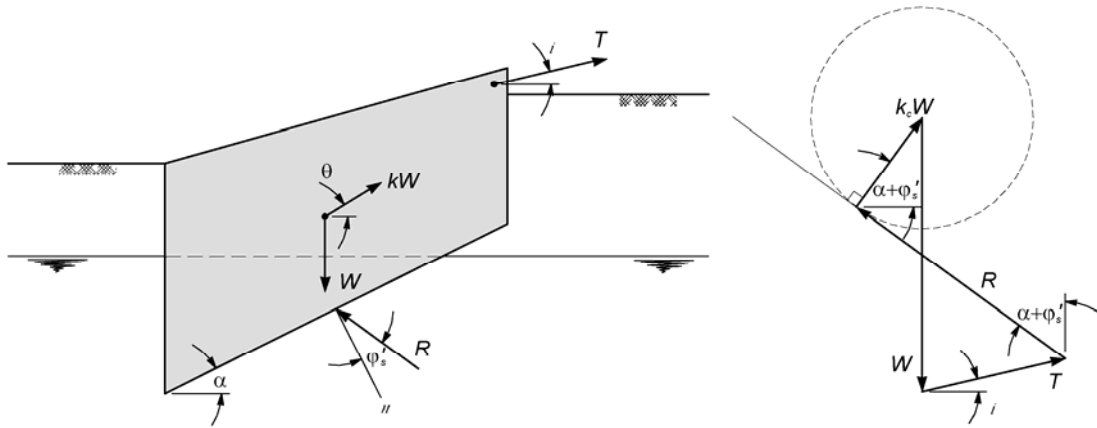


Figure 4.3. Rigid block, critical seismic coefficient

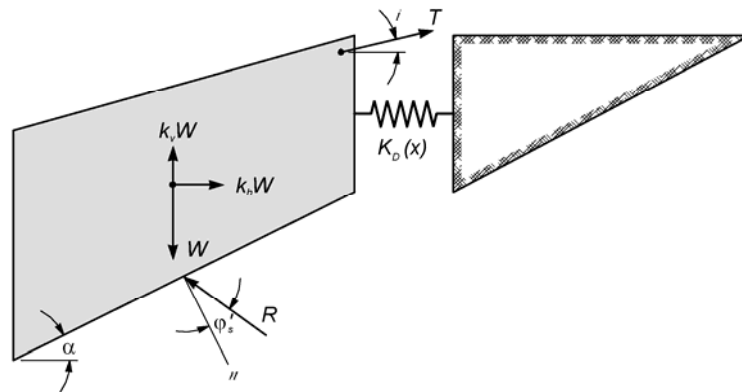


Figure 4.4. Rigid block, displacement dependent passive earth resistance

		<b>Ponte sullo Stretto di Messina</b> <b>PROGETTO DEFINITIVO</b>		
Sicily Anchor Block – earthquake induced displacements and safety against ultimate limit states, Annex		<i>Codice documento</i> PF0064_F0_ANX	<i>Rev</i> F0	<i>Data</i> 20/06/2011

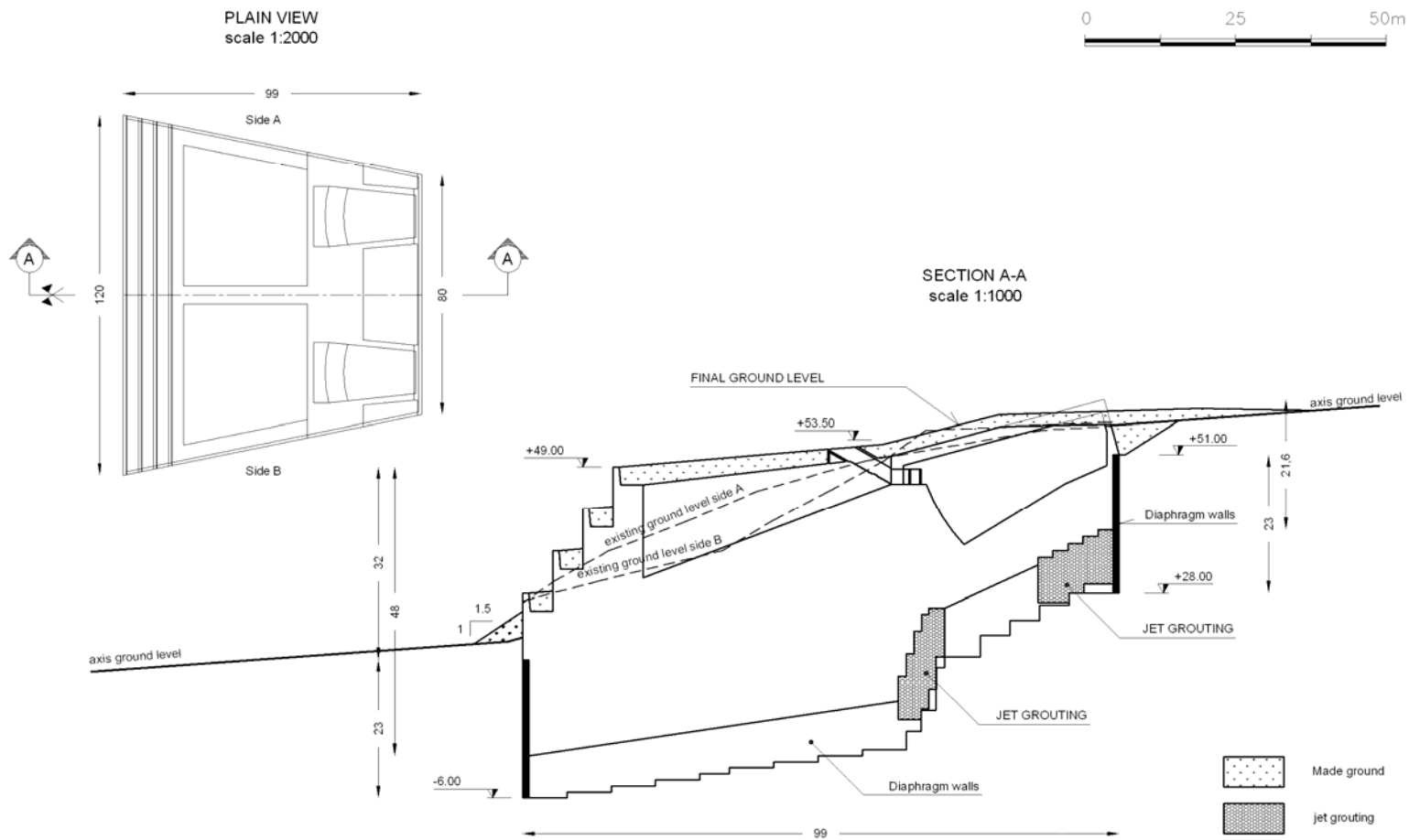




Figure 5.1. Plan view and cross section of Sicily anchor block

		<b>Ponte sullo Stretto di Messina</b> <b>PROGETTO DEFINITIVO</b>		
Sicily Anchor Block – earthquake induced displacements and safety against ultimate limit states, Annex	<i>Codice documento</i> PF0064_F0_ANX	<i>Rev</i> F0	<i>Data</i> 20/06/2011	

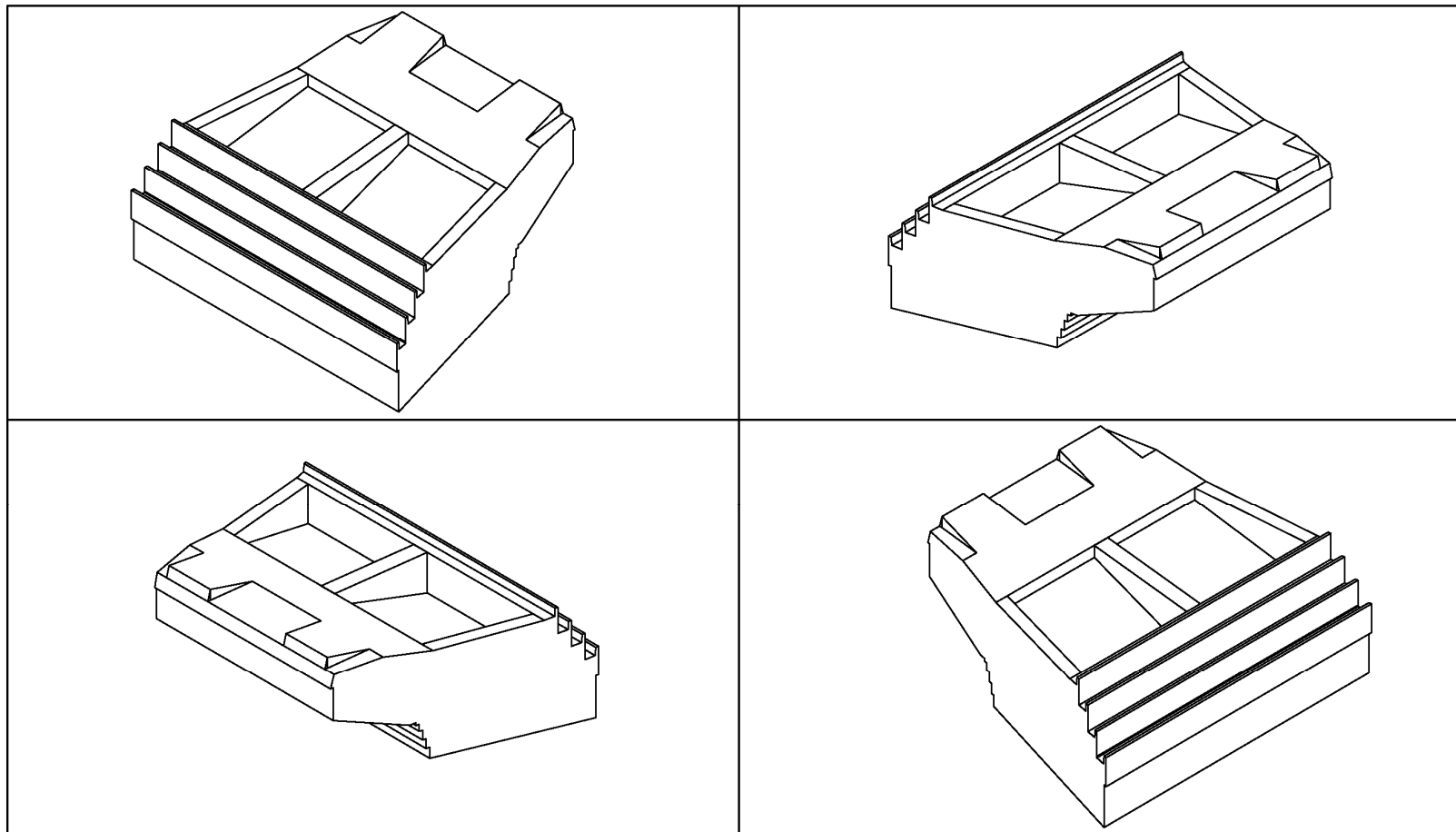


Figure 5.2. Sicily anchor block 3D CAD model

		<b>Ponte sullo Stretto di Messina</b> <b>PROGETTO DEFINITIVO</b>		
Sicily Anchor Block – earthquake induced displacements and safety against ultimate limit states, Annex		<i>Codice documento</i> PF0064_F0_ANX	<i>Rev</i> F0	<i>Data</i> 20/06/2011

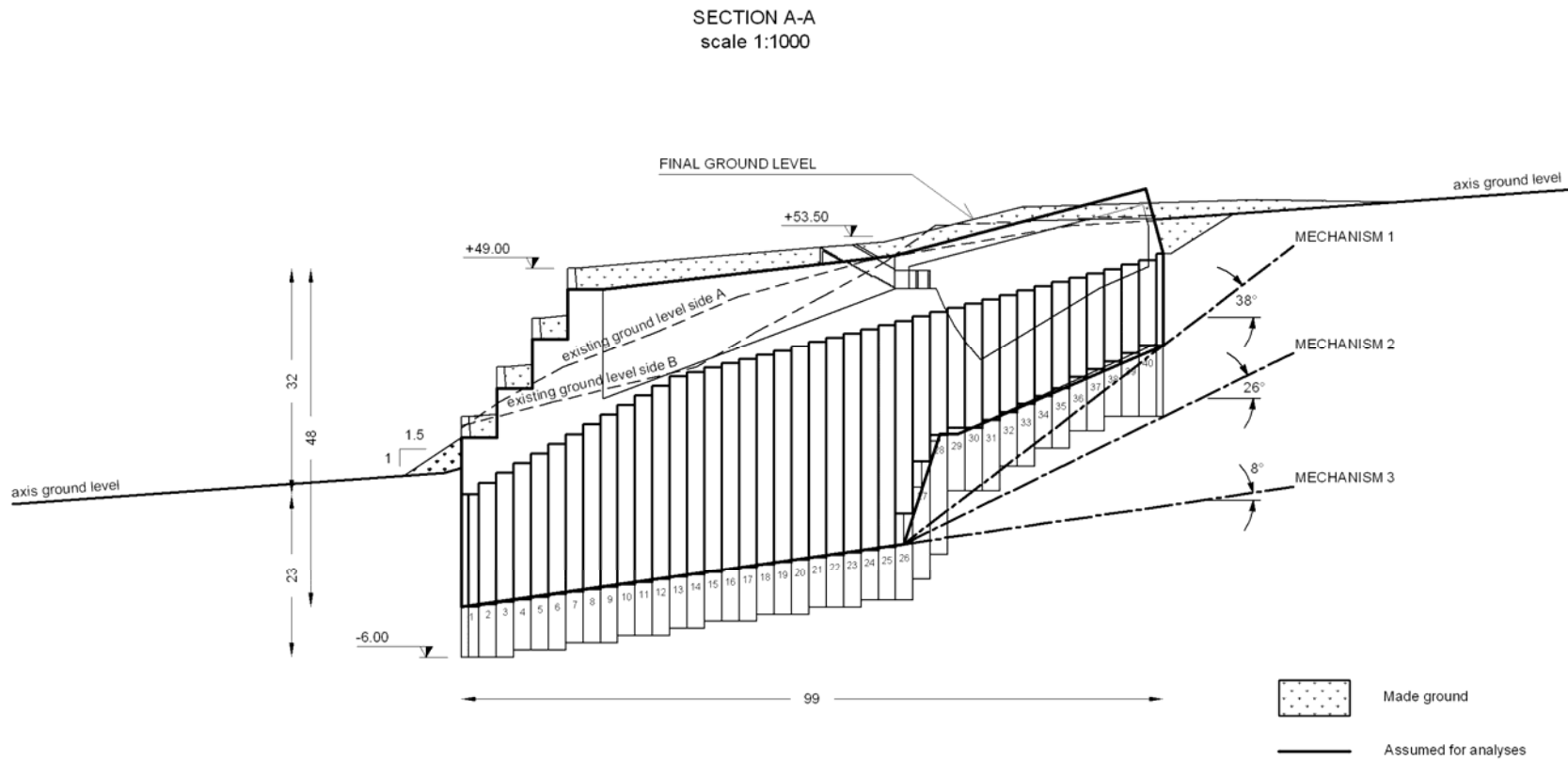




Figure 5.3. Sliding mechanisms



		<b>Ponte sullo Stretto di Messina</b> <b>PROGETTO DEFINITIVO</b>		
Sicily Anchor Block – earthquake induced displacements and safety against ultimate limit states, Annex		<i>Codice documento</i> PF0064_F0_ANX	<i>Rev</i> F0	<i>Data</i> 20/06/2011

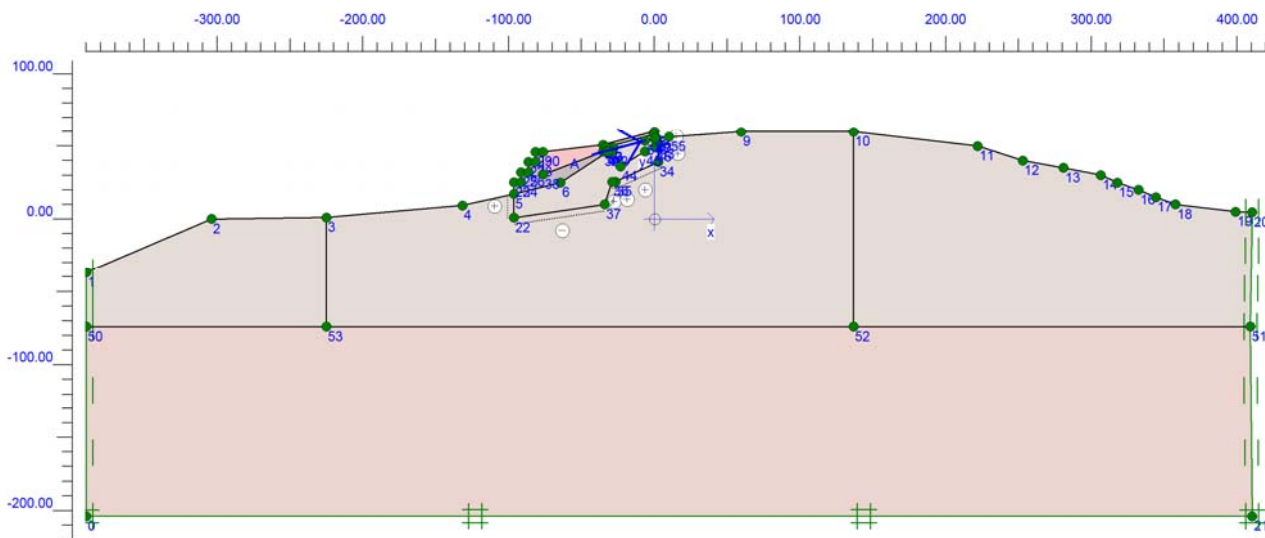


Figure 5.4. Mesh used for plane strain F.E. simulations

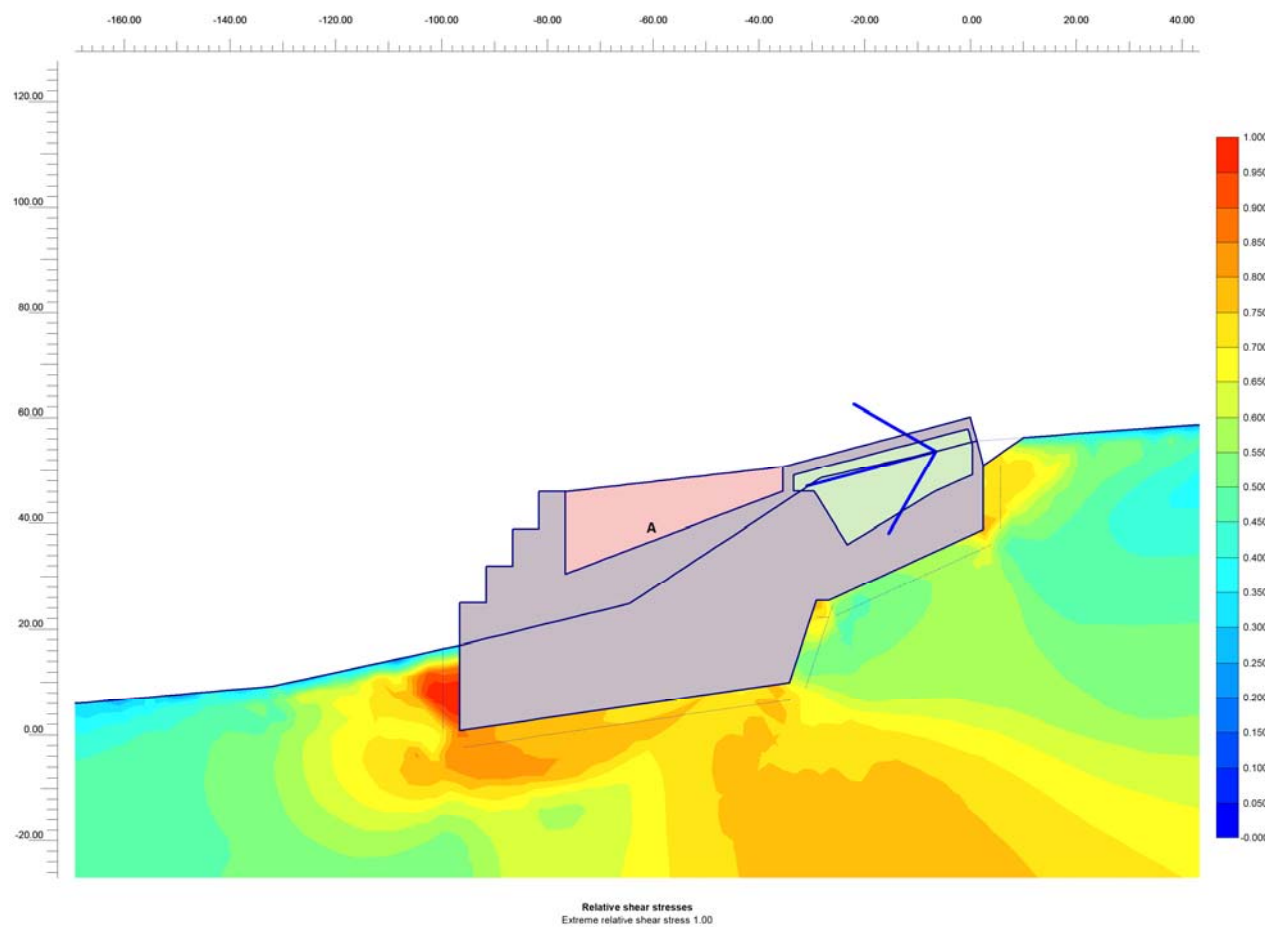




Figure 5.5. Relative shear stress ( $t/t_{max}$ ) contours

		<b>Ponte sullo Stretto di Messina</b> <b>PROGETTO DEFINITIVO</b>		
Sicily Anchor Block – earthquake induced displacements and safety against ultimate limit states, Annex		<i>Codice documento</i> PF0064_F0_ANX	<i>Rev</i> F0	<i>Data</i> 20/06/2011

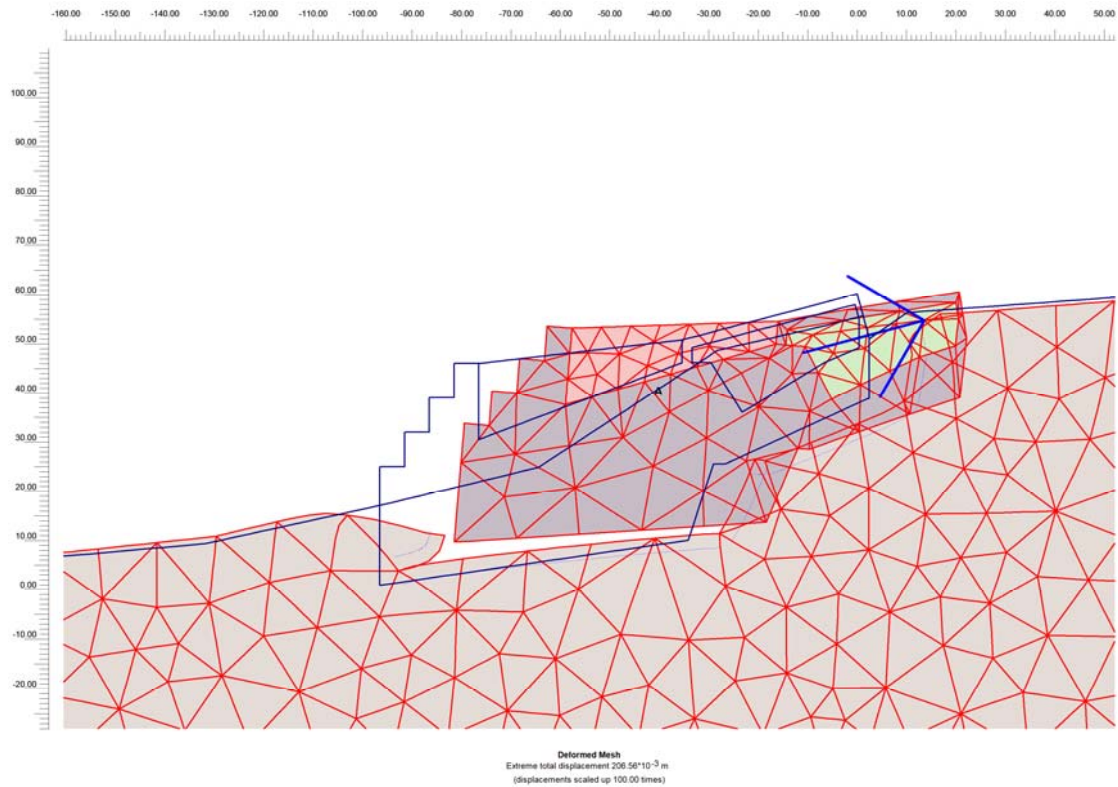


Figure 5.6. Deformed mesh

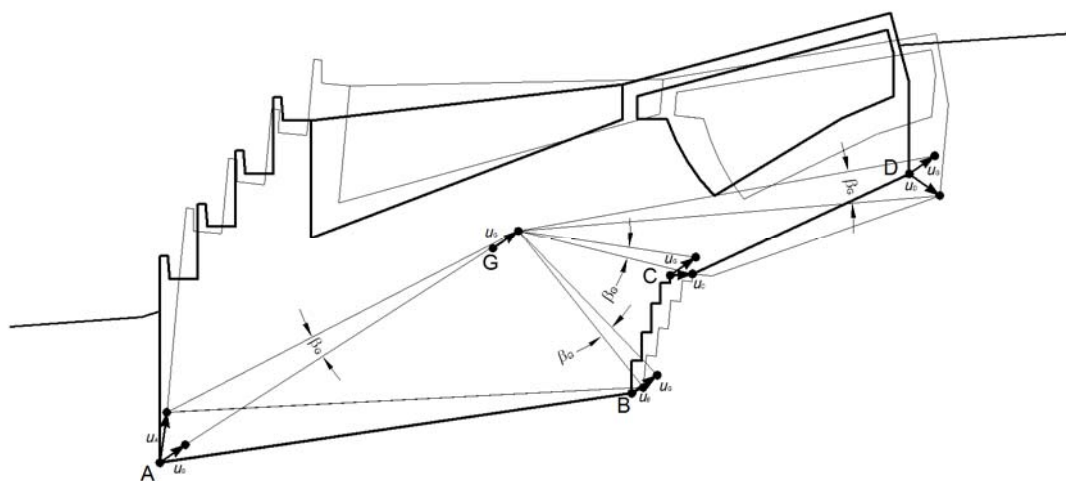




Figure 5.7. Reference displacement points for 2D F.E. simulation results

		<b>Ponte sullo Stretto di Messina</b> <b>PROGETTO DEFINITIVO</b>		
Sicily Anchor Block – earthquake induced displacements and safety against ultimate limit states, Annex	<i>Codice documento</i> PF0064_F0_ANX	<i>Rev</i> F0	<i>Data</i> 20/06/2011	

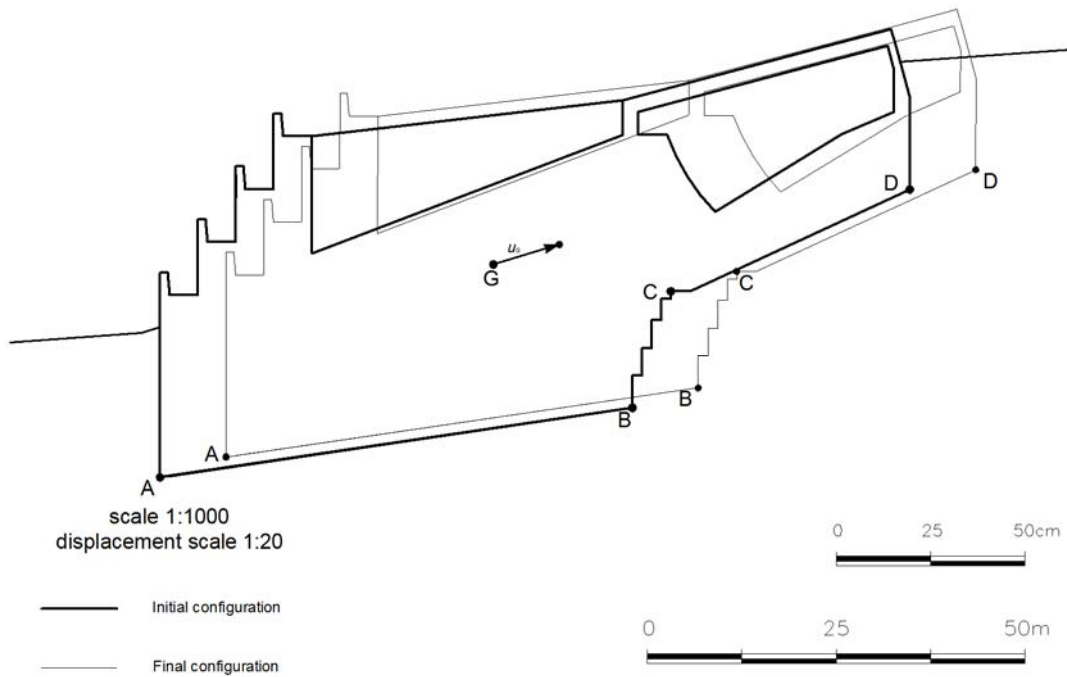


Figure 5.8. 2D F.E. simulations, sliding mechanism

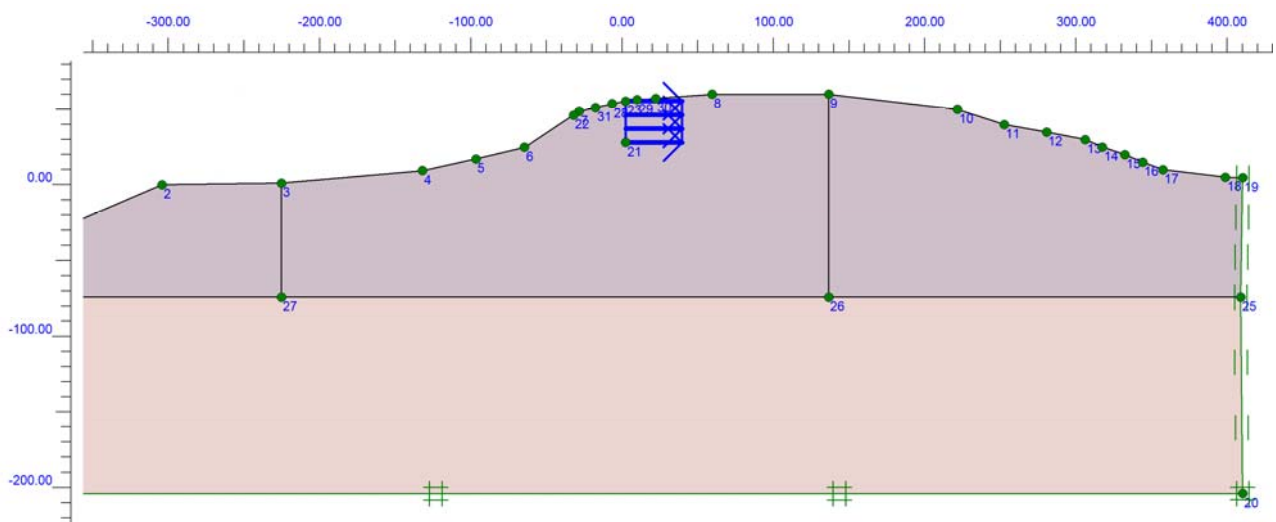


Figure 5.9. Mesh used in plane strain F.E. for simulating the earth resistance in front of the anchor block (mechanism 2)

		<b>Ponte sullo Stretto di Messina</b> <b>PROGETTO DEFINITIVO</b>	
Sicily Anchor Block – earthquake induced displacements and safety against ultimate limit states, Annex	<i>Codice documento</i> PF0064_F0_ANX	<i>Rev</i> F0	<i>Data</i> 20/06/2011

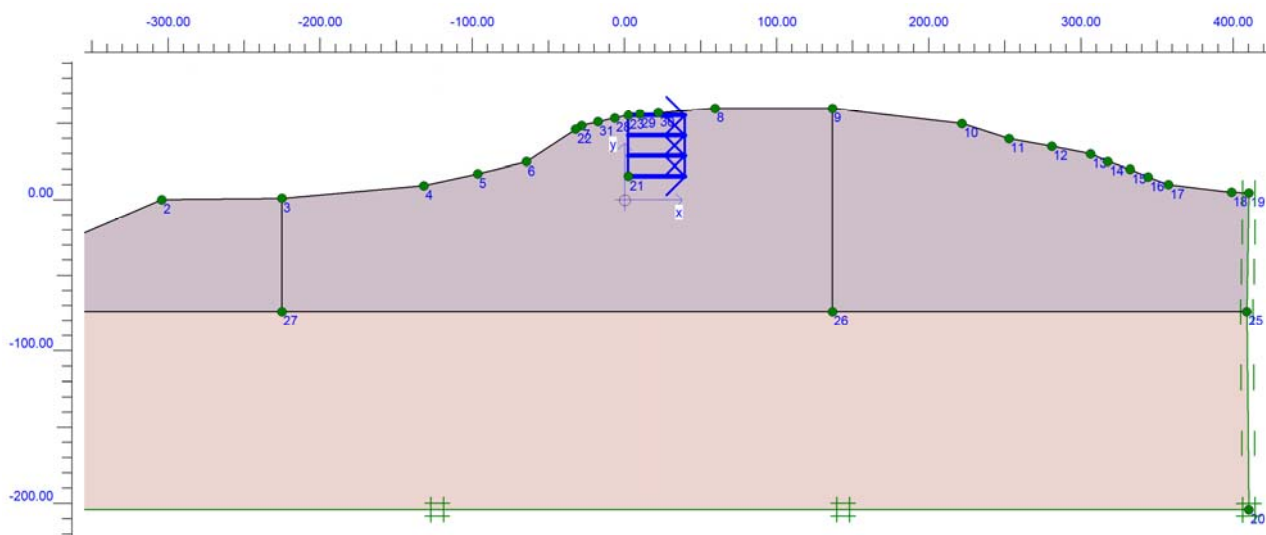




Figure 5.10. Mesh used in plane strain F.E. for simulating the earth resistance in front of the anchor block (mechanism 3)

		<b>Ponte sullo Stretto di Messina</b> <b>PROGETTO DEFINITIVO</b>		
Sicily Anchor Block – earthquake induced displacements and safety against ultimate limit states, Annex		<i>Codice documento</i> PF0064_F0_ANX	<i>Rev</i> F0	<i>Data</i> 20/06/2011

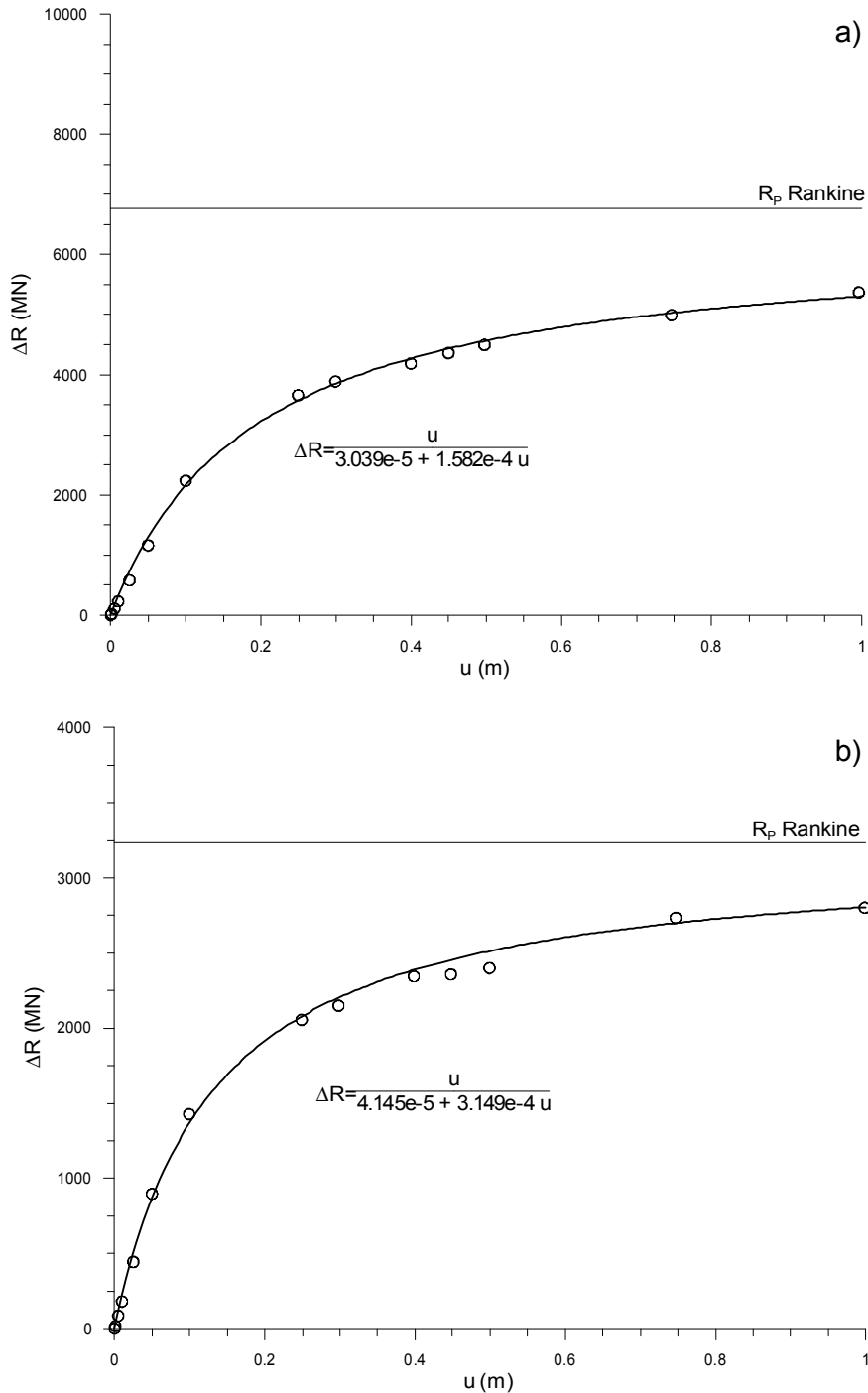


Figure 5.11.  $\Delta R = f(u)$  equation; a) mechanism 3; b) mechanism 2

		<b>Ponte sullo Stretto di Messina</b> <b>PROGETTO DEFINITIVO</b>	
Sicily Anchor Block – earthquake induced displacements and safety against ultimate limit states, Annex	<i>Codice documento</i> PF0064_F0_ANX	<i>Rev</i> F0	<i>Data</i> 20/06/2011

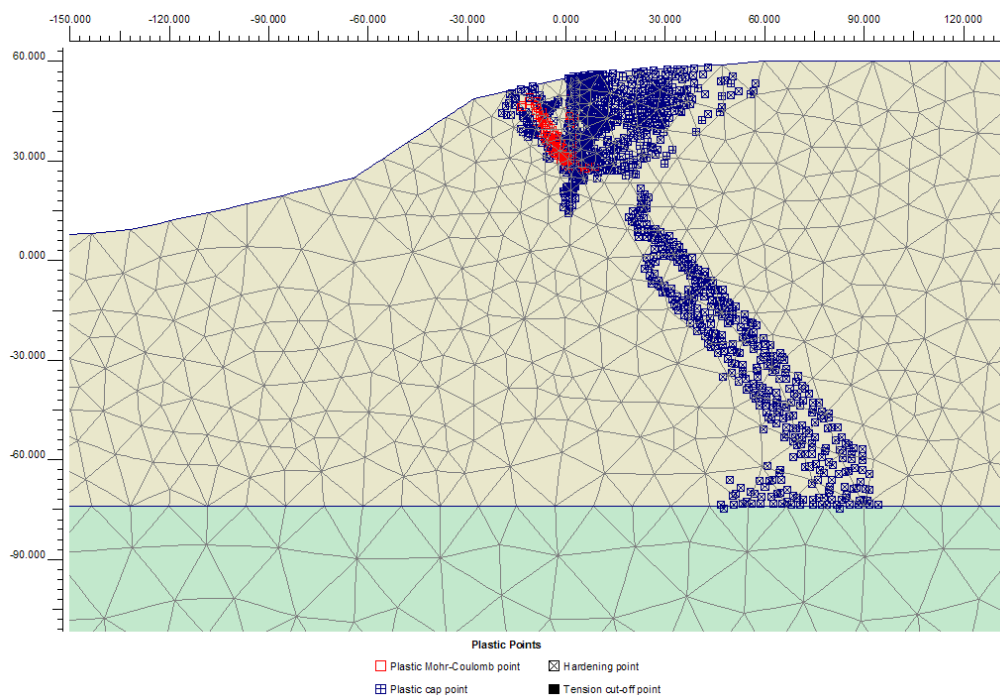


Figure 5.12. 2D F.E. simulation of earth resistance, mechanism 2, plastic points

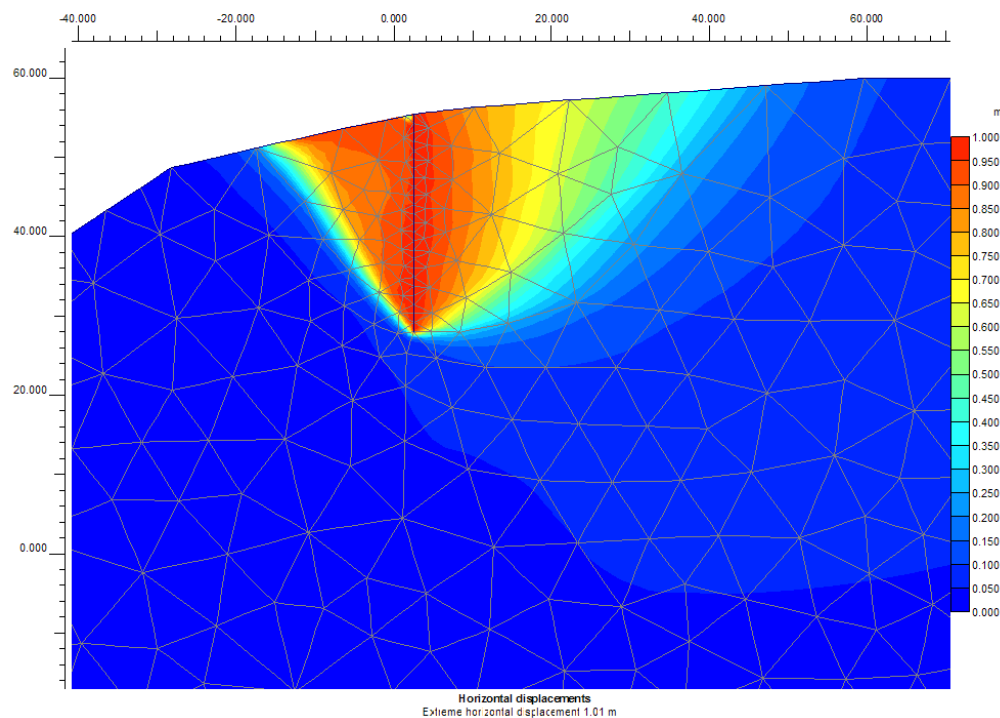


Figure 5.13. 2D F.E. simulation of earth resistance, mechanism 2, horizontal displacements contours

		<b>Ponte sullo Stretto di Messina</b> <b>PROGETTO DEFINITIVO</b>	
Sicily Anchor Block – earthquake induced displacements and safety against ultimate limit states, Annex	<i>Codice documento</i> PF0064_F0_ANX	<i>Rev</i> F0	<i>Data</i> 20/06/2011

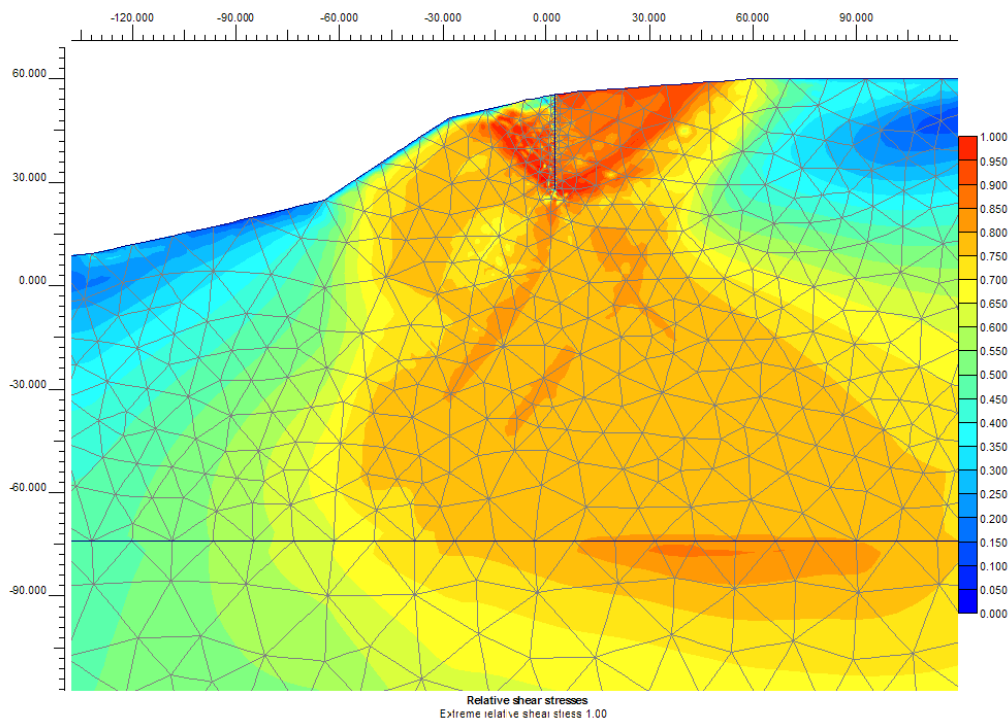


Figure 5.14. 2D F.E. simulation of earth resistance, mechanism 2, relative shear ( $t/t_{max}$ ) contours

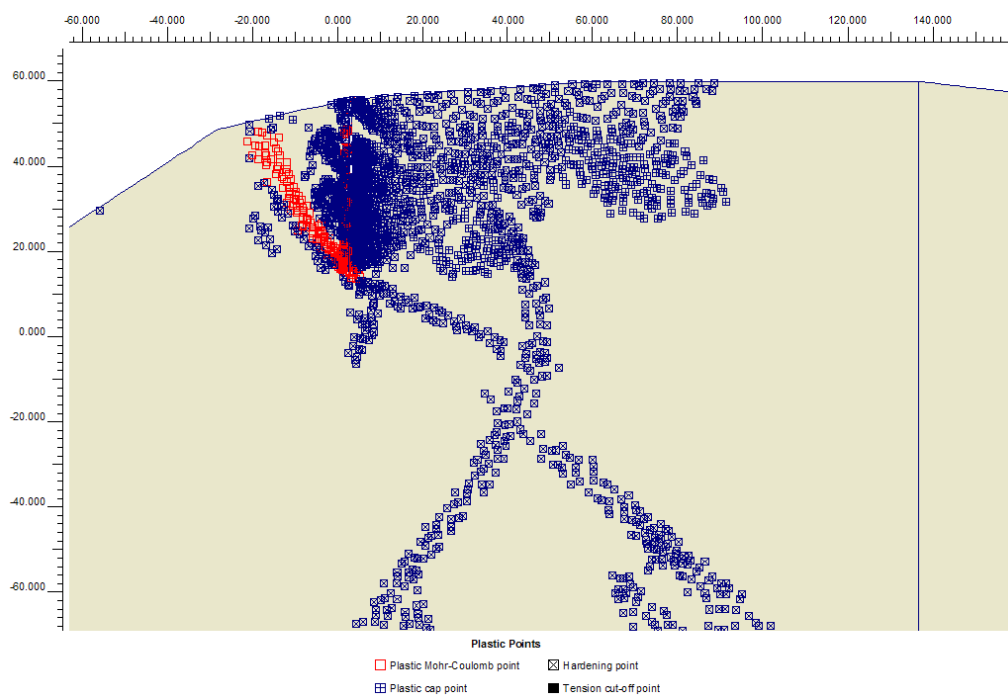




Figure 5.15. 2D F.E. simulation of earth resistance, mechanism 3, plastic points

		<b>Ponte sullo Stretto di Messina</b> <b>PROGETTO DEFINITIVO</b>		
Sicily Anchor Block – earthquake induced displacements and safety against ultimate limit states, Annex		<i>Codice documento</i> PF0064_F0_ANX	<i>Rev</i> F0	<i>Data</i> 20/06/2011

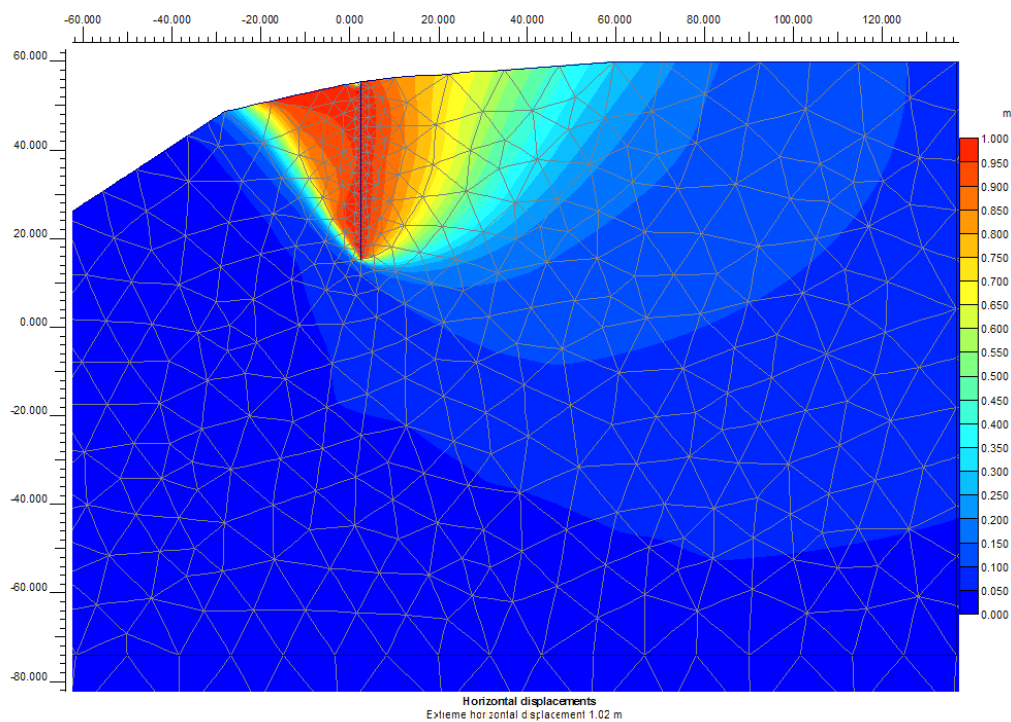


Figure 5.16 2D F.E. simulation of earth resistance, mechanism 3, horizontal displacements contours

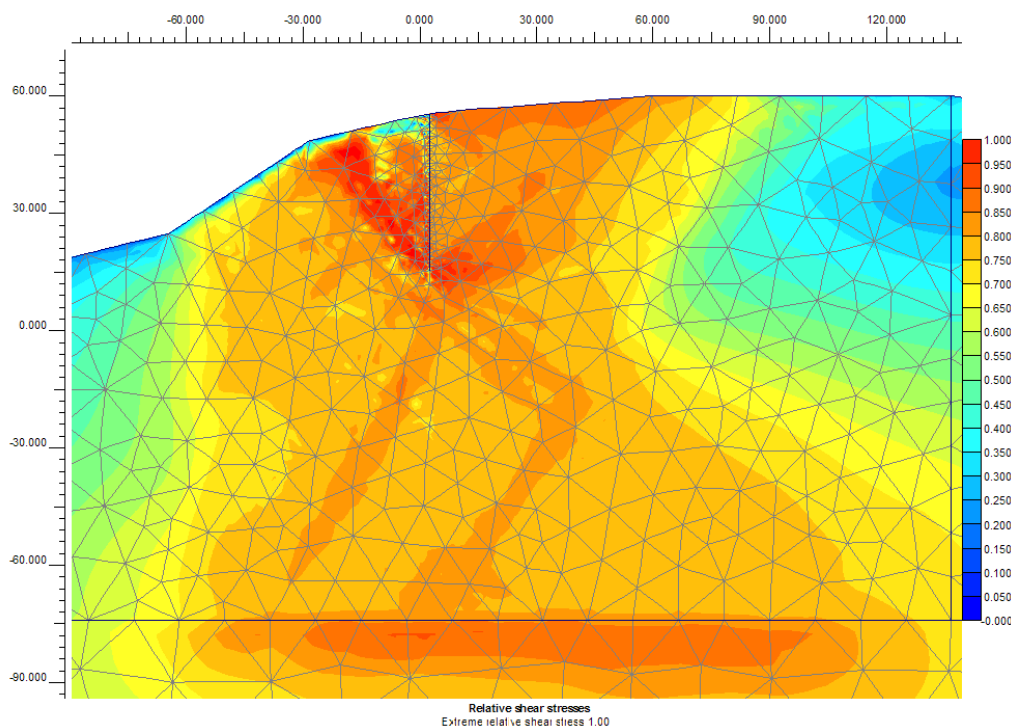


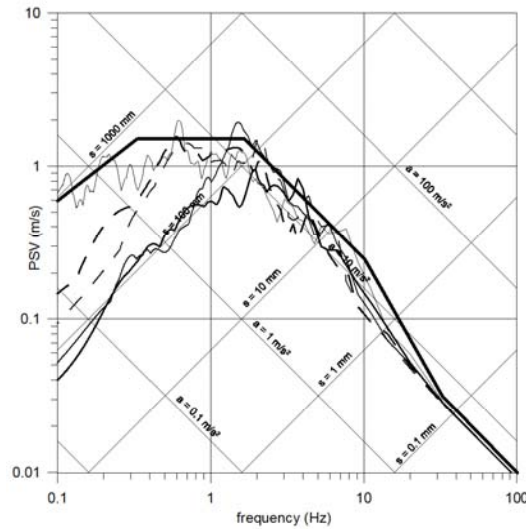


Figure 5.17. 2D F.E. simulation of earth resistance, mechanism 3, relative shear ( $t/t_{max}$ ) contours



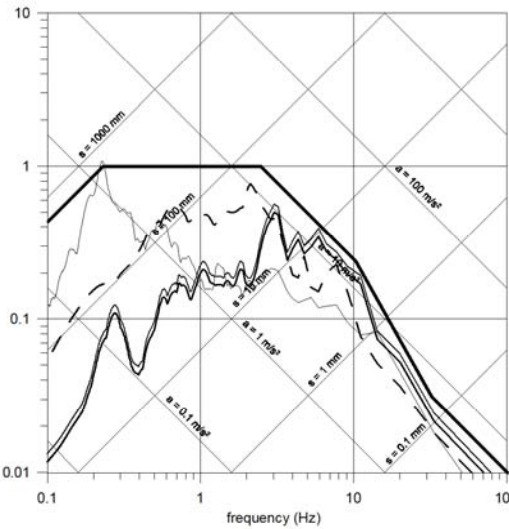
		<b>Ponte sullo Stretto di Messina</b> <b>PROGETTO DEFINITIVO</b>		
Sicily Anchor Block – earthquake induced displacements and safety against ultimate limit states, Annex	<i>Codice documento</i> PF0064_F0_ANX	<i>Rev</i> F0	<i>Data</i> 20/06/2011	

Elastic response spectra, horizontal components damping 5%, scaled to 0.58g



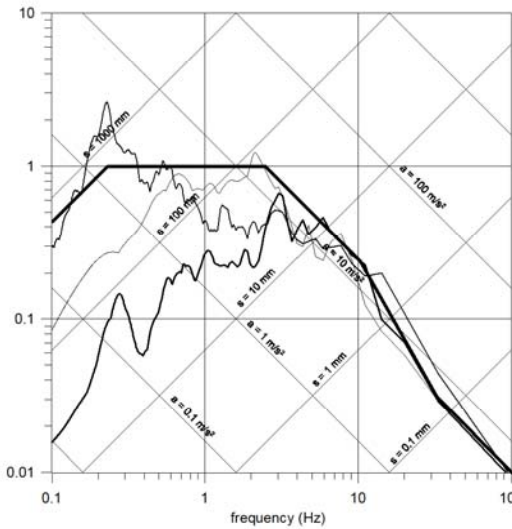
- Design response spectrum, hor. comp.
- Friuli 76 TOLXC
- Friuli 76 TOLYC
- Imperial Valley 79 DLT352
- - Kobe 95 TAZ000
- - Kobe 95 TAZ090

Elastic response spectra, vertical components damping 5%, scaled by the same factor of the corresponding horizontal components





- Design response spectrum, vert. comp.
- Friuli 76 TOLZC S=1.6246
- Friuli 76 TOLZC S=1.8354
- Imperial Valley 79 DLTDW S=1.6524
- - Kobe 95 TAZUP S=0.8357
- - Kobe 95 TAZUP S=0.8369

Elastic response spectra, vertical components damping 5%, scaled to 0.58g

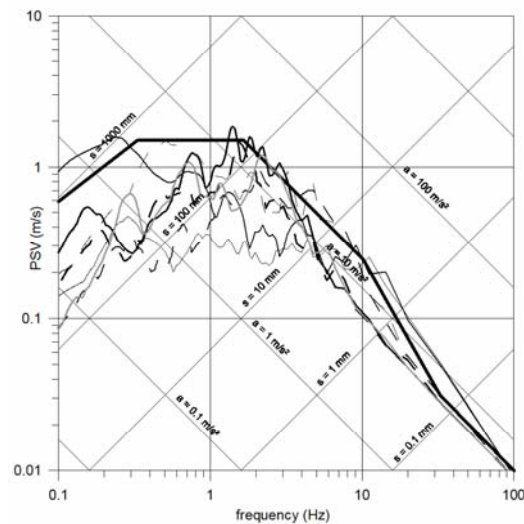


- Design response spectrum, vert. comp.
- Friuli 76 TOLZC
- Imperial Valley 79 DLTDW
- Kobe 95 TAZUP

Figure 5.18. Elastic response spectra of the accelerograms used in the analyses

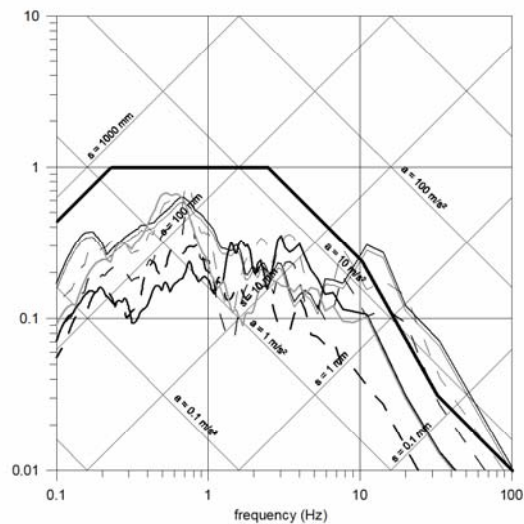
		<b>Ponte sullo Stretto di Messina</b> <b>PROGETTO DEFINITIVO</b>		
Sicily Anchor Block – earthquake induced displacements and safety against ultimate limit states, Annex		<i>Codice documento</i> PF0064_F0_ANX	<i>Rev</i> F0	<i>Data</i> 20/06/2011

Elastic response spectra, horizontal components damping 5%, scaled to 0.58g



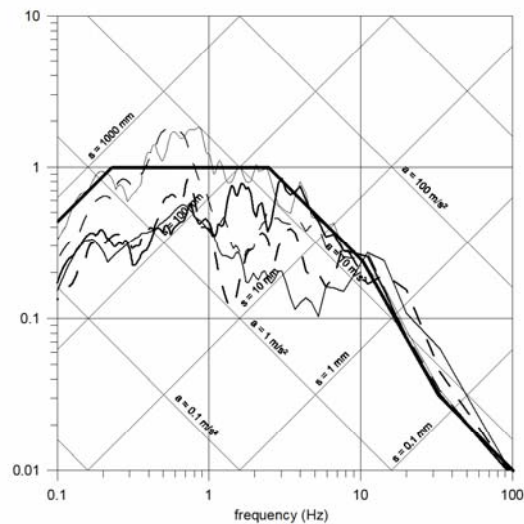
- Design response spectrum, hor. comp.
- Landers 92 CLWTR
- Landers 92 LCN260
- Landers 92 LCN345
- - Loma Prieta 89 CYC285
- - Loma Prieta 89 G03000
- - Loma Prieta 89 G03090
- Loma Prieta 89 G04000

Elastic response spectra, vertical components damping 5%, scaled by the same factor of the corresponding horizontal components



- Design response spectrum, vert. comp.
- Landers 92 CLWUP S=1.3909
- Landers 92 LCNUP S=0.7351
- Landers 92 LCNUP S=0.7978
- - Loma Prieta 89 CYCUP S=1.1983
- - Loma Prieta 89 G03UP S=1.0405
- - Loma Prieta 89 G03UP S=1.5804
- Loma Prieta 89 G04UP 1.3909

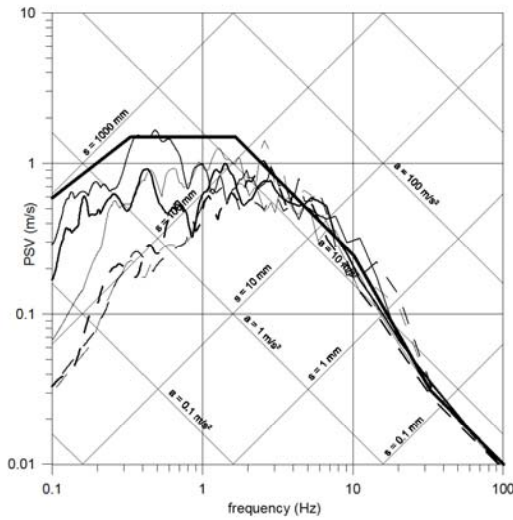
Elastic response spectra, vertical components damping 5%, scaled to 0.58g



- Design response spectrum, vert. comp.
- Landers 92 CLWUP
- Landers 92 LCNUP
- Loma Prieta 89 CYCUP
- - Loma Prieta 89 G03UP
- - Loma Prieta 89 G04UP

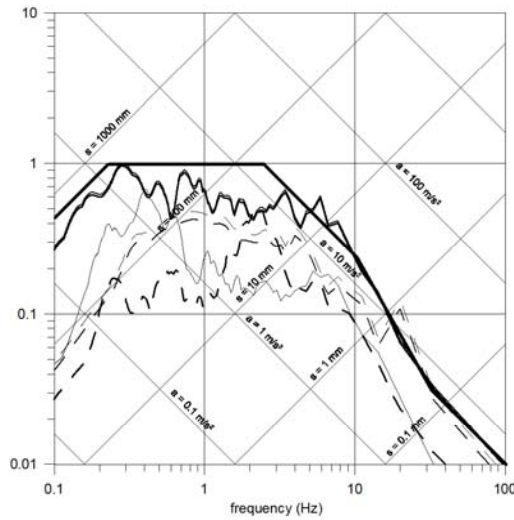
Figure 5.19. Elastic response spectra of the accelerograms used in the analyses

Elastic response spectra, horizontal components damping 5%, scaled to 0.58g



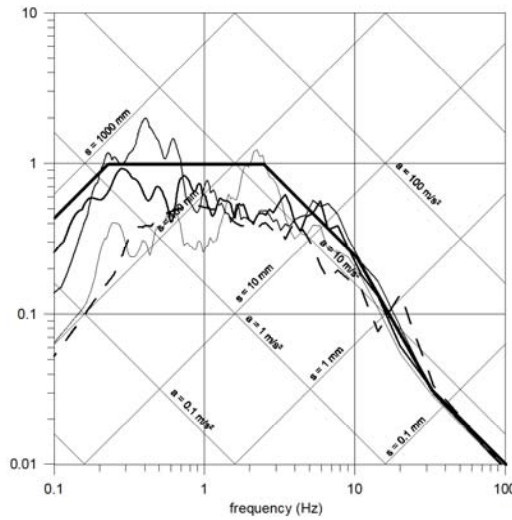
- Design response spectrum, hor. comp.
- Manjil 90 ABBL
- Manjil 90 ABBT
- Northridge 94 CEN245
- Northridge 94 LAC180
- Umbria Marche 97 NCRXC
- Umbria Marche 97 NCRYC

Elastic response spectra, vertical components damping 5%, scaled by the same factor of the corresponding horizontal components





- Design response spectrum, vert. comp.
- Manjil 90 ABBV S=1.1262
- Manjil 90 ABBV S=1.1694
- Northridge 94 CENUP S=1.8012
- Northridge 94 LACUP S=1.8354
- Umbria Marche 97 NCRZC S=1.1069
- Umbria Marche 97 NCRZC S=1.2527

Elastic response spectra, vertical components damping 5%, scaled to 0.58g

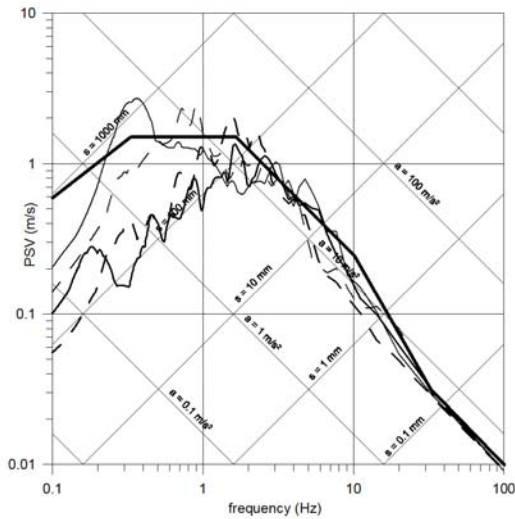


- Design response spectrum, vert. comp.
- Manjil 90 ABBV
- Northridge 94 CENUP
- Northridge 94 LACUP
- Umbria Marche 97 NCRZC

Figure 5.20. Elastic response spectra of the accelerograms used in the analyses

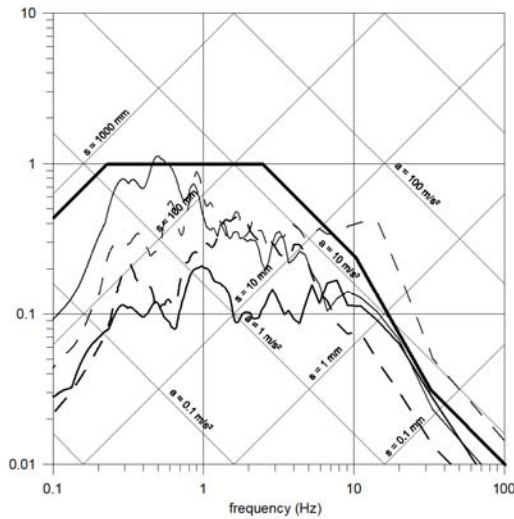
		<b>Ponte sullo Stretto di Messina</b> <b>PROGETTO DEFINITIVO</b>		
Sicily Anchor Block – earthquake induced displacements and safety against ultimate limit states, Annex		<i>Codice documento</i> PF0064_F0_ANX	<i>Rev</i> F0	<i>Data</i> 20/06/2011

Elastic response spectra, horizontal components damping 5%, scaled to 0.58g



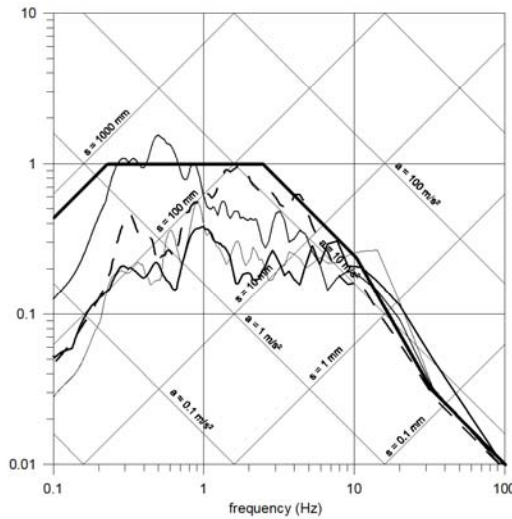
- Design response spectrum, hor. comp.
- Imperial Valley 79 BC230
- Irpinia 80 STUYC
- - Montenegro 79 PETXC
- - Montenegro 79 ULCXC

Elastic response spectra, vertical components damping 5%, scaled by the same factor of the corresponding horizontal components





- Design response spectrum, vert. comp.
- Imperial Valley 79 BCUP S=0.7484
- Irpinia 80 STUZC S=1.7957
- - Montenegro 79 PETZC S=1.2775
- - Montenegro 79 ULCZC S=1.9728

Elastic response spectra, vertical components damping 5%, scaled to 0.58g

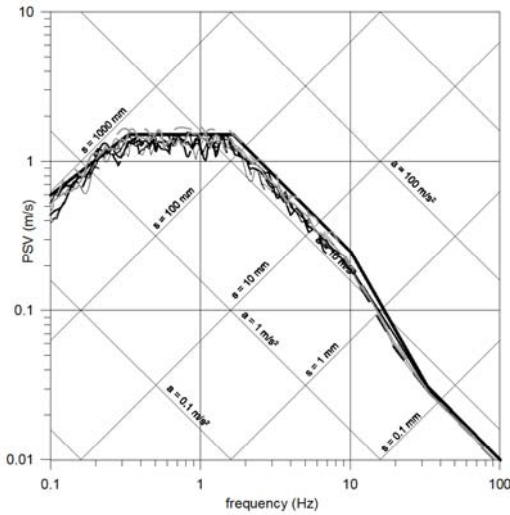


- Design response spectrum, vert. comp.
- Imperial Valley 79 BCUP
- Irpinia 80 STUZC
- Montenegro 79 ULCZC
- - Montenegro 79 PETZC

Figure 5.21. Elastic response spectra of the accelerograms used in the analyses

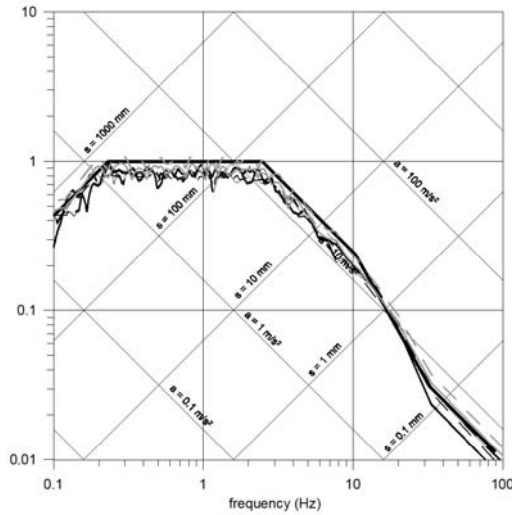
		<b>Ponte sullo Stretto di Messina</b> <b>PROGETTO DEFINITIVO</b>		
Sicily Anchor Block – earthquake induced displacements and safety against ultimate limit states, Annex		<i>Codice documento</i> PF0064_F0_ANX	<i>Rev</i> F0	<i>Data</i> 20/06/2011

Elastic response spectra, horizontal components damping 5%, scaled to 0.58g



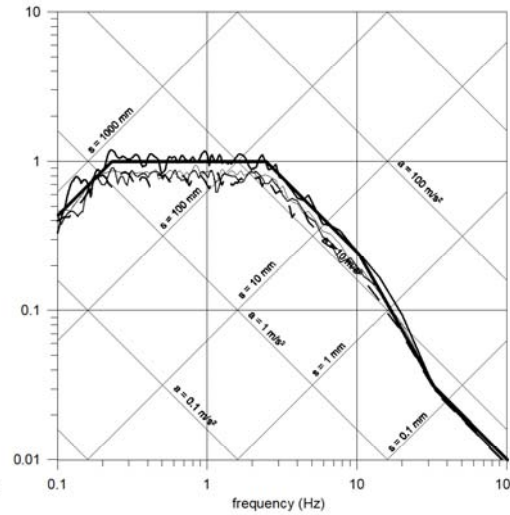
- Design response spectrum, hor. comp.
- Art. 1 comp. 1
- Art. 1 comp. 2
- Art. 2 comp. 1
- - Art. 2 comp. 2
- - Art. 3 comp. 1
- - Art. 3 comp. 2
- Art. 4 comp. 1
- - Art. 4 comp. 2

Elastic response spectra, vertical components damping 5%, scaled by the same factor of the corresponding horizontal components





- Design response spectrum, vert. comp.
- Art. 1 comp. V S=0.9034
- Art. 1 comp. V S=0.9163
- Art. 2 comp. V S=0.8841
- - Art. 2 comp. V S=0.9063
- - Art. 3 comp. V S=0.8593
- - Art. 3 comp. V S=0.9493
- Art. 4 comp. V S=0.9539
- - Art. 4 comp. V S=1.0861

Elastic response spectra, vertical components damping 5%, scaled to 0.58g



- Design response spectrum, vert. comp.
- Art. 1 comp. V
- Art. 2 comp. V
- Art. 3 comp. V
- - Art. 4 comp. V

Figure 5.22. Elastic response spectra of the accelerograms used in the analyses

		<b>Ponte sullo Stretto di Messina</b> <b>PROGETTO DEFINITIVO</b>		
Sicily Anchor Block – earthquake induced displacements and safety against ultimate limit states, Annex	<i>Codice documento</i> PF0064_F0_ANX	<i>Rev</i> F0	<i>Data</i> 20/06/2011	

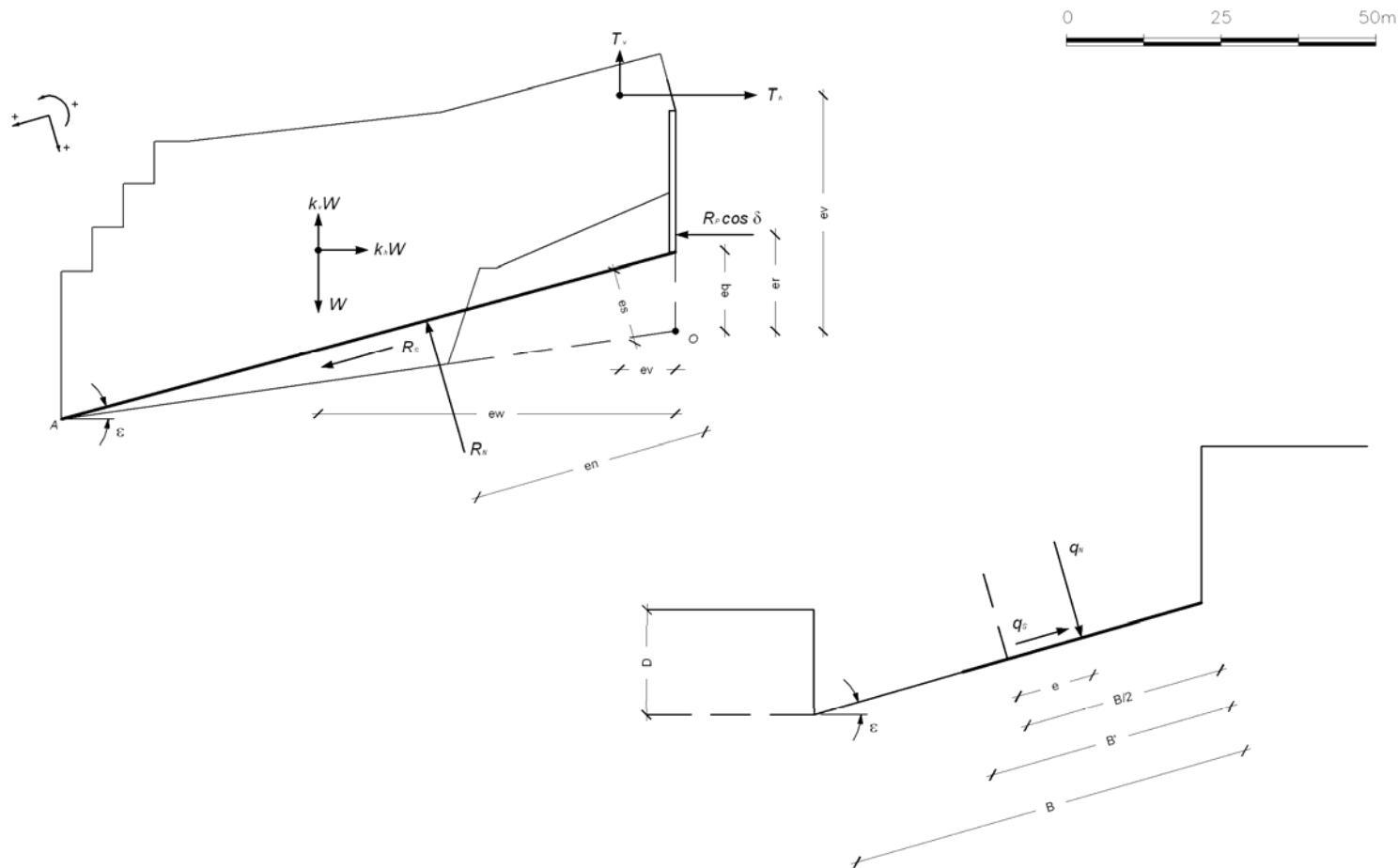





Figure 6.1. Assumptions for evaluating safety against rotation and bearing capacity failure

		<p align="center"><b>Ponte sullo Stretto di Messina</b> PROGETTO DEFINITIVO</p>		
<p>Sicity Anchor Block – earthquake induced displacements and safety against ultimate limit states, Annex</p>	<p><i>Codice documento</i> PF0064_F0_ANX</p>		<p><i>Rev</i> F0</p>	<p><i>Data</i> 20/06/2011</p>

## Appendices

		<b>Ponte sullo Stretto di Messina</b> <b>PROGETTO DEFINITIVO</b>		
Sicily Anchor Block – earthquake induced displacements and safety against ultimate limit states, Annex		<i>Codice documento</i> PF0064_F0_ANX	<i>Rev</i> F0	<i>Data</i> 20/06/2011

## Appendix A – Sliding resistance along the block sides

### Mechanism 1

characteristic values of  $T_L$

Diaphragm wall	Head m	Toe m	Length m	$\tau_{\text{Head}}$ kPa	$\tau_{\text{TOE}}$ kPa	$T_{Lk}$ kN/m	Width m	$T_{Lk}/\text{wall}$ kN
1	0.0	16.3	16.3	0.0	40.9	333.5	2.5	833.8
2	6.3	23.9	17.6	15.8	60.0	667.2	2.5	1668.0
3	4.9	23.6	18.7	12.3	59.3	669.0	2.5	1672.5
4	10.5	30.2	19.7	26.4	75.8	1006.5	2.5	2516.2
5	9.1	29.8	20.7	22.8	74.8	1010.8	2.5	2527.0
6	14.7	36.5	21.8	36.9	91.6	1401.1	2.5	3502.8
7	13.3	36.1	22.8	33.4	90.6	1413.9	2.5	3534.7
8	18.9	42.8	23.9	47.5	107.5	1851.1	2.5	4627.8
9	17.5	42.4	24.9	43.9	106.4	1872.3	2.5	4680.7
10	16.3	42.2	25.9	40.9	105.9	1902.0	2.5	4754.9
11	15.2	42.2	27.0	38.2	105.9	1945.5	2.5	4863.7
12	14.1	42.1	28.0	35.4	105.7	1975.3	2.5	4938.3
13	13.0	42.0	29.0	32.6	105.4	2002.2	2.5	5005.5
14	12.7	42.0	29.3	31.9	105.4	2011.9	2.5	5029.7
15	12.4	41.9	29.5	31.1	105.2	2010.8	2.5	5027.0
16	12.1	41.8	29.7	30.4	104.9	2009.5	2.5	5023.8
17	11.7	41.7	30.0	29.4	104.7	2011.0	2.5	5027.5
18	11.4	41.7	30.3	28.6	104.7	2019.7	2.5	5049.2
19	11.1	41.6	30.5	27.9	104.4	2017.7	2.5	5044.3
20	10.7	41.5	30.8	26.9	104.2	2018.2	2.5	5045.5
21	10.4	41.5	31.1	26.1	104.2	2026.2	2.5	5065.4
22	10.1	41.4	31.3	25.4	103.9	2023.5	2.5	5058.7
23	9.7	41.3	31.6	24.4	103.7	2023.0	2.5	5057.6
24	9.4	41.2	31.8	23.6	103.4	2019.9	2.5	5049.7
25	9.1	41.2	32.1	22.8	103.4	2026.8	2.5	5067.1
26	8.8	40.7	31.9	22.1	102.2	1982.2	2.5	4955.4
27	8.9	39.2	30.3	22.3	98.4	1829.5	2.5	4573.8
28	8.9	38.6	29.7	22.3	96.9	1770.9	2.5	4427.3
29	9.0	37.3	28.3	22.6	93.6	1644.8	2.5	4112.0
30	9.0	36.1	27.1	22.6	90.6	1534.2	2.5	3835.6
31	9.1	34.8	25.7	22.8	87.4	1416.3	2.5	3540.7
32	9.1	33.5	24.4	22.8	84.1	1304.8	2.5	3262.0
33	9.1	32.3	23.2	22.8	81.1	1205.7	2.5	3014.2
34	9.2	31.0	21.8	23.1	77.8	1100.1	2.5	2750.2
35	9.2	29.8	20.6	23.1	74.8	1008.5	2.5	2521.3
36	9.0	28.2	19.2	22.6	70.8	896.6	2.5	2241.5



		<b>Ponte sullo Stretto di Messina</b> <b>PROGETTO DEFINITIVO</b>		
Sicily Anchor Block – earthquake induced displacements and safety against ultimate limit states, Annex		<i>Codice documento</i> PF0064_F0_ANX	<i>Rev</i> F0	<i>Data</i> 20/06/2011

Diaphragm wall	Head m	Toe m	Length m	$\tau_{\text{Head}}$ kPa	$\tau_{\text{TOE}}$ kPa	$T_{\text{Lk}}$ kN/m	Width m	$T_{\text{Lk}}/\text{wall}$ kN
37	8.4	26.3	17.9	21.1	66.0	779.7	2.5	1949.3
38	7.7	24.4	16.7	19.3	61.3	672.9	2.5	1682.3
39	7.1	22.4	15.3	17.8	56.2	566.6	2.5	1416.4
40	6.5	20.1	13.6	16.3	50.5	454.1	3.5	1589.4
total								151543

$$\varphi'_k (\text{°}) \quad 40.0 \quad K_{ak} \quad 0.217$$

$$\varphi'_{sk} (\text{°}) \quad 30.0 \quad \gamma \text{ (kN/m}^3\text{)} \quad 20$$

$$T_{\text{Lk}} = 2 \times \text{total} = \quad \mathbf{303.1 \text{ MN}}$$

### Mechanism 1

design values of  $T_L$

Diaphragm wall	Head m	Toe m	Length m	$\tau_{\text{Head}}$ kPa	$\tau_{\text{TOE}}$ kPa	$T_{\text{Ld}}$ kN/m	Width m	$T_{\text{Ld}}/\text{wall}$ kN
1	0	16.3	16.3	0.0	32.7	266.8	2.5	667.0
2	6.3	23.9	17.6	12.7	48.0	533.8	2.5	1334.4
3	4.9	23.6	18.7	9.8	47.4	535.2	2.5	1338.0
4	10.5	30.2	19.7	21.1	60.7	805.2	2.5	2013.0
5	9.1	29.8	20.7	18.3	59.9	808.6	2.5	2021.6
6	14.7	36.5	21.8	29.5	73.3	1120.9	2.5	2802.2
7	13.3	36.1	22.8	26.7	72.5	1131.1	2.5	2827.7
8	18.9	42.8	23.9	38.0	86.0	1480.9	2.5	3702.2
9	17.5	42.4	24.9	35.1	85.2	1497.8	2.5	3744.6
10	16.3	42.2	25.9	32.7	84.8	1521.6	2.5	3803.9
11	15.2	42.2	27.0	30.5	84.8	1556.4	2.5	3890.9
12	14.1	42.1	28.0	28.3	84.6	1580.3	2.5	3950.7
13	13	42.0	29.0	26.1	84.4	1601.8	2.5	4004.4
14	12.7	42.0	29.3	25.5	84.4	1609.5	2.5	4023.8
15	12.4	41.9	29.5	24.9	84.2	1608.6	2.5	4021.6
16	12.1	41.8	29.7	24.3	84.0	1607.6	2.5	4019.0
17	11.7	41.7	30.0	23.5	83.8	1608.8	2.5	4022.0
18	11.4	41.7	30.3	22.9	83.8	1615.8	2.5	4039.4
19	11.1	41.6	30.5	22.3	83.6	1614.2	2.5	4035.4
20	10.7	41.5	30.8	21.5	83.4	1614.6	2.5	4036.4
21	10.4	41.5	31.1	20.9	83.4	1620.9	2.5	4052.3
22	10.1	41.4	31.3	20.3	83.2	1618.8	2.5	4047.0
23	9.7	41.3	31.6	19.5	83.0	1618.4	2.5	4046.1
24	9.4	41.2	31.8	18.9	82.7	1615.9	2.5	4039.8

		<b>Ponte sullo Stretto di Messina</b> <b>PROGETTO DEFINITIVO</b>		
Sicily Anchor Block – earthquake induced displacements and safety against ultimate limit states, Annex		<i>Codice documento</i> PF0064_F0_ANX	<i>Rev</i> F0	<i>Data</i> 20/06/2011

Diaphragm wall	Head m	Toe m	Length m	$\tau_{\text{Head}}$ kPa	$\tau_{\text{TOE}}$ kPa	$T_{\text{Ld}}$ kN/m	Width m	$T_{\text{Ld}}/\text{wall}$ kN
25	9.1	41.2	32.1	18.3	82.7	1621.5	2.5	4053.7
26	8.8	40.7	31.9	17.7	81.7	1585.7	2.5	3964.4
27	8.9	39.2	30.3	17.9	78.7	1463.6	2.5	3659.0
28	8.9	38.6	29.7	17.9	77.5	1416.7	2.5	3541.8
29	9	37.3	28.3	18.1	74.9	1315.8	2.5	3289.6
30	9	36.1	27.1	18.1	72.5	1227.4	2.5	3068.5
31	9.1	34.8	25.7	18.3	69.9	1133.0	2.5	2832.5
32	9.1	33.5	24.4	18.3	67.3	1043.8	2.5	2609.6
33	9.1	32.3	23.2	18.3	64.9	964.6	2.5	2411.4
34	9.2	31.0	21.8	18.5	62.3	880.1	2.5	2200.2
35	9.2	29.8	20.6	18.5	59.9	806.8	2.5	2017.0
36	9.0	28.2	19.2	18.1	56.6	717.3	2.5	1793.2
37	8.4	26.3	17.9	16.9	52.8	623.8	2.5	1559.4
38	7.7	24.4	16.7	15.5	49.0	538.3	2.5	1345.9
39	7.1	22.4	15.3	14.3	45.0	453.3	2.5	1133.2
40	6.5	20.1	13.6	13.1	40.4	363.3	3.5	1271.5
<b>total</b>								<b>121234.3</b>

$\varphi'_k$  (°)      40.0    $K_{ak}$       0.217

$\varphi'_{sd}$  (°)      24.8    $\gamma$  (kN/m<sup>3</sup>)      20

$T_{\text{Ld}} = 2 \times \text{total} = \quad \mathbf{242.5 \text{ MN}}$

		<b>Ponte sullo Stretto di Messina</b> <b>PROGETTO DEFINITIVO</b>		
Sicily Anchor Block – earthquake induced displacements and safety against ultimate limit states, Annex		<i>Codice documento</i> PF0064_F0_ANX	<i>Rev</i> F0	<i>Data</i> 20/06/2011

## Mechanism 2

characteristic values of  $T_L$

Diaphragm wall	Head m	Toe m	Length m	$\tau_{Head}$ kPa	$\tau_{TOE}$ kPa	$T_{Lk}$ kN/m	Width m	$T_{Lk}/wall$ kN
1	0.0	16.3	16.3	0	40.9	333.5	2.5	833.8
2	6.3	23.9	17.6	15.8168	60.0	667.2	2.5	1668.0
3	4.9	23.6	18.7	12.3019	59.3	669.0	2.5	1672.5
4	10.5	30.2	19.7	26.3613	75.8	1006.5	2.5	2516.2
5	9.1	29.8	20.7	22.8464	74.8	1010.8	2.5	2527.0
6	14.7	36.5	21.8	36.9058	91.6	1401.1	2.5	3502.8
7	13.3	36.1	22.8	33.3909	90.6	1413.9	2.5	3534.7
8	18.9	42.8	23.9	47.4503	107.5	1851.1	2.5	4627.8
9	17.5	42.4	24.9	43.9355	106.4	1872.3	2.5	4680.7
10	16.3	42.2	25.9	40.9227	105.9	1902.0	2.5	4754.9
11	15.2	42.2	27.0	38.1611	105.9	1945.5	2.5	4863.7
12	14.1	42.1	28.0	35.3994	105.7	1975.3	2.5	4938.3
13	13.0	42.0	29.0	32.6378	105.4	2002.2	2.5	5005.5
14	12.7	42.0	29.3	31.8846	105.4	2011.9	2.5	5029.7
15	12.4	41.9	29.5	31.1314	105.2	2010.8	2.5	5027.0
16	12.1	41.8	29.7	30.3782	104.9	2009.5	2.5	5023.8
17	11.7	41.7	30.0	29.374	104.7	2011.0	2.5	5027.5
18	11.4	41.7	30.3	28.6208	104.7	2019.7	2.5	5049.2
19	11.1	41.6	30.5	27.8676	104.4	2017.7	2.5	5044.3
20	10.7	41.5	30.8	26.8634	104.2	2018.2	2.5	5045.5
21	10.4	41.5	31.1	26.1102	104.2	2026.2	2.5	5065.4
22	10.1	41.4	31.3	25.357	103.9	2023.5	2.5	5058.7
23	9.7	41.3	31.6	24.3528	103.7	2023.0	2.5	5057.6
24	9.4	41.2	31.8	23.5996	103.4	2019.9	2.5	5049.7
25	9.1	41.2	32.1	22.8464	103.4	2026.8	2.5	5067.1
26	8.8	40.7	31.9	22.0933	102.2	1982.2	2.5	4955.4
27	8.9	40.6	31.7	22.3443	101.9	1969.8	2.5	4924.4
28	8.9	40.0	31.1	22.3443	100.4	1909.0	2.5	4772.6
29	9.0	39.5	30.5	22.5954	99.2	1856.9	2.5	4642.3
30	9.0	38.9	29.9	22.5954	97.7	1797.9	2.5	4494.6
31	9.1	38.4	29.3	22.8464	96.4	1747.1	2.5	4367.7
32	9.1	37.8	28.7	22.8464	94.9	1689.7	2.5	4224.2
33	9.1	37.2	28.1	22.8464	93.4	1633.2	2.5	4083.0
34	9.2	36.7	27.5	23.0975	92.1	1584.5	2.5	3961.3
35	9.2	36.1	26.9	23.0975	90.6	1529.7	2.5	3824.2
36	9.0	35.3	26.3	22.5954	88.6	1462.5	2.5	3656.3
37	8.4	34.0	25.6	21.089	85.4	1362.6	2.5	3406.4
38	7.7	32.8	25.1	19.3316	82.3	1276.1	2.5	3190.2
39	7.1	31.6	24.5	17.8252	79.3	1190.2	2.5	2975.5

		<b>Ponte sullo Stretto di Messina</b> <b>PROGETTO DEFINITIVO</b>		
Sicily Anchor Block – earthquake induced displacements and safety against ultimate limit states, Annex		<i>Codice documento</i> PF0064_F0_ANX	<i>Rev</i> F0	<i>Data</i> 20/06/2011

Diaphragm wall	Head m	Toe m	Length m	$\tau_{\text{Head}}$ kPa	$\tau_{\text{TOE}}$ kPa	$T_{\text{Lk}}$ kN/m	Width m	$T_{\text{Lk}}/\text{wall}$ kN
40	6.5	30.1	23.6	16.3189	75.6	1084.3	3.5	3795.0
total								166944

$\varphi'_k$  (°)      40.0     $K_{\text{ak}}$                       0.217  
 $\varphi'_{\text{sk}}$  (°)      30.0     $\gamma$  (kN/m<sup>3</sup>)                      20                       $T_{\text{Lk}} = 2 \times \text{total} =$                       **333.9 MN**

### Mechanism 2

design values of  $T_L$

Diaphragm wall	Head m	Toe m	Length m	$\tau_{\text{Head}}$ kPa	$\tau_{\text{TOE}}$ kPa	$T_{\text{Ld}}$ kN/m	Width m	$T_{\text{Ld}}/\text{wall}$ kN
1	0.0	16.3	16.3	0	32.7	266.8	2.5	667.0
2	6.3	23.9	17.6	12.653	48.0	533.8	2.5	1334.4
3	4.9	23.6	18.7	9.8415	47.4	535.2	2.5	1338.0
4	10.5	30.2	19.7	21.089	60.7	805.2	2.5	2013.0
5	9.1	29.8	20.7	18.277	59.9	808.6	2.5	2021.6
6	14.7	36.5	21.8	29.525	73.3	1120.9	2.5	2802.2
7	13.3	36.1	22.8	27	72.5	1131.1	2.5	2827.7
8	18.9	42.8	23.9	37.96	86.0	1480.9	2.5	3702.2
9	17.5	42.4	24.9	35.148	85.2	1497.8	2.5	3744.6
10	16.3	42.2	25.9	32.738	84.8	1521.6	2.5	3803.9
11	15.2	42.2	27.0	30.529	84.8	1556.4	2.5	3890.9
12	14.1	42.1	28.0	28.32	84.6	1580.3	2.5	3950.7
13	13.0	42.0	29.0	26.11	84.4	1601.8	2.5	4004.4
14	12.7	42.0	29.3	25.508	84.4	1609.5	2.5	4023.8
15	12.4	41.9	29.5	24.905	84.2	1608.6	2.5	4021.6
16	12.1	41.8	29.7	24.303	84.0	1607.6	2.5	4019.0
17	11.7	41.7	30.0	23.499	83.8	1608.8	2.5	4022.0
18	11.4	41.7	30.3	22.897	83.8	1615.8	2.5	4039.4
19	11.1	41.6	30.5	22.294	83.6	1614.2	2.5	4035.4
20	10.7	41.5	30.8	21.491	83.4	1614.6	2.5	4036.4
21	10.4	41.5	31.1	20.888	83.4	1620.9	2.5	4052.3
22	10.1	41.4	31.3	20.286	83.2	1618.8	2.5	4047.0
23	9.7	41.3	31.6	19.482	83.0	1618.4	2.5	4046.1
24	9.4	41.2	31.8	18.88	82.7	1615.9	2.5	4039.8
25	9.1	41.2	32.1	18.277	82.7	1621.5	2.5	4053.7
26	8.8	40.7	31.9	17.675	81.7	1585.7	2.5	3964.4
27	8.9	40.6	31.7	17.875	81.5	1575.8	2.5	3939.5
28	8.9	40.0	31.1	17.875	80.3	1527.2	2.5	3818.1

		<b>Ponte sullo Stretto di Messina</b> <b>PROGETTO DEFINITIVO</b>		
Sicily Anchor Block – earthquake induced displacements and safety against ultimate limit states, Annex		<i>Codice documento</i> PF0064_F0_ANX	<i>Rev</i> F0	<i>Data</i> 20/06/2011

Diaphragm wall	Head m	Toe m	Length m	$\tau_{\text{Head}}$ kPa	$\tau_{\text{TOE}}$ kPa	$T_{\text{Ld}}$ kN/m	Width m	$T_{\text{Ld}}/\text{wall}$ kN
29	9.0	39.5	30.5	18.076	79.3	1485.5	2.5	3713.8
30	9.0	38.9	29.9	18.076	78.1	1438.3	2.5	3595.7
31	9.1	38.4	29.3	18.277	77.1	1397.6	2.5	3494.1
32	9.1	37.8	28.7	18.277	75.9	1351.7	2.5	3379.3
33	9.1	37.2	28.1	18.277	74.7	1306.5	2.5	3266.4
34	9.2	36.7	27.5	18.478	73.7	1267.6	2.5	3169.0
35	9.2	36.1	26.9	18.478	72.5	1223.7	2.5	3059.3
36	9.0	35.3	26.3	18.076	70.9	1170.0	2.5	2925.1
37	8.4	34.0	25.6	16.871	68.3	1090.0	2.5	2725.1
38	7.7	32.8	25.1	15.465	65.9	1020.9	2.5	2552.1
39	7.1	31.6	24.5	14.26	63.5	952.2	2.5	2380.4
40	6.5	30.1	23.6	13.055	60.5	867.4	3.5	3036.0
total								133555.5

$\varphi'_k$  (°)      40.0  $K_{ak}$       0.217

$\varphi'_{sd}$  (°)      24.8  $\gamma$  (kN/m<sup>3</sup>)      20

$T_{\text{Ld}} = 2 \times \text{total} = \mathbf{267.1 \text{ MN}}$

		<b>Ponte sullo Stretto di Messina</b> <b>PROGETTO DEFINITIVO</b>		
Sicily Anchor Block – earthquake induced displacements and safety against ultimate limit states, Annex		<i>Codice documento</i> PF0064_F0_ANX	<i>Rev</i> F0	<i>Data</i> 20/06/2011

### Mechanism 3

characteristic values of  $T_L$

Diaphragm wall	Head m	Toe m	Length m	$\tau_{Head}$ kPa	$\tau_{TOE}$ kPa	$T_L$ kN/m	Width m	$T_L/wall$ kN
1	0.0	16.3	16.3	0	40.9	333.5	2.5	833.8
2	6.3	23.9	17.6	15.8168	60.0	667.2	2.5	1668.0
3	4.9	23.6	18.7	12.3019	59.3	669.0	2.5	1672.5
4	10.5	30.2	19.7	26.3613	75.8	1006.5	2.5	2516.2
5	9.1	29.8	20.7	22.8464	74.8	1010.8	2.5	2527.0
6	14.7	36.5	21.8	36.9058	91.6	1401.1	2.5	3502.8
7	13.3	36.1	22.8	33.3909	90.6	1413.9	2.5	3534.7
8	18.9	42.8	23.9	47.4503	107.5	1851.1	2.5	4627.8
9	17.5	42.4	24.9	43.9355	106.4	1872.3	2.5	4680.7
10	16.3	42.2	25.9	40.9227	105.9	1902.0	2.5	4754.9
11	15.2	42.2	27.0	38.1611	105.9	1945.5	2.5	4863.7
12	14.1	42.1	28.0	35.3994	105.7	1975.3	2.5	4938.3
13	13.0	42.0	29.0	32.6378	105.4	2002.2	2.5	5005.5
14	12.7	42.0	29.3	31.8846	105.4	2011.9	2.5	5029.7
15	12.4	41.9	29.5	31.1314	105.2	2010.8	2.5	5027.0
16	12.1	41.8	29.7	30.3782	104.9	2009.5	2.5	5023.8
17	11.7	41.7	30.0	29.374	104.7	2011.0	2.5	5027.5
18	11.4	41.7	30.3	28.6208	104.7	2019.7	2.5	5049.2
19	11.1	41.6	30.5	27.8676	104.4	2017.7	2.5	5044.3
20	10.7	41.5	30.8	26.8634	104.2	2018.2	2.5	5045.5
21	10.4	41.5	31.1	26.1102	104.2	2026.2	2.5	5065.4
22	10.1	41.4	31.3	25.357	103.9	2023.5	2.5	5058.7
23	9.7	41.3	31.6	24.3528	103.7	2023.0	2.5	5057.6
24	9.4	41.2	31.8	23.5996	103.4	2019.9	2.5	5049.7
25	9.1	41.2	32.1	22.8464	103.4	2026.8	2.5	5067.1
26	8.8	40.7	31.9	22.0933	102.2	1982.2	2.5	4955.4
27	8.9	41.9	33.0	22.3443	105.2	2104.4	2.5	5261.0
28	8.9	42.5	33.6	22.3443	106.7	2168.0	2.5	5419.9
29	9.0	43.2	34.2	22.5954	108.5	2241.0	2.5	5602.5
30	9.0	43.9	34.9	22.5954	110.2	2317.5	2.5	5793.9
31	9.1	44.5	35.4	22.8464	111.7	2381.9	2.5	5954.6
32	9.1	45.2	36.1	22.8464	113.5	2460.7	2.5	6151.7
33	9.1	45.9	36.8	22.8464	115.2	2540.7	2.5	6351.8
34	9.2	46.5	37.3	23.0975	116.7	2608.0	2.5	6520.1
35	9.2	47.2	38.0	23.0975	118.5	2690.4	2.5	6725.9
36	9.0	47.6	38.6	22.5954	119.5	2742.5	2.5	6856.3
37	8.4	47.6	39.2	21.089	119.5	2755.6	2.5	6889.1
38	7.7	47.6	39.9	19.3316	119.5	2769.8	2.5	6924.4
39	7.1	47.6	40.5	17.8252	119.5	2780.9	2.5	6952.3
40	6.5	47.6	41.1	16.3189	119.5	2791.2	3.5	9769.1

		<b>Ponte sullo Stretto di Messina</b> PROGETTO DEFINITIVO		
Sicily Anchor Block – earthquake induced displacements and safety against ultimate limit states, Annex		Codice documento PF0064_F0_ANX	Rev F0	Data 20/06/2011

Diaphragm wall	Head m	Toe m	Length m	$\tau_{\text{Head}}$ kPa	$\tau_{\text{TOE}}$ kPa	$T_L$ kN/m	Width m	$T_L/\text{wall}$ kN
total								201799


$$\varphi'_k (^\circ) \quad 40.0 \quad K_{ak} \quad 0.217$$

$$\varphi'_{sk} (^\circ) \quad 30.0 \quad \gamma \text{ (kN/m}^3\text{)} \quad 20 \quad T_{Lk} = 2 \times \text{total} = \quad \mathbf{403.6 \text{ MN}}$$

### Mechanism 3

design values of  $T_L$

Diaphragm wall	Head m	Toe m	Length m	$\tau_{\text{Head}}$ kPa	$\tau_{\text{TOE}}$ kPa	$T_L$ kN/m	Width m	$T_L/\text{wall}$ kN
1	0	16.3	16.3	0	32.7	266.8	2.5	667.0
2	6.3	23.9	17.6	12.653	48.0	533.8	2.5	1334.4
3	4.9	23.6	18.7	9.8415	47.4	535.2	2.5	1338.0
4	10.5	30.2	19.7	21.089	60.7	805.2	2.5	2013.0
5	9.1	29.8	20.7	18.277	59.9	808.6	2.5	2021.6
6	14.7	36.5	21.8	29.525	73.3	1120.9	2.5	2802.2
7	13.3	36.1	22.8	27	72.5	1131.1	2.5	2827.7
8	18.9	42.8	23.9	37.96	86.0	1480.9	2.5	3702.2
9	17.5	42.4	24.9	35.148	85.2	1497.8	2.5	3744.6
10	16.3	42.2	25.9	32.738	84.8	1521.6	2.5	3803.9
11	15.2	42.2	27.0	30.529	84.8	1556.4	2.5	3890.9
12	14.1	42.1	28.0	28.32	84.6	1580.3	2.5	3950.7
13	13	42.0	29.0	26.11	84.4	1601.8	2.5	4004.4
14	12.7	42.0	29.3	25.508	84.4	1609.5	2.5	4023.8
15	12.4	41.9	29.5	24.905	84.2	1608.6	2.5	4021.6
16	12.1	41.8	29.7	24.303	84.0	1607.6	2.5	4019.0
17	11.7	41.7	30.0	23.499	83.8	1608.8	2.5	4022.0
18	11.4	41.7	30.3	22.897	83.8	1615.8	2.5	4039.4
19	11.1	41.6	30.5	22.294	83.6	1614.2	2.5	4035.4
20	10.7	41.5	30.8	21.491	83.4	1614.6	2.5	4036.4
21	10.4	41.5	31.1	20.888	83.4	1620.9	2.5	4052.3
22	10.1	41.4	31.3	20.286	83.2	1618.8	2.5	4047.0
23	9.7	41.3	31.6	19.482	83.0	1618.4	2.5	4046.1
24	9.4	41.2	31.8	18.88	82.7	1615.9	2.5	4039.8
25	9.1	41.2	32.1	18.277	82.7	1621.5	2.5	4053.7
26	8.8	40.7	31.9	17.675	81.7	1585.7	2.5	3964.4
27	8.9	41.9	33.0	17.875	84.2	1683.5	2.5	4208.8
28	8.9	42.5	33.6	17.875	85.4	1734.4	2.5	4335.9
29	9	43.2	34.2	18.076	86.8	1792.8	2.5	4482.0

		<b>Ponte sullo Stretto di Messina</b> <b>PROGETTO DEFINITIVO</b>		
Sicily Anchor Block – earthquake induced displacements and safety against ultimate limit states, Annex		<i>Codice documento</i> PF0064_F0_ANX	<i>Rev</i> F0	<i>Data</i> 20/06/2011

Diaphragm wall	Head m	Toe m	Length m	$\tau_{\text{Head}}$ kPa	$\tau_{\text{TOE}}$ kPa	$T_L$ kN/m	Width m	$T_L/\text{wall}$ kN
30	9	43.9	34.9	18.076	88.2	1854.0	2.5	4635.1
31	9.1	44.5	35.4	18.277	89.4	1905.5	2.5	4763.7
32	9.1	45.2	36.1	18.277	90.8	1968.5	2.5	4921.3
33	9.1	45.9	36.8	18.277	92.2	2032.6	2.5	5081.4
34	9.2	46.5	37.3	18.478	93.4	2086.4	2.5	5216.0
35	9.2	47.2	38.0	18.478	94.8	2152.3	2.5	5380.7
36	9	47.6	38.6	18.076	95.6	2194.0	2.5	5485.1
37	8.4	47.6	39.2	16.871	95.6	2204.5	2.5	5511.3
38	7.7	47.6	39.9	15.465	95.6	2215.8	2.5	5539.6
39	7.1	47.6	40.5	14.26	95.6	2224.7	2.5	5561.9
40	6.5	47.6	41.1	13.055	95.6	2232.9	3.5	7815.3
total								161439.6

$\varphi'_k$  (°)      40.0  $K_{ak}$       0.217

$\varphi'_{sd}$  (°)      24.8  $\gamma$  (kN/m<sup>3</sup>)      20

$T_{Ld} = 2 \times \text{total} = \quad \mathbf{322.9 \text{ MN}}$



		<b>Ponte sullo Stretto di Messina</b> <b>PROGETTO DEFINITIVO</b>	
Sicily Anchor Block – earthquake induced displacements and safety against ultimate limit states, Annex	<i>Codice documento</i> PF0064_F0_ANX	<i>Rev</i> F0	<i>Data</i> 20/06/2011

## Appendix B – Passive earth resistance in front of the anchor block

### Mechanism 1 ( $z = 18.8$ m)

	<b>SLS2</b>	<b>ULS</b>	<b>SLIS</b>
$K_h$	0.097	0.216	0.238
$K_v$	0.048	0.108	0.119
$K_{Pk}$	9.005	7.655	7.395
diaphragm wall head depth (m)	6.5	6.5	6.5
diaphragm wall toe depth (m)	18.8	18.8	18.8
$\sigma'_{hp(k)}$ head (kPa)	1170.65	995.15	961.35
$\sigma'_{hp(k)}$ toe (kPa)	3385.9	2878.3	2780.5
$R'_{Pk}$ (kN/m)	28022.7	23821.6	23012.5
pore pressure resultant (kN/m)	0	0	0
$R_{Pk}$ (MN)	2241.8	1905.7	1841.0

	<b>SLS2</b>	<b>ULS</b>	<b>SLIS</b>
$K_h$	0.097	0.216	0.238
$K_v$	0.048	0.108	0.119
$K_{Pd}$	5.481	4.577	4.401
diaphragm wall head depth (m)	6.5	6.5	6.5
diaphragm wall toe depth (m)	18.8	18.8	18.8
$\sigma'_{hp(d)}$ testa (kPa)	712.5	595.0	572.1
$\sigma'_{hp(d)}$ piede (kPa)	2060.9	1721.0	1654.8
$R'_{Pd}$ per metro lin. (kN/m)	17056.3	14243.2	13695.5
pore pressure resultant (kN/m)	0	0	0
$R_{Pd}$ totale (MN)	1364.5	1139.5	1095.6

		<b>Ponte sullo Stretto di Messina</b> <b>PROGETTO DEFINITIVO</b>	
Sicily Anchor Block – earthquake induced displacements and safety against ultimate limit states, Annex	<i>Codice documento</i> PF0064_F0_ANX	<i>Rev</i> F0	<i>Data</i> 20/06/2011

*Mechanism 2 (z = 29.2 m)*

	<b>SLS2</b>	<b>ULS</b>	<b>SLIS</b>
$K_h$	0.097	0.216	0.238
$K_v$	0.048	0.108	0.119
$K_{Pk}$	9.005	7.655	7.395
diaphragm wall head depth (m)	6.5	6.5	6.5
diaphragm wall toe depth (m)	29.2	29.2	29.2
$\sigma_{hp(k)} \text{ head (kPa)}$	1170.65	995.15	961.35
$\sigma_{hp(k)} \text{ toe (kPa)}$	5258.9	4470.5	4318.7
$R'_{Pk}$ (kN/m)	72975.6	62035.4	59928.3
pore pressure resultant (kN/m)	0	0	0
$R_{Pk}$ (MN)	5838.0	4962.8	4794.3

	<b>SLS2</b>	<b>ULS</b>	<b>SLIS</b>
$K_h$	0.097	0.216	0.238
$K_v$	0.048	0.108	0.119
$K_{Pd}$	5.481	4.577	4.401
diaphragm wall head depth (m)	6.5	6.5	6.5
diaphragm wall toe depth (m)	29.2	29.2	29.2
$\sigma_{hp(d)} \text{ testa (kPa)}$	712.5	595.0	572.1
$\sigma_{hp(d)} \text{ piede (kPa)}$	3200.9	2673.0	2570.2
$R'_{Pd}$ per metro lin. (kN/m)	44417.5	37091.6	35665.3
pore pressure resultant (kN/m)	0	0	0
$R_{Pd}$ totale (MN)	3553.4	2967.3	2853.2

		<b>Ponte sullo Stretto di Messina</b> <b>PROGETTO DEFINITIVO</b>	
Sicily Anchor Block – earthquake induced displacements and safety against ultimate limit states, Annex	<i>Codice documento</i> PF0064_F0_ANX	<i>Rev</i> F0	<i>Data</i> 20/06/2011

*Mechanism 3 (z = 47.6 m)*

	<b>SLS2</b>	<b>ULS</b>	<b>SLIS</b>
$K_h$	0.097	0.216	0.238
$K_v$	0.048	0.108	0.119
$K_{Pk}$	9.005	7.655	7.395
diaphragm wall head depth (m)	6.5	6.5	6.5
diaphragm wall toe depth (m)	47.6	47.6	47.6
$\sigma'_{hp(k)}$ head (kPa)	1170.65	995.15	961.35
$\sigma'_{hp(k)}$ toe (kPa)	8572.8	7287.6	7040.0
$R'_{Pk}$ (kN/m)	200227.1	170209.7	164428.6
pore pressure resultant (kN/m)	0	0	0
$R_{Pk}$ (MN)	16018.2	13616.8	13154.3

	<b>SLS2</b>	<b>ULS</b>	<b>SLIS</b>
$K_h$	0.097	0.216	0.238
$K_v$	0.048	0.108	0.119
$K_{Pd}$	5.481	4.577	4.401
diaphragm wall head depth (m)	6.5	6.5	6.5
diaphragm wall toe depth (m)	47.6	47.6	47.6
$\sigma'_{hp(d)}$ testa (kPa)	712.5	595.0	572.1
$\sigma'_{hp(d)}$ piede (kPa)	5217.9	4357.3	4189.8
$R'_{Pd}$ per metro lin. (kN/m)	121870.6	101770.1	97856.7
pore pressure resultant (kN/m)	0	0	0
$R_{Pd}$ totale (MN)	9749.6	8141.6	7828.5

		<b>Ponte sullo Stretto di Messina</b> <b>PROGETTO DEFINITIVO</b>		
Sicily Anchor Block – earthquake induced displacements and safety against ultimate limit states, Annex	<i>Codice documento</i> PF0064_F0_ANX	<i>Rev</i> F0	<i>Data</i> 20/06/2011	

## Appendix C – Safety against sliding, pseudo-static approach

### General input parameters

Anchor block weight $W_b$	7502 MN
Anchor block width	80 m
Pore pressure resultant force $U$	0 MN
Anchor block submerged weight $W_b'$	7502 MN
Cable force angle $i$	15 °
Unit weight of soil	20 kN/m <sup>3</sup>
Characteristic angle of shear resistance of soil $\phi'_k$	40 °
Design angle of shear resistance of soil $\phi'_d$	33.9 °
Characteristic angle of shear resistance on the sliding surface $\phi'_{sk}$	36 °
Design angle of shear resistance on the sliding surface $\phi'_{sd}$	30.2 °
Characteristic friction angle at soil-concrete interface $\delta_k$	20 °
Design friction angle at soil-concrete interface $\delta_d$	16.9 °

#### CABLE FORCE (MN)

	SLS2	ULS	SLIS
	3250	3964	3146

#### SEISMIC COEFFICIENT

	SLS2	ULS	SLIS
$K_h$	0.097	0.216	0.238
$K_v$	0.048	0.108	0.119
$a_{tr}/g$	0.26	0.58	0.64

$S_T \times S_s \times \beta_m$	0.372
---------------------------------	-------

#### PASSIVE EARTH PRESSURE COEFFICIENT

	SLS2	ULS	SLIS
$K_{Pk}$	9.005	7.655	7.395
$K_{Pd}$	5.481	4.577	4.401

		<b>Ponte sullo Stretto di Messina</b> <b>PROGETTO DEFINITIVO</b>		
Sicily Anchor Block – earthquake induced displacements and safety against ultimate limit states, Annex	<i>Codice documento</i> PF0064_F0_ANX	<i>Rev</i> F0	<i>Data</i> 20/06/2011	

### Mechanism 1

#### Input parameters

sliding surface inclination	38 °
Soil volume above the sliding surface	17340.0 m <sup>3</sup>
Submerged soil volume above the sliding surface	0.0 m <sup>3</sup>
Soil weight above the sliding surface	347 MN
Submerged soil weight above the sliding surface	347 MN
Total weight $W$	7849 MN
Total submerged $W'$	7849 MN
$\theta$ critical ( $\alpha + \phi'_s$ )	74 °
Design sliding resistance along the block side $T_{Ld}$	242.5 MN
Passive earth resistance	

	SLS2	ULS	SILS
$R_{Pk}$ (MN)	2241.8	1905.7	1841.0
$R_{Pd}$ (MN)	1364.5	1139.5	1095.6

$R_d$ (MN)	SLS2	ULS	SLIS
$W' \cos\alpha \tan\phi'_k$	4493.6	4493.6	4493.6
$W (K_h \sin\alpha - K_v \cos\alpha) \tan\phi'_k$	122.3	272.7	300.9
$T \sin(\alpha-i) \tan\phi'_k$	922.6	1125.3	893.1
$E_d$ (MN)	SLS2	ULS	SLIS
$W' \sin\alpha$	4832.2	4832.2	4832.2
$W (K_h \cos\alpha + K_v \sin\alpha)$	831.9	1855.8	2047.7
$T \cos(\alpha-i)$	2991.6	3648.9	2895.9
$\Sigma R_d / \Sigma E_d$ (MN)	-5.4	8.1	47.4

		<b>Ponte sullo Stretto di Messina</b> <b>PROGETTO DEFINITIVO</b>		
Sicily Anchor Block – earthquake induced displacements and safety against ultimate limit states, Annex		<i>Codice documento</i> PF0064_F0_ANX	<i>Rev</i> F0	<i>Data</i> 20/06/2011

## Mechanism 2

### Input parameters

sliding surface inclination	26 °
Soil volume above the sliding surface	32900.0 m <sup>3</sup>
Submerged soil volume above the sliding surface	0.0 m <sup>3</sup>
Soil weight above the sliding surface	658 MN
Submerged soil weight above the sliding surface	658 MN
Total weight $W$	8160 MN
Total submerged $W'$	8160 MN
$\theta$ critical ( $\alpha + \phi'_s$ )	62 °
Design sliding resistance along the block side $T_{Ld}$	267.1 MN

### Passive earth resistance

	SLS2	ULS	SILS
$R_{Pk}$ (MN)	5838.0	4962.8	4794.3
$R_{Pd}$ (MN)	3553.4	2967.3	2853.2

$R_d$ (MN)	SLS2	ULS	SLIS
$W' \cos \alpha \tan \phi'_k$	5328.6	5328.6	5328.6
$W (K_h \sin \alpha - K_v \cos \alpha) \tan \phi'_k$	-6.3	-14.1	-15.6
$T \sin(\alpha - i) \tan \phi'_k$	450.6	549.5	436.1
$E_d$ (MN)	SLS2	ULS	SLIS
$W' \sin \alpha$	3577.1	3577.1	3577.1
$W (K_h \cos \alpha + K_v \sin \alpha)$	882.3	1968.3	2171.9
$T \cos(\alpha - i)$	3190.3	3891.2	3088.2
$\Sigma R_d / \Sigma E_d$ (MN)	15.4	3.1	4.2

		<b>Ponte sullo Stretto di Messina</b> <b>PROGETTO DEFINITIVO</b>		
Sicily Anchor Block – earthquake induced displacements and safety against ultimate limit states, Annex	<i>Codice documento</i> PF0064_F0_ANX	<i>Rev</i> F0	<i>Data</i> 20/06/2011	

### Mechanism 3



#### Input parameters

sliding surface inclination	8 °
Soil volume above the sliding surface	51835 m <sup>3</sup>
Submerged soil volume above the sliding surface	0 m <sup>3</sup>
Soil weight above the sliding surface	1036.7 MN
Submerged soil weight above the sliding surface	1036.7 MN
Total weight $W$	8539 MN
Total submerged $W'$	8539 MN
$\theta$ critical ( $\alpha + \phi'_s$ )	44 °
Design sliding resistance along the block side $T_{Ld}$	322.9 MN

#### Passive earth resistance

	SLS2	ULS	SILS
$R_{Pk}$ (MN)	16018.2	13616.8	13154.3
$R_{Pd}$ (MN)	9749.6	8141.6	7828.5

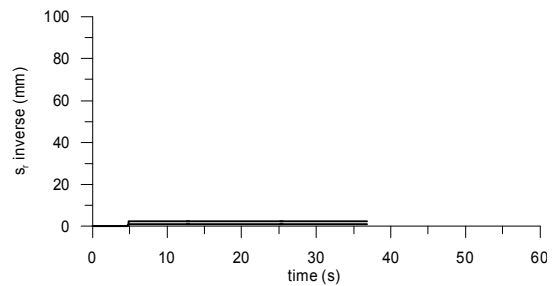
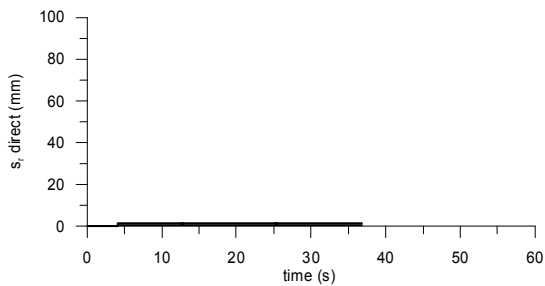
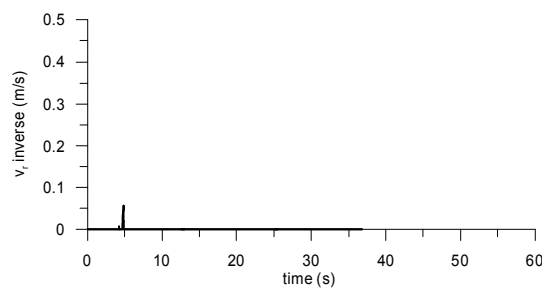
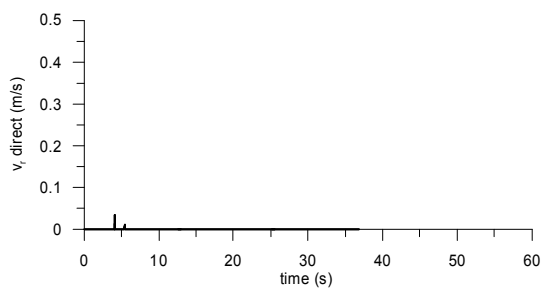
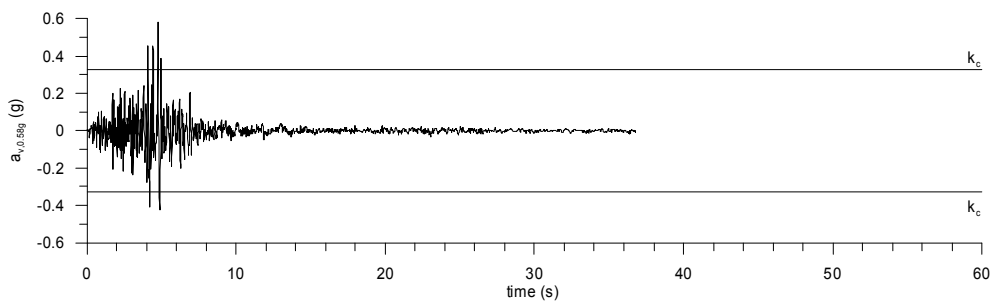
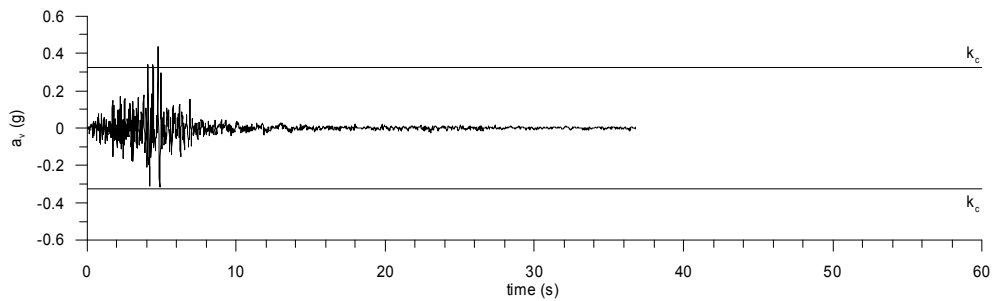
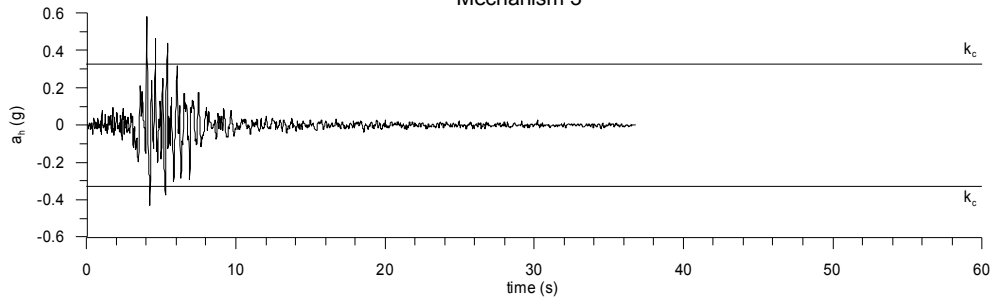
$R_d$ (MN)	SLS2	ULS	SLIS
$W' \cos \alpha \tan \phi'_k$	6143.4	6143.4	6143.4
$W (K_h \sin \alpha - K_v \cos \alpha) \tan \phi'_k$	-213.6	-476.5	-525.7
$T \sin(\alpha - i) \tan \phi'_k$	-287.8	-351.0	-278.6
$E_d$ (MN)	SLS2	ULS	SLIS
$W' \sin \alpha$	1188.4	1188.4	1188.4
$W (K_h \cos \alpha + K_v \sin \alpha)$	875.3	1952.6	2154.6
$T \cos(\alpha - i)$	3225.8	3934.5	3122.6
$\Sigma R_d / \Sigma E_d$ (MN)	4.5	2.4	2.7

		<b>Ponte sullo Stretto di Messina</b> <b>PROGETTO DEFINITIVO</b>		
Sicily Anchor Block – earthquake induced displacements and safety against ultimate limit states, Annex	<i>Codice documento</i> PF0064_F0_ANX		<i>Rev</i> F0	<i>Data</i> 20/06/2011

## Appendix D – Time histories

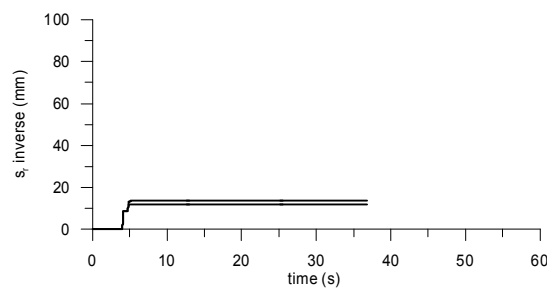
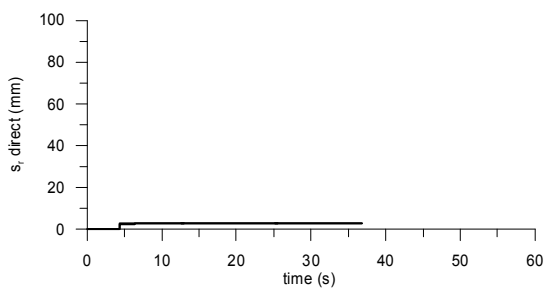
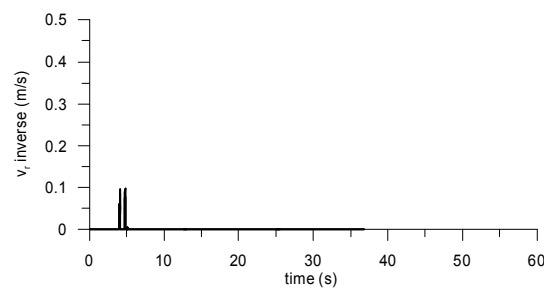
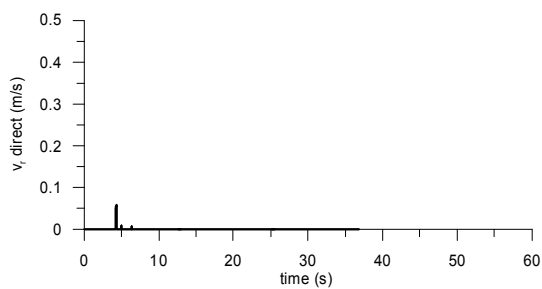
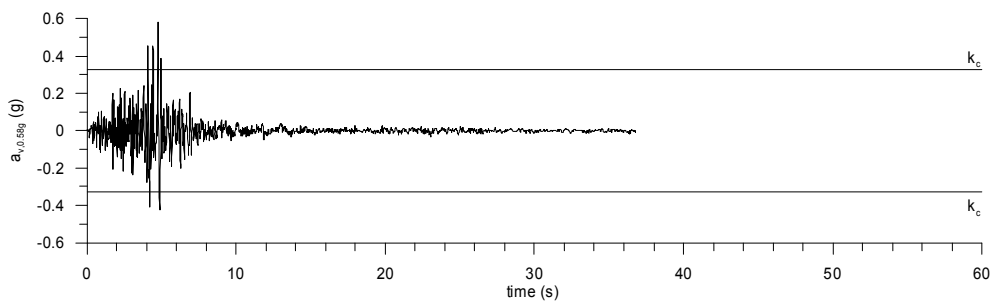
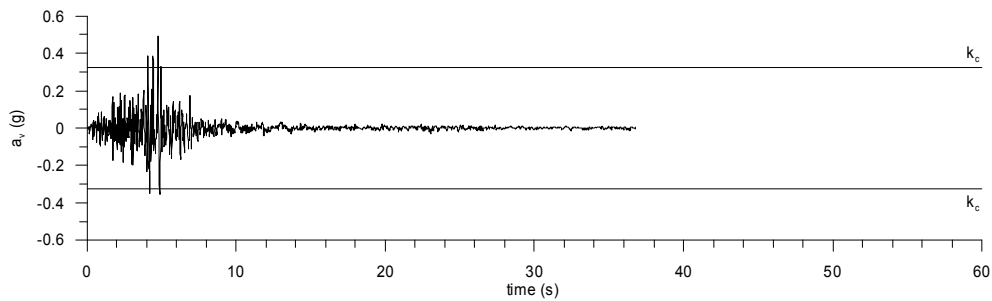
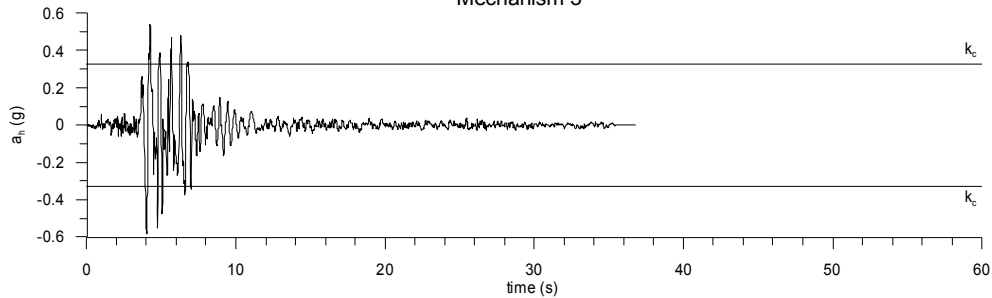


Friuli 76 TOLXC  
Mechanism 3



— same scaling factor for  $a_x$  and  $a_y$   
—  $a_{v,max}=0.58g$

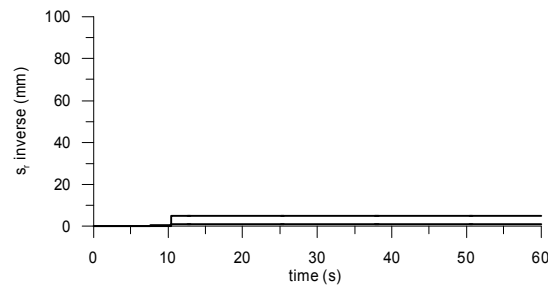
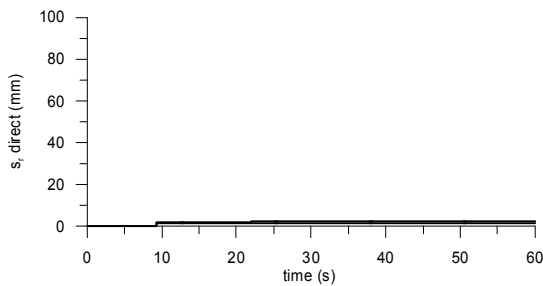
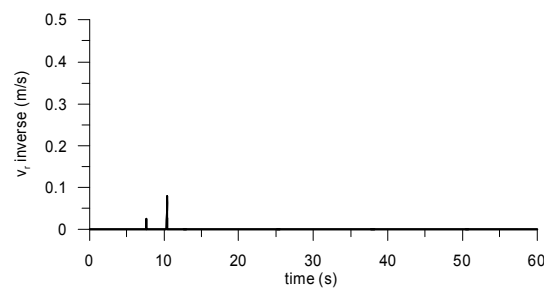
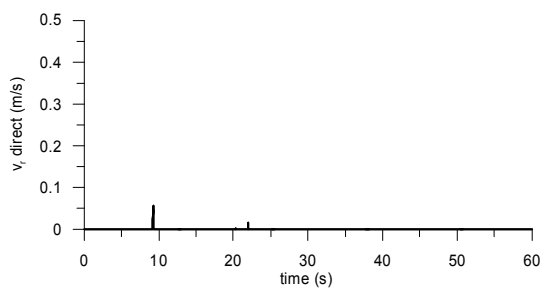
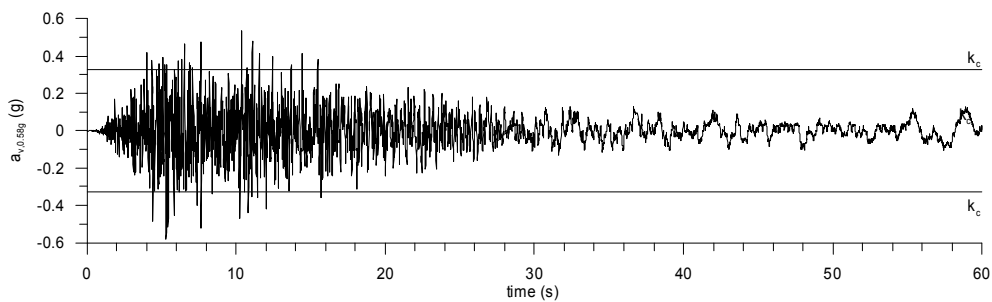
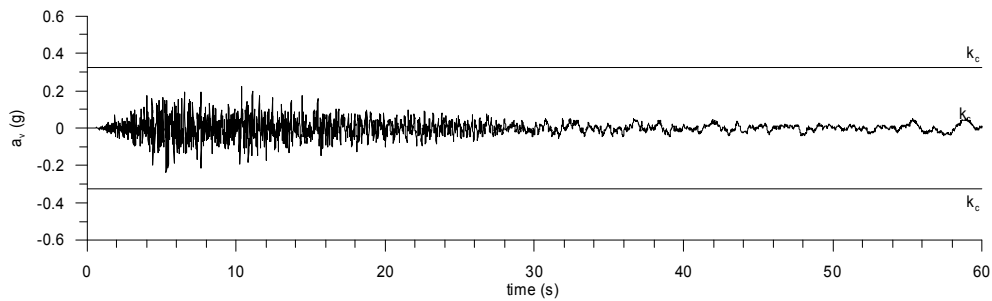
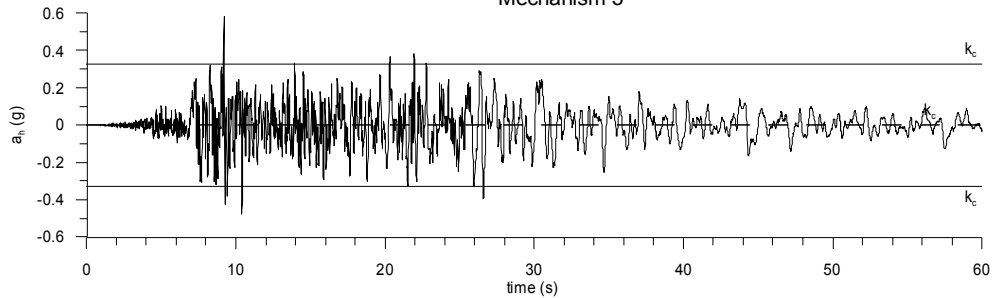
Friuli 76 TOLYC  
Mechanism 3



— same scaling factor for  $a_x$  and  $a_v$   
—  $a_{v,max}=0.58g$

Imperial Valley 79 DLT352

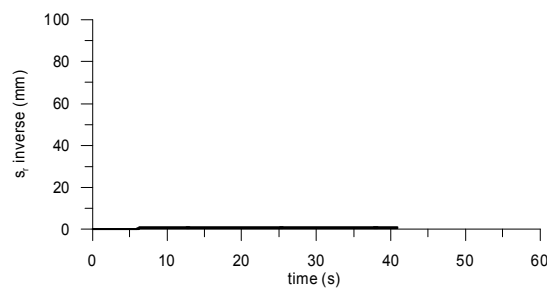
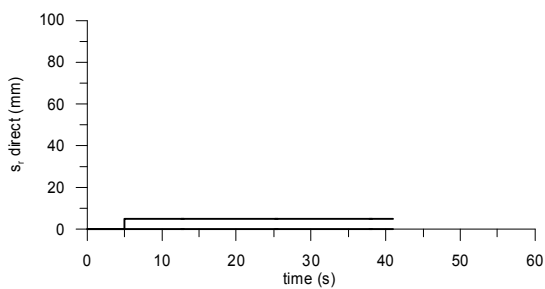
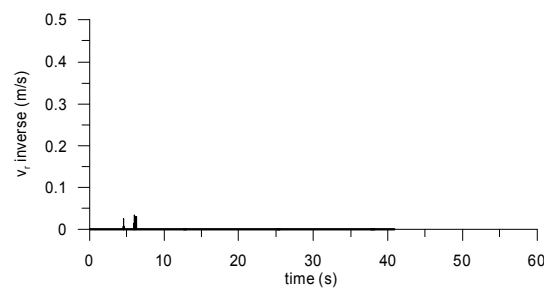
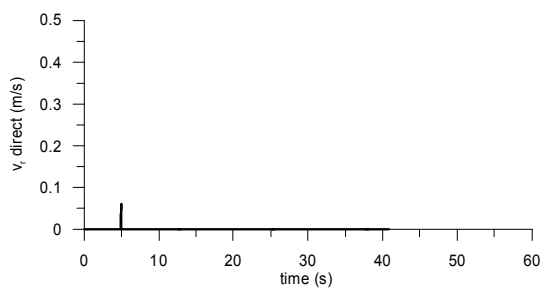
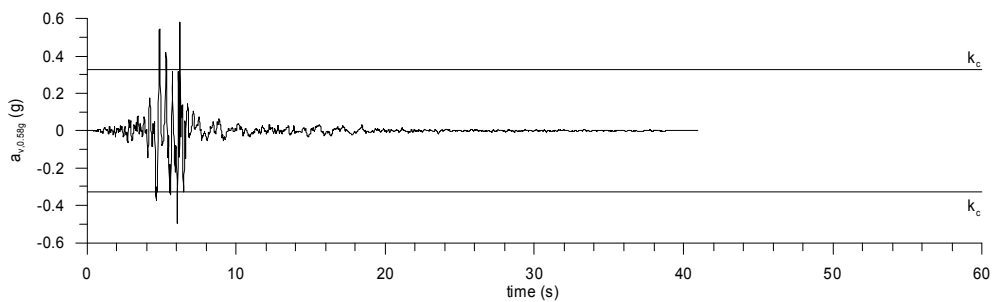
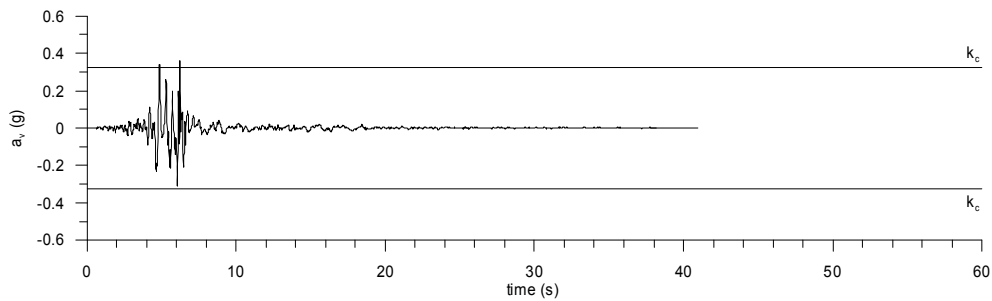
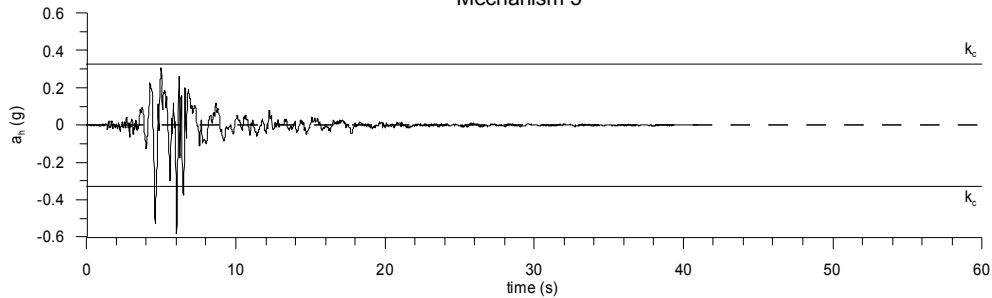
Mechanism 3



— same scaling factor for  $a_x$  and  $a_y$   
—  $a_{v,max}=0.58g$

Kobe 95 TAZ000

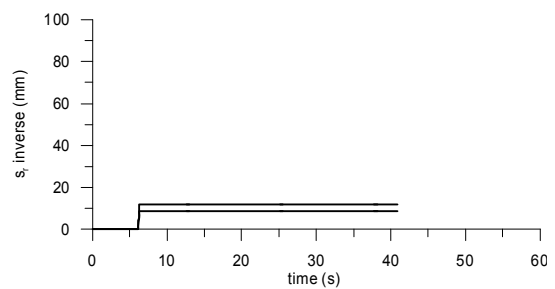
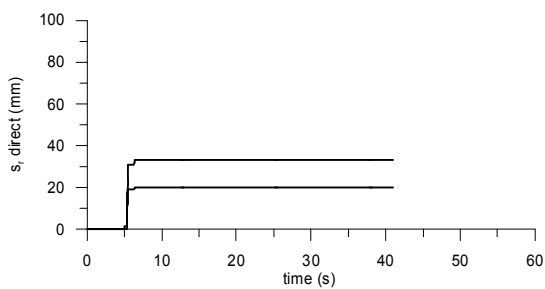
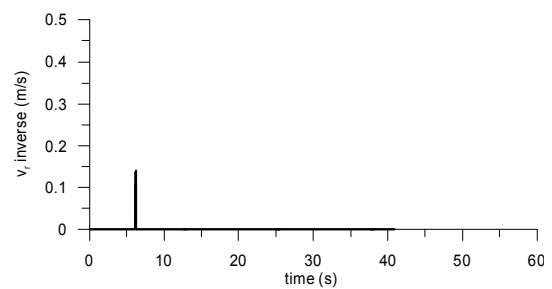
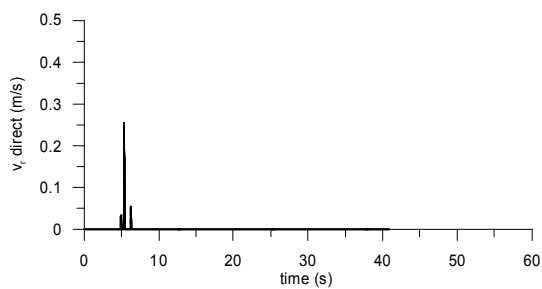
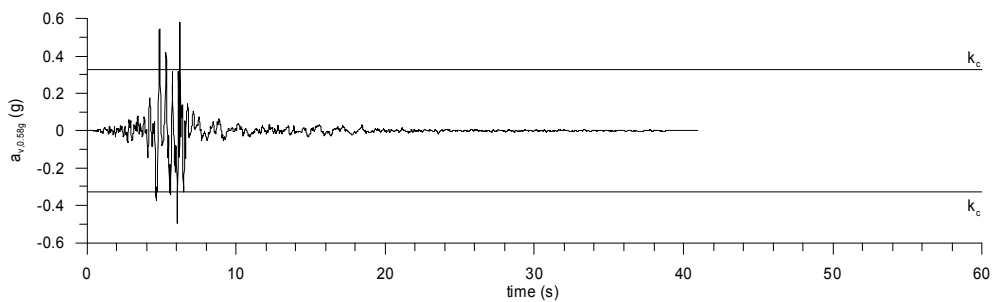
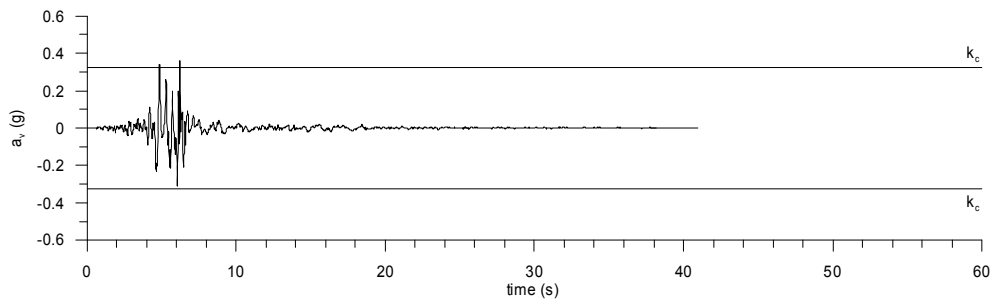
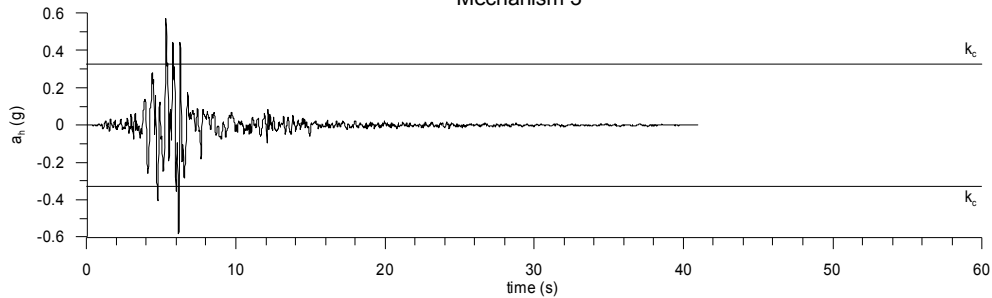
Mechanism 3



— same scaling factor for  $a_x$  and  $a_y$   
—  $a_{v,max}=0.58g$

Kobe 95 TAZ090

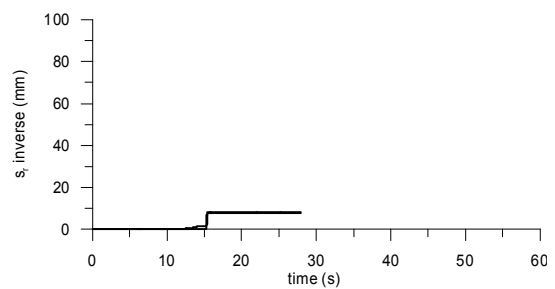
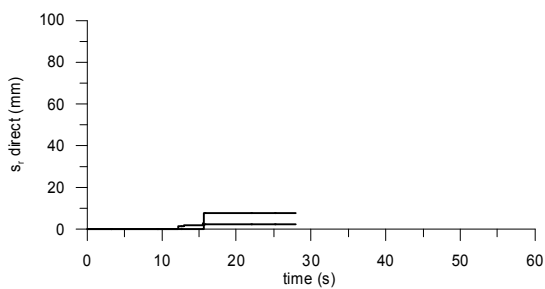
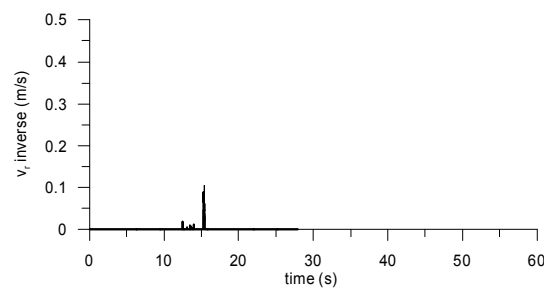
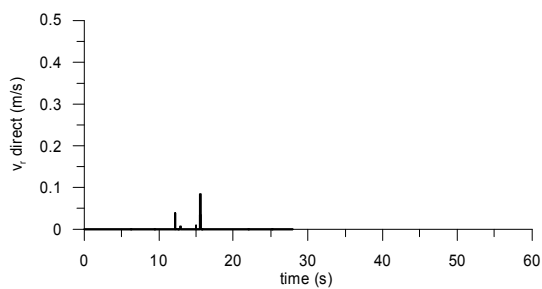
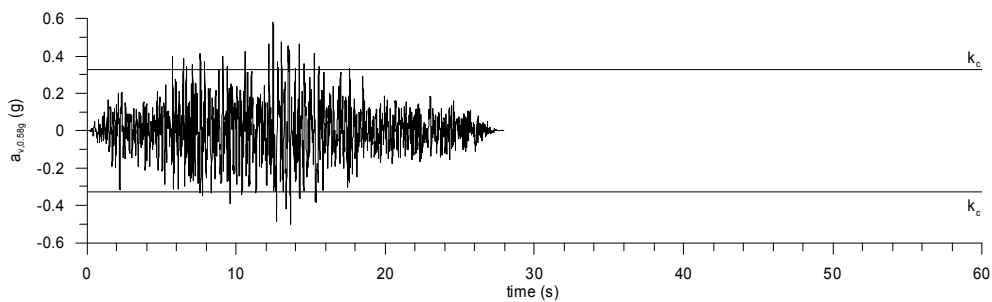
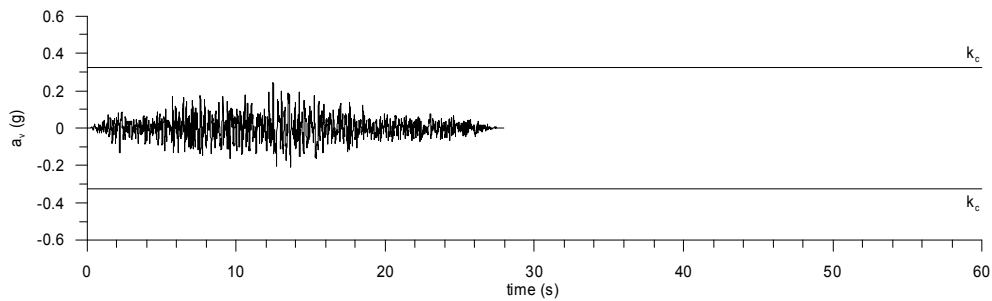
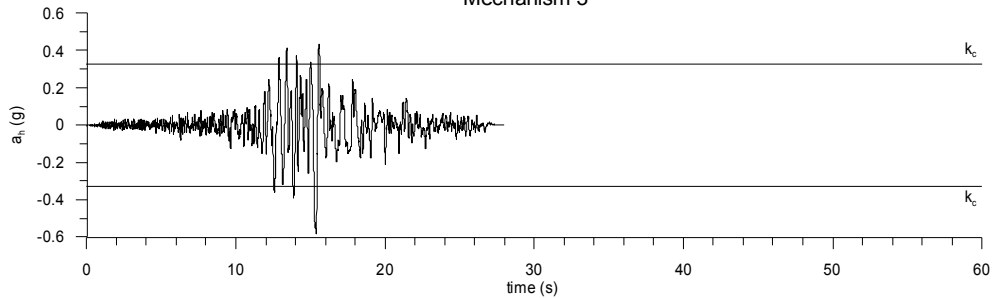
Mechanism 3



— same scaling factor for  $a_x$  and  $a_v$   
—  $a_{v,max}=0.58g$

Landers 92 CLWTR

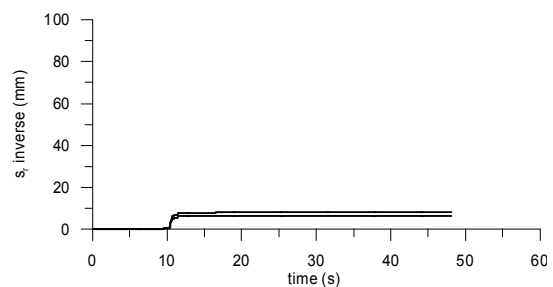
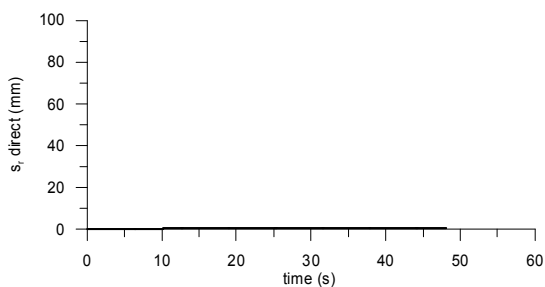
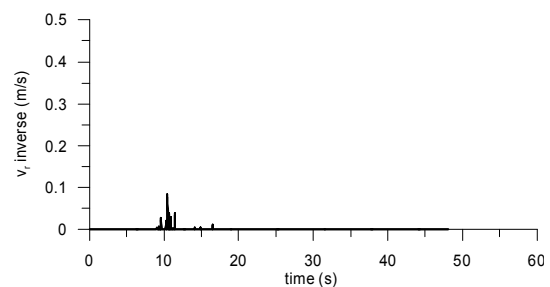
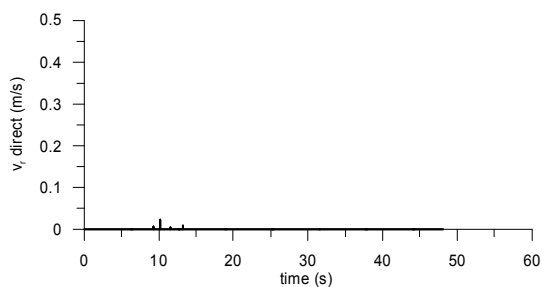
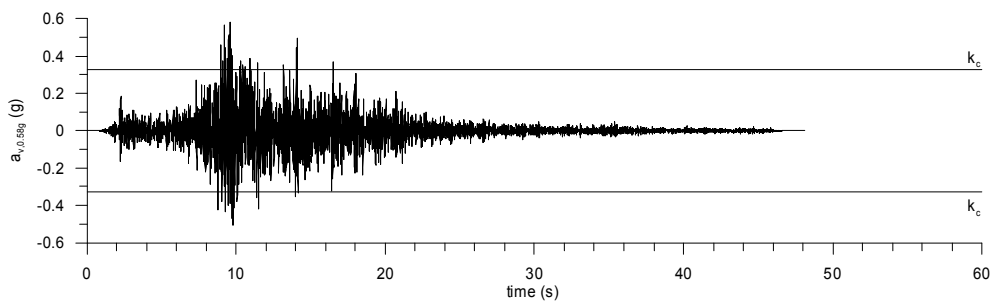
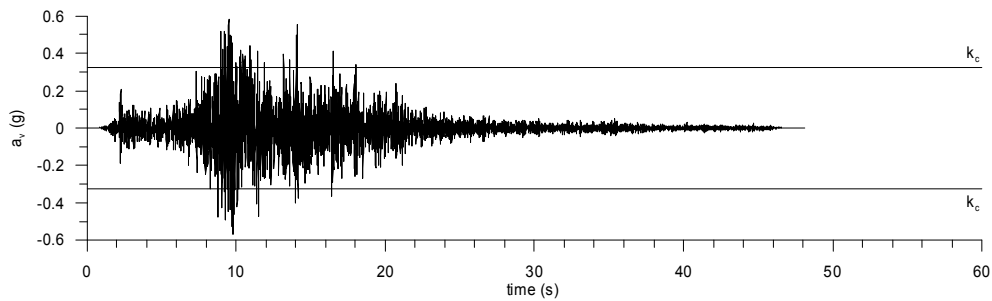
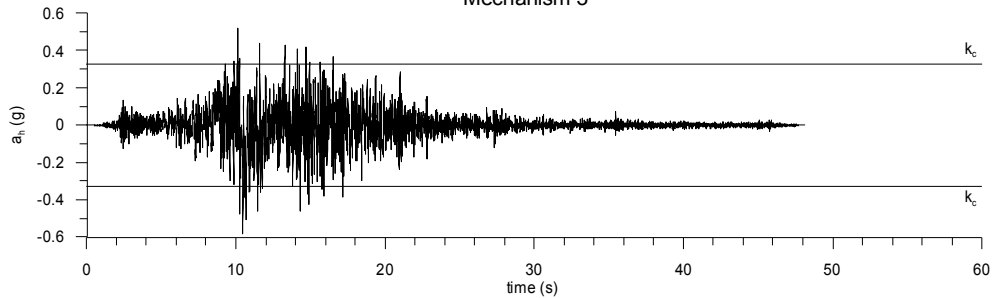
Mechanism 3



— same scaling factor for  $a_x$  and  $a_y$   
—  $a_{v,max}=0.58g$

Landers 92 LCN260

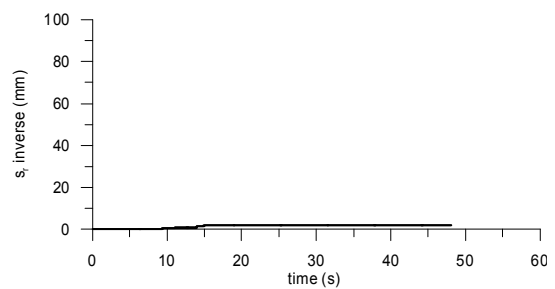
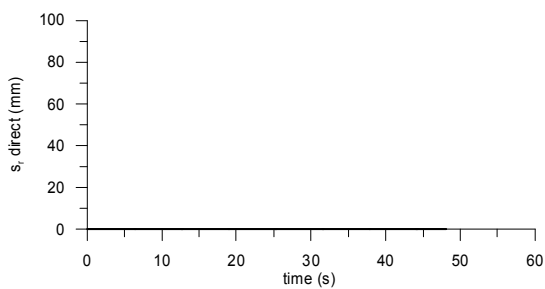
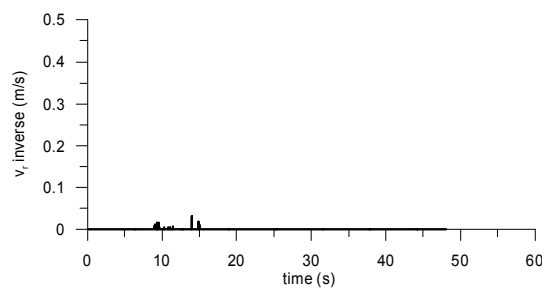
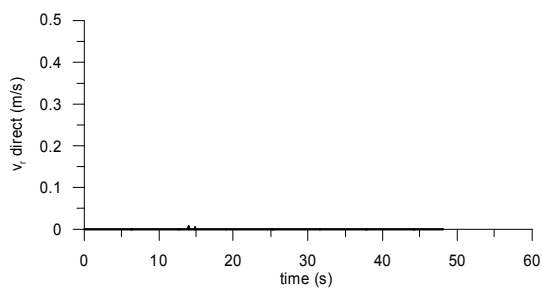
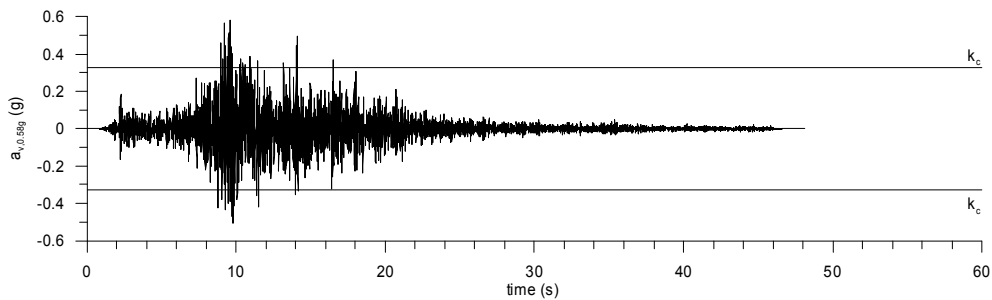
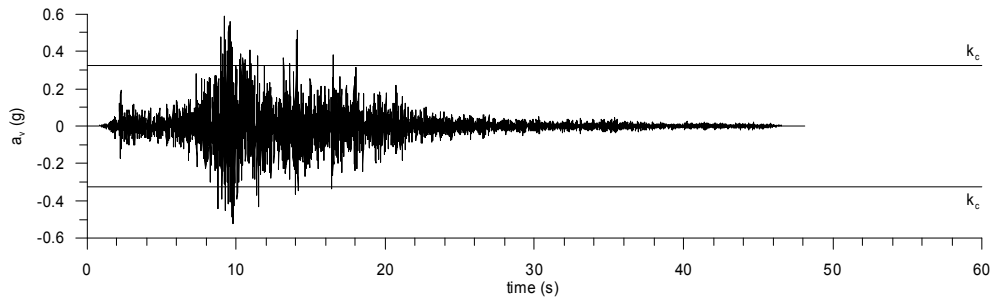
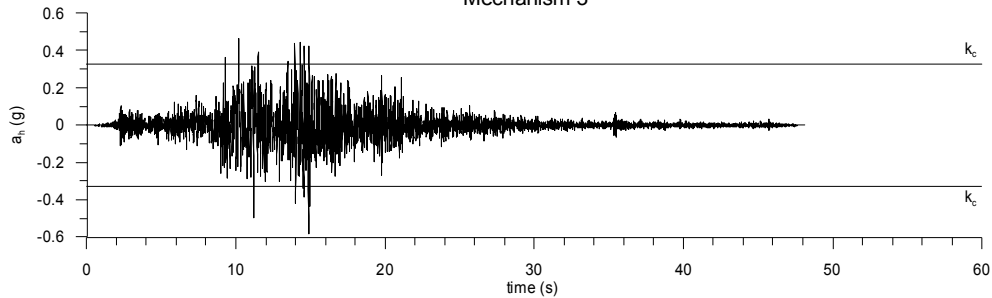
Mechanism 3



— same scaling factor for  $a_x$  and  $a_y$   
—  $a_{v,max}=0.58g$

Landers 92 LCN345

Mechanism 3

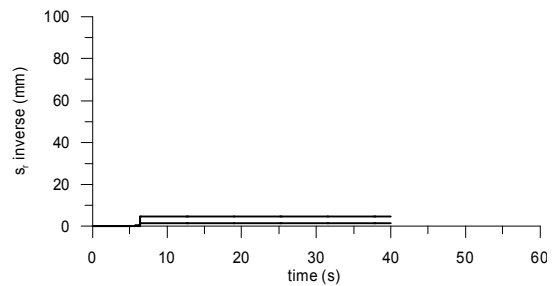
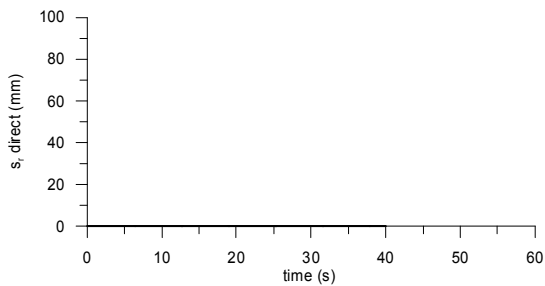
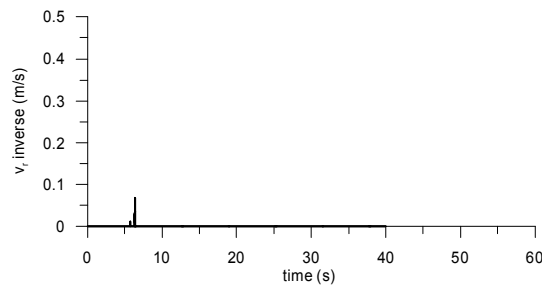
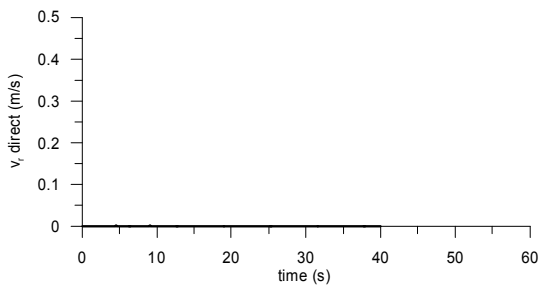
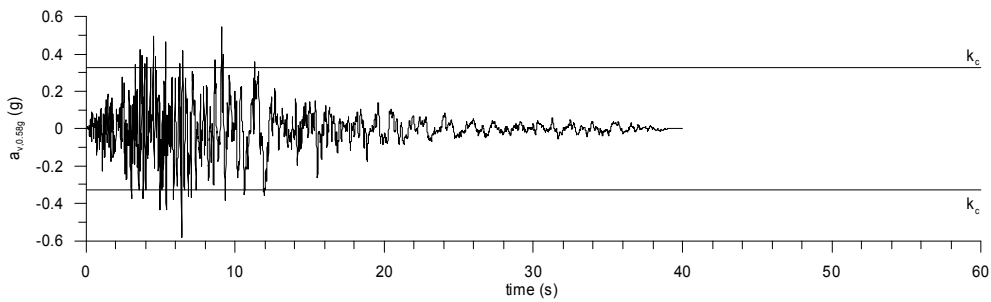
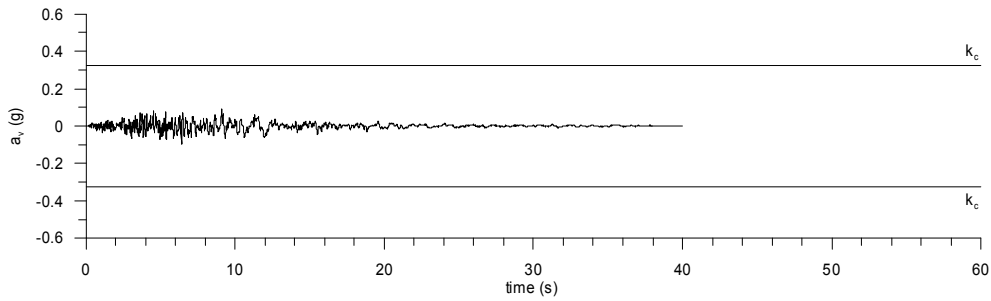
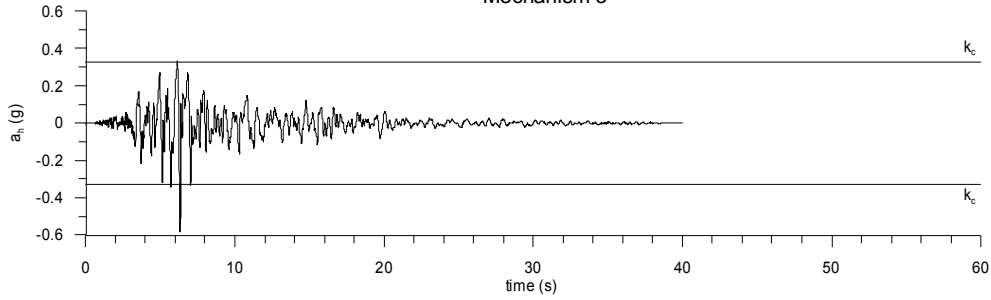


— same scaling factor for  $a_x$  and  $a_y$   
—  $a_{v,max}=0.58g$



Loma Prieta 89 CYC285

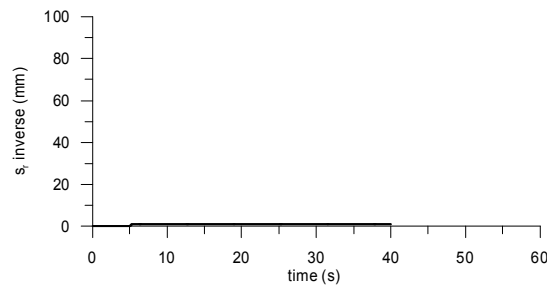
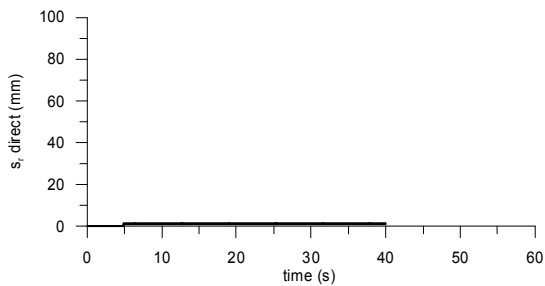
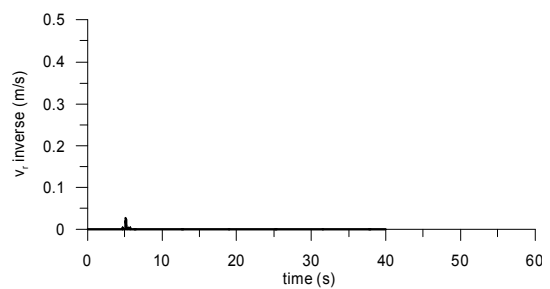
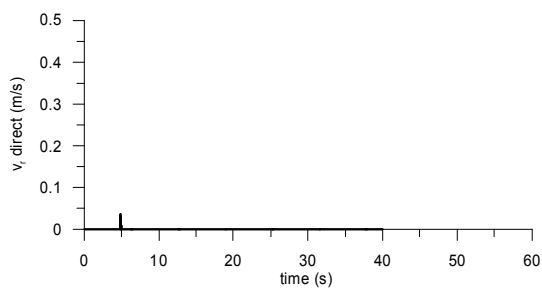
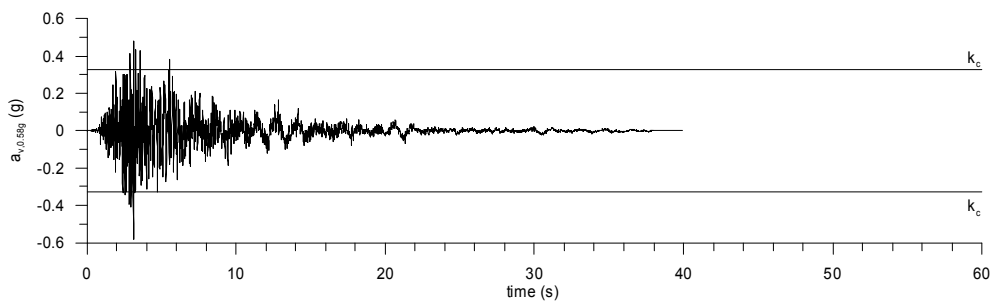
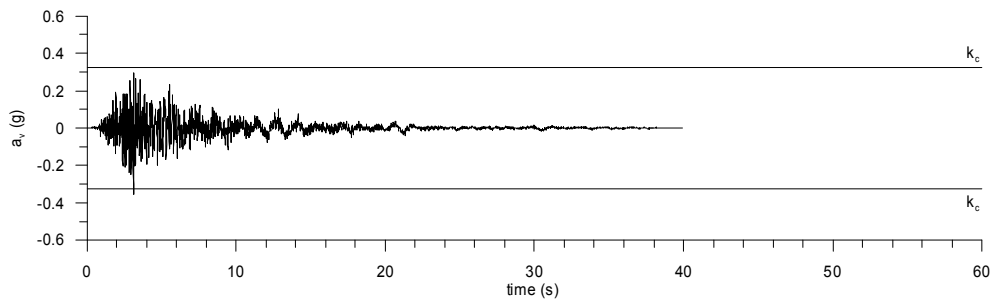
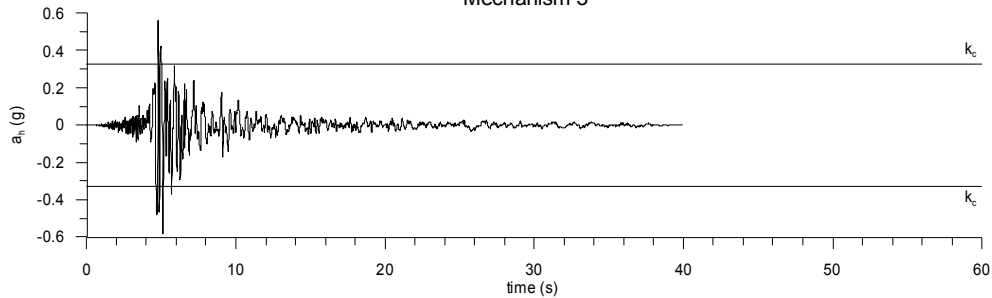
Mechanism 3



— same scaling factor for  $a_x$  and  $a_v$   
—  $a_{v,max}=0.58g$

Loma Prieta 89 G03000

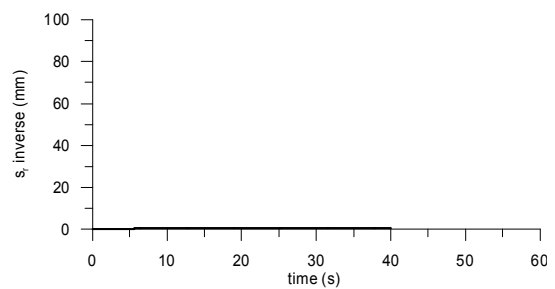
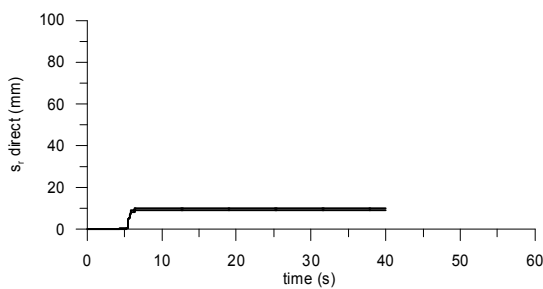
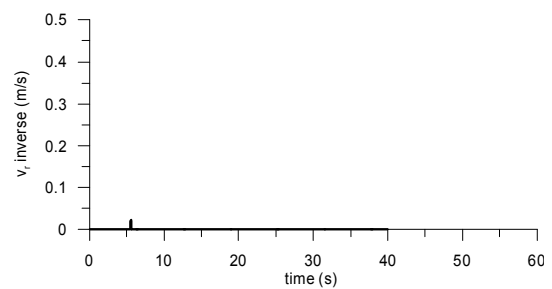
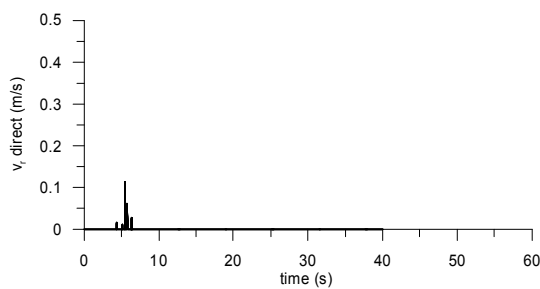
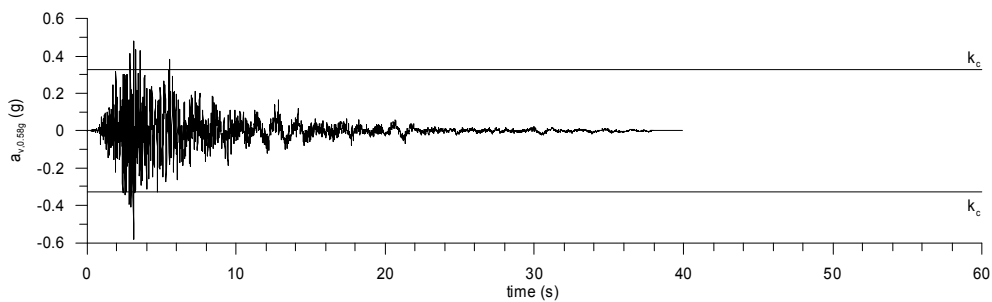
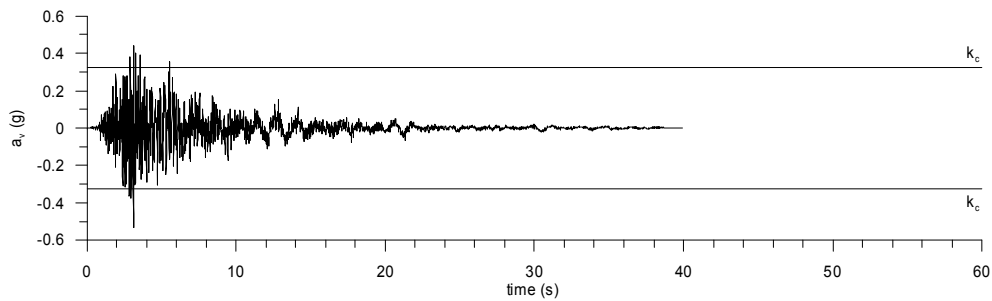
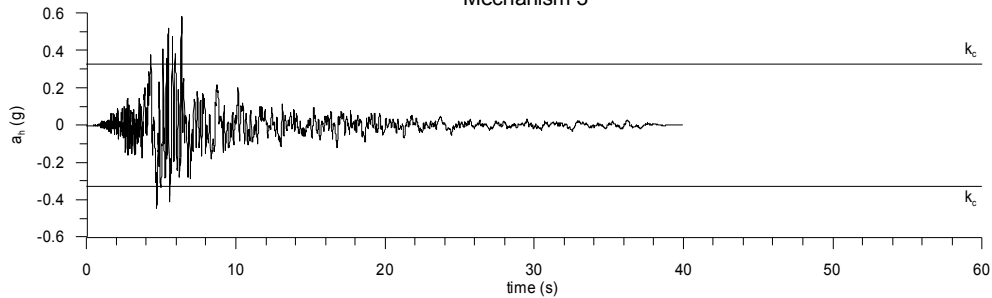
Mechanism 3



— same scaling factor for  $a_x$  and  $a_v$   
—  $a_{v,max}=0.58g$

Loma Prieta 89 G03090

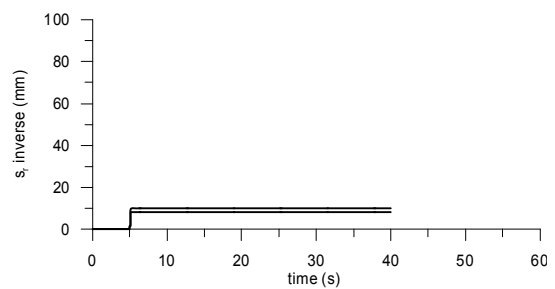
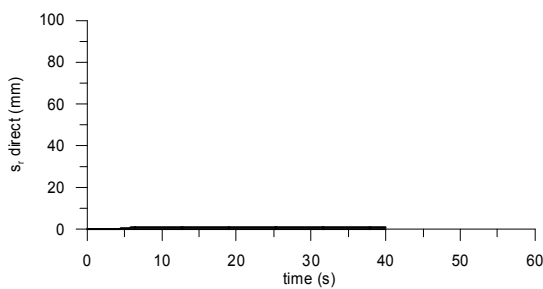
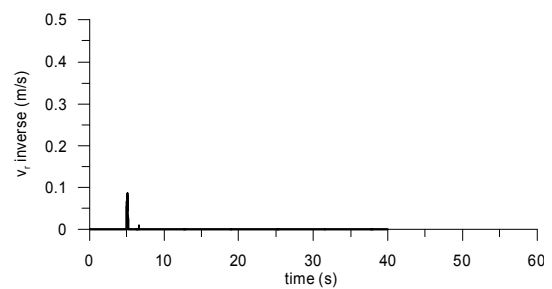
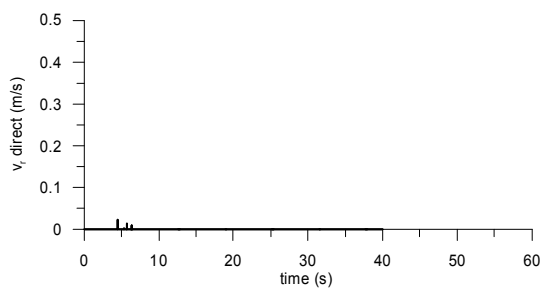
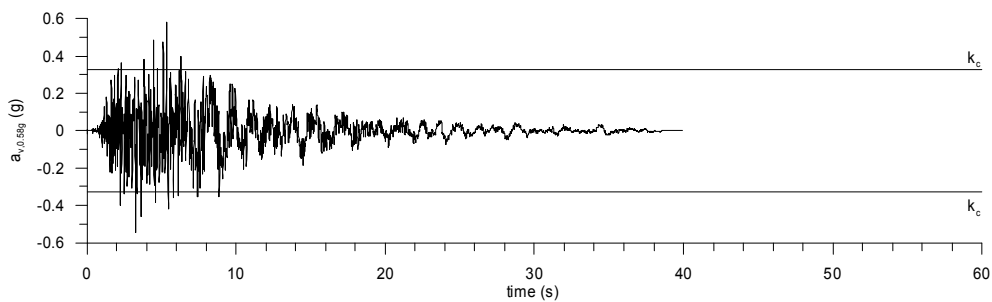
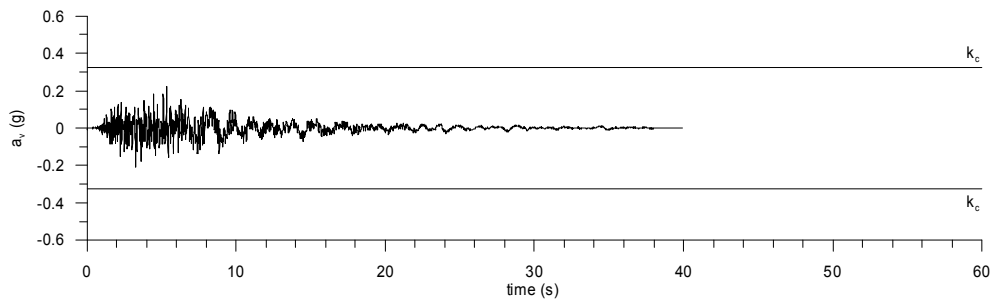
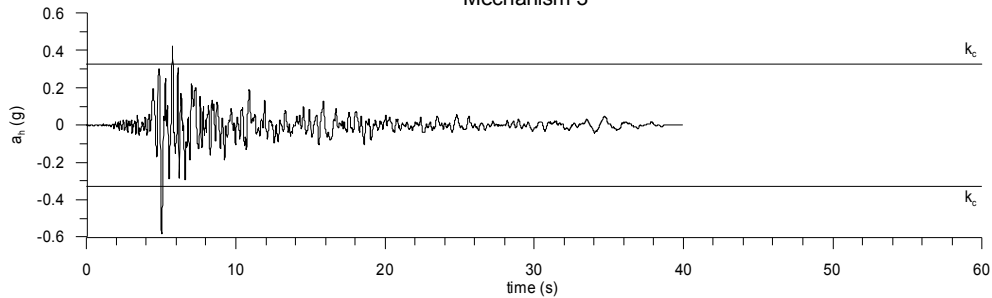
Mechanism 3



— same scaling factor for  $a_x$  and  $a_v$   
—  $a_{v,max}=0.58g$

Loma Prieta 89 G04000

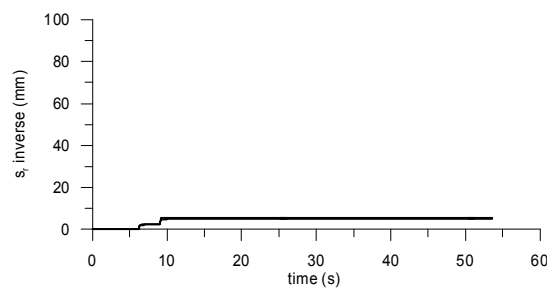
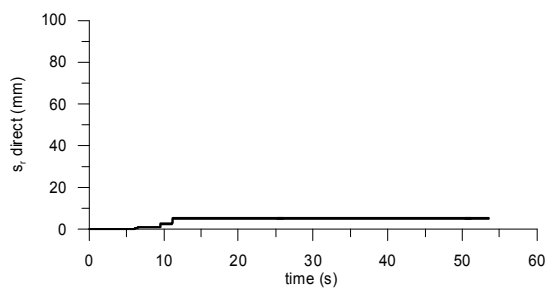
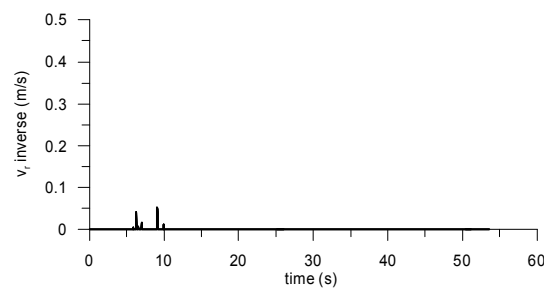
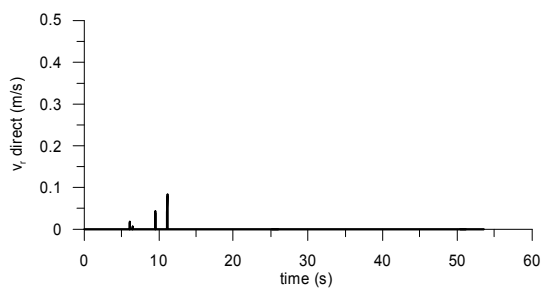
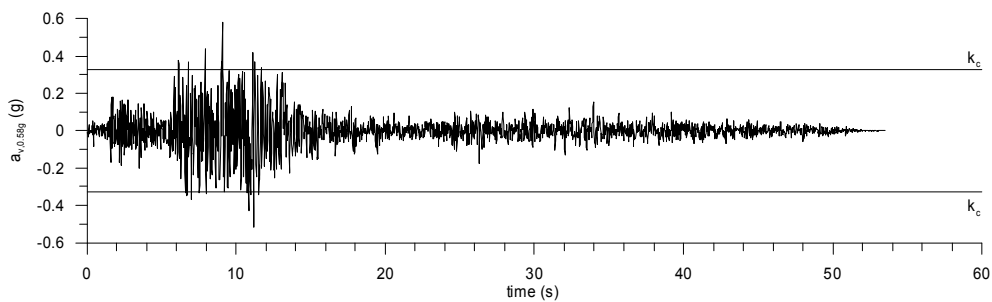
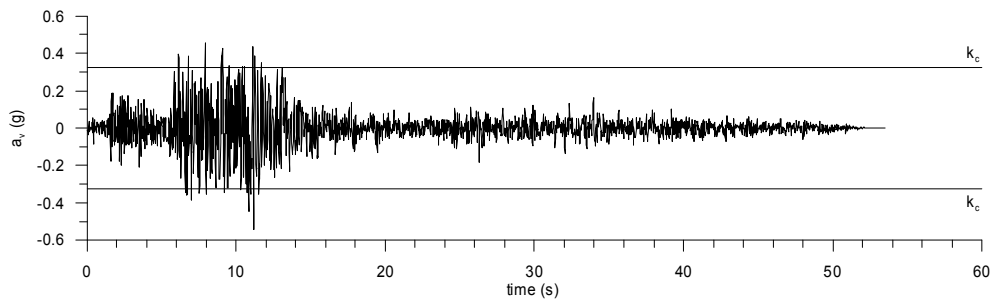
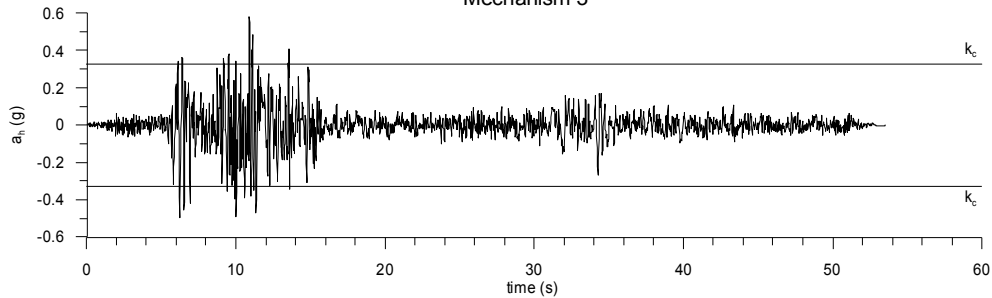
Mechanism 3



— same scaling factor for  $a_h$  and  $a_v$   
—  $a_{v,max}=0.58g$

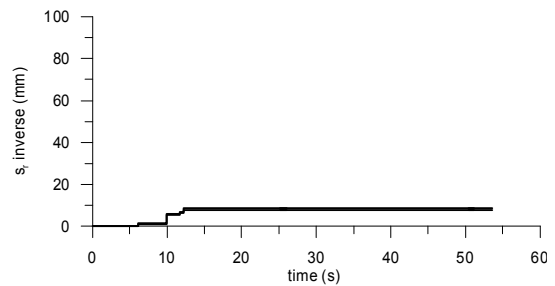
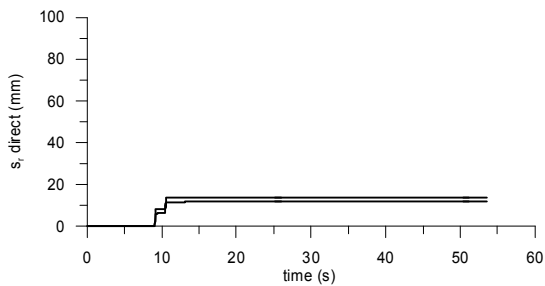
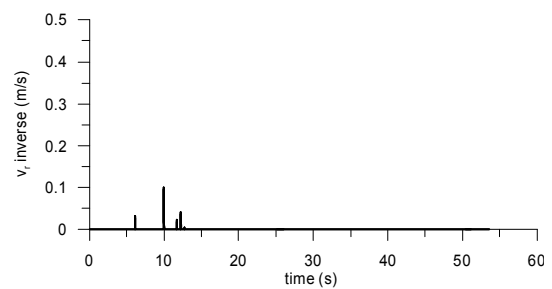
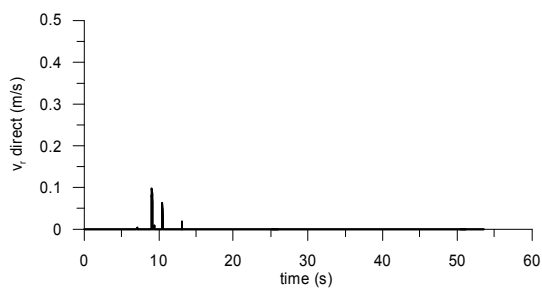
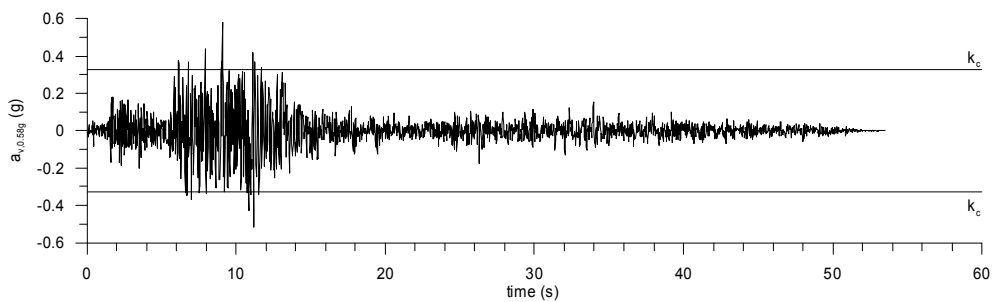
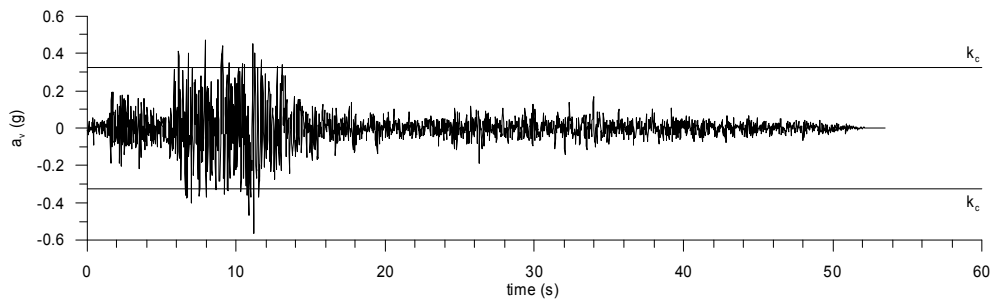
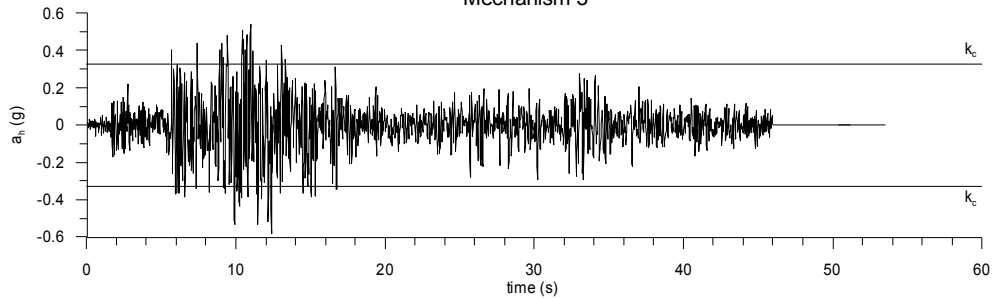
Manjil 90 ABBL

Mechanism 3



— same scaling factor for  $a_x$  and  $a_v$   
—  $a_{v,max}=0.58g$

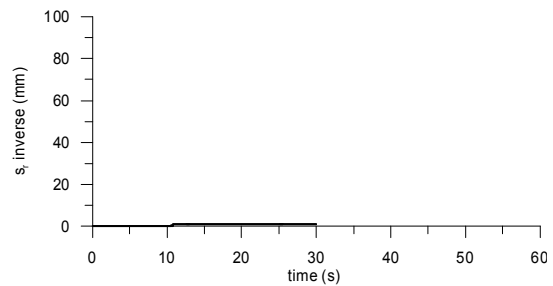
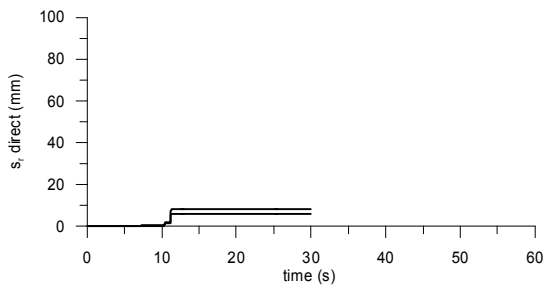
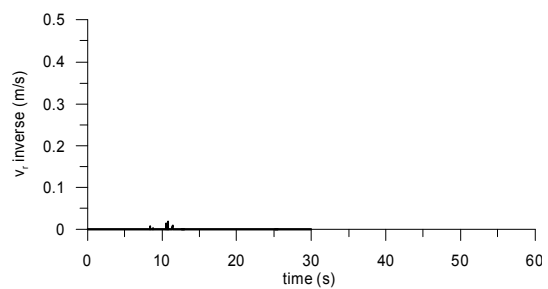
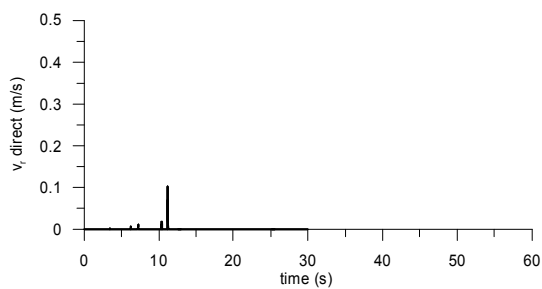
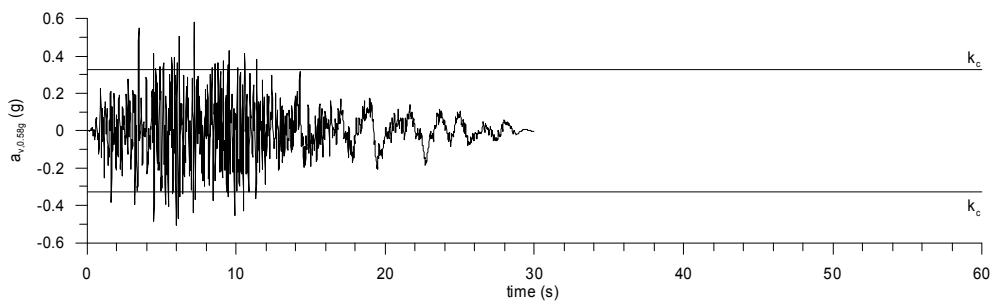
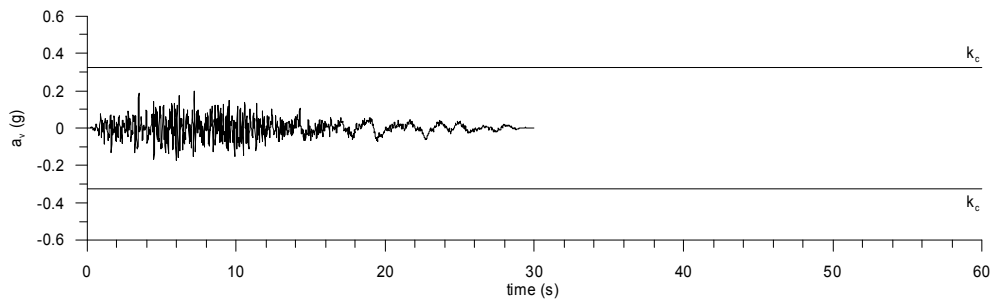
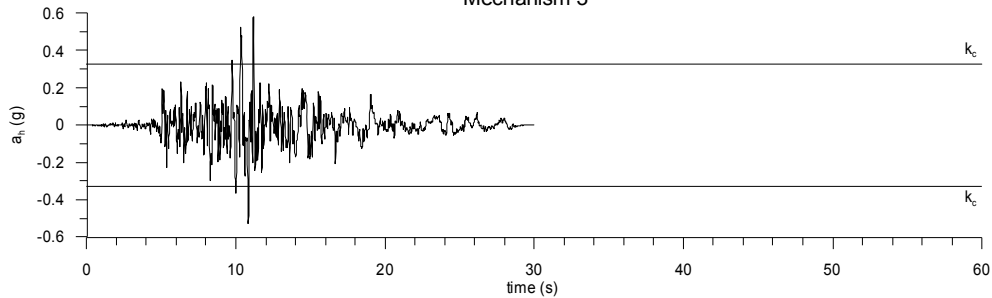
Manjil 90 ABBT  
Mechanism 3



— same scaling factor for  $a_v$  and  $a_v$   
—  $a_{v,max}=0.58g$

Northridge 94 CEN245

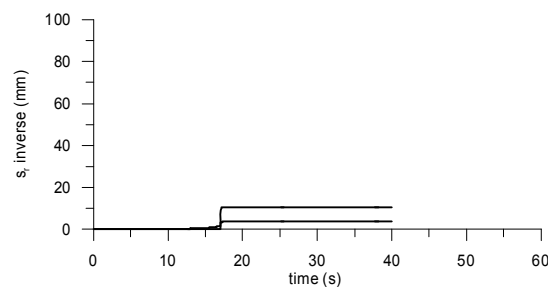
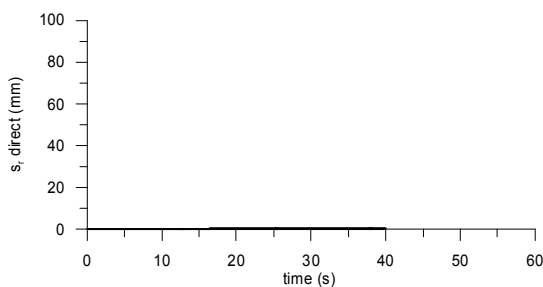
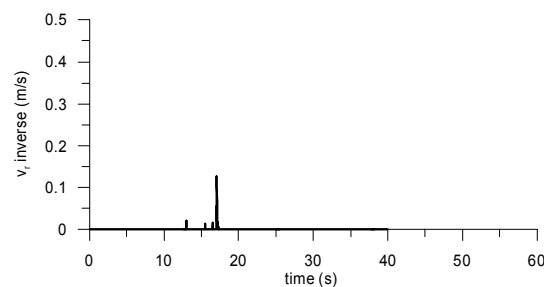
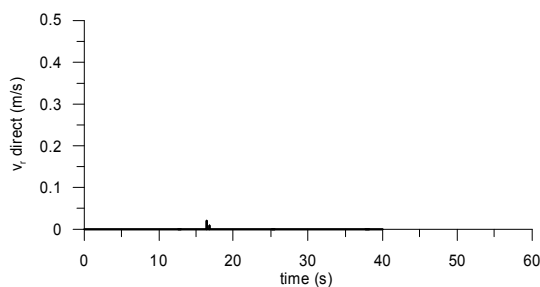
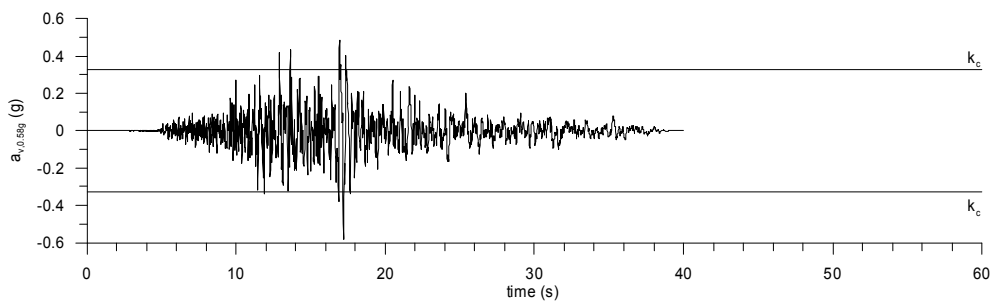
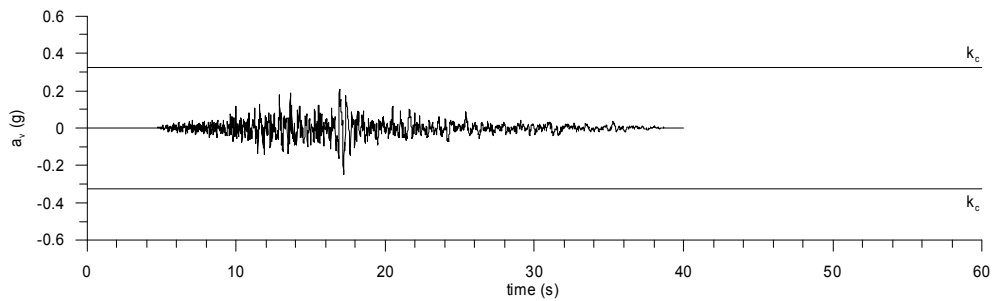
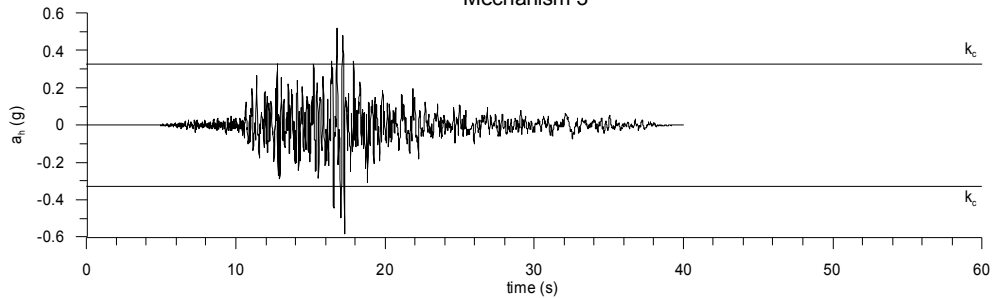
Mechanism 3



— same scaling factor for  $a_x$  and  $a_v$   
—  $a_{v,max}=0.58g$

Northridge 94 LAC180

Mechanism 3

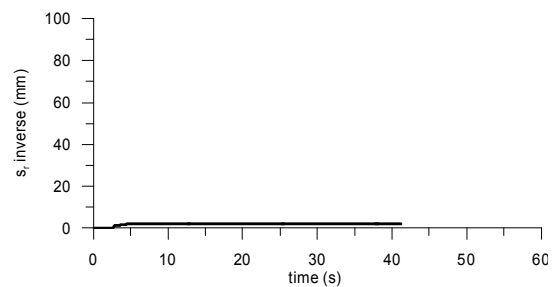
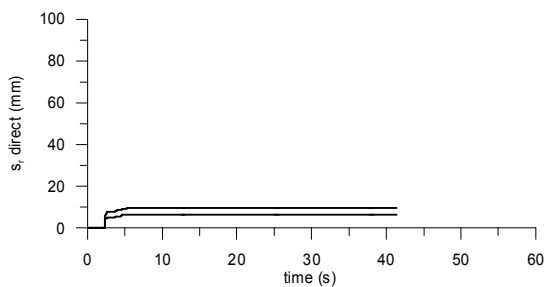
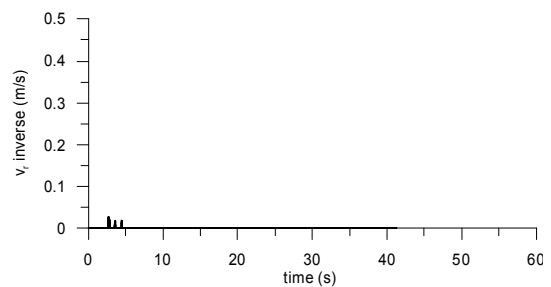
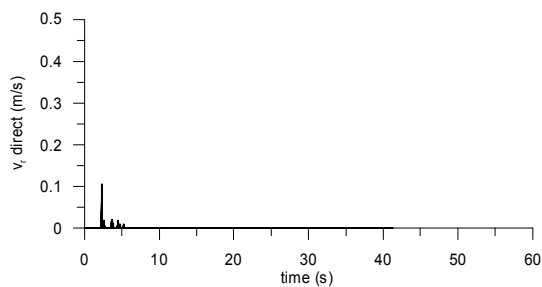
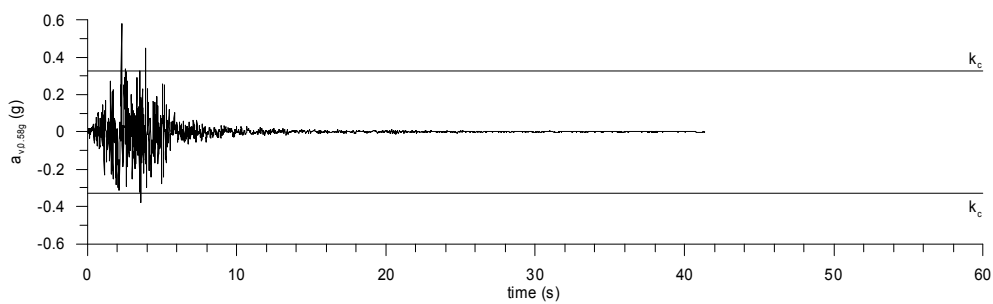
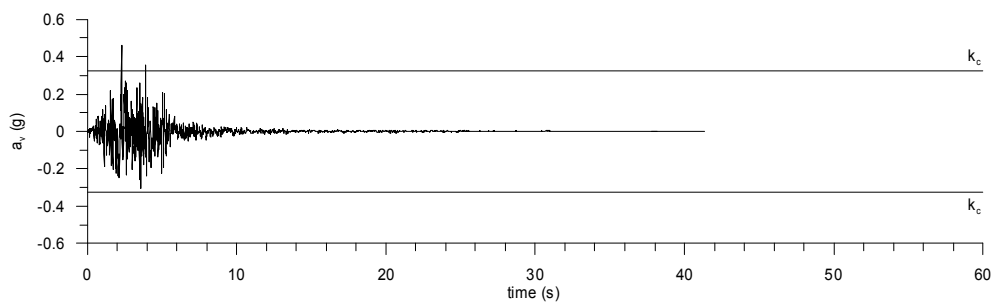
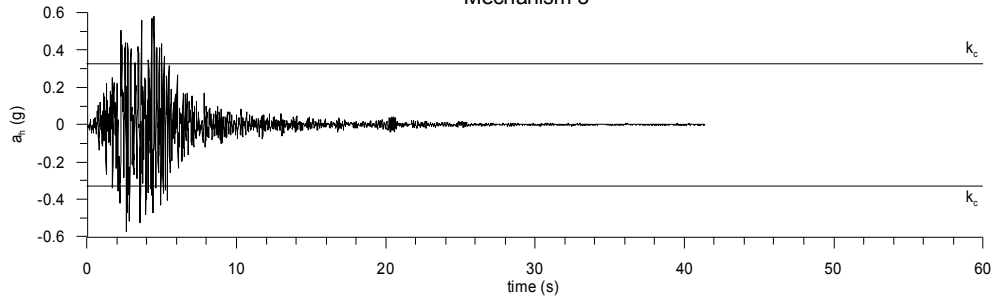


— same scaling factor for  $a_x$  and  $a_y$   
—  $a_{v,max}=0.58g$



Umbria Marche 97 NCRXC

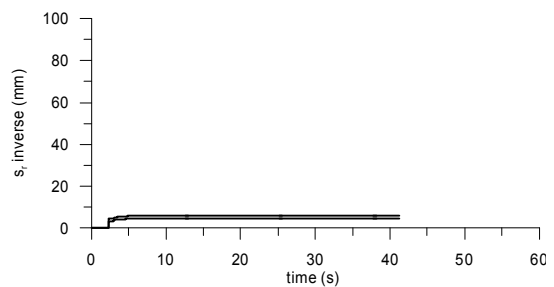
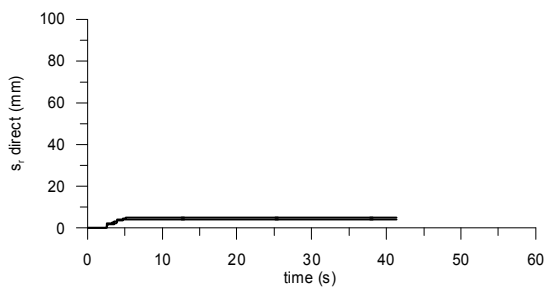
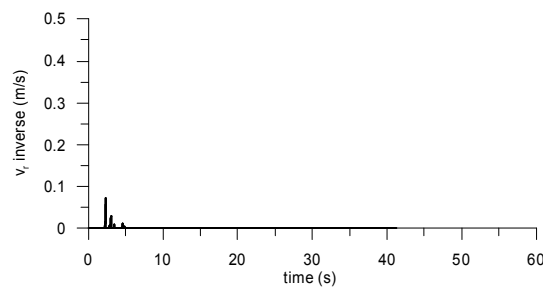
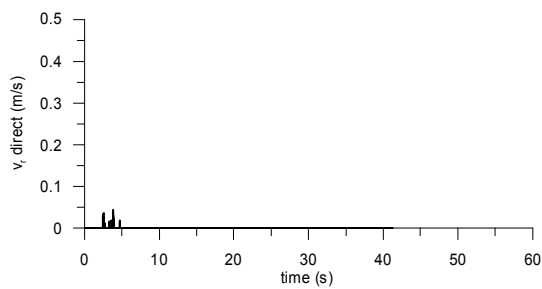
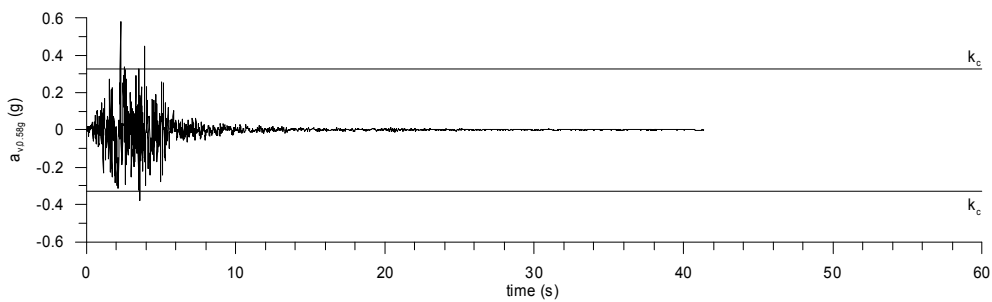
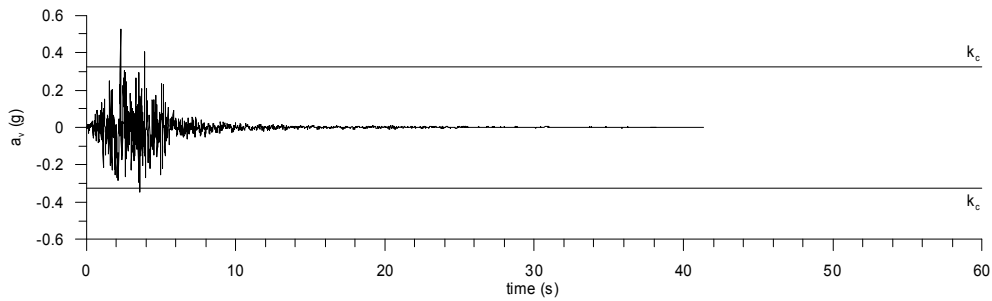
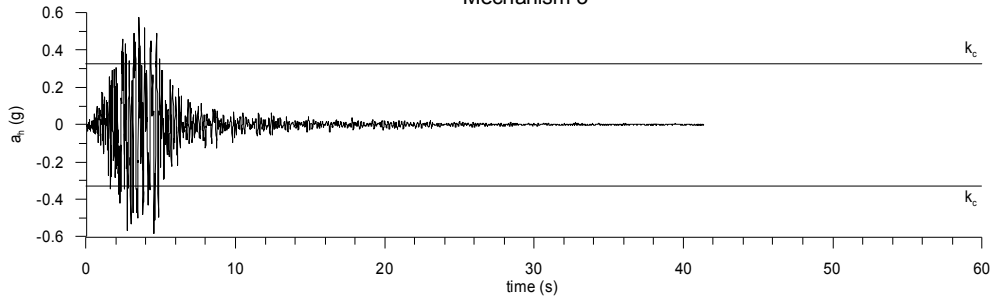
Mechanism 3



— same scaling factor for  $a_x$  and  $a_y$   
—  $a_{v,max}=0.58g$

Umbria Marche 97 NCRYC

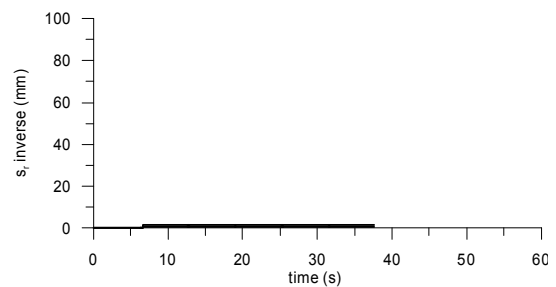
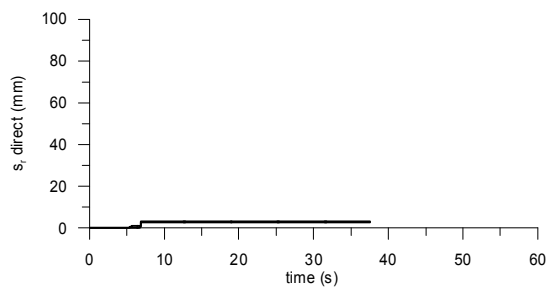
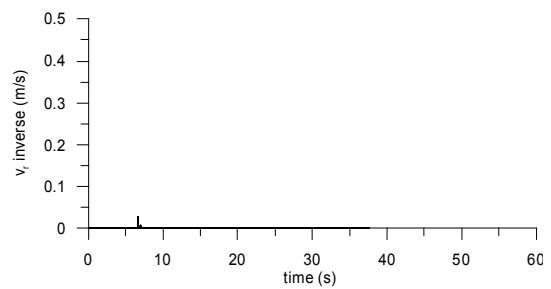
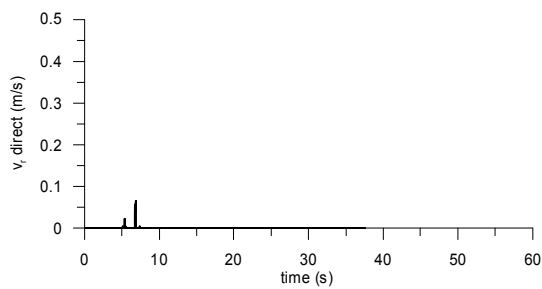
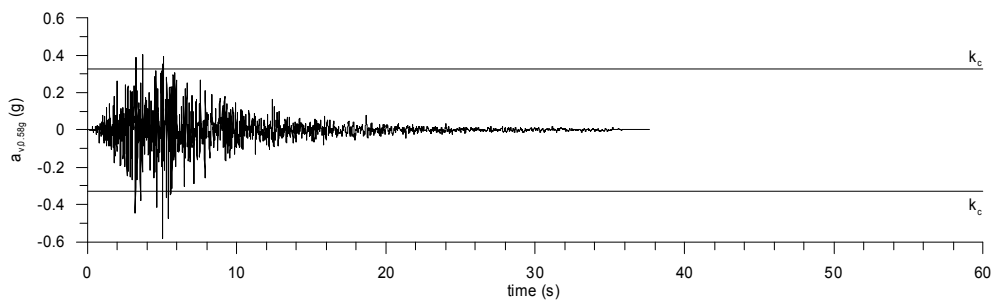
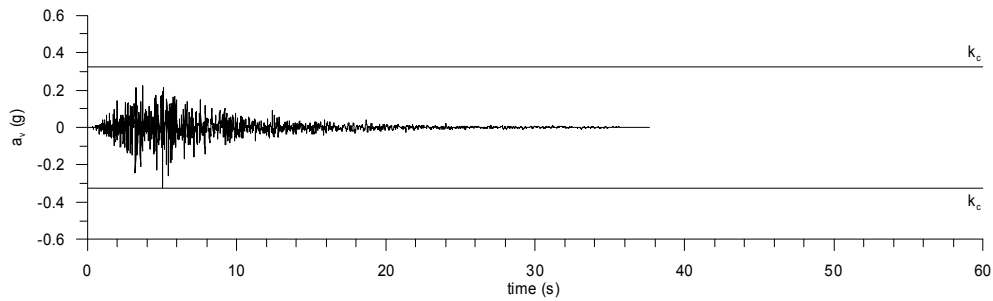
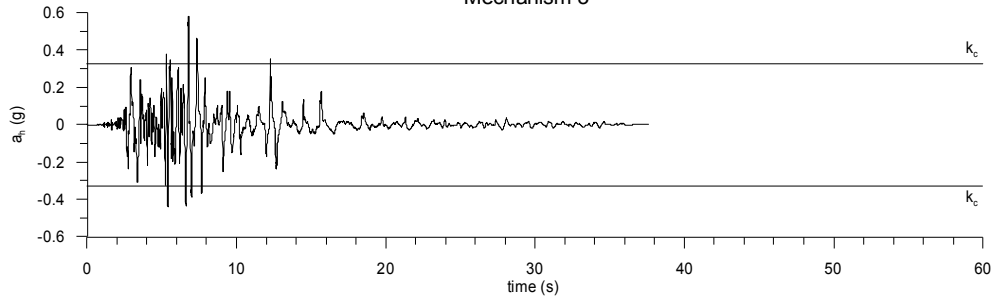
Mechanism 3



— same scaling factor for  $a_n$  and  $a_v$   
—  $a_{v,max}=0.58g$

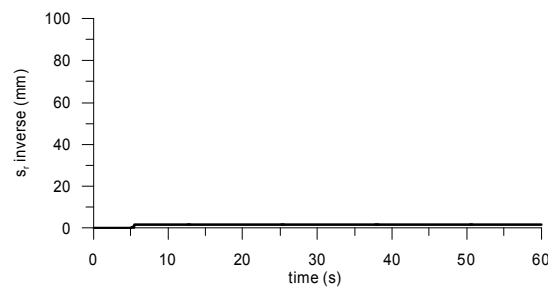
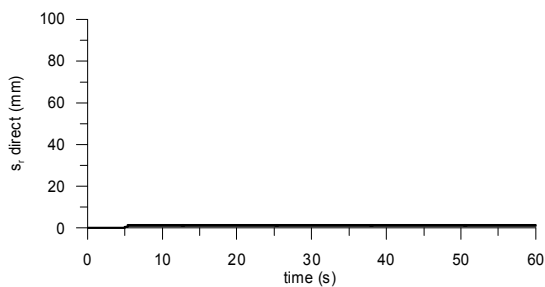
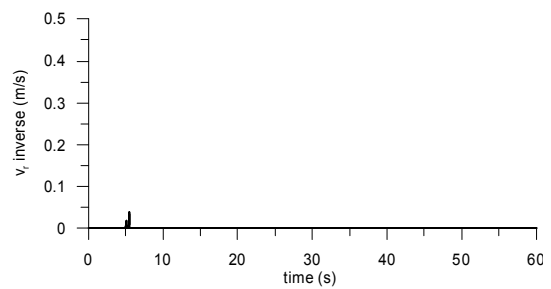
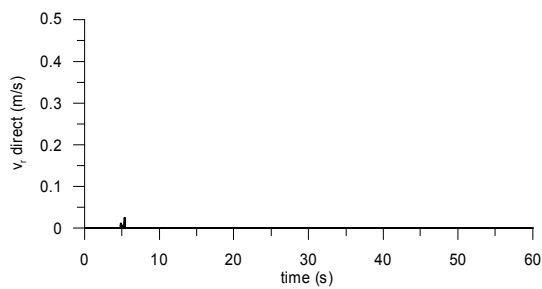
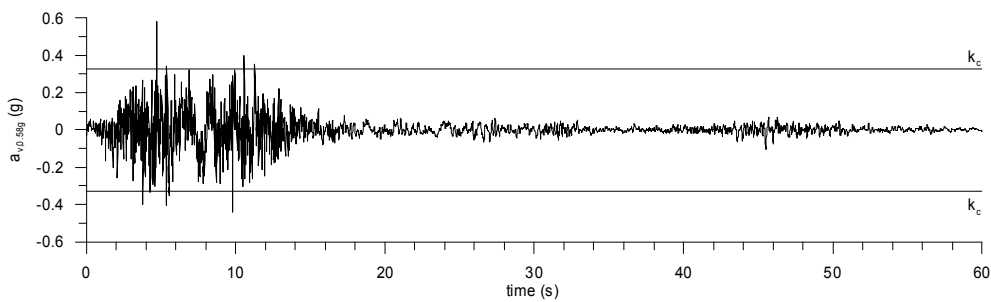
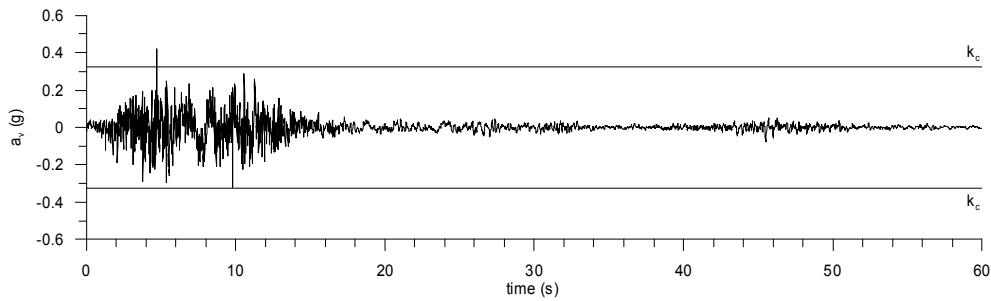
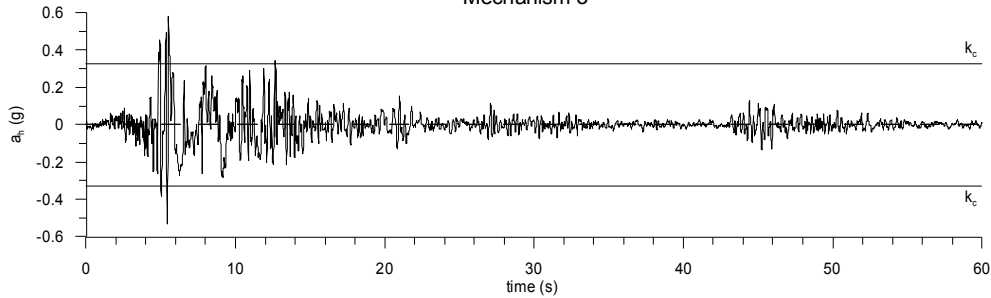
Imperial Valley 79 BC230

Mechanism 3



— same scaling factor for  $a_n$  and  $a_v$   
—  $a_{v,max}=0.58g$

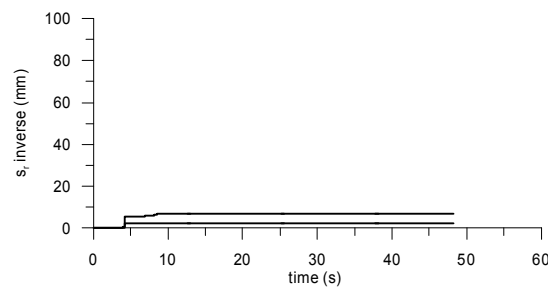
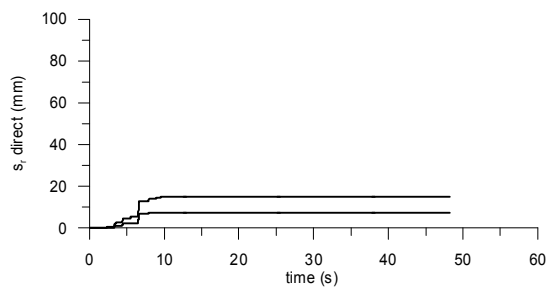
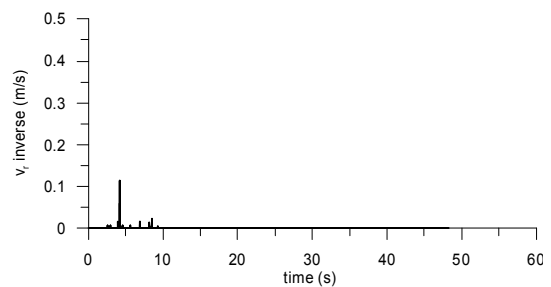
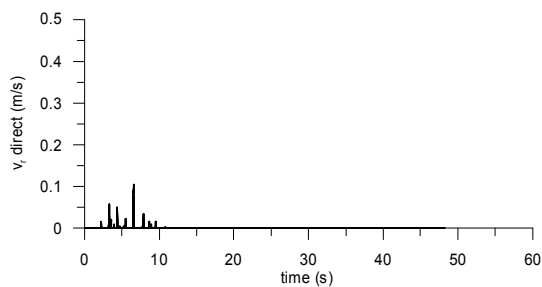
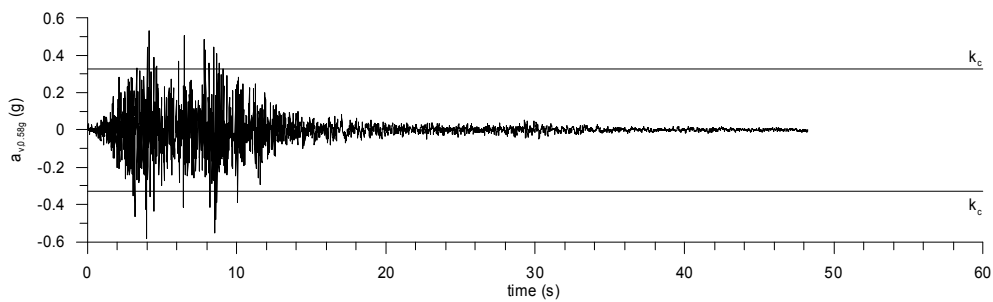
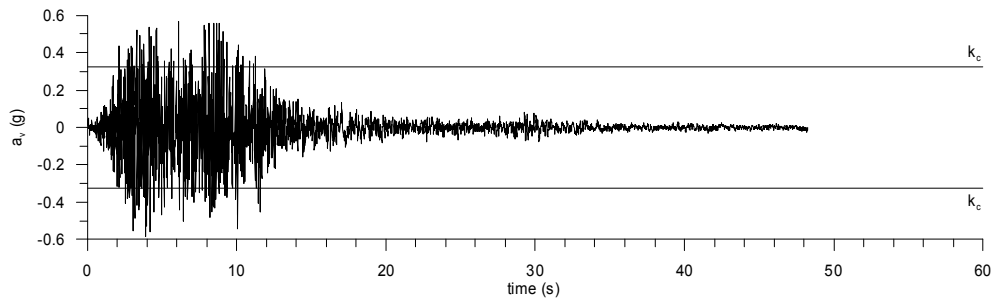
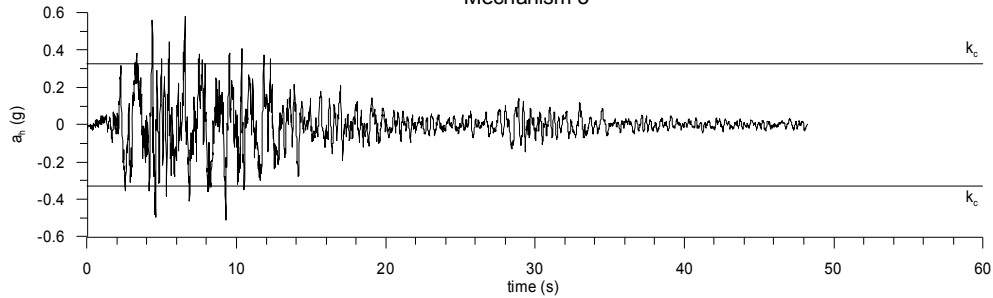
Irpinia 80 STUYC  
Mechanism 3



— same scaling factor for  $a_n$  and  $a_v$   
—  $a_{v,max}=0.58g$

Montenegro 79 ULCXC

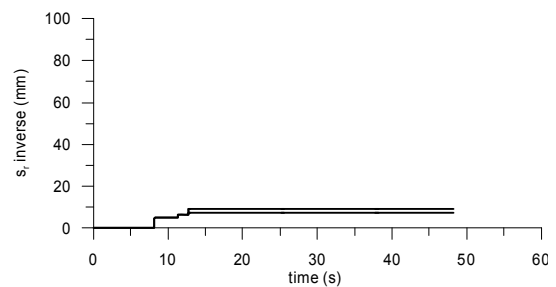
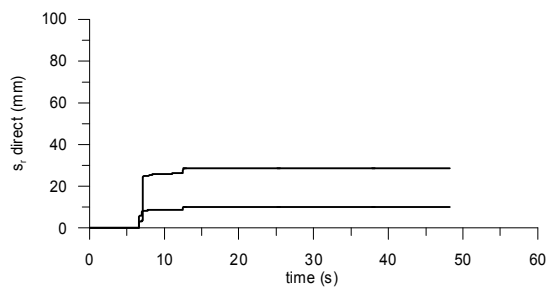
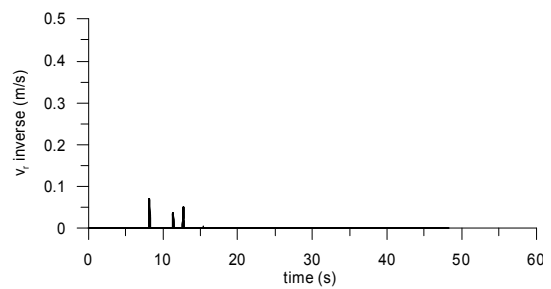
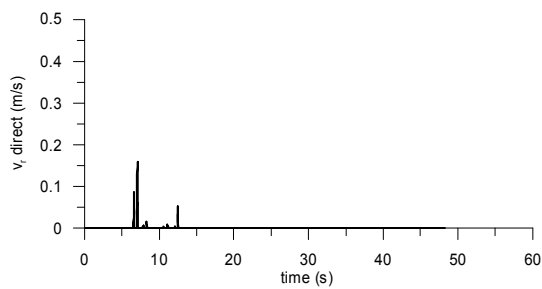
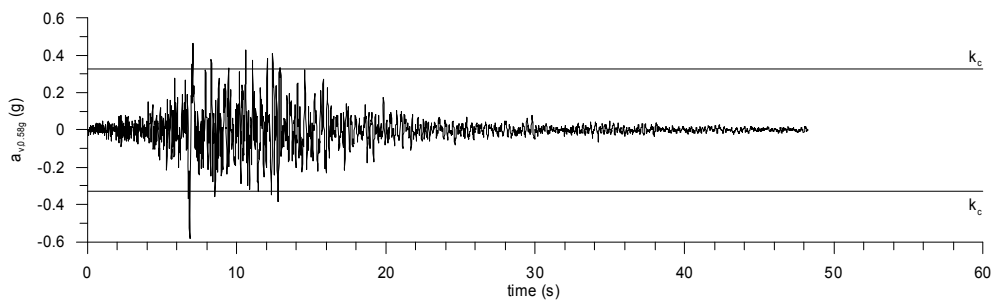
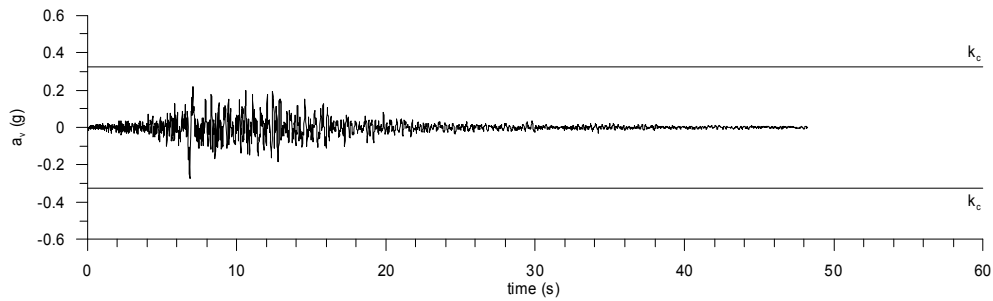
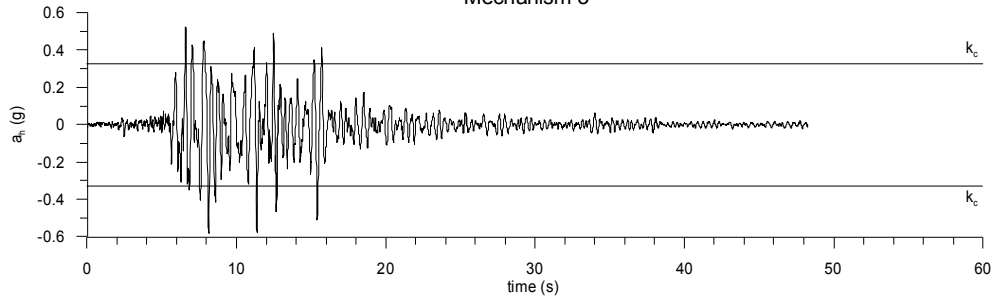
Mechanism 3



— same scaling factor for  $a_x$  and  $a_v$   
—  $a_{v,max}=0.58g$

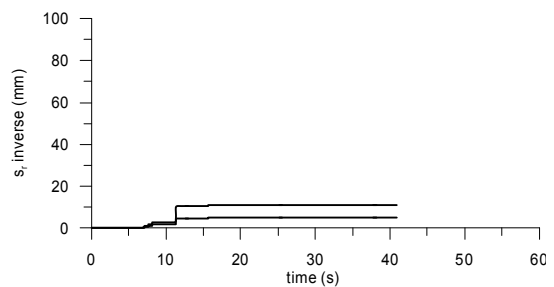
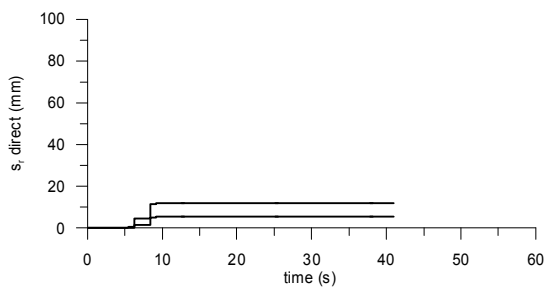
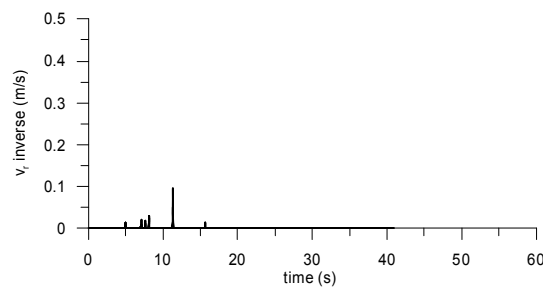
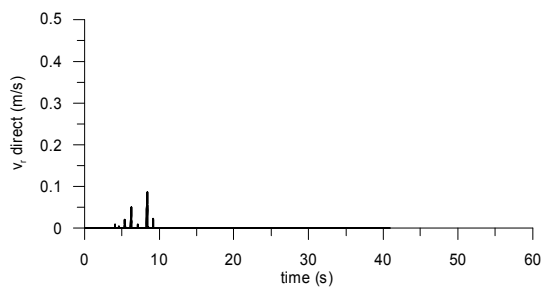
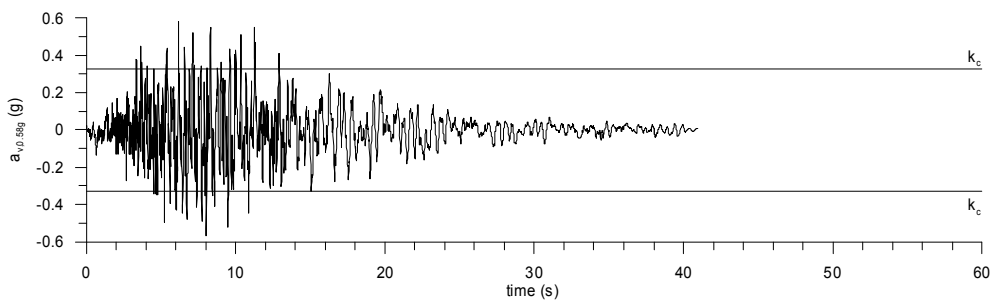
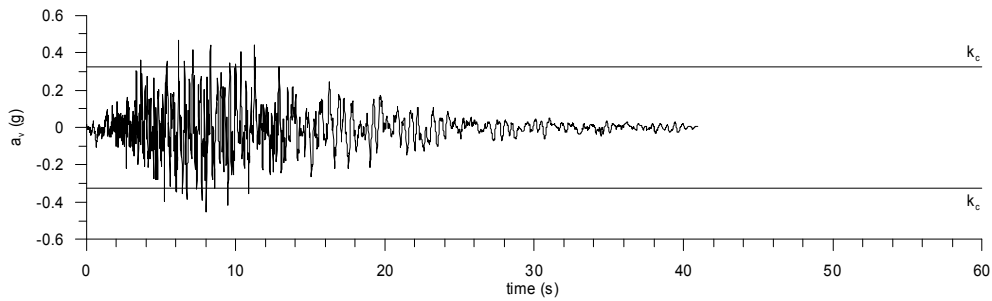
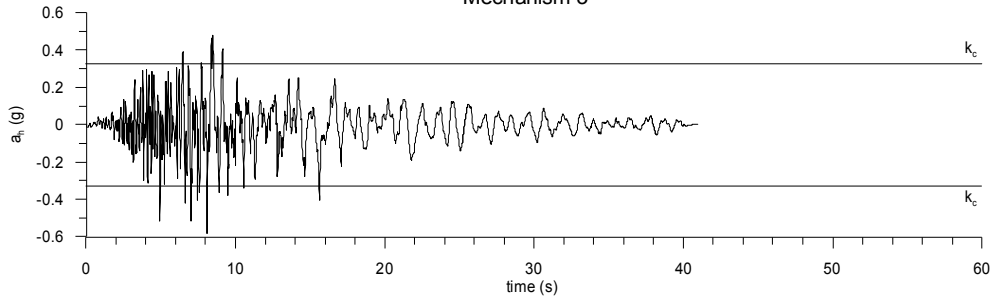
Montenegro 79 PETXC

Mechanism 3



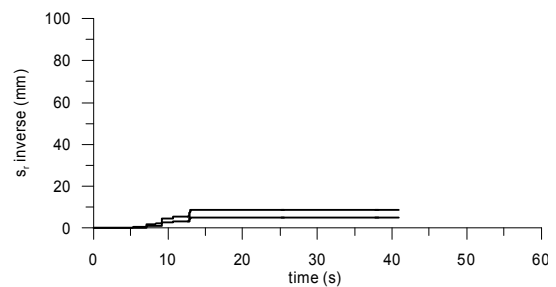
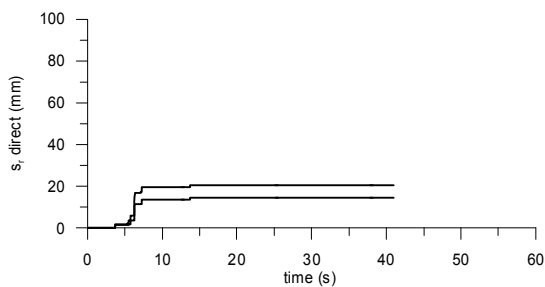
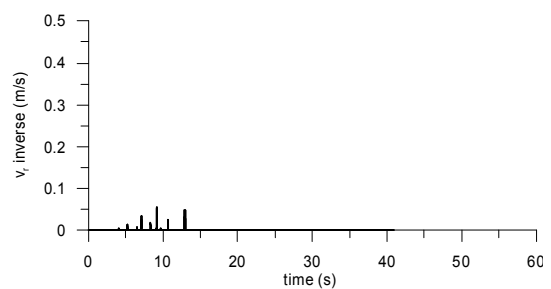
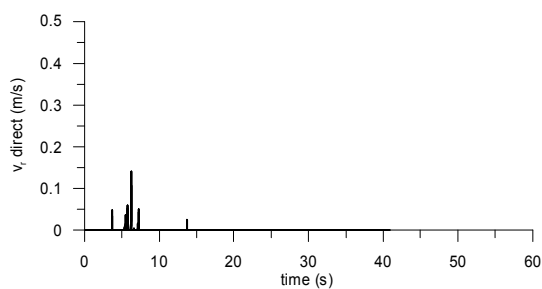
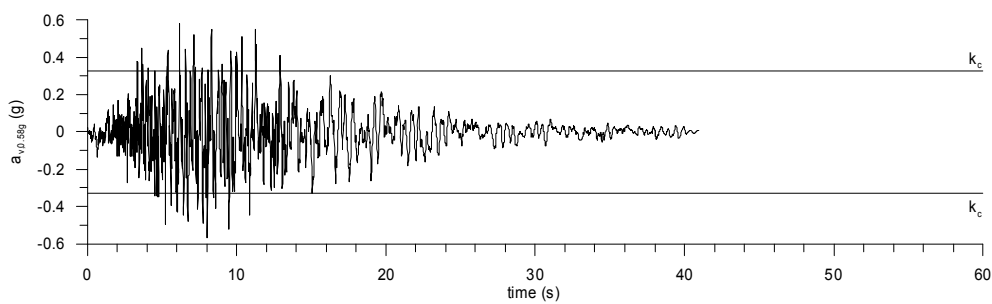
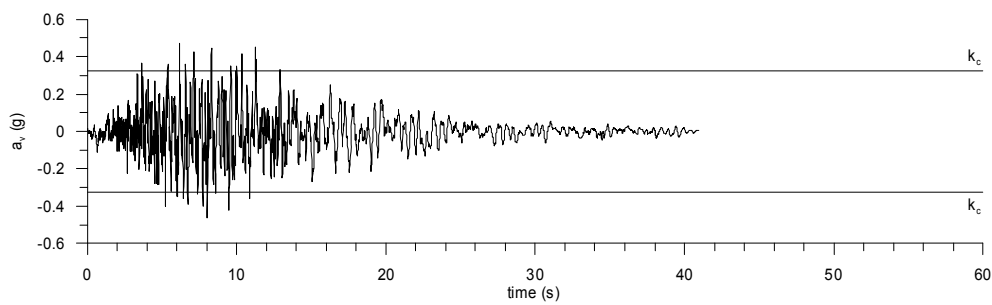
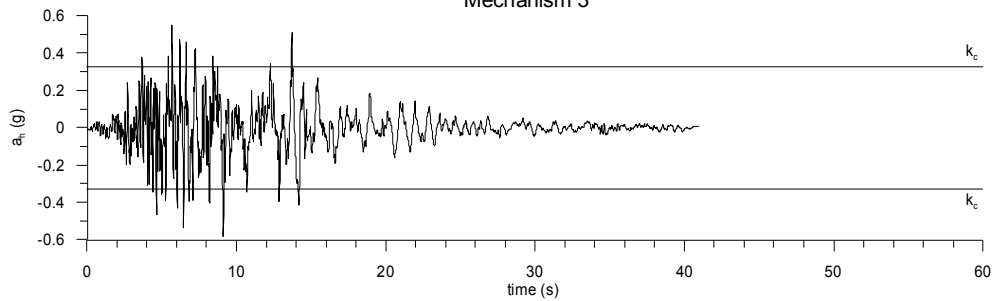
— same scaling factor for  $a_v$  and  $a_r$   
—  $a_{v,max}=0.58g$

Artificial 1 component 1  
Mechanism 3



— same scaling factor for  $a_x$  and  $a_y$   
—  $a_{v,max}=0.58g$

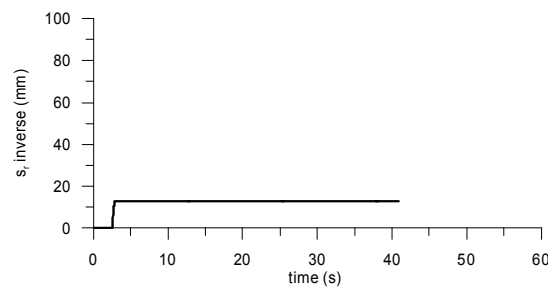
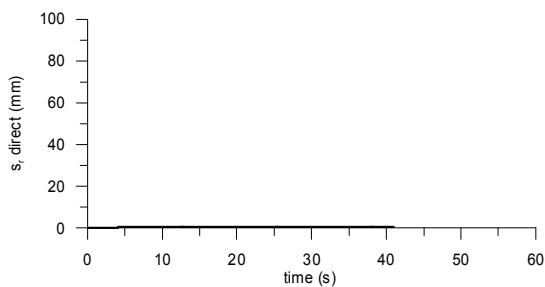
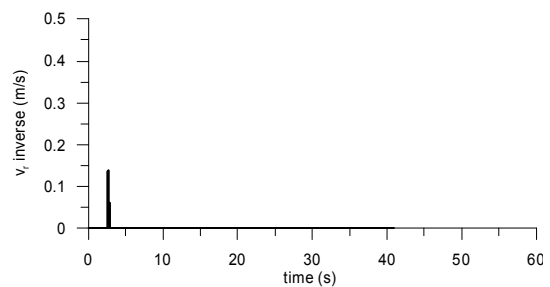
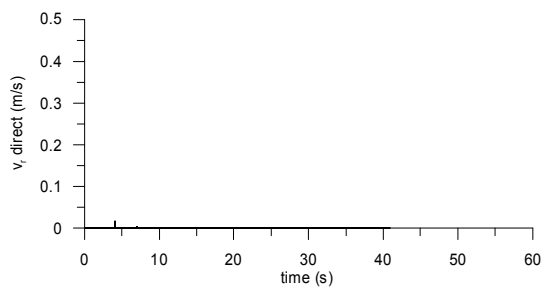
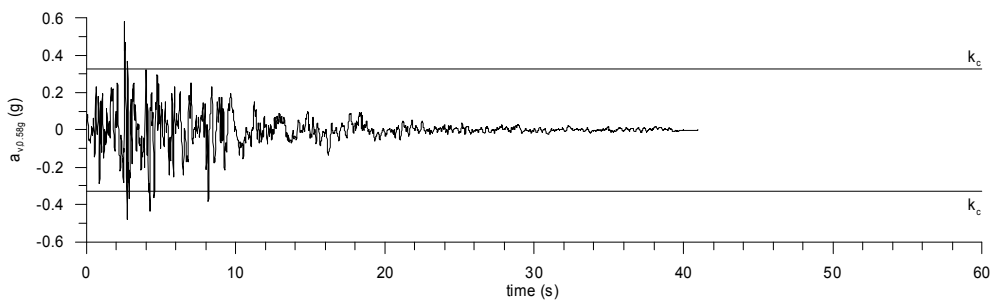
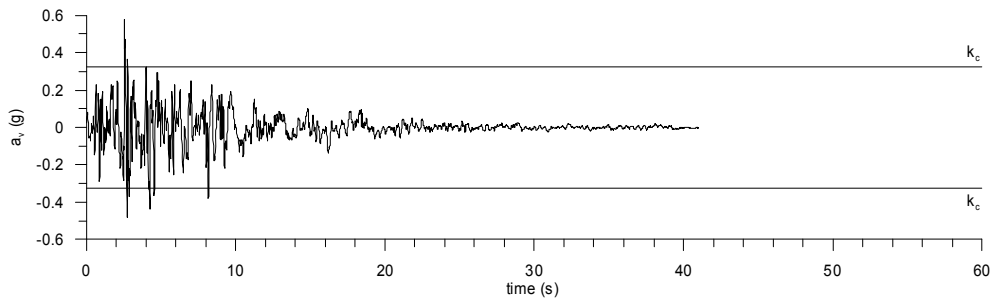
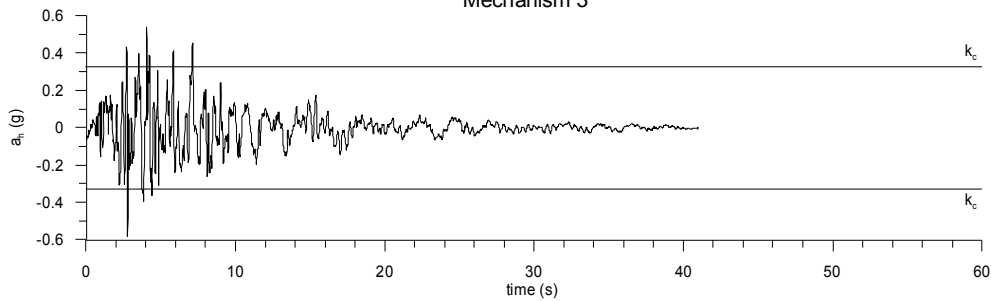
Artificial 1 component 2  
Mechanism 3



— same scaling factor for  $a_x$  and  $a_y$   
—  $a_{v,max}=0.58g$



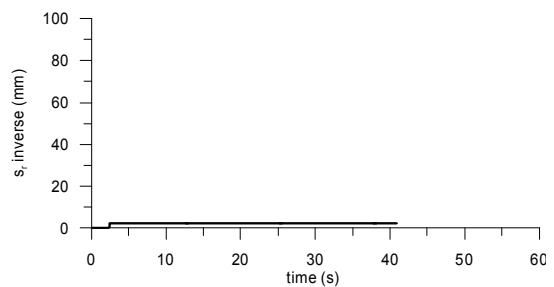
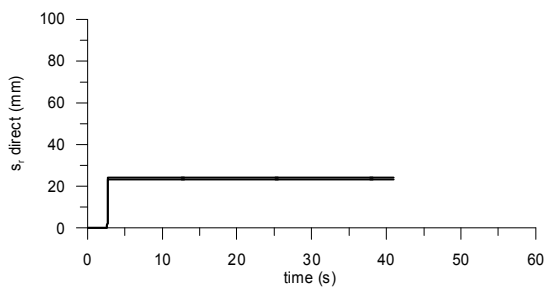
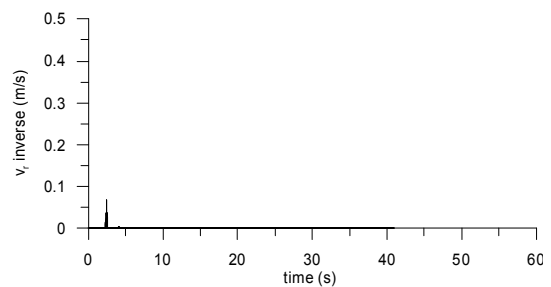
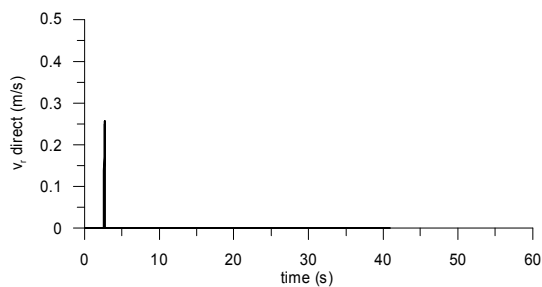
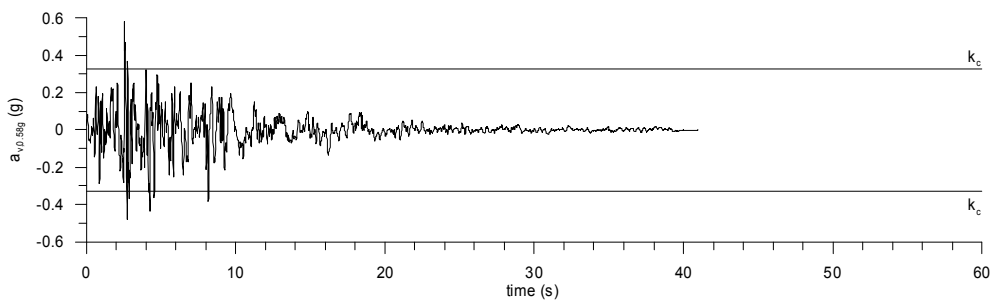
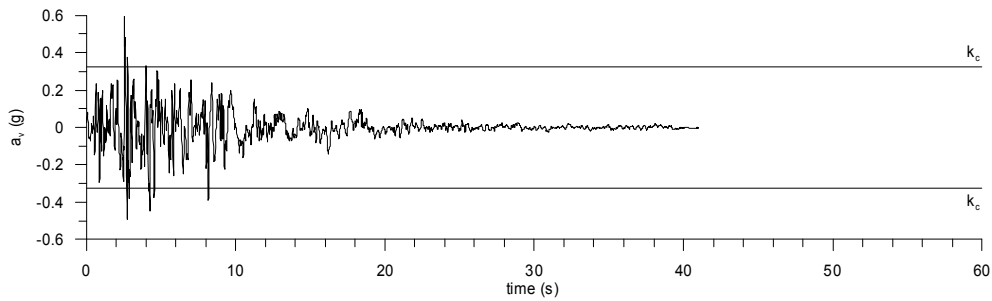
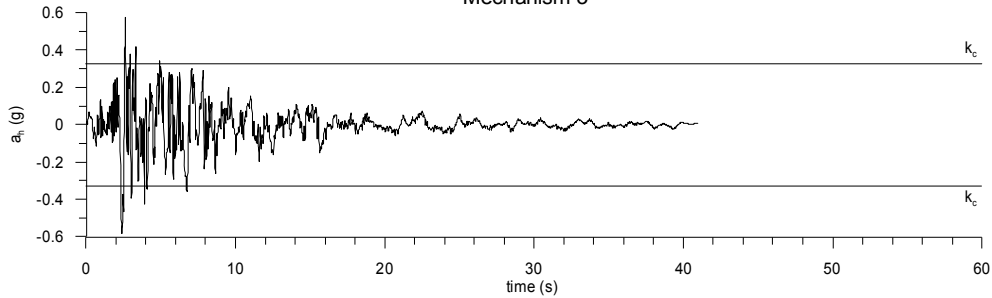
Artificial 2 component 1  
Mechanism 3



— same scaling factor for  $a_u$  and  $a_v$   
—  $a_{v,max}=0.58g$

Artificial 2 component 2

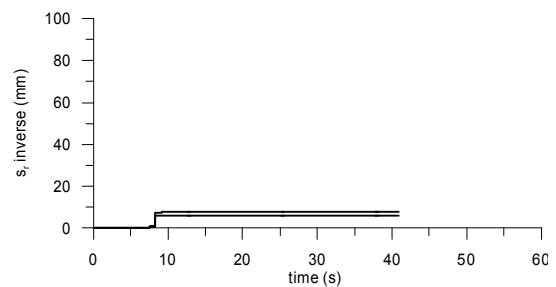
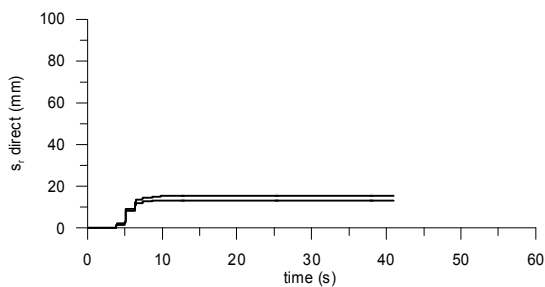
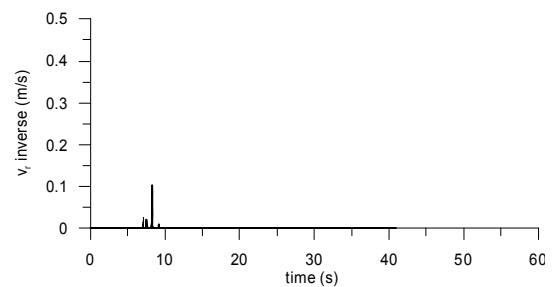
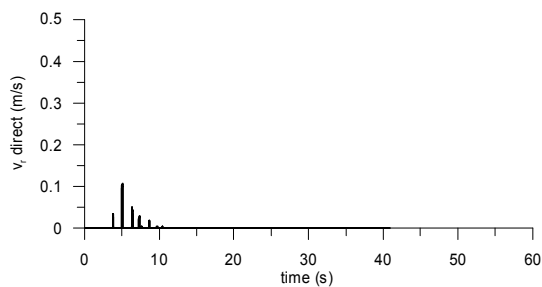
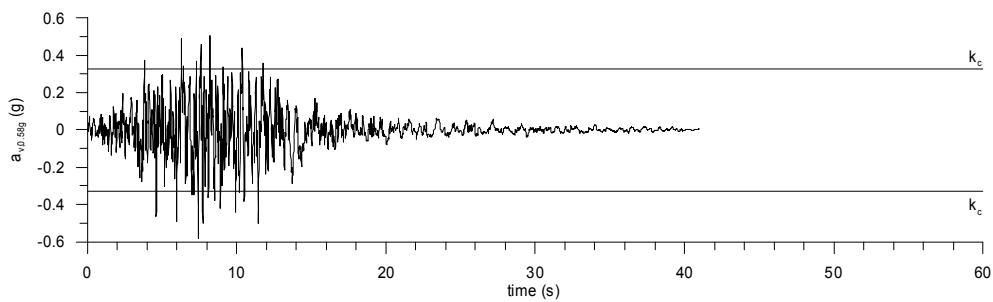
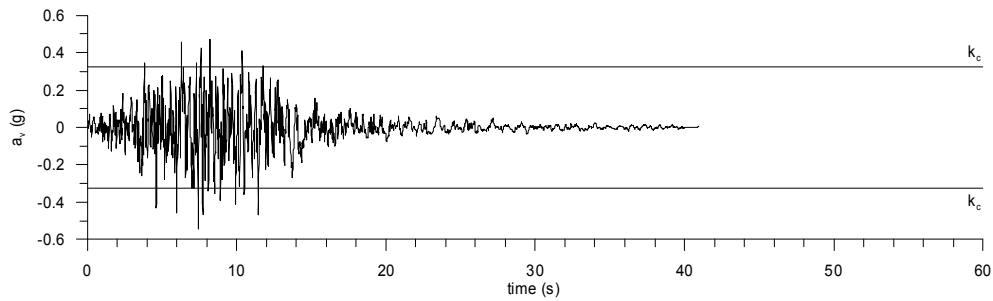
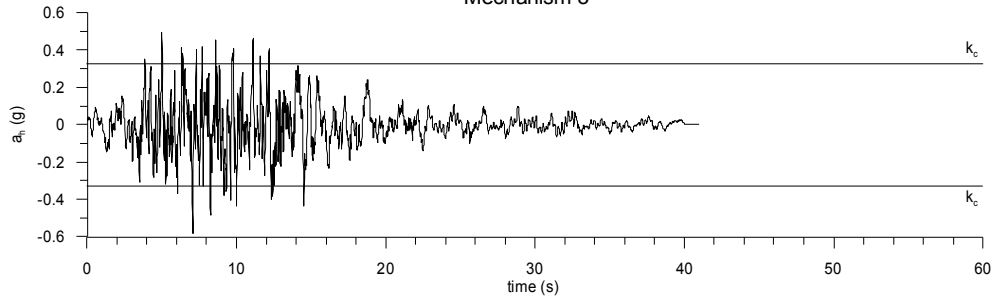
Mechanism 3



— same scaling factor for  $a_x$  and  $a_y$   
—  $a_{v,max}=0.58g$

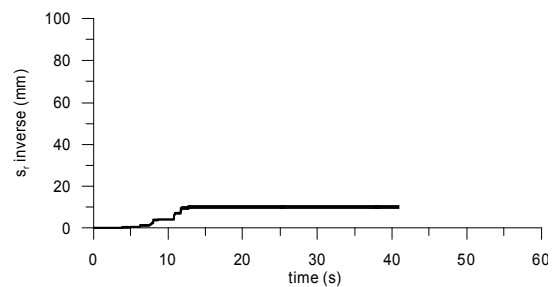
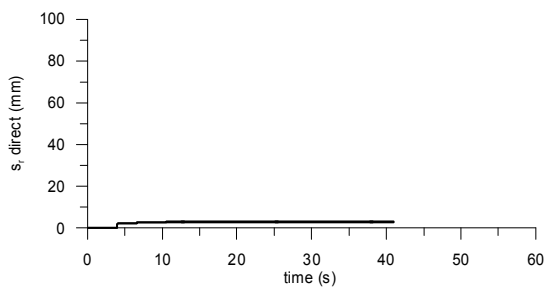
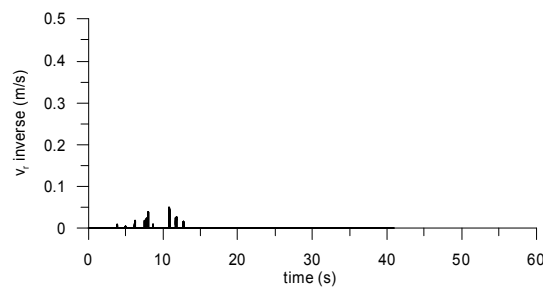
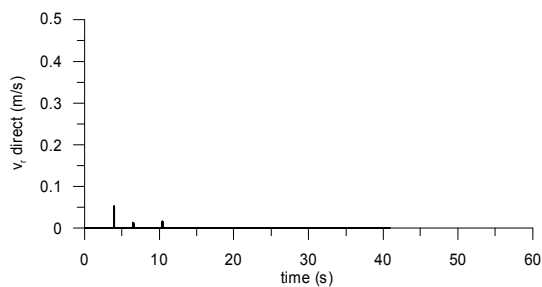
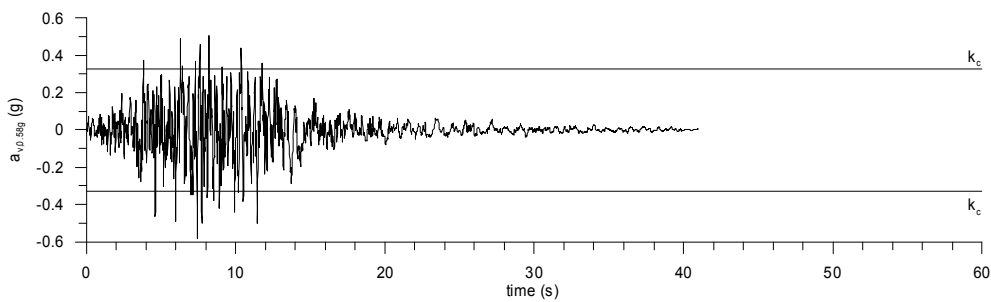
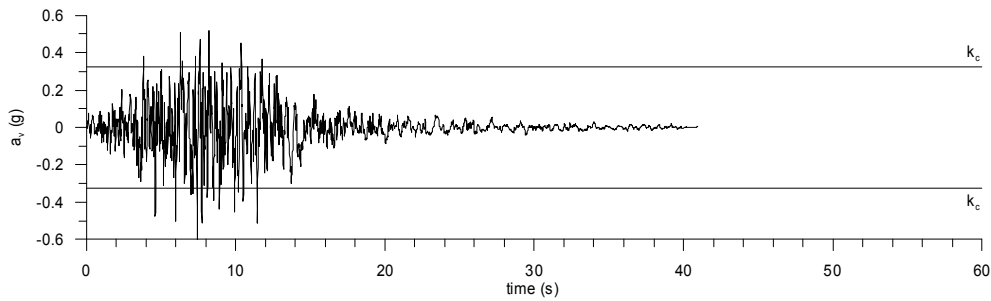
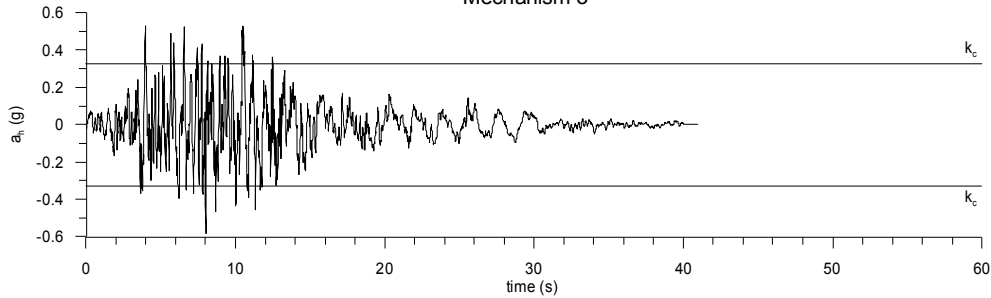
Artificial 3 component 1

Mechanism 3



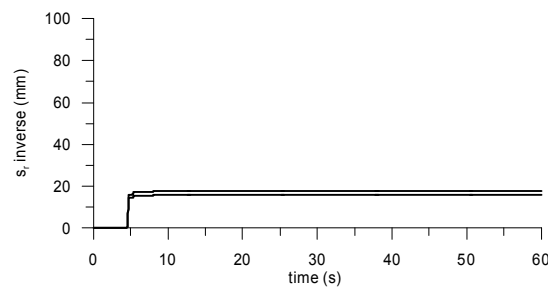
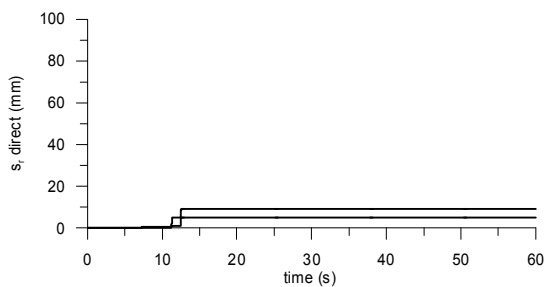
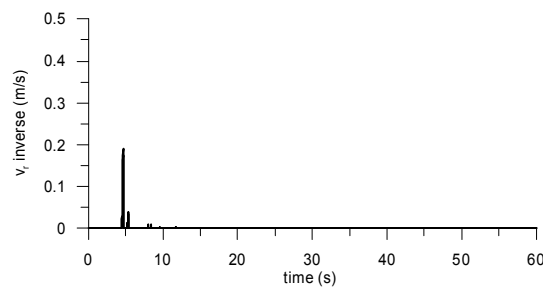
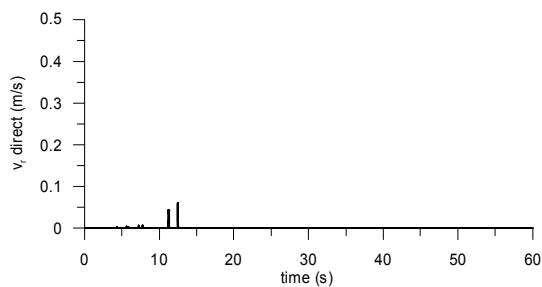
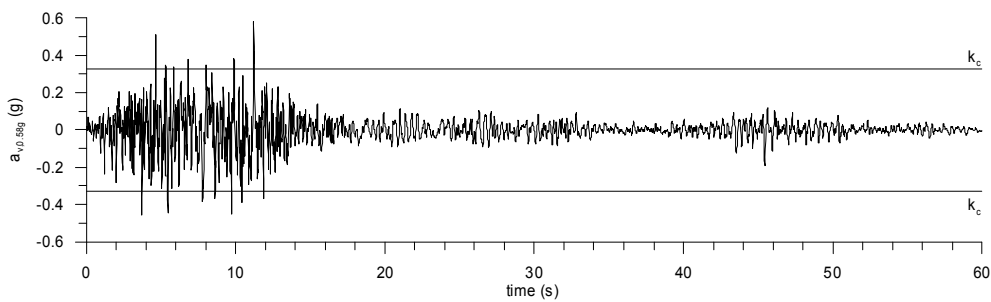
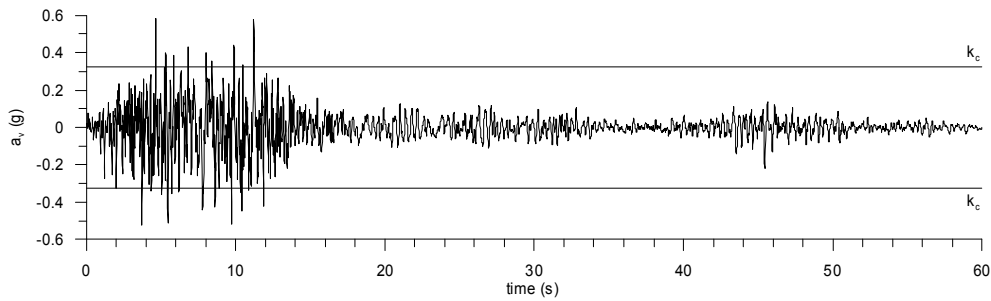
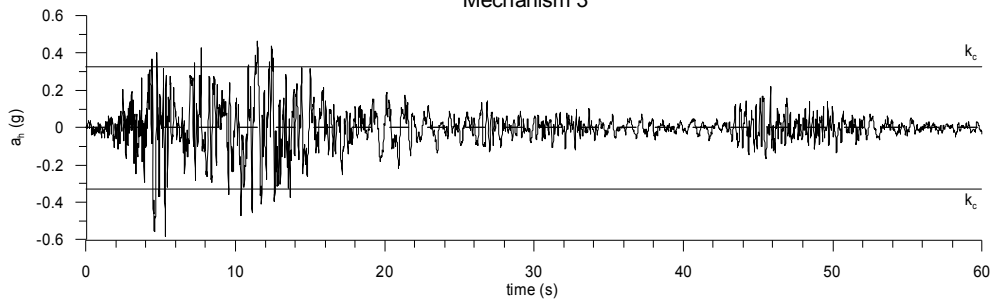
— same scaling factor for  $a_x$  and  $a_y$   
—  $a_{v,max}=0.58g$

Artificial 3 component 2  
Mechanism 3



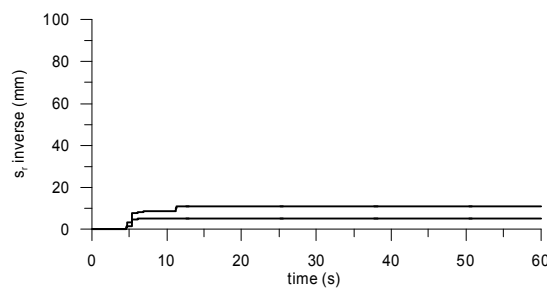
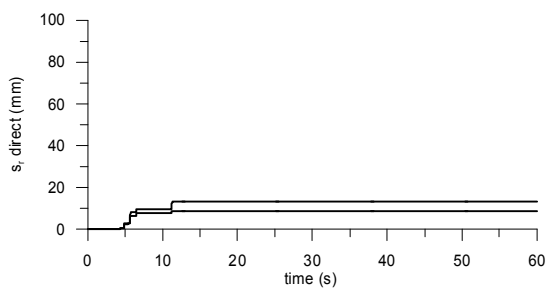
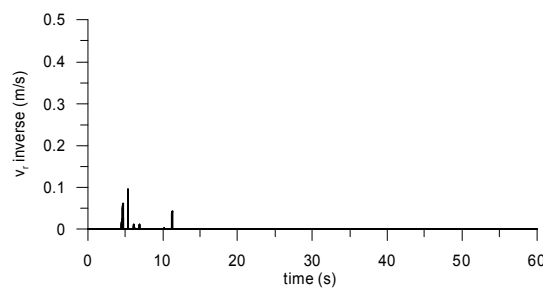
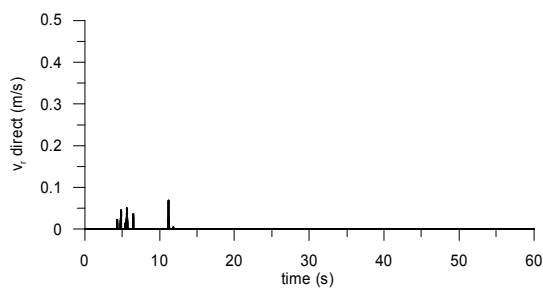
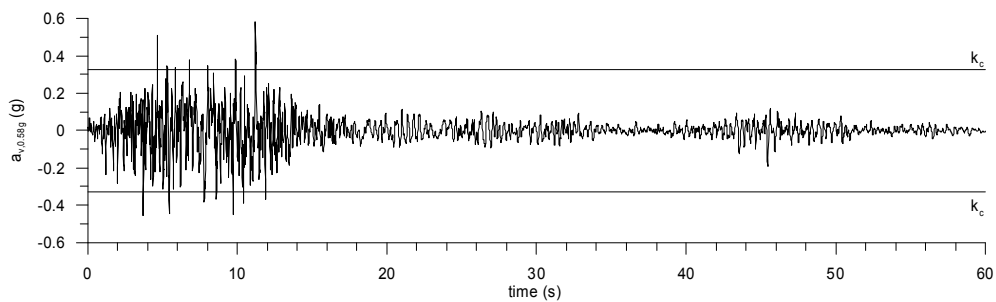
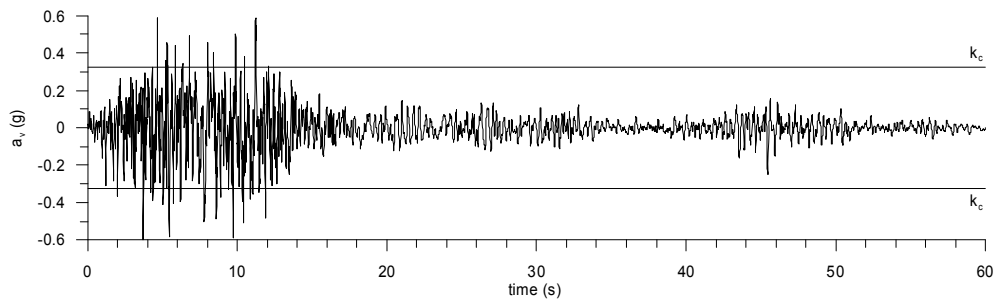
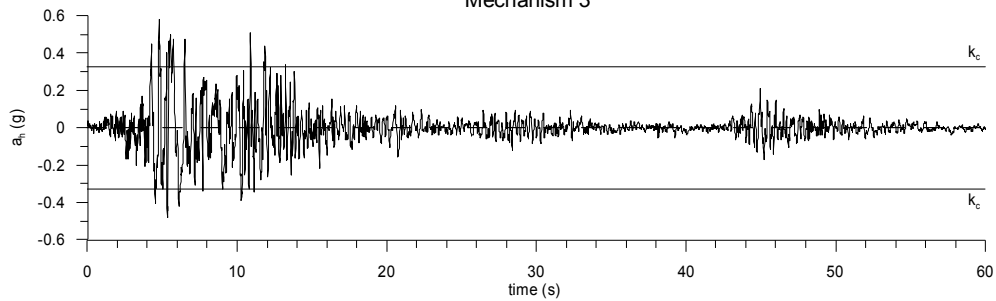
— same scaling factor for  $a_u$  and  $a_v$   
—  $a_{v,max}=0.58g$



Artificial 4 component 1  
Mechanism 3



— same scaling factor for  $a_x$  and  $a_y$   
—  $a_{v,max}=0.58g$

Artificial 4 component 2  
Mechanism 3



		<b>Ponte sullo Stretto di Messina</b> <b>PROGETTO DEFINITIVO</b>		
Sicily Anchor Block – earthquake induced displacements and safety against ultimate limit states, Annex	<i>Codice documento</i> PF0064_F0_ANX	<i>Rev</i> F0	<i>Data</i> 20/06/2011	

### **Appendix E – Updated cable forces obtained from global IBDAS model version 3.3b**

The forces transmitted by the main cables to the Sicilia Anchor Block have been recently re-evaluated using the global IBDAS model version 3.3b. The worst load combinations were selected for each limit state (SILS, SLS2 and ULS) for both static and seismic conditions, using 6 different criteria. Table E.1 resumes the values obtained for static loading conditions, while Table E.2 refers to seismic loading conditions.

Low differences are observed between values of the cable forces computed in the tender design and those recently provided by the global IBDAS model version 3.3b. Considering the maximum values of cable forces given by the different criteria for each load case, the ratio of the tender design cable forces to those provided by IBDAS model are in the range 1.06 to 0.90 (Table E.3); the higher ratio refers to the ULS load combination, while the lower is obtained for the SILS load combination.

For the Ultimate Limit State (ULS) cable forces provided by the tender design are 5.8% higher than the corresponding IBDAS values, this resulting in a conservative estimate of the behaviour of the Sicilia Anchor Block.



		<b>Ponte sullo Stretto di Messina</b> <b>PROGETTO DEFINITIVO</b>		
Sicily Anchor Block – earthquake induced displacements and safety against ultimate limit states, Annex	<i>Codice documento</i> PF0064_F0_ANX	<i>Rev</i> F0	<i>Data</i> 20/06/2011	

Table E.1 – Static Loading Conditions – updated global IBIDAS model version 3.3b

Criteria	Load case	F <sub>long</sub> (MN)	F <sub>vert</sub> (MN)	F (MN)
min u <sub>vert</sub>	ULS	2184	605	2266
max u <sub>vert</sub>		3575	1081	<b>3735</b>
min u <sub>hor</sub>		2184	605	2266
max u <sub>hor</sub>		3575	1081	3735
min R <sub>transv</sub>		2184	605	2266
max R <sub>transv</sub>		3575	1081	3735
min u <sub>vert</sub>	SILS	2479	710	2578
max u <sub>vert</sub>		3245	945	<b>3380</b>
min u <sub>hor</sub>		2479	710	2578
max u <sub>hor</sub>		3245	945	3380
min R <sub>transv</sub>		2479	710	2578
max R <sub>transv</sub>		3245	945	3380
min u <sub>vert</sub>	SLS2	2188	607	2271
max u <sub>vert</sub>		3215	958	<b>3355</b>
min u <sub>hor</sub>		2188	607	2271
max u <sub>hor</sub>		3215	958	3355
min R <sub>transv</sub>		2188	607	2271
max R <sub>transv</sub>		3215	958	3355







		<b>Ponte sullo Stretto di Messina</b> <b>PROGETTO DEFINITIVO</b>		
Sicily Anchor Block – earthquake induced displacements and safety against ultimate limit states, Annex		<i>Codice documento</i> PF0064_F0_ANX	<i>Rev</i> F0	<i>Data</i> 20/06/2011

Table E.2 – Seismic Loading Conditions – updated global IBDAS model version 3.3b

Criteria	Load case	$F_{long}$ (MN)	$F_{vert}$ (MN)	F (MN)
min $u_{vert}$	ULS	2071	553	2143
max $u_{vert}$		3488	1064	<b>3647</b>
min $u_{hor}$		2199	629	2287
max $u_{hor}$		3360	988	3502
min $R_{transv}$		2173	623	2260
max $R_{transv}$		3386	994	3529
min $u_{vert}$	SILS	2357	653	2446
max $u_{vert}$		3341	992	<b>3485</b>
min $u_{hor}$		2498	737	2605
max $u_{hor}$		3199	909	3326
min $R_{transv}$		2469	730	2575
max $R_{transv}$		3228	916	3355
min $u_{vert}$	SLS2	2143	585	2221
max $u_{vert}$		3244	974	<b>3387</b>
min $u_{hor}$		2201	620	2287
max $u_{hor}$		3185	939	3321
min $R_{transv}$		2189	617	2275
max $R_{transv}$		3197	942	3333

Table E.3: Cable forces in the Sicilia Anchor Block: Tender Design and IBDAS values

Load case	Tender Design	Static IBDAS	Seismic IBDAS	$F_{TD}/F_{IBDAS}$
	F (MN)	F (MN)	F (MN)	
ULS	3964	3735	3647	1.06
SILS	3146	3380	3485	0.90
SLS2	3250	3355	3387	0.96

		<b>Ponte sullo Stretto di Messina</b> <b>PROGETTO DEFINITIVO</b>		
Sicily Anchor Block – earthquake induced displacements and safety against ultimate limit states, Annex	<i>Codice documento</i> PF0064_F0_ANX	<i>Rev</i> F0	<i>Data</i> 20/06/2011	

## Appendix F – Updated cable forces obtained from global IBDAS model version 3.3f

The forces transmitted by the main cables to the Sicilia Anchor Block have been further re-evaluated using the global IBDAS model version 3.3f. The worst load combinations were selected for each limit state (SILS, SLS2 and ULS) for both static and seismic conditions, using 6 different criteria. Table F.1 resumes the values obtained for static loading conditions, while Table F.2 refers to seismic loading conditions.

Low differences are observed between values of the cable forces computed in the tender design and those recently provided by the global IBDAS model version 3.3f. Considering the maximum values of cable forces given by the different criteria for each load case, the ratio of the tender design cable forces to those provided by IBDAS model are in the range 1.08 to 0.93 (Table F.3); the higher ratio refers to the ULS load combination, while the lower is obtained for the SILS load combination.

For the Ultimate Limit State (ULS) cable forces provided by the tender design are 8% higher than the corresponding IBDAS values, this resulting in a conservative estimate of the behaviour of the Sicilia Anchor Block.



		<b>Ponte sullo Stretto di Messina</b> <b>PROGETTO DEFINITIVO</b>		
Sicily Anchor Block – earthquake induced displacements and safety against ultimate limit states, Annex	<i>Codice documento</i> PF0064_F0_ANX	<i>Rev</i> F0	<i>Data</i> 20/06/2011	

Table F.1 – Static Loading Conditions – updated global IBDAS model version 3.3f

Criteria	Load case	F <sub>long</sub> (MN)	F <sub>vert</sub> (MN)	F (MN)
min u <sub>vert</sub>	ULS	2176	596	2256
max u <sub>vert</sub>		<b>3525</b>	<b>1057</b>	<b>3680</b>
min u <sub>hor</sub>		2176	597	2256
max u <sub>hor</sub>		3525	1057	3680
min R <sub>transv</sub>		2176	597	2256
max R <sub>transv</sub>		3525	1057	3680
min u <sub>vert</sub>	SILS	2439	690	2535
max u <sub>vert</sub>		3205	924	3336
min u <sub>hor</sub>		2439	690	2535
max u <sub>hor</sub>		3205	924	3336
min R <sub>transv</sub>		2439	691	2535
max R <sub>transv</sub>		3205	924	3336
min u <sub>vert</sub>	SLS2	2181	598	2261
max u <sub>vert</sub>		3175	937	3311
min u <sub>hor</sub>		2181	598	2261
max u <sub>hor</sub>		3175	937	3311
min R <sub>transv</sub>		2181	598	2261
max R <sub>transv</sub>		3175	937	3311





		<b>Ponte sullo Stretto di Messina</b> <b>PROGETTO DEFINITIVO</b>		
Sicily Anchor Block – earthquake induced displacements and safety against ultimate limit states, Annex		<i>Codice documento</i> PF0064_F0_ANX	<i>Rev</i> F0	<i>Data</i> 20/06/2011

Table F.2 – Seismic Loading Conditions – updated global IBDAS model version 3.3f

Criteria	Load case	F <sub>long</sub> (MN)	F <sub>vert</sub> (MN)	F (MN)
min u <sub>vert</sub>	ULS	2105	554	2177
max u <sub>vert</sub>		3397	1030	3550
min u <sub>hor</sub>		2138	587	2217
max u <sub>hor</sub>		3364	997	3509
min R <sub>transv</sub>		2250	638	2339
max R <sub>transv</sub>		3252	946	3387
min u <sub>vert</sub>	SILS	2363	645	2449
max u <sub>vert</sub>		<b>3255</b>	<b>960</b>	<b>3394</b>
min u <sub>hor</sub>		2399	681	2494
max u <sub>hor</sub>		3218	924	3348
min R <sub>transv</sub>		2523	737	2629
max R <sub>transv</sub>		3094	868	3214
min u <sub>vert</sub>	SLS2	2154	581	2231
max u <sub>vert</sub>		<b>3185</b>	<b>949</b>	<b>3323</b>
min u <sub>hor</sub>		2169	596	2250
max u <sub>hor</sub>		3170	934	3304
min R <sub>transv</sub>		2220	619	2305
max R <sub>transv</sub>		3117	910	3249

Table F.3: Cable forces in the Sicilia Anchor Block: Tender Design and IBDAS values (model version 3.3f)

	Tender Design	Static IBDAS	Seismic IBDAS	
Load case	F (MN)	F (MN)	F (MN)	F <sub>TD</sub> /F <sub>IBDAS</sub>
ULS	3964	3680	3550	1.08
SILS	3146	3336	3394	0.93
SLS2	3250	3311	3323	0.98

		<b>Ponte sullo Stretto di Messina</b> <b>PROGETTO DEFINITIVO</b>	
Sicily Anchor Block – earthquake induced displacements and safety against ultimate limit states, Annex	<i>Codice documento</i> PF0064_F0_ANX	<i>Rev</i> F0	<i>Data</i> 20/06/2011

## References

- Berezantzev W.G. (1964). *Calculation of foundation basis*. Construction Literature, Leningrad, U.S.S.R.
- Bolton M.D. (1986). *The strength and dilatancy of sands*, Géotechnique, 1, 65-78
- Cubrinovski M. and Ishihara K. (1999). *Empirical correlation between SPT N-value and relative density for sandy soils*. Soils and Foundations, 39 n. 5, 61 – 71.
- Jamiolkowski M., Leroueil S., and Lo Presti D. C. F. (1991). "Theme lecture: Design parameters from theory to practice." Proc., Geo-Coast'91, 1–41.
- Newmark N.M. (1965). *Effect of earthquakes on dam and embankment*. Geotèchnique, 15 (2), 139-160.
- Rowe P.W. (1962). *The stress – dilatancy relation for static equilibrium of an assembly of particles in contact*. Proceedings Royal Society, London, Ser. A 269, 500 – 527.
- Schmertmann J.H. (1975). *Measurement of in situ shear strength. State – of – the – art report*. ASCE Speciality Conference on in Situ Measurements of Soil Properties, 2, 57 – 138
- Tanaka Y., Kudo Y., Yoshida Y. & Ikemi M. (1987). *A study on the mechanical properties of sandy gravel – dynamic properties of reconstituted samples*. Central Research Institute of Electric Power Industry, Report U87019.